Pacific Gas and Electric Company®

Paula Gerfen
Senior Vice President and
Chief Nuclear Officer

Diablo Canyon Power Plant
P.O. Box 56
Avila Beach, CA 93424

805.545.4596
Fax: 805.545.4234
Paula.Gerfen@pge.com

PG&E Letter DCL-26-046

ATTN: Document Control Desk
U.S. Nuclear Regulatory Commission
Washington, DC 20555-0001

10 CFR 50, Appendix H

Docket No. 50-275, OL-DPR-80
Diablo Canyon Power Plant Unit 1
<u>Diablo Canyon Unit 1 Reactor Vessel Material Surveillance Program Capsule B Technical Report</u>

Dear Commissioners and Staff:

On April 21, 2025, Surveillance Program Capsule B was withdrawn from the Diablo Canyon Power Plant (DCPP) Unit 1 reactor vessel and shipped to Westinghouse for extensive testing. Pursuant to 10 CFR 50 Appendix H, Pacific Gas and Electric Company (PG&E) is submitting the enclosed non-proprietary summary technical report, WCAP-19173-NP, Revision 0, “Analysis of Capsule B from the Pacific Gas and Electric Company Diablo Canyon Unit 1 Reactor Vessel Radiation Surveillance Program,” which meets applicable NRC regulatory requirements for surveillance capsule withdrawal and testing.

As discussed in the DCPP License Renewal Application and independently confirmed by NRC in their safety evaluation report,[1] existing capsule data evaluations demonstrate that both Units 1 and 2 meet the reactor vessel integrity criteria for 60 years. The results of this additional analysis (WCAP-19173-NP) support the NRC's previous conclusions for DCPP license renewal and confirm that the DCPP Unit 1 reactor vessel continues to remain safe for at least 60 years of operation. Thus, in summary, both DCPP Units 1 and 2 meet the reactor vessel integrity criteria for at least 60 years (i.e., through November 2, 2044, and August 26, 2045, respectively).

The results in WCAP-19173-NP do not cause any changes to the DCPP Unit 1 and 2 Technical Specifications (TS) 3.4.3, “RCS Pressure and Temperature (P/T) Limits,” TS 3.4.12, “Low Temperature Overpressure Protection (LTOP) System,” or TS 5.6.6, “Reactor Coolant System (RCS) PRESSURE AND TEMPERATURE LIMITS REPORT (PTLR).”

PG&E makes no new or revised regulatory commitments (as defined by NEI 99-04) in this letter.

---

[1] See Sections 3.0.3.2.13 and 4.2 at https://www.nrc.gov/docs/ML2515/ML25153A508.pdf

If you have any questions, please contact Mr. Philippe Soenen, Director, at (805) 459-3701.

Sincerely,

Paula Gerfen
Senior Vice President and Chief Nuclear Officer

June 29, 2026
Date

mma0/50943986
Enclosure
cc: Diablo Distribution
cc/Enc: DCISC
Nathan E. Garcia, Acting NRC Senior Resident Inspector
Brian Harris, NRC Senior Project Manager
Samson S. Lee, NRC Project Manager
John Monninger, NRC Region IV Administrator

WCAP-19173-NP, Revision 0, "Analysis of Capsule B from the Pacific Gas and Electric Company Diablo Canyon Unit 1 Reactor Vessel Radiation Surveillance Program"

WCAP-19173-NP
Revision 0

June 2026

Analysis of Capsule B from the Pacific Gas and Electric Company Diablo Canyon Unit 1 Reactor Vessel Radiation Surveillance Program

Westinghouse

WCAP-19173-NP
Revision 0

Analysis of Capsule B from the Pacific Gas and Electric Company Diablo Canyon Unit 1 Reactor Vessel Radiation Surveillance Program

Margaret L. Long
Reactor Vessel/Containment Vessel (RV/CV)
Design & Analysis

Alberto Guillen Marcos
Radiation Engineering & Analysis

June 2026

Reviewers: D. Brett Lynch
Reactor Vessel/Containment Vessel (RV/CV)
Design & Analysis

Andrew E. Hawk
Radiation Engineering & Analysis

Approved: Ryan R. Lowes, Director
Reactor Component Engineering

Jesse J Klingensmith, Manager
Radiation Engineering & Analysis

Westinghouse Electric Company LLC
1000 Westinghouse Drive
Cranberry Township, PA 16066, USA

Revision	Description	Completed
0	Original Issue.	June 2026

Originator/Author Names	Originator/Author Scope
Margaret L. Long Reactor Vessel/Containment Vessel (RV/CV) Design and Analysis	All
Alberto Guillen Marcos Radiation Engineering and Analysis	>Section 6, Radiation Analysis and Neutron Dosimetry >Appendix A, Validation of the Radiation Transport Models Based on Neutron Dosimetry Measurements
Reviewer Names	
D. Brett Lynch Reactor Vessel/Containment Vessel (RV/CV) Design and Analysis	All
Andrew E. Hawk Radiation Engineering and Analysis	>Section 6, Radiation Analysis and Neutron Dosimetry >Appendix A, Validation of the Radiation Transport Models Based on Neutron Dosimetry Measurements
Manager Names	
Ryan R. Lowes Reactor Component Engineering	All
Jesse J Klingensmith Radiation Engineering and Analysis	>Section 6, Radiation Analysis and Neutron Dosimetry >Appendix A, Validation of the Radiation Transport Models Based on Neutron Dosimetry Measurements

TABLE OF CONTENTS

LIST OF TABLES

LIST OF FIGURES

EXECUTIVE SUMMARY

The purpose of this report is to document the testing results of surveillance Capsule B from Diablo Canyon Unit 1 in accordance with Nuclear Regulatory Commission (NRC) regulatory requirements and guidance. Capsule B was removed at the end of Cycle 25 and post-irradiation mechanical tests of the Charpy V-notch and tensile specimens were performed. As summarized below, the test and analysis results do not cause any changes to the conclusions for Diablo Canyon license renewal [22] and confirm that the Diablo Canyon Unit 1 reactor vessel continues to remain safe for at least 60 years of operation.

A fluence evaluation utilizing the neutron transport and dosimetry cross-section libraries was derived from the Evaluated Nuclear Data File (ENDF) database (specifically, ENDF/B-VI). Capsule B received a fluence of 3.62 x 10^{19} n/cm^2 (E > 1.0 MeV) and included specimens of the Diablo Canyon Lower Shell Plate B4107-1, surveillance weld, and surrogate weld. The surveillance weld specimens in Capsule B were previously irradiated in Capsule S, which received an exposure of 0.293 x 10^{19} n/cm^2. Therefore, these surveillance weld specimens received an accumulative fluence of 3.913 x 10^{19} n/cm^2 (E > 1.0 MeV). The peak clad/base metal interface vessel fluence at 54 EFPY, corresponding to the end-of-license extension (EOLE) of plant operation, is projected to be 2.14 x 10^{19} n/cm^2 (E > 1.0 MeV).

In order to assess the impact of the irradiation on the embrittlement of the reactor vessel materials, the 30 ft-lb reference temperature (T_{30}) and Upper-Shelf Energy (USE) were determined per ASTM E185-16 [6] from the irradiated specimens contained with Capsule B and compared to unirradiated data. All Charpy V-notch data were plotted using a symmetric hyperbolic tangent curve-fitting program. This evaluation led to the following conclusions:

(1) As shown in Table 5-10, for the measured shifts in the 30 ft-lb reference temperature (ΔRT_{NDT}):

   a. The measured Lower Shell Plate B4107-1 T_{30} (transverse orientation) shift is higher than the Regulatory Guide 1.99, Rev. 2 [1], Position 1.1 predictions, but within 2-sigma, (2σ, 34°F) applied to embrittlement predictions for plates and forgings to account for uncertainties.

   b. The measured surveillance weld (Heat # 27204) shift is within 1-sigma, (σ, 28°F) of the Regulatory Guide 1.99, Rev. 2 [1], Position 1.1 prediction for welds; thus, demonstrating good agreement.

   c. The measured surrogate weld (Heat # 27204) shift is less than the Regulatory Guide 1.99, Rev. 2 [1], Position 1.1 prediction, thus demonstrating predictions are conservative and bounding.

(2) As shown in Table 5-10, the measured percent decreases in USE are less than the Regulatory Guide 1.99, Rev. 2, Position 1.2 predictions for the Lower Shell Plate B4107-1 (transverse orientation), surveillance weld (Heat # 27204, Flux Linde 1092), and surrogate weld (Heat # 27204, Flux Linde 1092). This demonstrates the Regulatory Guide 1.99, Rev. 2, Position 1.2 predictions are conservative and bound the actual measurements of DCPP Unit 1 reactor vessel materials.

(3) The Diablo Canyon Unit 1 surveillance weld data are deemed “credible” per Regulatory Guide 1.99, Rev. 2 [1] (i.e., results follow expected trends); therefore, these data were used in the analysis and are acceptable to be used for performing embrittlement projection per Regulatory Guide 1.99, Rev. 2, Position 2.1 and Position 2.2. This determination includes data from the surrogate weld and sister-plant data. This credibility evaluation can be found in Appendix D.

(4) Comparison with WCAP-18924-NP [21], the analysis of record (AOR) for DCPP Unit 1 for reactor vessel integrity, shows good agreement. The AOR is bounding when considering the Capsule B surveillance data results because:

a. There are no changes to the credibility conclusions (i.e., results follow expected trends).
b. Neutron fluence projections for 60 years of operation roughly equate to those used in the AOR.
c. The pressurized thermal shock reference temperature (RT_{PTS}) inputs are bounding or equal to the AOR (e.g., increase in ΔRT_{NDT}, margin term, unirradiated RT_{NDT}, etc.)
d. The USE inputs are bounding or equal to the AOR (e.g., copper content, 1/4T fluence at 60 years, unirradiated USE, etc.).

(5) The test and analysis results do not cause any changes to the Diablo Canyon Technical Specifications [25] (TS) 3.4.3, “RCS Pressure and Temperature (P/T) Limits,” TS 3.4.12, “Low Temperature Overpressure Protection (LTOP) System,” or TS 5.6.6, “REACTOR COOLANT SYSTEM (RCS) PRESSURE AND TEMPERATURE LIMITS REPORT (PTLR) [26].”

1 SUMMARY OF RESULTS

The analysis of the reactor vessel materials contained in surveillance Capsule B, the fourth capsule removed and tested from the Diablo Canyon Unit 1 reactor pressure vessel, led to the following conclusions:

- Charpy V-notch test data were plotted using a symmetric hyperbolic tangent curve-fitting program. Appendix C presents the CVGRAPH, Version 6.02, Charpy V-notch plots for Capsule B, along with data from the program baseline and previous capsules.

- Capsule B received a cumulative fast neutron fluence (E > 1.0 MeV) of 3.62 x 10^{19} n/cm^2.

- Irradiation of the reactor vessel Lower Shell Plate B4107-1 Charpy specimens, oriented with the longitudinal axis of the specimen parallel to the major surfaces of the plate and normal to the major working direction (transverse orientation), resulted in an irradiated 30 ft-lb transition temperature of 155.2°F. This corresponds to a 30 ft-lb transition temperature increase of 136.9°F for the transversely oriented specimens.

- Irradiation of the surrogate weld (Heat # 27204) Charpy specimens resulted in an irradiated 30 ft-lb transition temperature of 201.5°F. This corresponds to a 30 ft-lb transition temperature increase of 242.6°F for the surrogate weld specimens.

- Irradiation of the surveillance weld (Heat # 27204) Charpy specimens resulted in an irradiated 30 ft-lb transition temperature of 243.7°F. This corresponds to a 30 ft-lb transition temperature increase of 308.7°F for the surveillance program weld specimens.

- Irradiation of the Correlation Monitor Material (CMM) Plate HSST02 Charpy specimens, oriented with the longitudinal axis of the specimen parallel to the major surfaces of the plate and normal to the major working direction (transverse orientation), resulted in an irradiated 30 ft-lb transition temperature of 210.8°F. This corresponds to a 30 ft-lb transition temperature increase of 163.8°F for the CMM specimens.

- The average upper-shelf energy of Lower Shell Plate B4107-1 (transverse orientation) resulted in an average energy decrease of 14.6 ft-lb after irradiation. This decrease results in an irradiated average upper-shelf energy of 98.0 ft-lb for the transversely oriented specimens.

- The average upper-shelf energy of the surrogate weld (Heat # 27204) Charpy specimens resulted in an average energy decrease of 45.7 ft-lb after irradiation. This decrease results in an irradiated average upper-shelf energy of 58.6 ft-lb for the surveillance program weld specimens.

- The average upper-shelf energy of the surveillance weld (Heat # 27204) Charpy specimens resulted in an average energy decrease of 37.6 ft-lb after irradiation. This decrease results in an irradiated average upper-shelf energy of 50.0 ft-lb for the surveillance program weld specimens.

- The average upper-shelf energy of the CMM resulted in an average energy decrease of 37.4 ft-lb after irradiation. This decrease results in an irradiated average upper-shelf energy of 83.0 ft-lb for the CMM specimens.

- Comparisons of the measured 30 ft-lb shift in transition temperature values and upper-shelf energy decreases to those predicted by Regulatory Guide 1.99, Rev. 2 [1] for the Diablo Canyon Unit 1 reactor vessel surveillance materials are presented in Table 5-10.

- Based on the credibility evaluation presented in Appendix D, the Diablo Canyon Unit 1 surveillance weld data are deemed "credible". This determination includes data from the surrogate weld and sister-plant data.

- The maximum calculated 54 EFPY (end-of-license extension) neutron fluence (E > 1.0 MeV) for the Diablo Canyon Unit 1 reactor vessel beltline using the Regulatory Guide 1.99, Rev. 2 [1] attenuation formula (i.e., Equation # 3 in the Guide) and a vessel thickness of 8.625 inches are as follows:

  Calculated (54 EFPY): Vessel peak clad/base metal interface fluence* = 2.14 x 10^{19} n/cm^2
  Vessel peak quarter-thickness (1/4T) fluence = 1.28 x 10^{19} n/cm^2
  Vessel peak three-quarter thickness (3/4T) fluence = 0.453 x 10^{19} n/cm^2

  *This fluence value is determined from data in Table 6-6.

2 INTRODUCTION

This report presents the results of the examination of Capsule B, the fourth capsule removed and tested in the continuing surveillance program, which monitors the effects of neutron irradiation on the Pacific Gas and Electric Company (PG&E) Diablo Canyon Unit 1 reactor pressure vessel materials under actual operating conditions.

The surveillance program for the Diablo Canyon Unit 1 reactor pressure vessel materials was designed and recommended by Westinghouse Electric Company LLC. The initial reactor vessel surveillance program, described in WCAP-8465 [2], was developed in accordance with ASTM E185-70 [3]. To enhance the program, PG&E implemented a supplemental surveillance program at the beginning of Cycle 6 which included four additional surveillance capsules, including Capsule B discussed herein. This supplemental surveillance program is described in WCAP-13440 [16]. Results from the supplemental surveillance capsules were intended to provide additional data on reactor vessel material embrittlement at fluence levels beyond those addressed by the initial surveillance program.

Capsule B was removed from the reactor after receiving fast neutron fluence (E > 1.0 MeV) of 3.62×10^{19} n/cm^2 and shipped to the Westinghouse Churchill Laboratory, where post-irradiation Charpy V-notch impact and tensile testing was performed on the surveillance specimens. This report summarizes the testing and post-irradiation data obtained from surveillance Capsule B removed from the Diablo Canyon Unit 1 reactor vessel and presents the analysis of the data.

3 BACKGROUND

The ability of the large steel pressure vessel containing the reactor core and its primary coolant to resist fracture constitutes an important factor in ensuring safety in the nuclear industry. The beltline region of the reactor pressure vessel is the most critical region of the vessel because it is subjected to significant fast neutron bombardment. The overall effects of fast neutron irradiation on the mechanical properties of low-alloy, ferritic pressure vessel steels such as SA533 Grade B, Class 1 (base metal of the Diablo Canyon Unit 1 reactor pressure vessel beltline) are well documented in the literature. Generally, low-alloy ferritic materials show an increase in hardness and tensile properties and a decrease in ductility and toughness during high-energy irradiation.

A method for ensuring the integrity of reactor pressure vessels has been presented in "Fracture Toughness Criteria for Protection Against Failure," Appendix G to Section XI of the ASME Boiler and Pressure Vessel Code [4]. The method uses fracture mechanics concepts and is based on the reference nil-ductility transition temperature (RT_{NDT}).

RT_{NDT} is defined as the greater of either the drop-weight nil-ductility transition temperature (NDTT) per American Society of Testing and Materials (ASTM) E208 [5] or the temperature 60°F less than the 50 ft-lb (and 35-mil lateral expansion) temperature as determined from Charpy specimens oriented perpendicular (transverse) to the major working direction of the plate. The RT_{NDT} of a given material is used to index that material to a reference stress intensity factor curve (K_{Ic} curve) which appears in Appendix G to Section XI of the ASME Code [4]. The K_{Ic} curve is a lower bound of static fracture toughness results obtained from several heats of pressure vessel steel. When a given material is indexed to the K_{Ic} curve, allowable stress intensity factors can be obtained for this material as a function of temperature. Allowable operating limits can then be determined using these allowable stress intensity factors.

RT_{NDT} are adjusted to account for the effects of radiation on the reactor vessel material properties. The changes in mechanical properties of a given reactor pressure vessel steel, due to irradiation, are monitored by a reactor vessel surveillance program, such as the Diablo Canyon Unit 1 reactor vessel radiation surveillance program, in which a surveillance capsule is periodically removed from the operating nuclear reactor and the encapsulated specimens are tested. The increase in the average Charpy V-notch 30 ft-lb temperature (ΔRT_{NDT}) due to irradiation is added to the initial RT_{NDT}, along with a margin (M) to cover uncertainties, to adjust the RT_{NDT} (ART) for radiation embrittlement. This ART (initial RT_{NDT} + M + ΔRT_{NDT}) is used to index the material to the K_{Ic} curve and, in turn, to set operating limits for the nuclear power plant that take into account the effects of irradiation on the reactor vessel materials.

4 DESCRIPTION OF PROGRAM

The original Diablo Canyon Unit 1 reactor vessel surveillance program, documented in WCAP-8465 [2], was established to monitor neutron irradiation effects on beltline materials. Eight surveillance capsules were installed prior to initial startup in holders welded to the thermal shield, located between the shield and vessel wall opposite the core center.

The original capsule set consisted of five Type I and three Type II capsules. Type I capsules contained Charpy, tensile, and Wedge Opening Loading (WOL) specimens fabricated from SA533 Grade B Class 1 Intermediate Shell Plate material, along with CMM specimens. Type II capsules contained similar specimens fabricated from the Intermediate Shell Plate and the reactor vessel limiting weld (Heat # 27204, Linde 1092 flux, Lot 3714), as well as Heat-Affected Zone (HAZ) and CMM specimens.

The initial surveillance program was intended to monitor embrittlement through 40 years of operation. In order to provide additional data to support extended operation, PG&E implemented a supplemental surveillance program, documented in WCAP-13440 [16], which included four additional surveillance capsules (A, B, C, and D) installed during the refueling outage at End-of-Cycle (EOC) 5 in October 1992.

The supplemental capsules contain Charpy V-notch, Charpy blank, tensile, and WOL specimens fabricated from Diablo Canyon Unit 1 Lower Shell Plate B4107-1, CMM Plate HSST02, and weld Heat # 27204, along with dosimeters for neutron fluence measurement and thermal monitors to determine irradiation temperature. In addition, the capsules also contain Charpy V-notch specimens supplied by the Electric Power Research Institute (EPRI). These materials were part of an EPRI research program and were not directly relevant to the PG&E Diablo Canyon Unit 1 surveillance program. Details of the specimen compositions are provided in WCAP-13440 [16]. Capsule B was removed at the end of Cycle 25 with a fast neutron fluence (E > 1.0 MeV) of 3.62×10^{19} n/cm^2.

The tensile and Charpy V-notch base metal specimens were obtained from Lower Shell Plate B4107-1, which is the limiting reactor vessel beltline plate for embrittlement at higher fluences. Specimens identified as AT and BT were machined from the one-quarter thickness location after stress relief, while specimens identified as CT were machined from the three-quarter thickness location after stress relief. All base metal were oriented transverse to the major working direction.

CMM Charpy V-notch specimens, identified as DT and ET, were fabricated from SA533 Grade B Class 1 plate material supplied by Westinghouse. These specimens were machined from the one-quarter thickness location. Charpy specimens were oriented transverse to the major working direction.

The tensile and Charpy V-notch weld specimens were fabricated from surrogate weld metal MIL-B4 weld wire (Heat # 27204, Linde 1092 flux, Lot 3714), provided by ABB/Combustion Engineering. This material is representative of the limiting Diablo Canyon Unit 1 beltline weld (intermediate and lower shell longitudinal weld seams) and is consistent with the weld metal used in the original surveillance program. These specimens are identified as SW.

Additional surveillance weld metal previously irradiated in Capsule S were used to include Charpy blanks and WOL specimens in Capsule B as well. Charpy blanks were produced from fractured weld Charpy V-notch specimens by removing the fractured ends. The WOL specimens were untested weld specimens which were fabricated with crack propagation oriented along the weld direction. Capsule S received an exposure of 0.293 x 10^{19} n/cm^2; therefore, these surveillance weld specimens in Capsule B received an accumulative fluence of 3.913 x 10^{19} n/cm^2 (E > 1.0 MeV). These specimens are identified as W.

The dosimeters included iron, nickel, copper, aluminum cobalt (0.15% cobalt) and aluminum cobalt (0.15% cobalt) wires shielded with cadmium or gadolinium tubing which were incorporated into spacers. In addition, a dosimetry block with cadmium oxide-shielded neptunium (Np-237) and uranium (U-238) was included to measure the integrated flux at specific neutron energy levels.

Thermal monitors comprised of low melting-point eutectic alloy specimens were also included in the capsule. These thermal monitors were used to define the maximum temperature attained by the test specimens during irradiation. The composition of the two eutectic alloys and their melting points are as follows:

2.5% Ag, 97.5% Pb	Melting point: 579°F (304°C)
1.75% Ag, 0.75% Sn, 97.5% Pb	Melting point: 590°F (310°C)

The chemical composition and the heat treatment of the various mechanical specimens in Capsule B are presented in Table 4-1 and Table 4-2, respectively. The arrangement of the surveillance capsules in the Diablo Canyon Unit 1 reactor vessel is shown in Figure 4-1. The arrangement of the various specimens, dosimeters, and thermal monitors contained in Capsule B is shown in Figure 4-2.

Table 4-1 Chemical Composition (wt. %) of the Diablo Canyon Unit 1 Reactor Vessel Surveillance Materials (Unirradiated)(1)

Element	Lower Shell Plate B4107-1	Surrogate Weld (Heat # 27204)	Surveillance Weld (Heat # 27204)	Correlation Monitor Material Plate HSST02	
				Ladle	Check
C	0.250	0.130	0.14	0.22	0.22
S	0.014	0.009	0.025	0.019	0.018
N	---	0.013	0.009	---	---
Co	---	0.011	0.001(2)	---	---
Cu	0.130	0.220	0.198(3)	---	0.14
Si	0.024	0.210	0.45	0.22	0.25
Mo	0.480	0.540	0.48	0.53	0.52
Ni	0.560	1.000	0.999(3)	0.62	0.68
Mn	1.360	1.230	1.36	1.45	1.48
Cr	---	0.050	0.06	---	---
V	---	0.002	0.001	---	---
P	0.011	0.014	0.016	0.011	0.012
Al	---	0.002	0.018	---	---
Sn	---	0.004	0.01	---	---
B	---	0.0002	0.003(2)	---	---
Nb	---	0.010(2)	---	---	---
Ti	---	0.010(2)	0.01	---	---
W	---	0.020	---	---	---
As	---	0.020	0.016	---	---
Zr	---	0.002	0.03	---	---
Zn	---	---	0.056	---	---
Sb	---	---	0.003	---	---

Notes:

1. Data for surveillance weld and CMM obtained from WCAP-8465 [2]. Data for Lower Shell Plate B4107-1 and surrogate weld obtained from WCAP-13440 [16].
2. Not detected; numbers represent the minimum limit of detection.
3. Defined as the Cu and Ni chemistry content of the surveillance weld in WCAP-15958 [13]. Represents the average of the measured Cu and Ni content from WCAP-8465 [2] (baseline), WCAP-11567 [23] (Capsule S), and WCAP-13750 [24] (Capsule Y).

Table 4-2 Heat Treatment History of the Diablo Canyon Unit 1 Supplemental Reactor Vessel Surveillance Program Materials(1)

Material	Temperature (°F)	Time (hrs.)	Coolant
Lower Shell Plate B4107-1	1550 - 1650	4	Water quenched
	1225 ± 25	4	Air cooled
	1150 ± 25	40(2)	Furnace cooled to 600°F
CMM HSST02 Plate	1675 ± 25	4	Air cooled
	1600 ± 25	4	Water quenched
	1225 ± 25	4	Furnace cooled
	1150 ± 25	40	Furnace cooled to 600°F
Surrogate Weld (Heat # 27204)	1100 - 1175	40-3/4	---

Notes:

1. Data obtained from WCAP-13440 [16] and duplicated herein for completeness.
2. Per WCAP-13440 [16], records documenting the heat treatment of the archived plate could not be located. It is known that some pieces were post weld heat treated at 1150°F for 40 hours. In order to claim, with certainty, that the archive plate received a heat treatment similar to the reactor vessel, the plate was heat treated at 1150°F for 20 hours. This represents a compromise that should provide acceptable properties whether or not the plate had already been post weld heat treated.

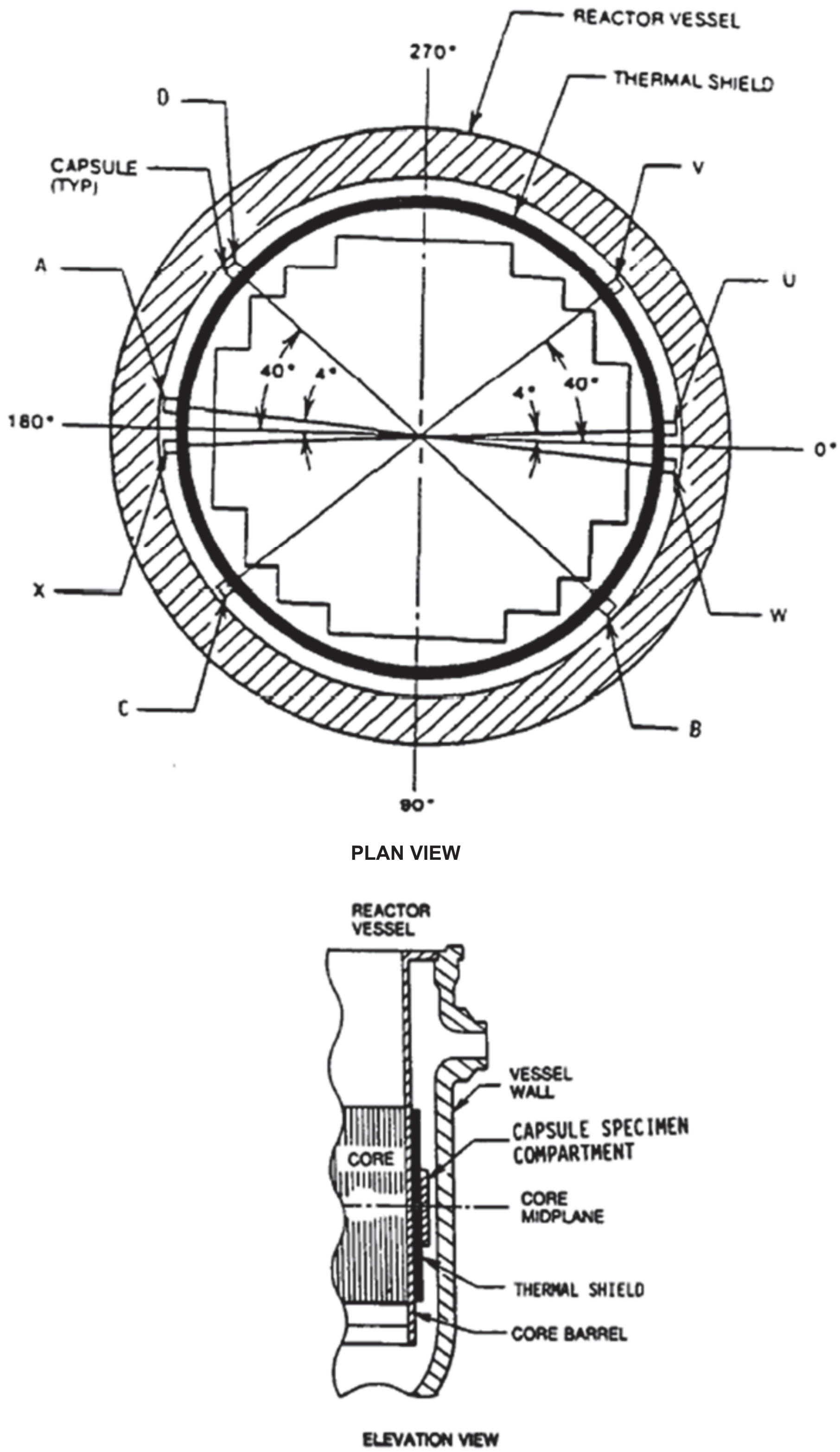

Figure 4-1 Location of Surveillance Capsules in the Diablo Canyon Unit 1 Reactor Vessel

LEGEND:			
	W	–	WELD METAL FROM CAPSULE S (HEAT # 27204)
	SW	–	SURROGATE WELD (HEAT # 27204)
	AT, BT, & CT	–	LOWER SHELL PLATE B4107-1 (TRANSVERSE)
	DT & ET	–	CORRELATION MONITOR MATERIAL
	WW, W8B, W9B & 72WP	–	EPRI SPECIMENS
	BTOP, BMID, & BBOT	–	DOSIMETRY WIRE AND THERMAL MONITOR SPACERS

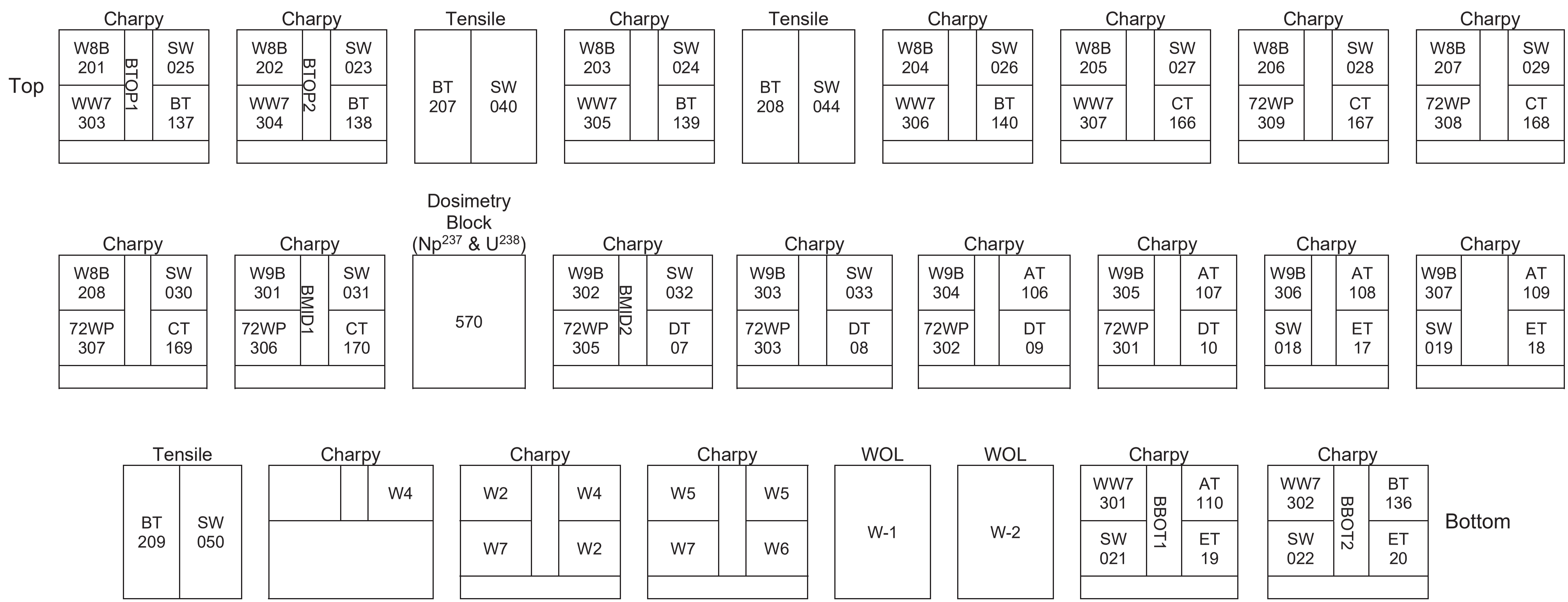

Figure 4-2 Diablo Canyon Unit 1 Surveillance Capsule B Specimen Locations per WCAP-13440

5 TESTING OF SPECIMENS FROM CAPSULE B

5.1 OVERVIEW

The post-irradiation mechanical testing of the Charpy V-notch impact specimens and tensile specimens was performed at the Westinghouse Churchill Hot Cell Facility. Testing was performed to meet the requirements of 10 CFR 50, Appendix H [9] and ASTM Specification E185-82 [10].

Capsule B was opened upon receipt at the hot cell laboratory. The specimens and spacer blocks were carefully removed, inspected for identification number, and checked against the master list in WCAP-13440 [16] and shown in Figure 4-2. All of the items were in their proper locations. The EPRI Charpy specimens were inventoried but not tested, as EPRI currently has no plans for testing them due to their insufficient accumulated fluence for long-term operation industry evaluations.

The temperature monitors were removed from the capsule compartments and were photographed and visually examined for evidence of melting. Visual examination revealed no definitive evidence indicating that the capsule experienced temperatures in excess of 579°F.

The Charpy blanks, which were originally broken Charpy specimens from Capsule S, were reconstituted into V-notch Charpy specimens according to ASTM E-23. Before starting the reconstitution process, these blanks (W2, W2, W4, W4, W5, W5, W6, W7 and W7)[1] were etched with a solution of 5% Nital along their length, until the weld microstructure was revealed. Only four (4) out of nine (9) blanks had enough weld material to be reconstituted into Charpy V-notch specimens (W2, W4, W5, and W7). The five (5) unsatisfactory specimens (W2, W4, W5, W6, and W7) were placed in storage. To increase the number of specimens for testing, four (4) new Charpy blanks were machined from the two WOL specimens (W-1 and W-2) present in Capsule B. These WOL specimens were also surveillance weld specimens from Capsule S. These blanks (W11, W12, W21, and W22) were reconstituted according to ASTM E1253. Remnants of W-1 and W-2 were retained.

Charpy V-notch testing was performed per ASTM E185-16 [6] and ASTM E23-18 [11] on a Tinius-Olsen Model 74, with 359J capacity impact test machine. The Charpy machine striker was instrumented with an Instron®[2] Dynatap Impulse system. Instrumented testing and calibration were performed to ASTM E2298-18 [12].

The instrumented striker load signal data acquisition rate was 819 kHz with data acquired for 10 ms. From the load-time curve, the general yield load (F_{gy}), the maximum load (F_m), and the time to maximum load were determined. Under some test conditions, a sharp drop in load, indicative of fast fracture, was observed. The load at which fast fracture was initiated is identified as the load at brittle fracture initiation/load at initiation of unstable crack propagation (F_{bf}). The termination load after the fast load drop is identified as

1 The specimens IDs contains repeats because these represent the 2 pieces resulting after testing the original specimen.

2 Instron® is a registered trademark of Instron Corporation. Other product and company names used herein are trademarks or trade names of their respective companies.

the arrest load/load at end of unstable crack propagation (F_a). F_{gy}, F_m, F_{bf}, and F_a were determined per the guidance in ASTM E2298-18 [12].

The maximum load energy (W_m) was determined by integrating the load-time record to the maximum load point via the instrumented Charpy software. The maximum load energy is approximately equivalent to the energy required to initiate a crack in the specimen. The integrated total impact energy (W_t) is compared to the absorbed energy measured from the dial energy (KV).

Percent shear was determined from post-fracture photographs using the ratio-of-areas method in compliance with ASTM E23-18 [11]. The lateral expansion was measured using a dial gauge rig similar to that shown in the same ASTM Standard.

Tensile tests were performed on a 250 kN capacity Instron® screw driven tensile machine (Model 5985) equipped with Instron Bluehill 3 Software and an Instron 22.48 kip load cell per ASTM E185-16 [6]. Testing met ASTM E8/E8M-16a [14] for room temperature or ASTM E21-17 [15] for elevated temperatures.

The tensile specimens were, nominally, 2.165 – 0.002 inches long with a 0.904 + 0.002-inch gauge section and a reduced section of 0.960 inches long by 0.226 ± 0.001 inches in diameter, as noted in WCAP-13440 [16]. Strain measurements were made using an extensometer (equipped with a Columbia Research Labs LVDT), which was attached to the 1.00-inch gauge section of the tensile specimen. The strain rate (crosshead speed controlled) obtained met the requirements of ASTM E8/E8M-16a [14] and ASTM E21-17 [15].

Elevated test temperatures were obtained with a three-zone electric resistance split-tube Instron SF-16 furnace with an 11-inch hot zone with an Instron Temperature Control System 3203 controller. For the elevated temperature tests, two Type-N thermocouples were placed in contact with the specimens on both ends of the gauge-length section of the specimen per ASTM E21-17 [15], Section 9.4.3. Tensile specimens were soaked at temperature (± 5ºF) for a minimum of 20 minutes before testing. All testing was conducted in air.

The yield load, ultimate load, fracture load, uniform elongation, and elongation at fracture were determined directly from the load-extension curve. The yield strength (0.2% offset method), ultimate tensile strength, and fracture strength were calculated using the original cross-sectional area. Yield point elongation (YPE) was calculated as the difference in strain between the upper yield strength and the onset of uniform strain hardening using the methodology described in ASTM E8/E8M-16a [14]. The final diameter and final gauge length were determined from post-fracture photographs. This final diameter measurement was used to calculate the fracture stress (fracture true stress) and the percent reduction in area. The final and original gauge lengths were used to calculate total elongation after fracture. The reported total elongation is the elongation at fracture.

All testing equipment was calibrated per Westinghouse procedures and in accordance with the ASTM standards cited herein. Records of calibration are available at Westinghouse.

5.2 CHARPY V-NOTCH IMPACT TEST RESULTS

The results of the Charpy V-notch impact tests performed on the various materials contained in Capsule B are presented in Table 5-1 through Table 5-8 and are compared with the unirradiated and previously withdrawn capsule results as shown in Figure 5-1 through Figure 5-12. The unirradiated capsule results were taken from WCAP-8465 [2] for the CMM and the surveillance weld, and from WCAP-13440 [16] for Lower Shell Plate B4107-1 and the surrogate weld. Results from the previous capsules were obtained from WCAP-15958 [13]. The data from the previous capsules, along with the original program unirradiated material data, were reevaluated using CVGRAPH, Version 6.02.

The transition temperature increases and decreases in upper-shelf energies for the Capsule B materials are summarized in Table 5-9 and led to the following results:

- Irradiation of the reactor vessel Lower Shell Plate B4107-1 Charpy specimens, oriented with the longitudinal axis of the specimen parallel to the major surfaces of the plate and normal to the major working direction (transverse orientation), resulted in an irradiated 30 ft-lb transition temperature of 155.2°F and an irradiated 50 ft-lb transition temperature of 177.9°F. This corresponds to a 30 ft-lb transition temperature increase of 136.9°F and a 50 ft-lb transition temperature increase of 115.2°F for the transversely oriented specimens.

- Irradiation of the surveillance program surrogate weld (Heat # 27204) Charpy specimens resulted in an irradiated 30 ft-lb transition temperature of 201.5°F and an irradiated 50 ft-lb transition temperature of 282.7°F. This corresponds to a 30 ft-lb transition temperature increase of 242.6°F and a 50 ft-lb transition temperature increase of 288.9°F.

- Irradiation of the surveillance program weld (Heat # 27204) Charpy specimens resulted in an irradiated 30 ft-lb transition temperature of 243.7°F and an irradiated 50 ft-lb transition temperature of 375.0°F. This corresponds to a 30 ft-lb transition temperature increase of 308.7°F and a 50 ft-lb transition temperature increase of 400.0°F.

- Irradiation of the CMM Plate HSST02 Charpy specimens resulted in an irradiated 30 ft-lb transition temperature of 210.8°F and an irradiated 50 ft-lb transition temperature of 253.7°F. This corresponds to a 30 ft-lb transition temperature increase of 163.8°F and a 50 ft-lb transition temperature increase of 175.7°F for the CMM specimens.

- The average upper-shelf energy of Lower Shell Plate B4107-1 (transverse orientation) resulted in an average energy decrease of 14.6 ft-lb after irradiation. This decrease results in an irradiated average upper-shelf energy of 98.0 ft-lb for the transversely oriented specimens.

- The average upper-shelf energy of the surrogate weld (Heat # 27204) resulted in an average energy decrease of 45.7 ft-lb after irradiation. This decrease results in an irradiated average upper-shelf energy of 58.6 ft-lb for the surrogate weld specimens.

- The average upper-shelf energy of the weld (Heat # 27204) resulted in an average energy decrease of 37.6 ft-lb after irradiation. This decrease results in an irradiated average upper-shelf energy of 50.0 ft-lb for the weld specimens.

- The average upper-shelf energy of the CMM resulted in an average energy decrease of 37.4 ft-lb after irradiation. This decrease results in an irradiated average upper-shelf energy of 83.0 ft-lb for the CMM specimens.

- Comparisons of the measured 30 ft-lb shift in transition temperature values and upper-shelf energy decreases to those predicted by Regulatory Guide 1.99, Rev. 2 [1] for the Diablo Canyon Unit 1 reactor vessel surveillance materials are presented in Table 5-10.

The fracture appearance of each irradiated Charpy specimen from the various materials is shown in Figure 5-13 through Figure 5-16. The fractures show an increasingly ductile or tougher appearance with increasing test temperature. Load-time records for the individual instrumented Charpy specimens are contained in Appendix B.

5.3 TENSILE TEST RESULTS

The results of the tensile tests performed on the various materials contained in Capsule B irradiated to 3.62×10^{19} n/cm^2 (E > 1.0 MeV) are presented in Table 5-11 and are compared with unirradiated results as shown in Figure 5-17 and Figure 5-18. Since 10 CFR 50, Appendix H only requires tensile testing at room and service temperature, only 2 of the 3 tensile specimens for each material were tested, with the remaining specimen being placed in storage.

The results of the tensile tests performed on Lower Shell Plate B4107-1 (transverse orientation) indicated that irradiation to 3.62×10^{19} n/cm^2 (E > 1.0 MeV) caused increases in the 0.2 percent offset yield strength and the ultimate tensile strength when compared to unirradiated data in WCAP-13440 [16]. See Figure 5-17.

The results of the tensile tests performed on the surrogate weld (Heat # 27204), indicated that irradiation to 3.62×10^{19} n/cm^2 (E > 1.0 MeV) caused increases in the 0.2 percent offset yield strength and the ultimate tensile strength when compared to unirradiated data in WCAP-13440 [16]. See Figure 5-18.

The fractured tensile specimens for Lower Shell Plate B4107-1 (transverse orientation) material are shown in Figure 5-19 and the fracture tensile specimens for the surrogate weld are shown in Figure 5-20. The engineering stress-strain curves for the tensile tests are shown in Figure 5-21 through Figure 5-24.

Table 5-1 Charpy V-notch Data for the Diablo Canyon Unit 1 Capsule B Lower Shell Plate B4107-1 Irradiated to a Fluence of 3.62 x 10^{19} n/cm^2 (E > 1.0 MeV)

Specimen ID	Temperature		Impact Energy		Lateral Expansion		Shear
	°F	°C(1)	ft-lb	Joules(1)	mils	mm(1)	%
AT106	74	23	14	19	12	0.30	5
BT140	100	38	19	26	20	0.51	10
AT107	125	52	19	26	20	0.51	10
AT109	150	66	24	33	22	0.56	15
CT170	160	71	29	39	30	0.76	15
AT110	180	82	33	45	31	0.79	20
CT166	190	88	68	92	47	1.19	50
BT137	190	88	80	108	51	1.30	50
BT139	200	93	61	83	48	1.22	40
BT136	210	99	76	103	56	1.42	55
CT169	225	107	92	125	64	1.63	70
CT167	250	121	93	126	76	1.93	90
BT138	300	149	98	133	74	1.88	100
CT168	350	177	102	138	78	1.98	100
AT108	375	191	94	127	77	1.96	100

Note:

(1) Calculated conversion values.

Table 5-2 Charpy V-notch Data for the Diablo Canyon Unit 1 Capsule B Surrogate Weld (Heat # 27204) Irradiated to a Fluence of 3.62 x 10^{19} n/cm^2 (E > 1.0 MeV)

Specimen ID	Temperature		Impact Energy		Lateral Expansion		Shear
	°F	°C(1)	ft-lb	Joules(1)	mils	mm(1)	%
SW027	125	52	12	16	8	0.20	5
SW031	150	66	17	23	15	0.38	20
SW019	180	82	17.5	24	15	0.38	40
SW033	190	88	33	45	24	0.61	45
SW025	200	93	28	38	24	0.61	55
SW022	210	99	30	41	24	0.61	60
SW030	225	107	44	60	40	1.02	85
SW026	225	107	37	50	27	0.69	85
SW023	250	121	40	54	28	0.71	80
SW028	275	135	43	58	36	0.91	90
SW024	300	149	53	72	43	1.09	98
SW018	325	163	55	75	42	1.07	100
SW029	350	177	61	83	53	1.35	100
SW032	375	191	63	85	46	1.17	100
SW021	400	204	61	83	49	1.24	100

Note:

(1) Calculated conversion values.

Table 5-3 Charpy V-notch Data for the Diablo Canyon Unit 1 Capsule B Surveillance Program CMM Irradiated to a Fluence of 3.62 x 10^{19} n/cm^2 (E > 1.0 MeV)

Specimen ID	Temperature		Impact Energy		Lateral Expansion		Shear
	°F	°C(1)	ft-lb	Joules(1)	mils	mm(1)	%
DT08	160	71	11	15	7	0.18	10
ET17	180	82	16	22	13	0.33	15
ET19	200	93	31	42	23	0.58	35
ET20	225	107	40	54	28	0.71	40
DT09	250	121	41	56	38	0.97	40
ET18	275	135	62	84	49	1.24	60
DT07	300	149	65	88	70	1.78	80
DT10	350	177	83	113	62	1.57	95

Note:

(1) Calculated conversion values.

Table 5-4 Charpy V-notch Data for the Diablo Canyon Unit 1 Capsule B Surveillance Program Reconstituted Surveillance Weld Irradiated to a Fluence of 3.913 x 10^{19} n/cm^2 (E > 1.0 MeV)

Specimen ID	Temperature		Impact Energy		Lateral Expansion		Shear
	°F	°C(1)	ft-lb	Joules(1)	mils	mm(1)	%
W11	180	82	20	27	14	0.36	30
W4	210	99	25.5	35	15	0.38	40
W5	240	116	25	34	19	0.48	45
W22	250	121	29	39	23	0.58	50
W12	260	127	26.5	36	18	0.46	50
W21	280	138	35	47	30	0.76	70
W7	300	149	53	72	46	1.17	91
W2	375	191	50	68	47	1.19	100

Note:

(1) Calculated conversion values.

Table 5-5 Instrumented Charpy Impact Test Results for the Diablo Canyon Unit 1 Capsule B Lower Shell Plate B4107-1 Irradiated to a Fluence of 3.62 x 10^{19} n/cm^2 (E > 1.0 MeV)

Specimen ID	Test Temp (°F)	Total Dial Energy, KV (ft-lb)	Total Instrumented Energy, W_t (ft-lb)	Difference, (KV-W_t)/KV (%)	Energy to Max Load, W_m (ft-lb)	Maximum Load, F_m (lb)	Time to F_m (msec)	General Yield Load, F_{gy} (lb)	Brittle Fracture Load, F_{bf} (lb)	Arrest Load, F_a (lb)
AT106	74	14	12.4	12	9.5	4102	0.19	3112	3785	0
BT140	100	19	17.7	7	15.1	3926	0.30	3205	3662	0
AT107	125	19	18.0	6	15.7	4131	0.29	3395	4112	0
AT109	150	24	22.7	5	19.8	4297	0.36	3344	4297	200
CT170	160	29	28.6	1	18.7	4064	0.36	3184	3632	400
AT110	180	33	29.6	10	19.5	4234	0.36	3288	4138	600
CT166	190	68	66.4	2	35.0	4262	0.61	3349	4124	2000
BT137	190	80	77.9	3	35.6	4390	0.61	3356	4218	2700
BT139	200	61	56.9	7	34.5	4226	0.61	3296	4181	2000
BT136	210	76	73.1	4	35.4	4333	0.6	3263	4240	2200
CT169	225	92	89.8	2	35.1	4309	0.61	3258	3300	2800
CT167	250	93	89.8	3	36.2	4207	0.60	2829	--	--
BT138	300	98	95.2	3	33.8	4093	0.61	2938	--	--
CT168	350	102	100.3	2	33.3	4033	0.61	3207	--	--
AT108	375	94	92.5	2	33.4	4063	0.61	3126	--	--

Table 5-6 Instrumented Charpy Impact Test Results for the Diablo Canyon Unit 1 Capsule B Surrogate Weld Irradiated to a Fluence of 3.62 x 10^{19} n/cm^2 (E >1.0 MeV)

Specimen ID	Test Temp (°F)	Total Dial Energy, KV (ft-lb)	Total Instrumented Energy, W_t (ft-lb)	Difference, $(KV-W_t)/KV$ (%)	Energy to Max Load, W_m (ft-lb)	Maximum Load, F_m (lb)	Time to F_m (msec)	General Yield Load, F_{gy} (lb)	Brittle Fracture Load, F_{bf} (lb)	Arrest Load, F_a (lb)
SW027	125	12	11.5	4	10.1	4555	0.19	3808	4533	0
SW031	150	17	15.5	9	10.0	4296	0.19	3616	4207	0
SW019	180	17.5	16.0	9	9.6	4206	0.19	3264	3730	500
SW033	190	33	31.8	4	16.7	4441	0.29	3675	4191	1600
SW025	200	28	28.4	-1	16.8	4495	0.29	3588	4179	1900
SW022	210	30	29.1	3	16.8	4460	0.29	3631	4405	1900
SW030	225	44	46.2	-5	20.8	4462	0.36	3580	4130	2650
SW026	225	37	36.5	1	16.4	4294	0.29	3722	4279	2800
SW023	250	40	40.1	0	17.0	4568	0.30	3850	4137	2300
SW028	275	43	42.7	1	21.1	4462	0.36	3466	4141	3100
SW024	300	53	53.5	-1	20.7	4438	0.37	3675	--	--
SW018	325	55	52.9	4	19.8	4213	0.36	3137	--	--
SW029	350	61	60.3	1	17.4	4403	0.28	3580	--	--
SW032	375	63	62.1	1	19.9	4367	0.36	3322	--	--
SW021	400	61	59.0	3	20	4289	0.36	3304	--	--

Table 5-7 Instrumented Charpy Impact Test Results for the Diablo Canyon Unit 1 Capsule B Surveillance Program CMM Irradiated to a Fluence of 3.62 x 10^{19} n/cm^2 (E > 1.0 MeV)

Specimen ID	Test Temp (°F)	Total Dial Energy, KV (ft-lb)	Total Instrumented Energy, W_t (ft-lb)	Difference, (KV-W_t)/KV (%)	Energy to Max Load, W_m (ft-lb)	Maximum Load, F_m (lb)	Time to F_m (msec)	General Yield Load, F_{gy} (lb)	Brittle Fracture Load, F_{bf} (lb)	Arrest Load, F_a (lb)
DT08	160	11	10.4	5	3.3	3875	0.09	3409	3670	0
ET17	180	16	14.7	8	13.1	3848	0.26	3656	3818	0
ET19	200	31	31.0	0	21.2	4536	0.36	3659	4521	1700
ET20	225	40	35.9	10	20.9	4496	0.36	3616	4492	2200
DT09	250	41	40.0	2	19.9	4397	0.36	3233	4069	2000
ET18	275	62	59.0	5	20.1	4364	0.36	3348	4148	3150
DT07	300	65	64.0	2	18.5	4021	0.36	3221	3903	2600
DT10	350	83	81.7	2	20.0	4301	0.36	3299	--	--

Table 5-8 Instrumented Charpy Impact Test Results for the Diablo Canyon Unit 1 Capsule B Surveillance Program Reconstituted Surveillance Weld Irradiated to a Fluence of 3.913 x 10^{19} n/cm^2 (E > 1.0 MeV)

Specimen ID	Test Temp (°F)	Total Dial Energy, KV (ft-lb)	Total Instrumented Energy, W_t (ft-lb)	Difference, (KV-W_t)/KV (%)	Energy to Max Load, W_m (ft-lb)	Maximum Load, F_m (lb)	Time to F_m (msec)	General Yield Load, F_{gy} (lb)	Brittle Fracture Load, F_{bf} (lb)	Arrest Load, F_a (lb)
W11	180	20	18.1	9	9.6	4289	0.19	3707	4091	1300
W4	210	25.5	23.6	7	13.8	4461	0.3	3262	4227	2600
W5	240	25	23.1	8	16.0	4256	0.29	3337	4032	2300
W22	250	29	27.7	5	20.7	4329	0.36	3358	4105	2000
W12	260	26.5	25.2	5	16.4	4295	0.29	3522	3800	2500
W21	280	35	34.7	1	15.9	4169	0.29	3259	3423	2900
W7	300	53	52.3	1	19.4	4232	0.36	3260	3167	2400
W2	375	50	48.4	3	18.7	4097	0.36	3087	--	--

Table 5-9 Effect of Irradiation on the Charpy V-notch Toughness Properties of the Diablo Canyon Unit 1 Reactor Vessel Surveillance Capsule B Materials

Material	Average 30 ft-lb Transition Temperature[1] (°F)			Average 35 mil Lateral Expansion Temperature[1] (°F)			Average 50 ft-lb Transition Temperature[1] (°F)			Average Energy Absorption ≥ 95% Shear[2] (ft-lb)		
	Unirradiated	Irradiated	ΔT	Unirradiated	Irradiated	ΔT	Unirradiated	Irradiated	ΔT	Unirradiated	Irradiated	ΔE
Lower Shell Plate B4107-1	18.3	155.2	136.9	38.1	166.8	128.7	62.7	177.9	115.2	112.6	98.0	-14.6
Surrogate Weld (Heat # 27204)	-41.1	201.5	242.6	-39.6	255.3	294.9	-6.2	282.7	288.9	104.3	58.6	-45.7
Surveillance Weld[4] (Heat # 27204)	-65.0	243.7	308.7	-46.3	293.9	340.2	-25.0	375.0[3]	400	87.6	50.0	-37.6
CMM	47.0	210.8	163.8	59.1	236.2	177.1	78.0	253.7	175.7	120.4	83.0	-37.4

Notes:
1. Average value is determined by CVGRAPH (see Appendix C).
2. USE values are a calculated average from unirradiated and Capsule B Charpy test results for specimens that achieved greater than or equal to 95% shear.
3. The fitted Charpy energy curve did not attain the 50 ft-lb energy level within the evaluated temperature range; therefore, the irradiated 50 ft-lb transition temperature was set to the highest temperature which achieved a measurement of 50 ft-lb.
4. The surveillance weld specimens are reconstituted tested specimens previously irradiated in Capsule S; therefore, the fluence is the sum of the fluences of Capsule S (0.293E+19 n/cm^2) and Capsule B (3.62E+19 n/cm^2).

Table 5-10 Comparison of the Diablo Canyon Unit 1 Surveillance Material 30 ft-lb Transition Temperature Shifts and Upper-Shelf Energy Decreases with Regulatory Guide 1.99, Rev. 2, Predictions

Material	Capsule	Capsule Fluence (x 10^{19} n/cm^2, E > 1.0 MeV)	30 ft-lb Transition Temperature Shift		Upper-Shelf Energy Decrease	
			Predicted(1) (°F)	Measured(2) (°F)	Predicted(1) (%)	Measured(2) (%)
Lower Shell Plate B4107-1	B	3.62	119.8	136.9	30	13
Surrogate Weld (Heat # 27204)	B	3.62	309.5	242.6	49	44
Surveillance Welds (Heat # 27204)	S	0.293	147.7	110.1	26	8
	Y	1.07	226.5	232.0	35	31
	V	1.35	240.8	200.2	37	25
	B	3.913(3)	300.4	308.7	48	43
Correlation Monitor Material HSST02	S	0.293	67.7	65.3	18	0
	Y	1.07	103.9	116.2	25	11
	V	1.35	110.5	116.4	26	3
	B	3.62	136.1	163.8	31	31

Notes:

1. Based on Regulatory Guide 1.99, Rev. 2 [1], Position 1.1 methodology for RT_{NDT} shift or 1.2 for USE decrease, using the capsule fluence and best-estimate weight percent values of copper and nickel of the surveillance material.
2. Calculated using measured Charpy data (See Appendix C).
3. The surveillance weld specimens are reconstituted tested specimens previously irradiated in Capsule S. The fluence is the sum of the fluences of Capsule S (0.293E+19 n/cm^2) and Capsule B (3.62E+19 n/cm^2).

Table 5-11 Tensile Test Properties of the Diablo Canyon Unit 1 Capsule B Reactor Vessel Surveillance Materials Irradiated to a Fluence of 3.62 x 10^{19} n/cm^2 (E > 1.0 MeV)

Material	Specimen ID	Test Temp (°F)	0.2% Yield Strength (ksi)	Ultimate Strength (ksi)	Fracture Load (kip)	Fracture Strength (ksi)	Fracture True Stress (ksi)	Uniform Elongation (%)	Total Elongation (%)	Reduction in Area (%)
Lower Shell Plate B4107-1 (Transverse Orientation)	BT207	77	82.9	103.5	2.9	72.7	192	9.0	22.3	62
	BT208	550	73.6	95.0	3.1	78.0	132	8.1	18.2	41
Surrogate Weld (Heat # 27204)	SW040	76	103.7	117.4	3.2	79.4	210	9.4	24.8	62
	SW044	550	87.7	102.3	3.2	79.2	150	7.1	17.7	47

Lower Shell Plate B4107-1

CVGraph 6.02: Hyperbolic Tangent Curve Printed on 6/10/2026 7:43 AM

Curve	Plant	Capsule	Material	Ori.	Heat #
1	Diablo Canyon 1	Unirrad	SA533B1	TL	C3121-1
2	Diablo Canyon 1	B	SA533B1	TL	C3121-1

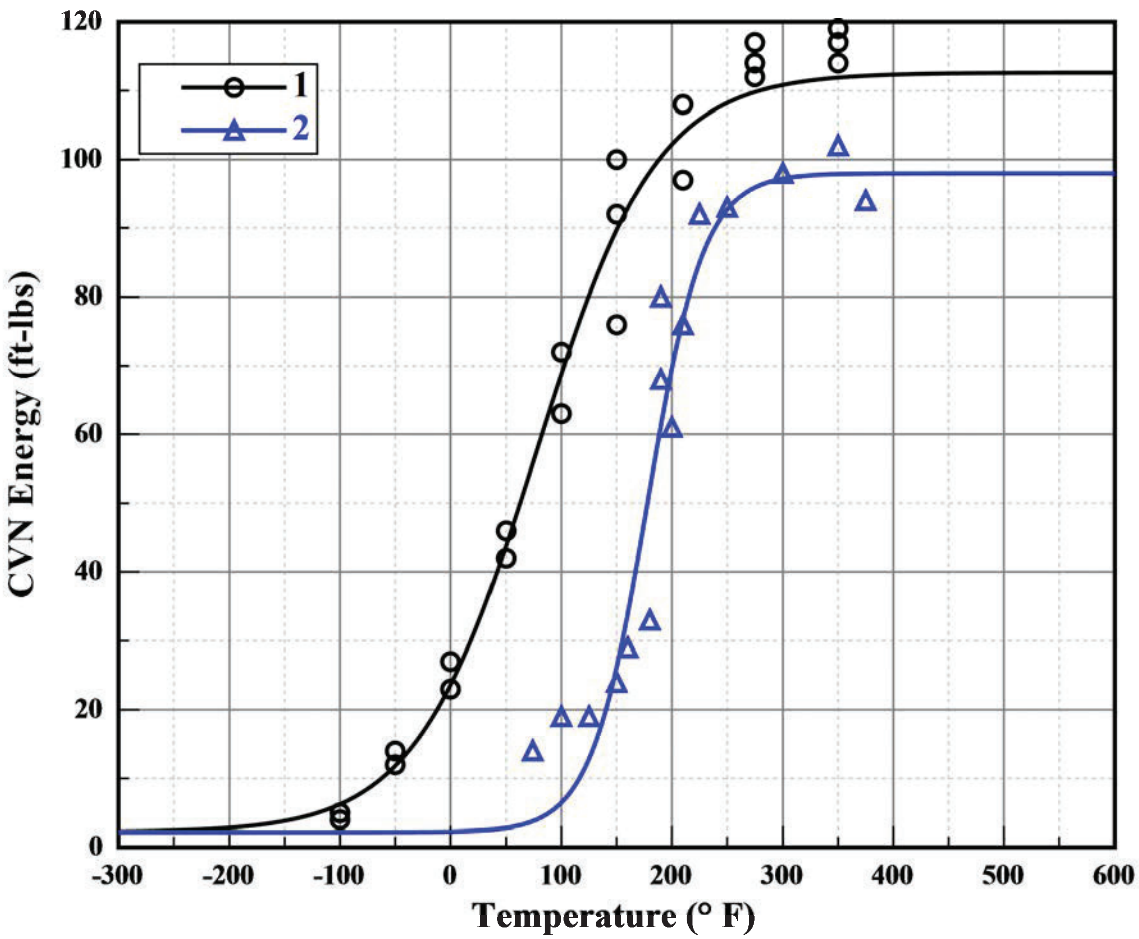

Curve	Fluence	LSE	USE	d-USE	T @30	d-T @30	T @50	d-T @50
1	0.00E+000	2.2	112.6	0	18.3	0	62.7	0
2	3.62E+019	2.2	98	-14.6	155.2	136.9	177.9	115.2

Figure 5-1 Charpy V-notch Impact Energy vs. Temperature for Diablo Canyon Unit 1 Reactor Vessel Surveillance Program Lower Shell Plate B4107-1 (Transverse Orientation)

Lower Shell Plate B4107-1

CVGraph 6.02: Hyperbolic Tangent Curve Printed on 5/29/2026 8:00 AM

Curve	Plant	Capsule	Material	Ori.	Heat #
1	Diablo Canyon 1	Unirrad	SA533B1	TL	C3121-1
2	Diablo Canyon 1	B	SA533B1	TL	C3121-1

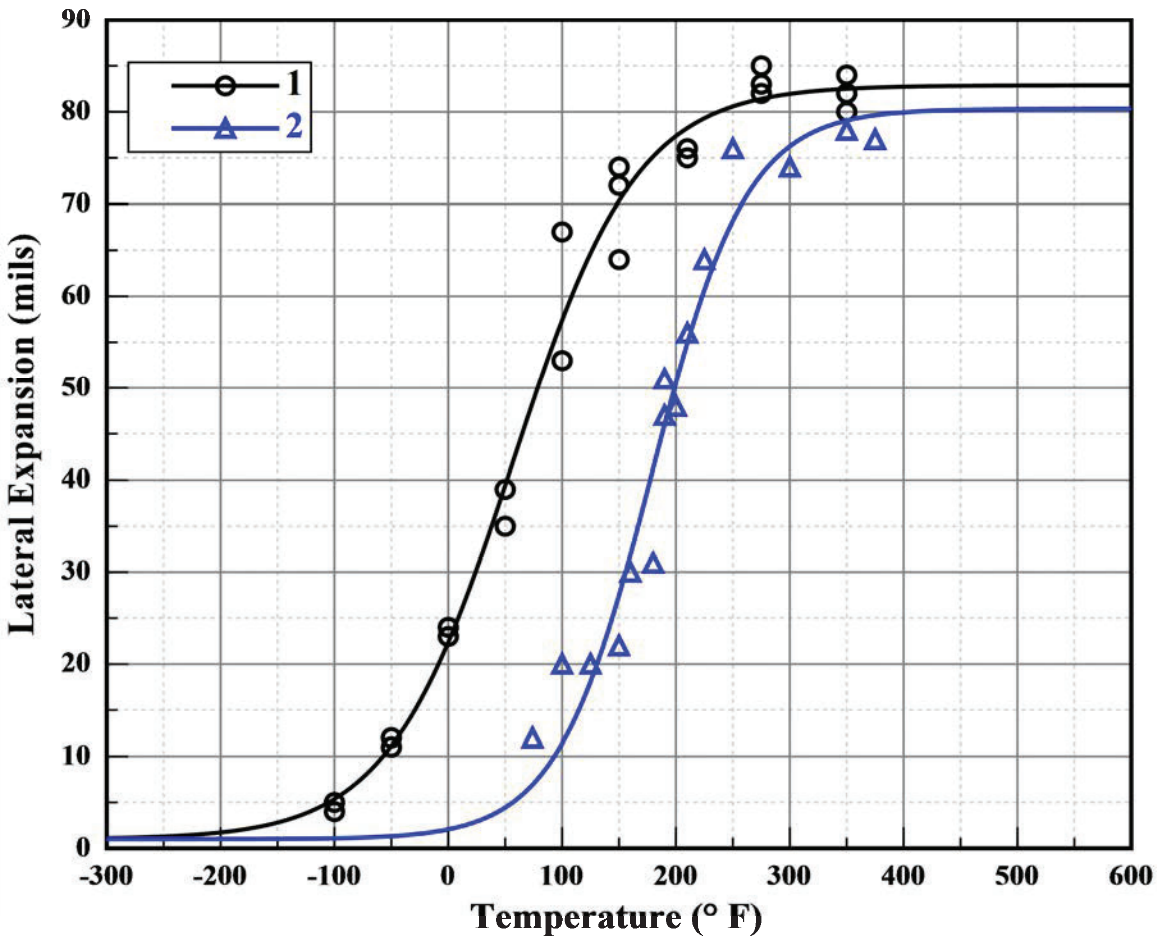

Curve	Fluence	LSE	USE	d-USE	T @35	d-T @35
1	0.00E+000	1	82.88	0	38.1	0
2	3.62E+019	1	80.33	-2.55	166.8	128.7

Figure 5-2 Charpy V-notch Lateral Expansion vs. Temperature for Diablo Canyon Unit 1 Reactor Vessel Surveillance Program Lower Shell Plate B4107-1 (Transverse Orientation)

Lower Shell Plate B4107-1

CVGraph 6.02: Hyperbolic Tangent Curve Printed on 5/29/2026 8:02 AM

Curve	Plant	Capsule	Material	Ori.	Heat #
1	Diablo Canyon 1	Unirrad	SA533B1	TL	C3121-1
2	Diablo Canyon 1	B	SA533B1	TL	C3121-1

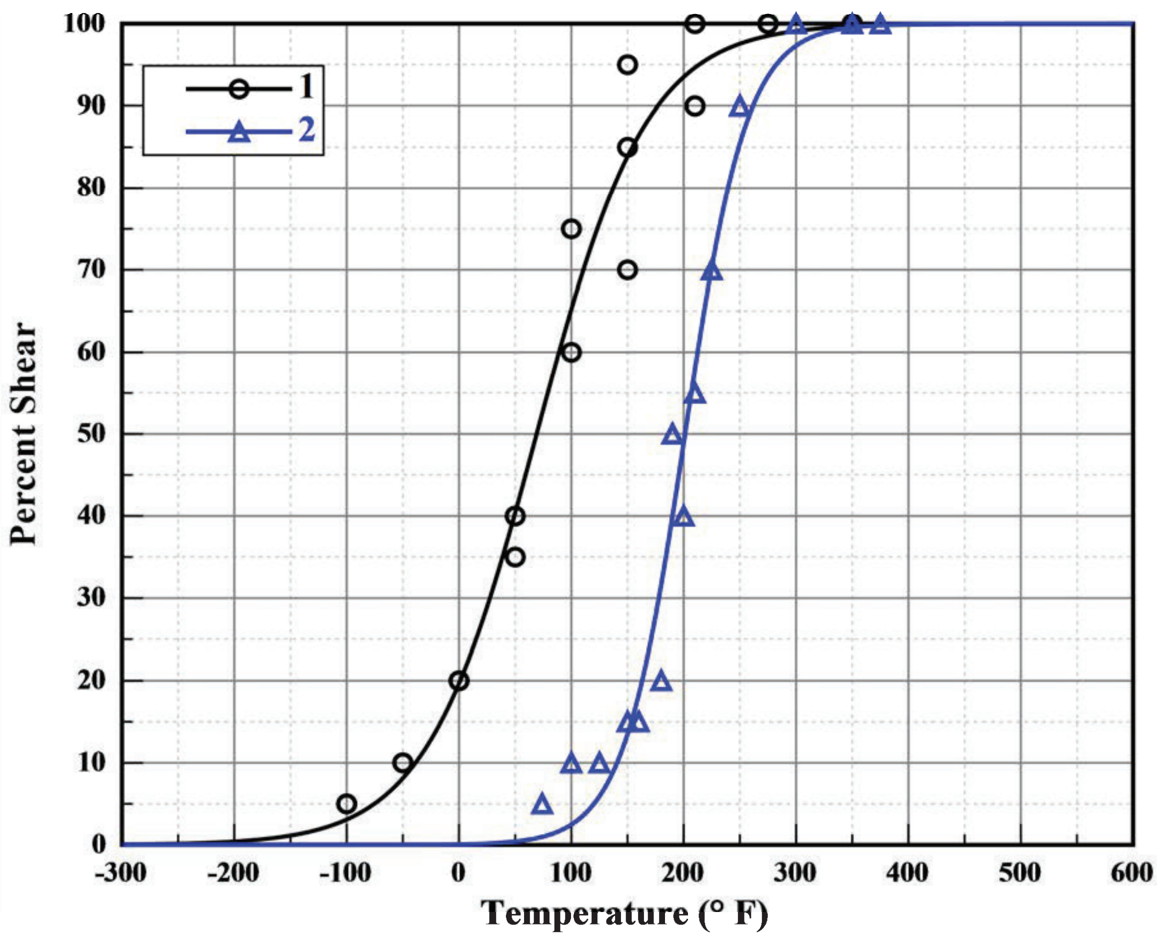

Curve	Fluence	LSE	USE	d-USE	T @50	d-T @50
1	0.00E+000	0	100	0	69.1	0
2	3.62E+019	0	100	0	201.2	132.1

Figure 5-3 Charpy V-notch Percent Shear vs. Temperature for Diablo Canyon Unit1 Reactor Vessel Surveillance Program Lower Shell Plate B4107-1 (Transverse Orientation)

Surrogate Weld (Heat # 27204)

CVGraph 6.02: Hyperbolic Tangent Curve Printed on 6/7/2026 1:23 PM

Curve	Plant	Capsule	Material	Ori.	Heat #
1	Diablo Canyon 1	Unirrad	Weld	NA	27204
2	Diablo Canyon 1	B	Weld	NA	27204

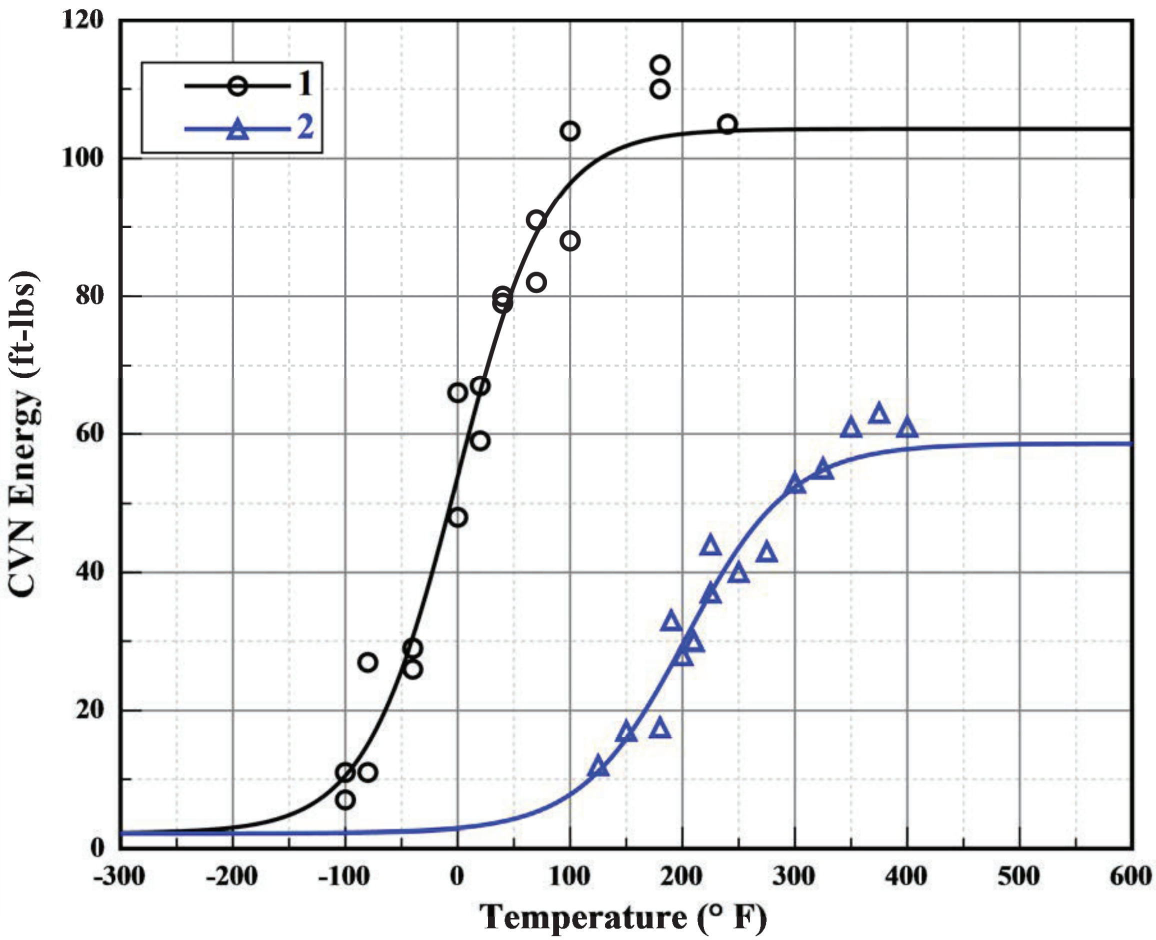

Curve	Fluence	LSE	USE	d-USE	T @30	d-T @30	T @50	d-T @50
1	0.00E+000	2.2	104.3	0	-41.1	0	-6.2	0
2	3.62E+019	2.2	58.6	-45.7	201.5	242.6	282.7	288.9

Figure 5-4 Charpy V-notch Impact Energy vs. Temperature for Diablo Canyon Unit 1 Reactor Vessel Surveillance Program Surrogate Weld

Surrogate Weld (Heat # 27204)

CVGraph 6.02: Hyperbolic Tangent Curve Printed on 6/7/2026 1:24 PM

Curve	Plant	Capsule	Material	Ori.	Heat #
1	Diablo Canyon 1	Unirrad	Weld	NA	27204
2	Diablo Canyon 1	B	Weld	NA	27204

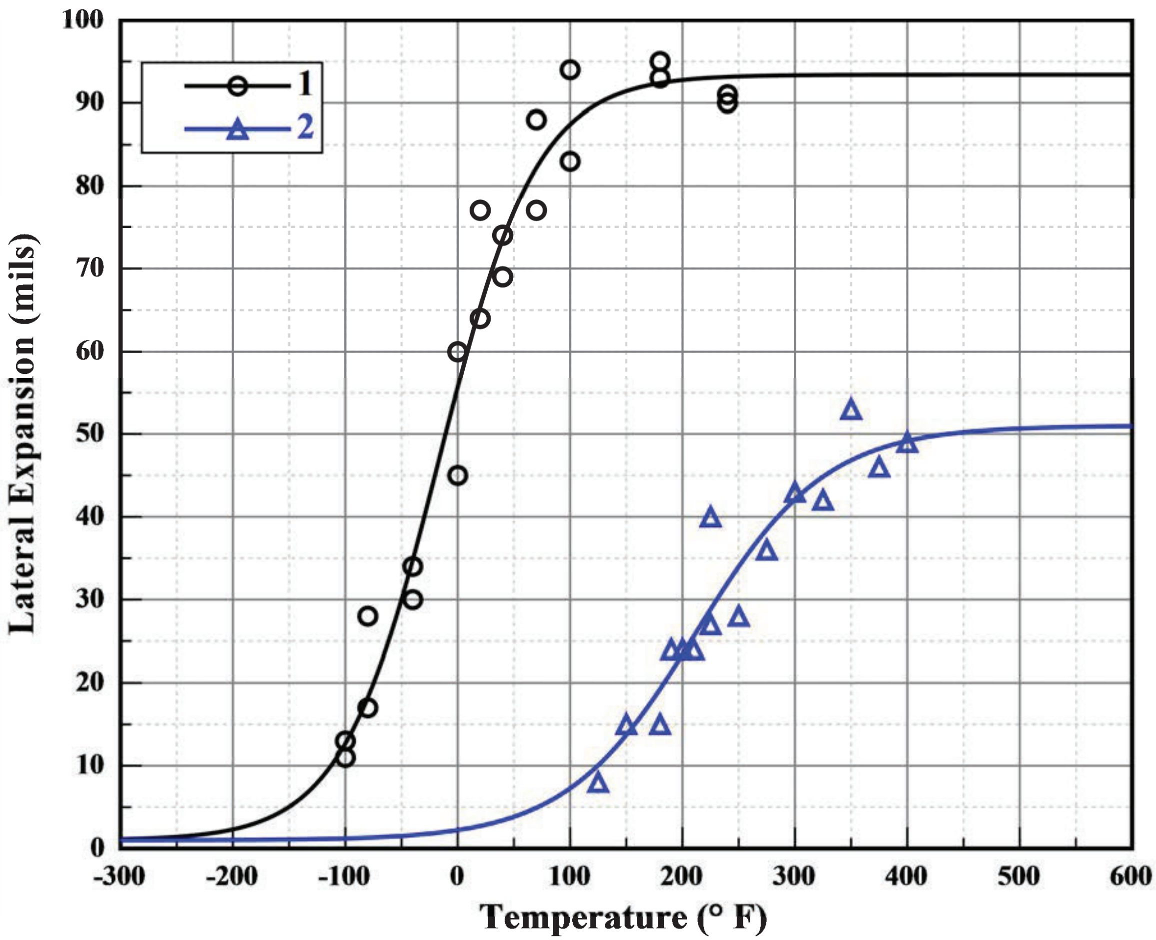

Curve	Fluence	LSE	USE	d-USE	T @35	d-T @35
1	0.00E+000	1	93.39	0	-39.6	0
2	3.62E+019	1	51	-42.39	255.3	294.9

Figure 5-5 Charpy V-notch Lateral Expansion vs. Temperature for Diablo Canyon Unit 1 Reactor Vessel Surveillance Program Surrogate Weld

Surrogate Weld (Heat # 27204)

CVGraph 6.02: Hyperbolic Tangent Curve Printed on 6/7/2026 1:25 PM

Curve	Plant	Capsule	Material	Ori.	Heat #
1	Diablo Canyon 1	Unirrad	Weld	NA	27204
2	Diablo Canyon 1	B	Weld	NA	27204

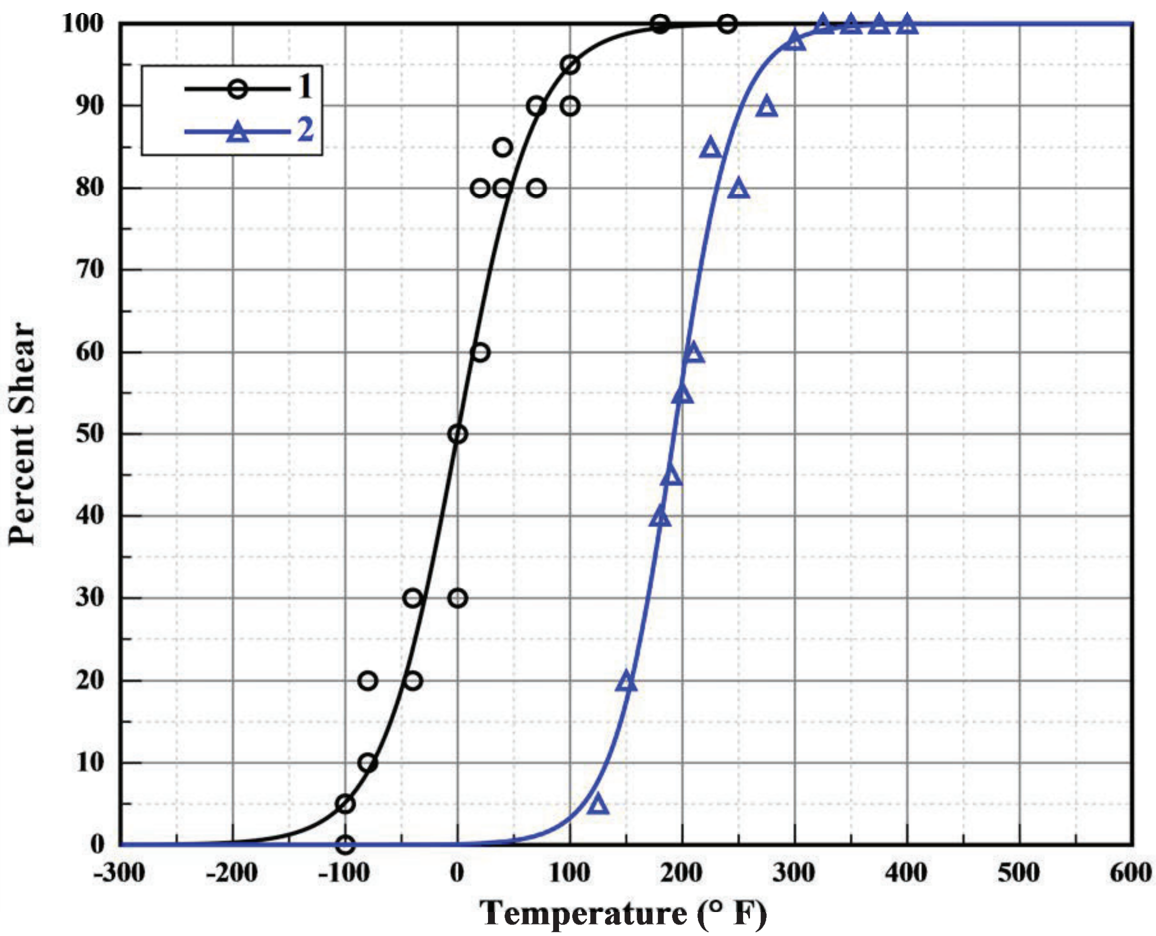

Curve	Fluence	LSE	USE	d-USE	T @50	d-T @50
1	0.00E+000	0	100	0	-0.1	0
2	3.62E+019	0	100	0	192.6	192.7

Figure 5-6 Charpy V-notch Percent Shear vs. Temperature for Diablo Canyon Unit 1 Reactor Vessel Surveillance Program Surrogate Weld

Weld Metal

CVGraph 6.02: Hyperbolic Tangent Curve Printed on 6/9/2026 4:06 AM

Curve	Plant	Capsule	Material	Ori.	Heat #
1	Diablo Canyon 1	Unirrad	Weld	NA	27204
2	Diablo Canyon 1	S	Weld	NA	27204
3	Diablo Canyon 1	Y	Weld	NA	27204
4	Diablo Canyon 1	V	Weld	NA	27204
5	Diablo Canyon 1	B	Weld	NA	27204

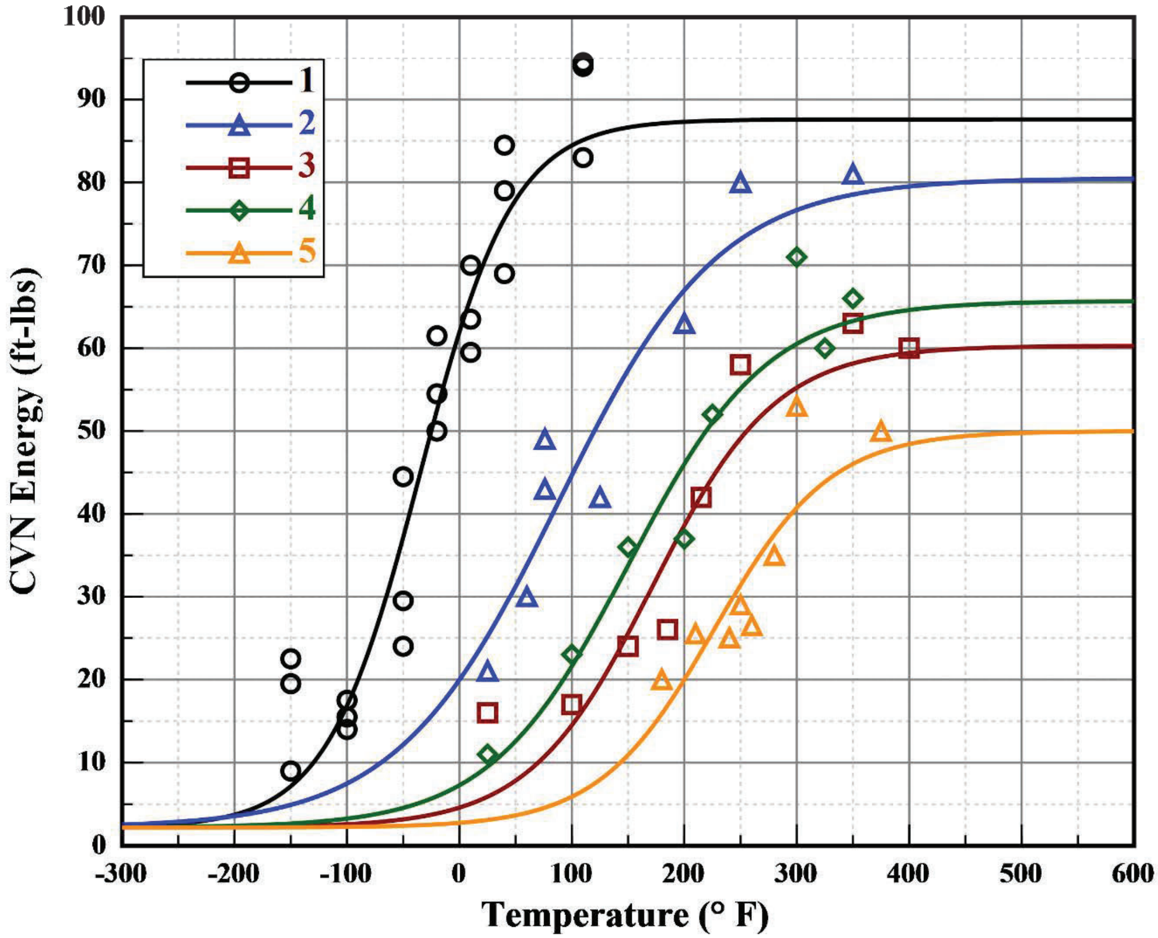

Figure 5-7 Charpy V-notch Impact Energy vs. Temperature for Diablo Canyon Unit 1 Reactor Vessel Surveillance Program Surveillance Welds

Weld Metal

CVGraph 6.02: Hyperbolic Tangent Curve Printed on 6/9/2026 4:06 AM

Curve	Fluence	LSE	USE	d-USE	T @30	d-T @30	T @50	d-T @50
1	0.00E+000	2.2	87.6	0	-65	0	-25	0
2	2.93E+018	2.2	80.5	-7.10	45.1	110.1	120	145
3	1.07E+019	2.2	60.3	-27.3	167	232	255.6	280.6
4	1.35E+019	2.2	65.7	-21.9	135.2	200.2	219.3	244.3
5	3.91E+019	2.2	50	-37.6	243.7	308.7	0 (1)	25

Note:
1. The fitted Charpy energy curve did not attain the 50 ft lb energy level within the evaluated temperature range; therefore, the irradiated 50 ft lb transition temperature was set to the highest temperature which achieved a measurement of 50 ft-lb.

Figure 5-7 Charpy V-notch Impact Energy vs. Temperature for Diablo Canyon Unit 1 Reactor Vessel Surveillance Program Surveillance Welds (cont.)

Weld Metal

CVGraph 6.02: Hyperbolic Tangent Curve Printed on 6/9/2026 4:08 AM

Curve	Plant	Capsule	Material	Ori.	Heat #
1	Diablo Canyon 1	Unirrad	Weld	NA	27204
2	Diablo Canyon 1	S	Weld	NA	27204
3	Diablo Canyon 1	Y	Weld	NA	27204
4	Diablo Canyon 1	V	Weld	NA	27204
5	Diablo Canyon 1	B	Weld	NA	27204

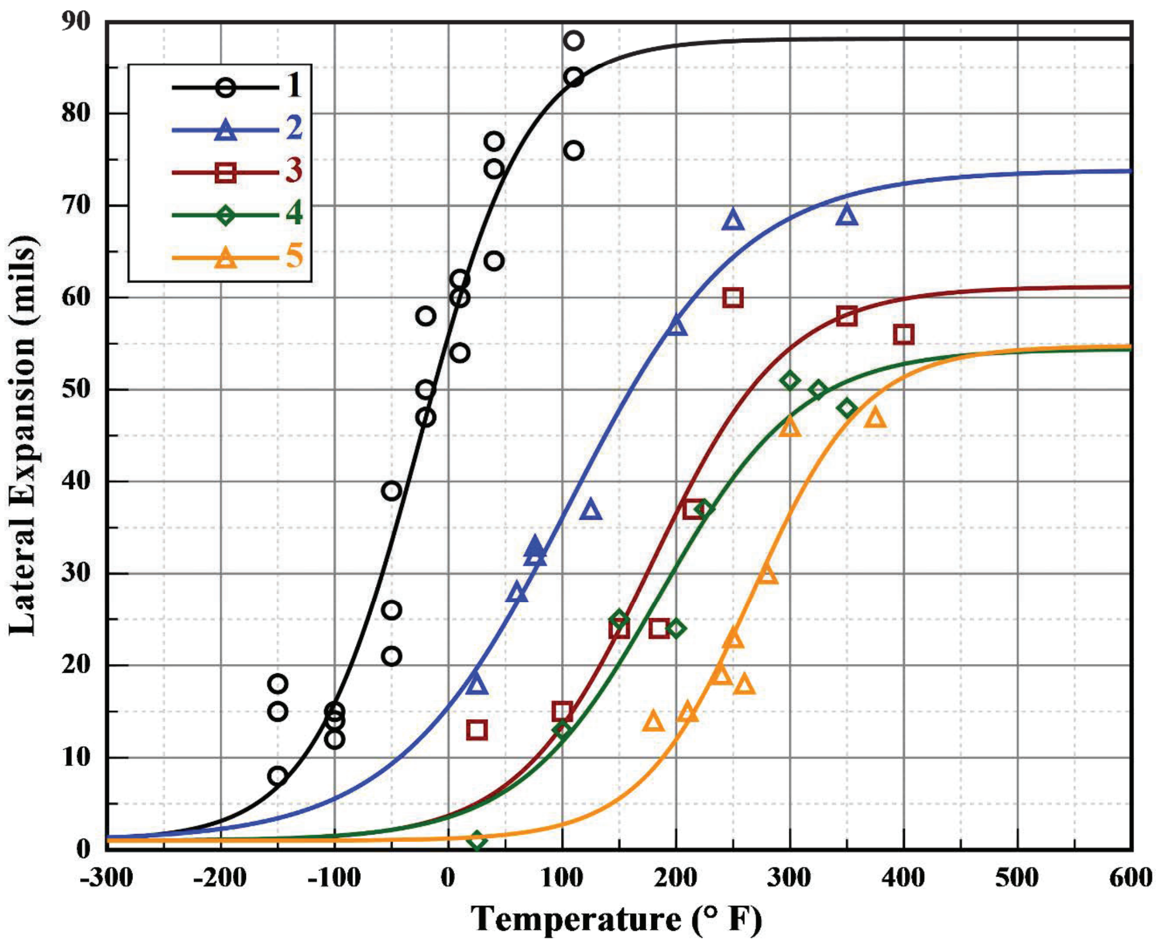

Figure 5-8 Charpy V-notch Lateral Expansion vs. Temperature for Diablo Canyon Unit 1 Reactor Vessel Surveillance Program Surveillance Welds

Weld Metal

CVGraph 6.02: Hyperbolic Tangent Curve Printed on 6/9/2026 4:08 AM

Curve	Fluence	LSE	USE	d-USE	T @35	d-T @35
1	0.00E+000	1	88.2	0	-46.3	0
2	2.93E+018	1	73.86	-14.34	95.5	141.8
3	1.07E+019	1	61.2	-27	193.9	240.2
4	1.35E+019	1	54.43	-33.77	220.6	266.9
5	3.91E+019	1	54.75	-33.45	293.9	340.2

Figure 5-8 Charpy V-notch Lateral Expansion vs. Temperature for Diablo Canyon Unit 1 Reactor Vessel Surveillance Program Surveillance Welds (cont.)

Weld Metal

CVGraph 6.02: Hyperbolic Tangent Curve Printed on 6/9/2026 4:11 AM

Curve	Plant	Capsule	Material	Ori.	Heat #
1	Diablo Canyon 1	Unirrad	Weld	NA	27204
2	Diablo Canyon 1	S	Weld	NA	27204
3	Diablo Canyon 1	Y	Weld	NA	27204
4	Diablo Canyon 1	V	Weld	NA	27204
5	Diablo Canyon 1	B	Weld	NA	27204

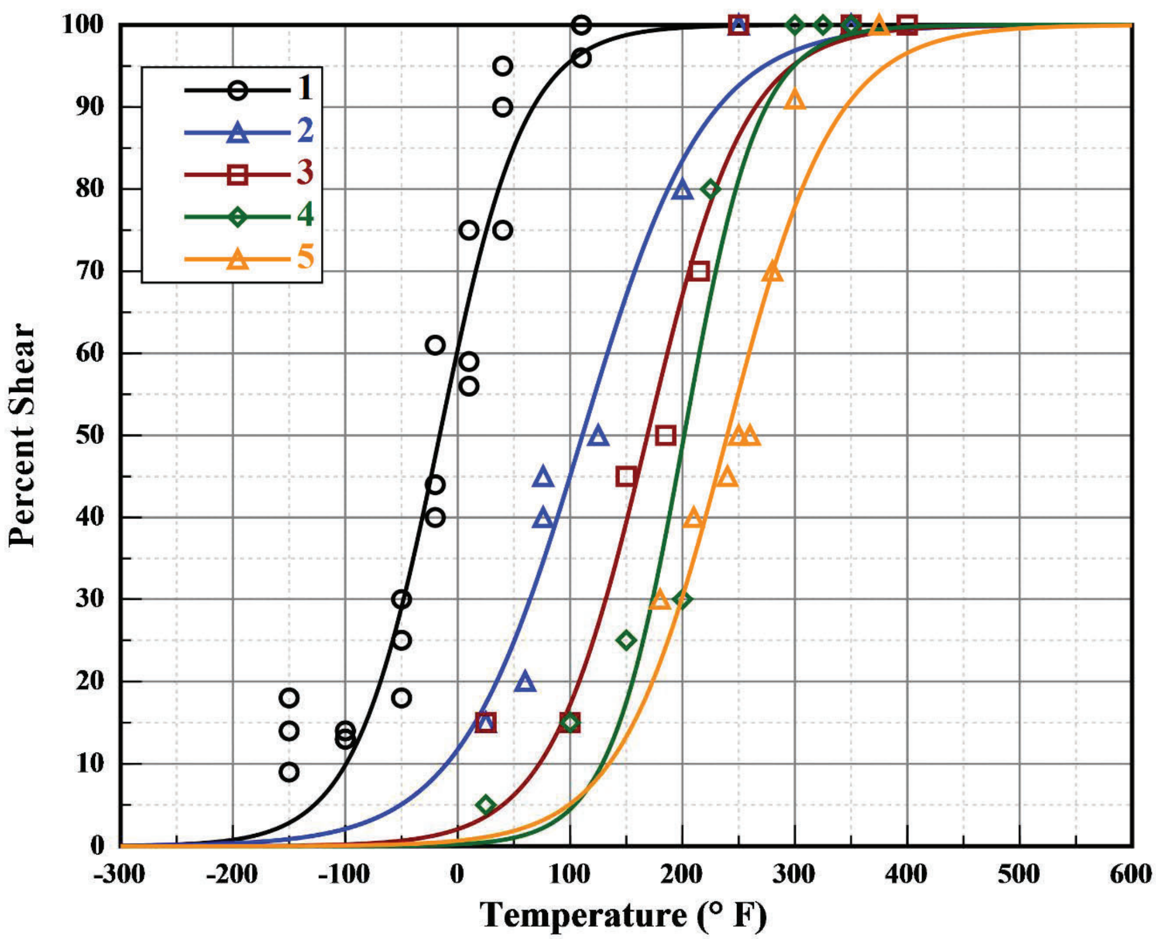

Figure 5-9 Charpy V-notch Percent Shear vs. Temperature for Diablo Canyon Unit 1 Reactor Vessel Surveillance Program Surveillance Welds

Weld Metal

CVGraph 6.02: Hyperbolic Tangent Curve Printed on 6/9/2026 4:11 AM

Curve	Fluence	LSE	USE	d-USE	T @50	d-T @50
1	0.00E+000	0	100	0	-16.1	0
2	2.93E+018	0	100	0	111	127.1
3	1.07E+019	0	100	0	168.8	184.9
4	1.35E+019	0	100	0	201.5	217.6
5	3.91E+019	0	100	0	239.8	255.9

Figure 5-9 Charpy V-notch Percent Shear vs. Temperature for Diablo Canyon Unit 1 Reactor Vessel Surveillance Program Surveillance Welds (cont.)

Correlation Monitor Material

CVGraph 6.02: Hyperbolic Tangent Curve Printed on 5/29/2026 7:24 AM

Curve	Plant	Capsule	Material	Ori.	Heat #
1	Diablo Canyon 1	Unirrad	SA533B1	NA	HSST02
2	Diablo Canyon 1	S	SA533B1	NA	HSST02
3	Diablo Canyon 1	Y	SA533B1	NA	HSST02
4	Diablo Canyon 1	V	SA533B1	NA	HSST02
5	Diablo Canyon 1	B	SA533B1	NA	HSST02

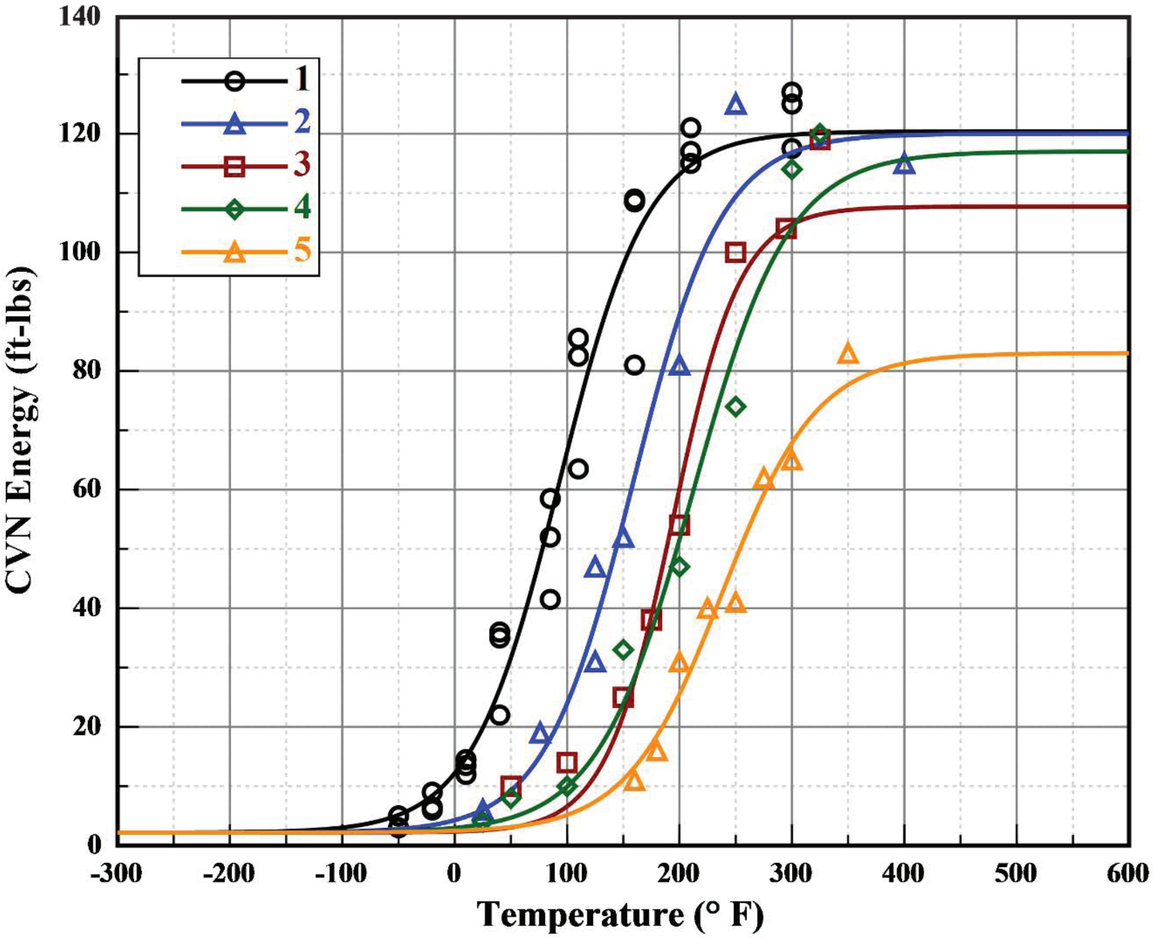

Figure 5-10 Charpy V-notch Impact Energy vs. Temperature for Diablo Canyon Unit 1 Reactor Vessel Surveillance Program CMM

Correlation Monitor Material

CVGraph 6.02: Hyperbolic Tangent Curve Printed on 5/29/2026 7:24 AM

Curve	Fluence	LSE	USE	d-USE	T @30	d-T @30	T @50	d-T @50
1	0.00E+000	2.2	120.4	0	47	0	78	0
2	2.93E+018	2.2	120	-0.40	112.3	65.3	143.6	65.6
3	1.07E+019	2.2	107.7	-12.7	163.2	116.2	188.4	110.4
4	1.35E+019	2.2	117	-3.40	163.4	116.4	197.6	119.6
5	3.62E+019	2.2	83	-37.4	210.8	163.8	253.7	175.7

Figure 5-10 Charpy V-notch Impact Energy vs. Temperature for Diablo Canyon Unit 1 Reactor Vessel Surveillance Program CMM (cont.)

Correlation Monitor Material

CVGraph 6.02: Hyperbolic Tangent Curve Printed on 5/28/2026 1:59 PM

Curve	Plant	Capsule	Material	Ori.	Heat #
1	Diablo Canyon 1	Unirrad	SA533B1	NA	HSST02
2	Diablo Canyon 1	S	SA533B1	NA	HSST02
3	Diablo Canyon 1	Y	SA533B1	NA	HSST02
4	Diablo Canyon 1	V	SA533B1	NA	HSST02
5	Diablo Canyon 1	B	SA533B1	NA	HSST02

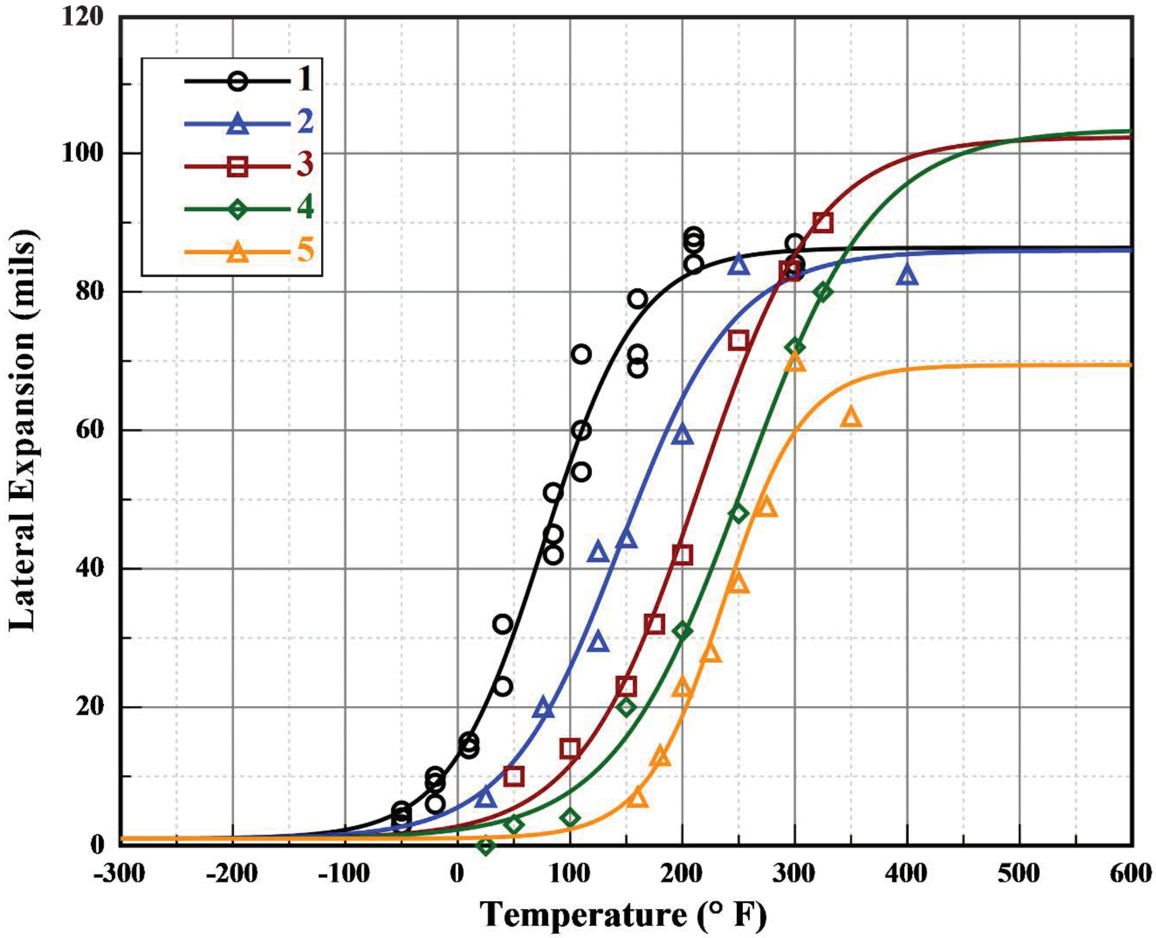

Figure 5-11 Charpy V-notch Lateral Expansion vs. Temperature for Diablo Canyon Unit 1 Reactor Vessel Surveillance Program CMM

Correlation Monitor Material

CVGraph 6.02: Hyperbolic Tangent Curve Printed on 5/28/2026 1:59 PM

Curve	Fluence	LSE	USE	d-USE	T @35	d-T @35
1	0.00E+000	1	86.37	0	59.1	0
2	2.93E+018	1	85.98	-0.39	124.5	65.4
3	1.07E+019	1	102.35	15.98	178.1	119
4	1.35E+019	1	103.52	17.15	213.5	154.4
5	3.62E+019	1	69.43	-16.94	236.2	177.1

Figure 5-11 Charpy V-notch Lateral Expansion vs. Temperature for Diablo Canyon Unit 1 Reactor Vessel Surveillance Program CMM (cont.)

Correlation Monitor Material

CVGraph 6.02: Hyperbolic Tangent Curve Printed on 5/28/2026 2:00 PM

Curve	Plant	Capsule	Material	Ori.	Heat #
1	Diablo Canyon 1	Unirrad	SA533B1	NA	HSST02
2	Diablo Canyon 1	S	SA533B1	NA	HSST02
3	Diablo Canyon 1	Y	SA533B1	NA	HSST02
4	Diablo Canyon 1	V	SA533B1	NA	HSST02
5	Diablo Canyon 1	B	SA533B1	NA	HSST02

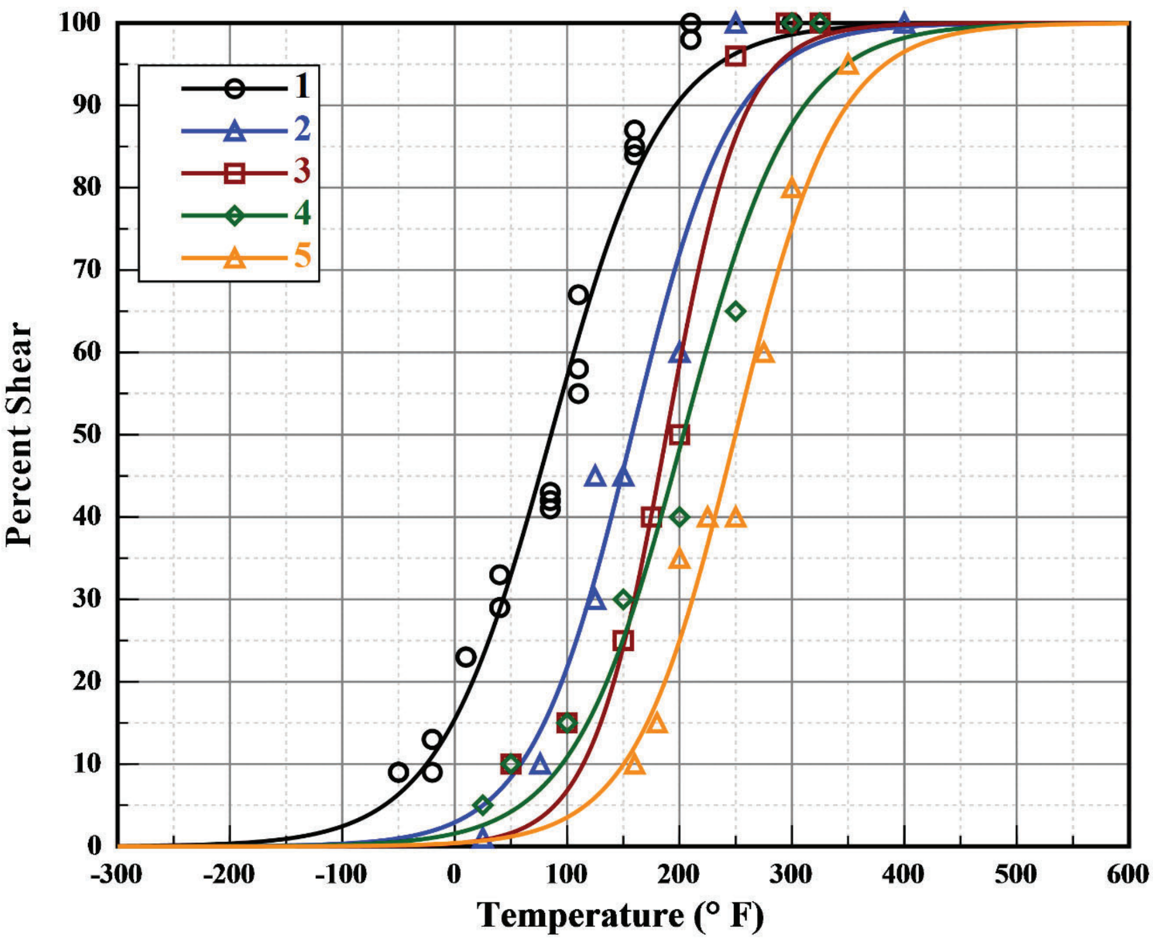

Figure 5-12 Charpy V-notch Percent Shear vs. Temperature for Diablo Canyon Unit 1 Reactor Vessel Surveillance Program CMM

Correlation Monitor Material

CVGraph 6.02: Hyperbolic Tangent Curve Printed on 5/28/2026 2:00 PM

Curve	Fluence	LSE	USE	d-USE	T @50	d-T @50
1	0.00E+000	0	100	0	85.7	0
2	2.93E+018	0	100	0	157.6	71.9
3	1.07E+019	0	100	0	188.4	102.7
4	1.35E+019	0	100	0	203.5	117.8
5	3.62E+019	0	100	0	249.8	164.1

Figure 5-12 Charpy V-notch Percent Shear vs. Temperature for Diablo Canyon Unit 1 Reactor Vessel Surveillance Program CMM (cont.)

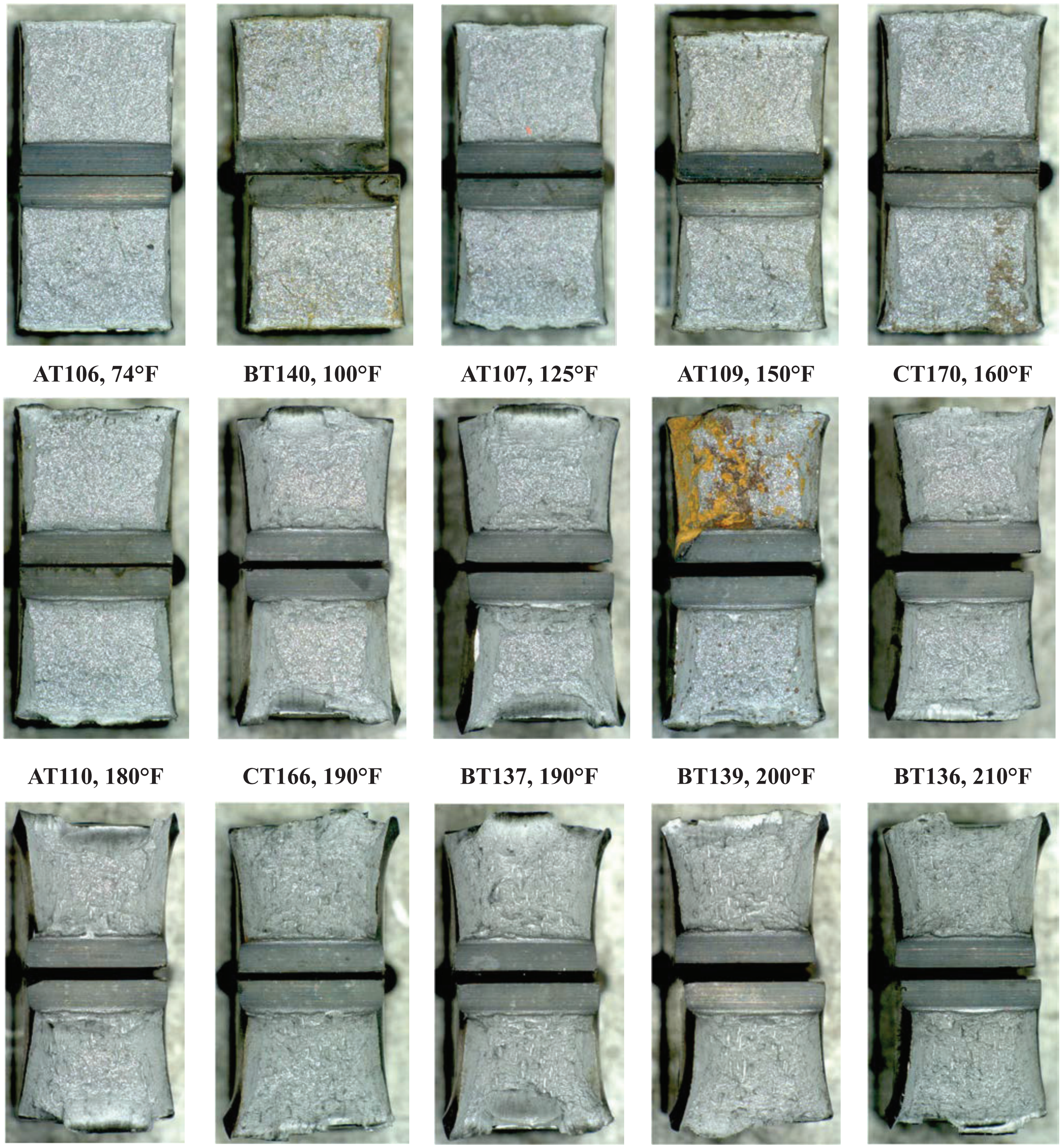

AT106, 74°F **BT140, 100°F** **AT107, 125°F** **AT109, 150°F** **CT170, 160°F**

AT110, 180°F **CT166, 190°F** **BT137, 190°F** **BT139, 200°F** **BT136, 210°F**

CT169, 225°F **CT167, 250°F** **BT138, 300°F** **CT168, 350°F** **AT108, 375°F**

Figure 5-13 Charpy Impact Specimen Fracture Surfaces of the Diablo Canyon Unit 1, Capsule B Lower Shell Plate B4107-1

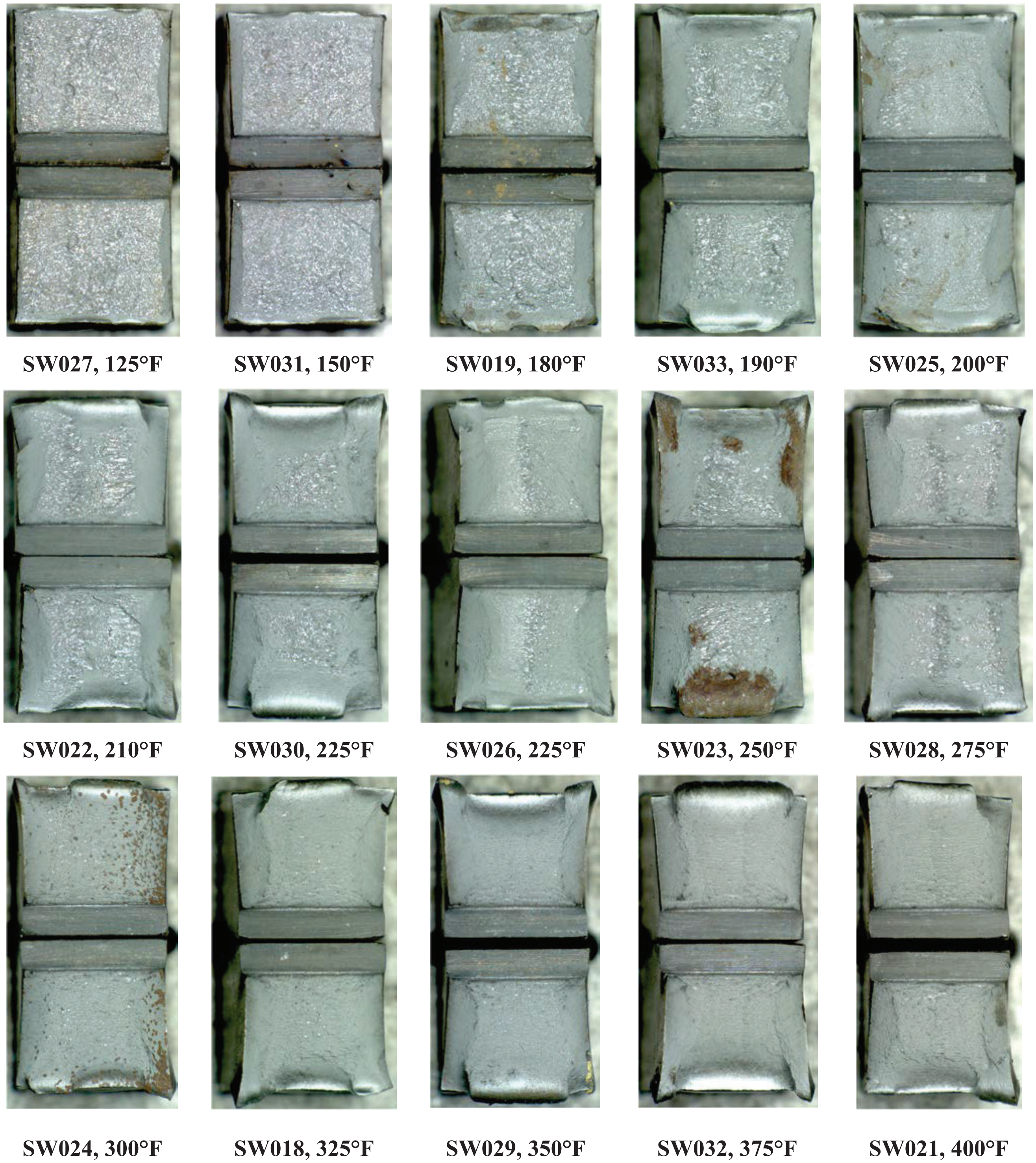

Figure 5-14 Charpy Impact Specimen Fracture Surfaces for the Diablo Canyon Unit 1 Capsule B Surrogate Weld

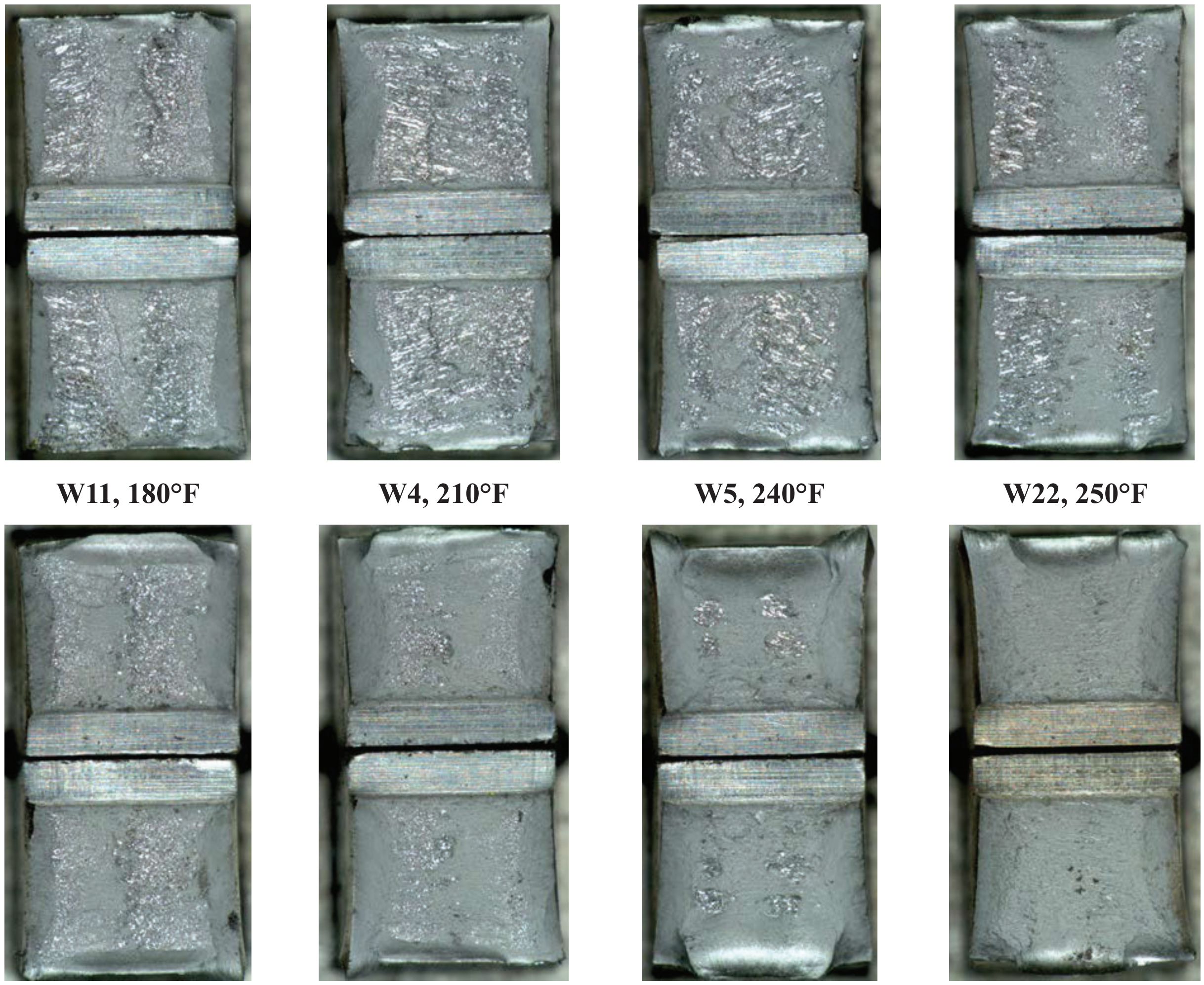

W11, 180°F **W4, 210°F** **W5, 240°F** **W22, 250°F**

W12, 260°F **W21, 280°F** **W7, 300°F** **W2, 375°F**

Figure 5-15 Charpy Impact Specimen Fracture Surfaces of the Diablo Canyon Unit 1, Capsule B Reconstituted Surveillance Weld

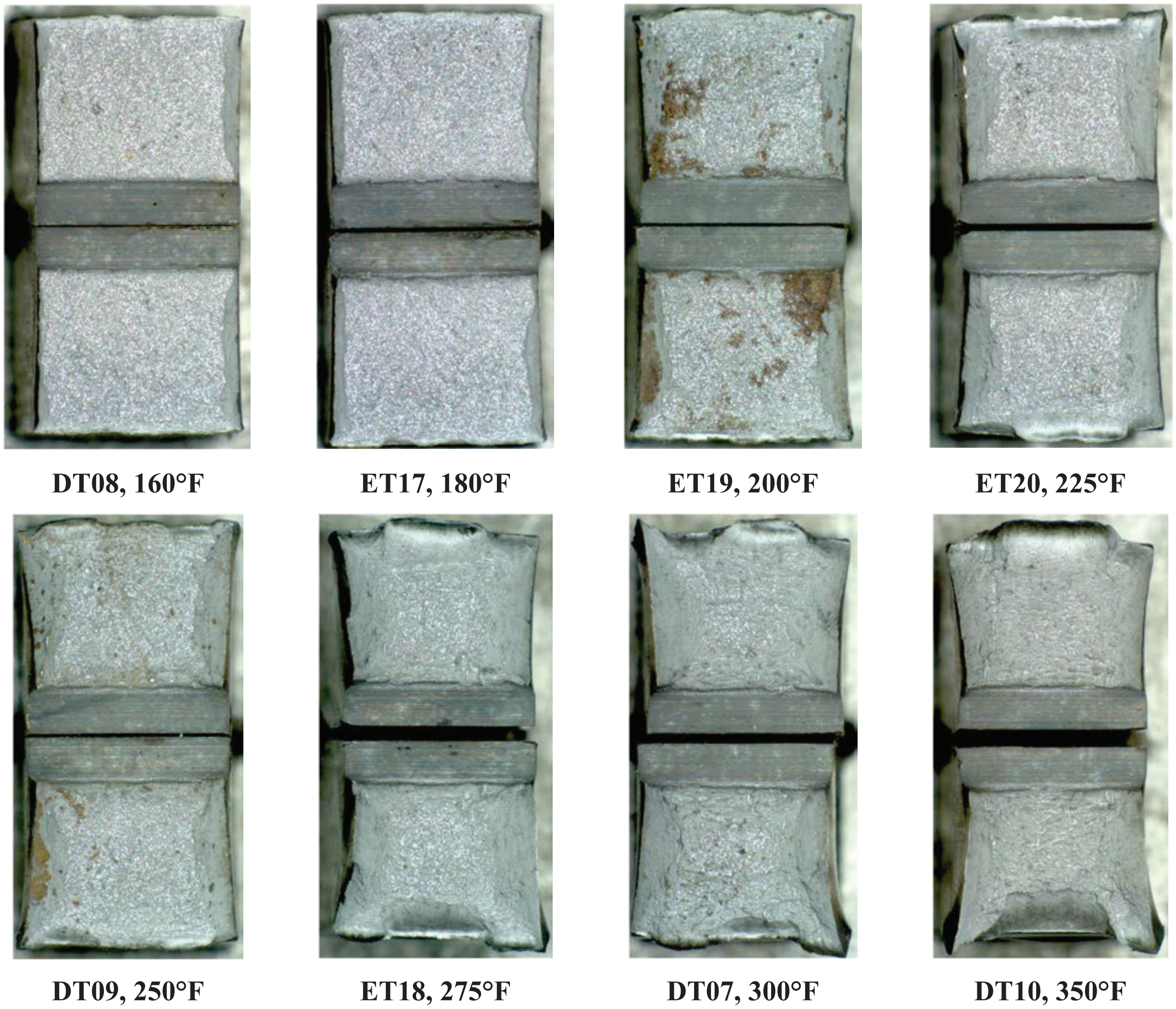

Figure 5-16 Charpy Impact Specimen Fracture Surfaces for the Diablo Canyon Unit 1 Capsule B CMM

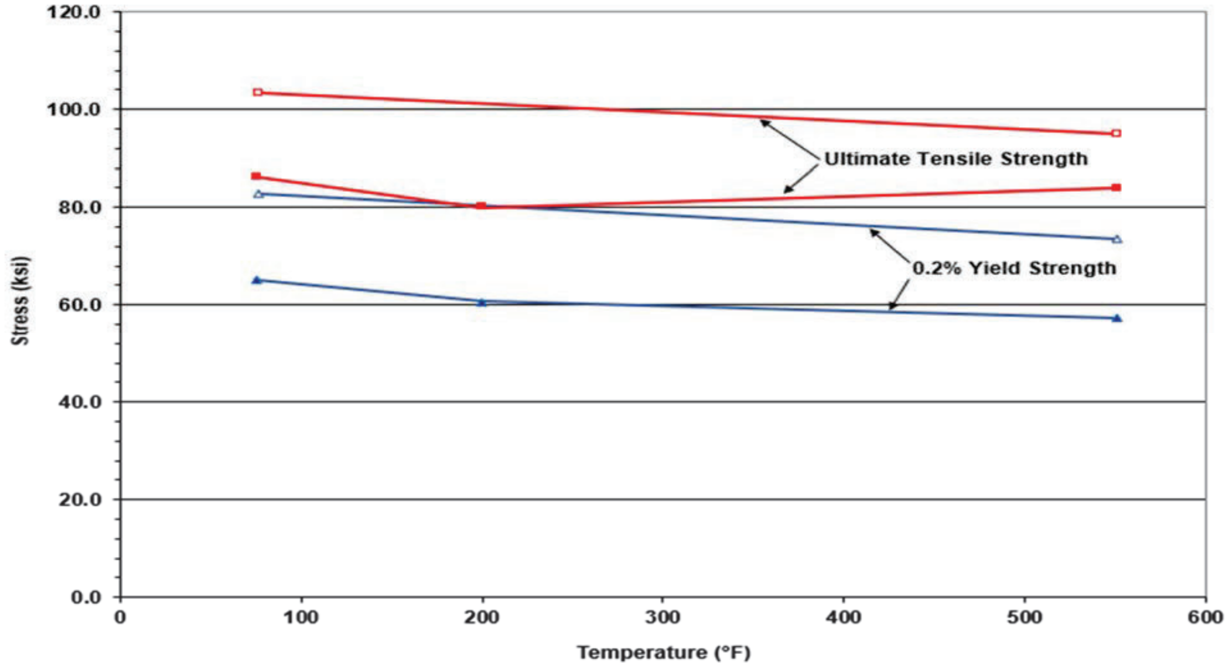

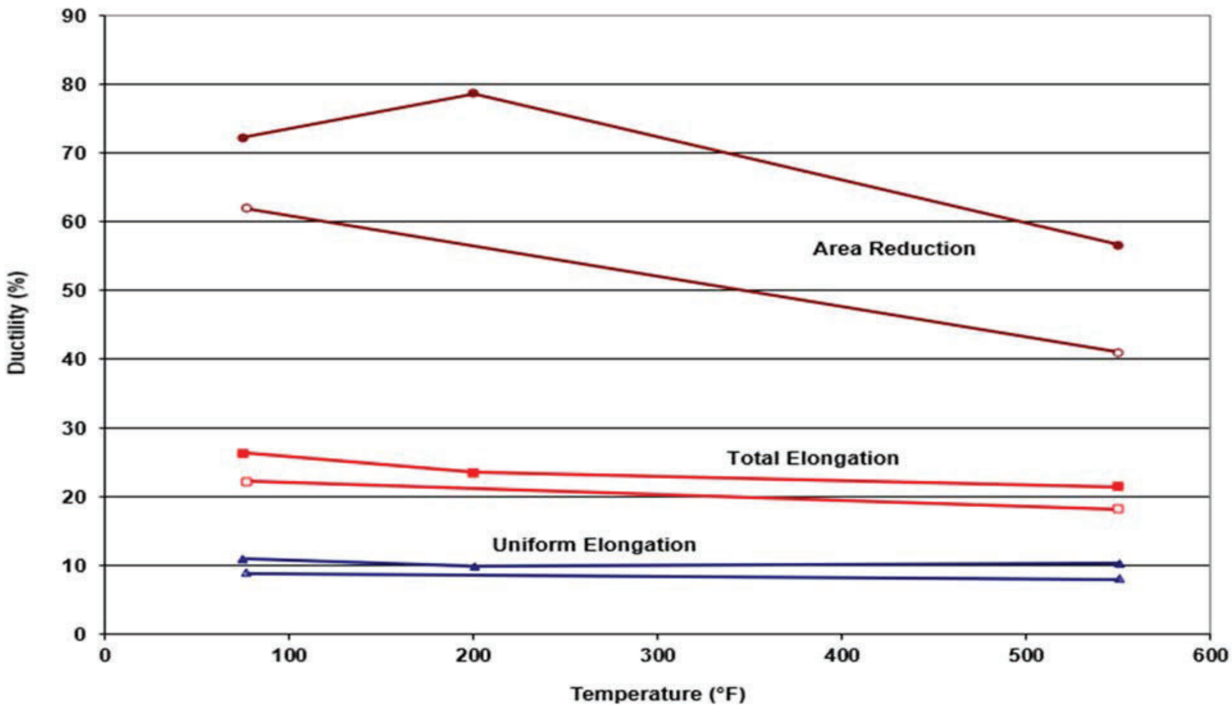

Legend: ▲, ●, and ■ are unirradiated
Δ, ○, and □ are irradiated to 3.62×10^{19} n/cm^2 (E > 1.0 MeV)

Figure 5-17 Tensile Properties for Diablo Canyon Unit 1 Reactor Vessel Lower Shell Plate B4107-1 (Transverse Orientation)

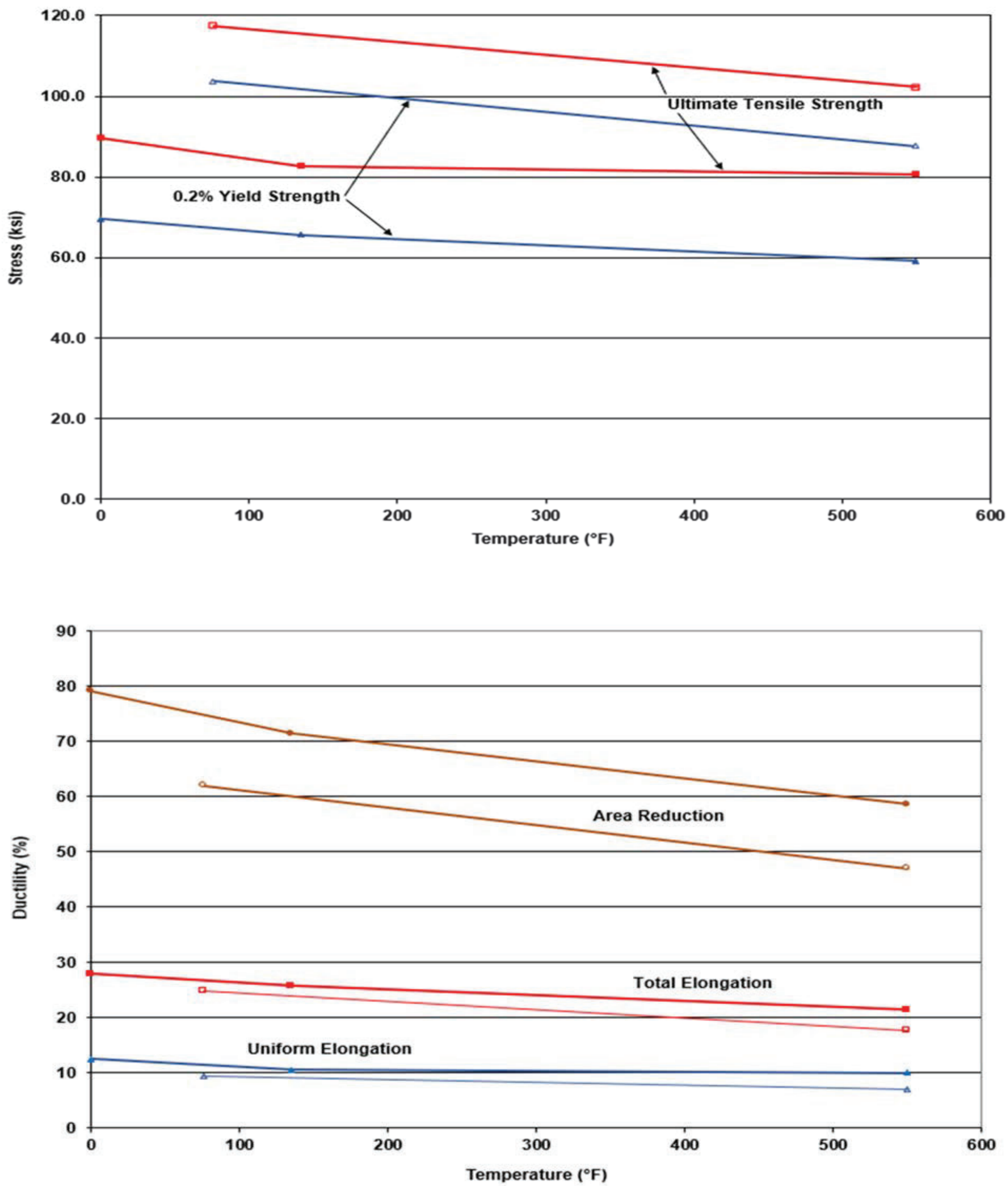

Legend: ▲, ●, and ■ are unirradiated
Δ, ○, and □ are irradiated to 3.62 x 10^{19} n/cm^2 (E > 1.0 MeV)

Figure 5-18 Tensile Properties for Diablo Canyon Unit 1 Surrogate Weld

BT207, 77 °F

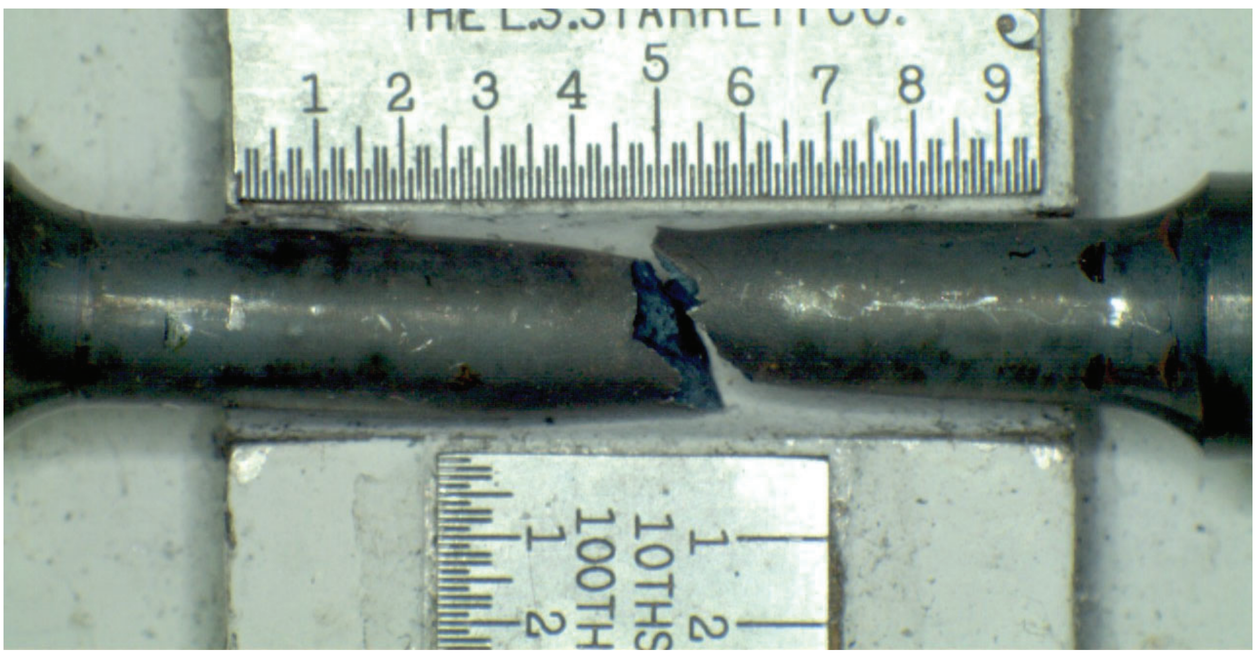

BT208, 550°F

Figure 5-19 Fractured Tensile Specimens from Diablo Canyon Unit 1, Capsule B, Lower Shell Plate B4107-1 (Transverse Orientation)

SW040, 76°F

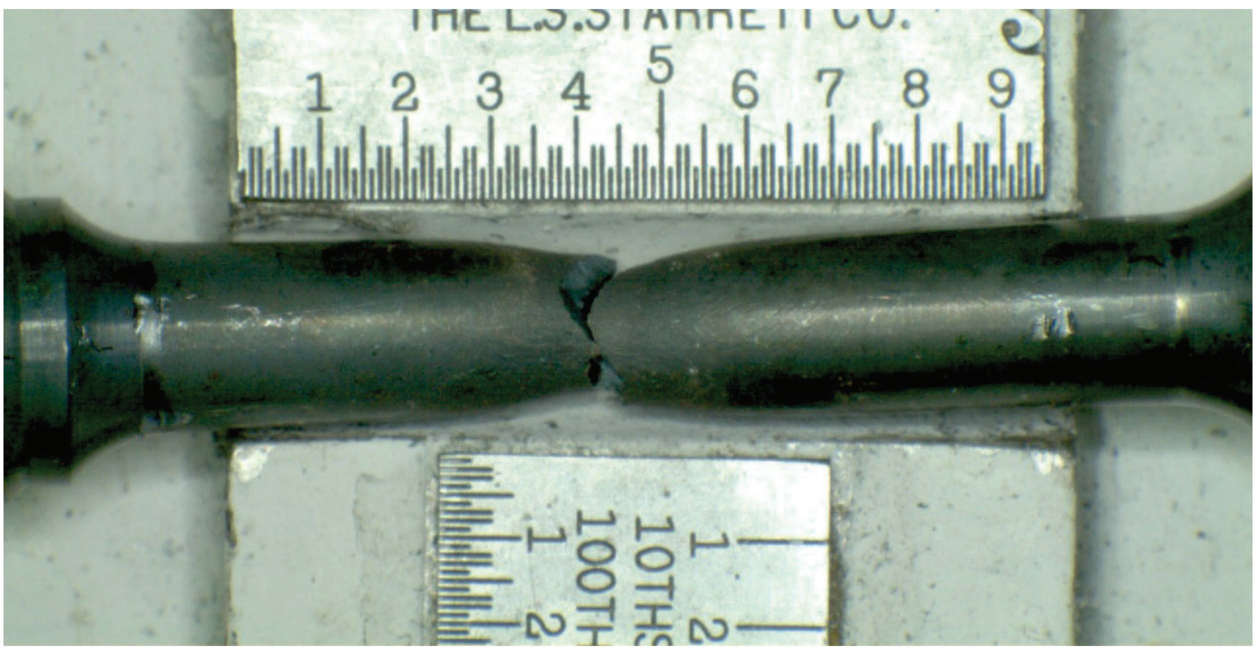

SW044, 550°F

Figure 5-20 Fractured Tensile Specimens from Diablo Canyon Unit 1, Capsule B, Surrogate Weld

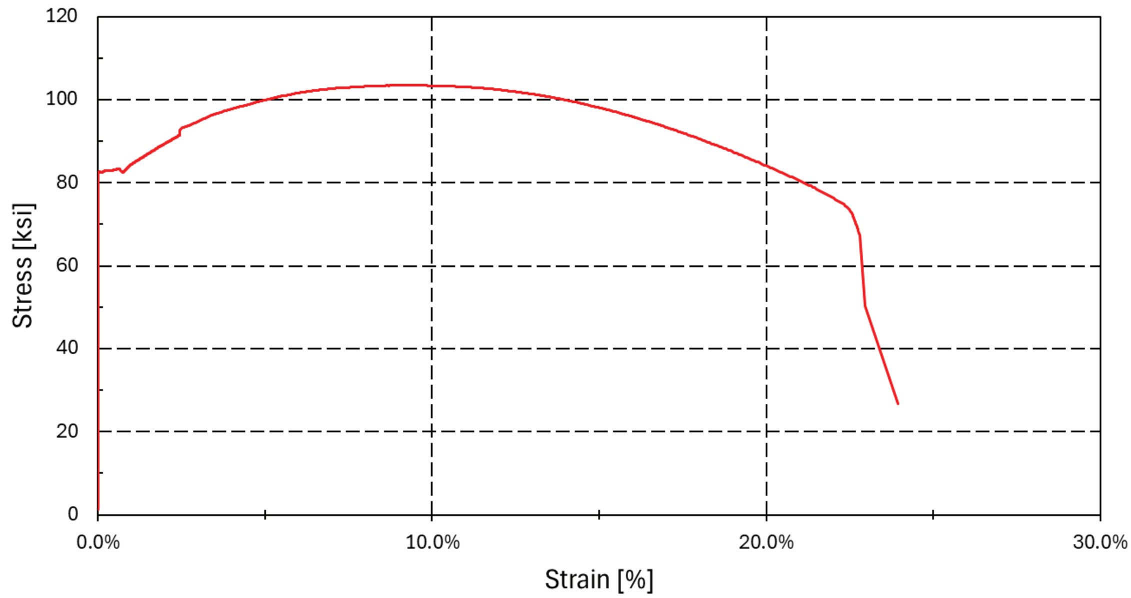

Figure 5-21 Engineering Stress-Strain Curve for Diablo Canyon Unit 1, Capsule B, Tensile Specimen BT207 (Plate B4107-1), Tested at 77°F

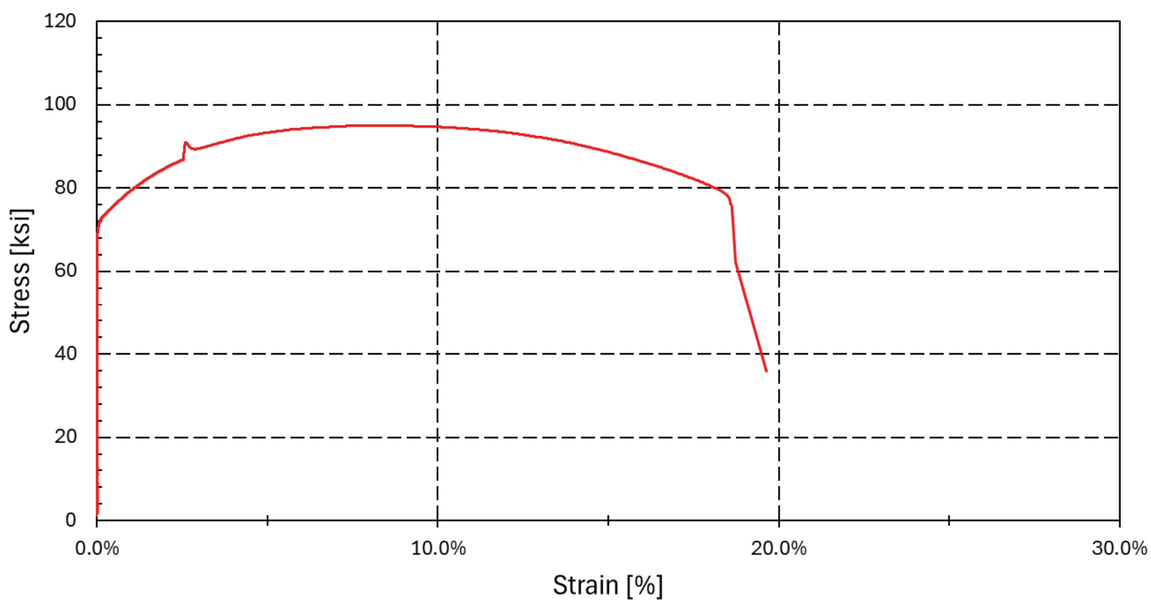

Figure 5-22 Engineering Stress-Strain Curve for Diablo Canyon Unit 1, Capsule B, Tensile Specimen BT208 (Plate B4107-1), Tested at 550°F

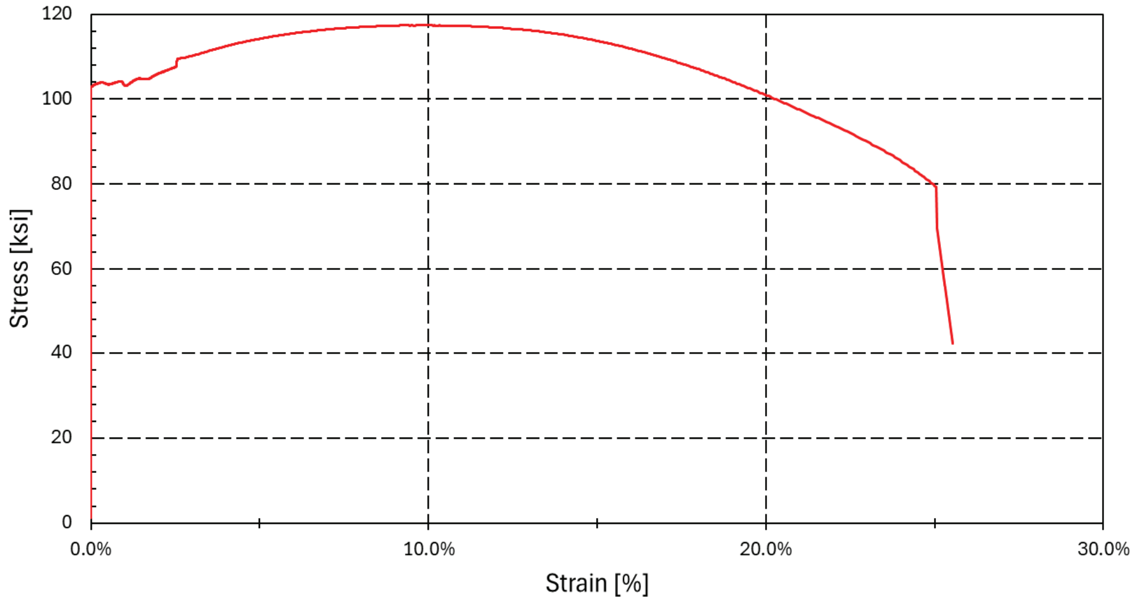

Figure 5-23 Engineering Stress-Strain Curve for Diablo Canyon Unit 1, Capsule B, Tensile Specimen SW040 (Surrogate Weld), Tested at 76°F

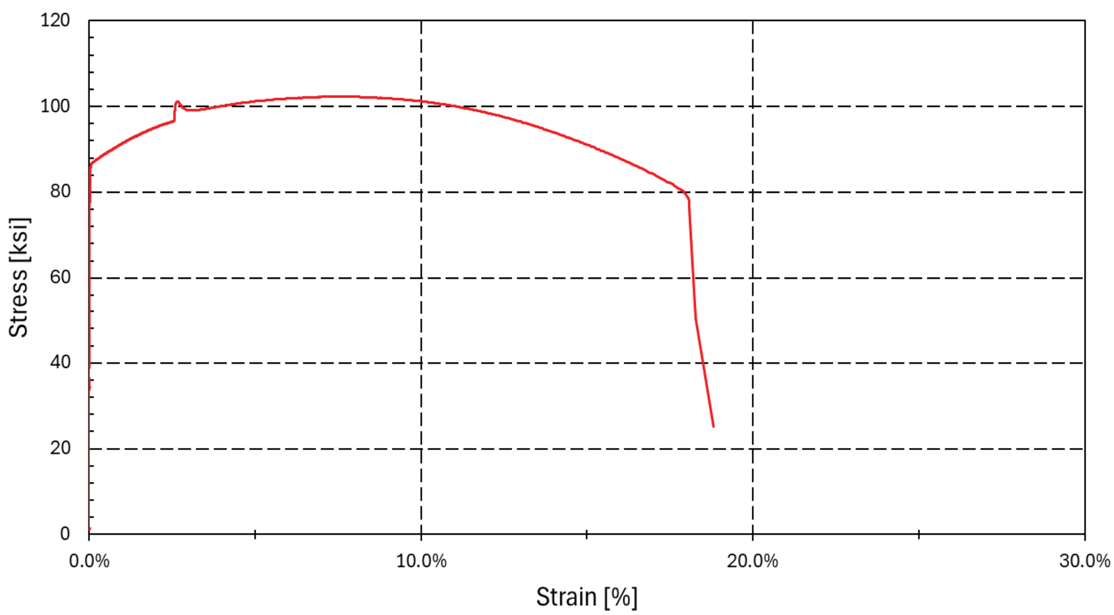

Figure 5-24 Engineering Stress-Strain Curve for Diablo Canyon Unit 1, Capsule B, Tensile Specimen SW044 (Surrogate Weld), Tested at 550°F

6 RADIATION ANALYSIS AND NEUTRON DOSIMETRY

6.1 INTRODUCTION

This section describes a discrete ordinates (S_n) transport analysis performed to determine the neutron radiation environment within the reactor pressure vessel and surveillance capsules. In this analysis, neutron exposure parameters in terms of fast neutron (E > 1.0 MeV) fluence and iron atom displacements (dpa) were established on a plant- and fuel-cycle-specific basis. In addition, the most recent neutron dosimetry sensors from surveillance Capsule B, withdrawn at the end of the 25th plant operating cycle, were evaluated. Comparisons of the results from the dosimetry evaluations with the analytical predictions served to validate the plant-specific neutron transport calculations. These validated calculations subsequently form the basis for projections of the neutron exposure of the reactor pressure vessel for operating periods extending to 54 effective full-power years (EFPY).

The use of fast neutron (E > 1.0 MeV) fluence to correlate measured material property changes to the neutron exposure of the material has traditionally been accepted for the development of damage trend curves as well as for the implementation of trend curve data to assess the condition of the vessel. However, it has been suggested that an exposure model that accounts for differences in neutron energy spectra between surveillance capsule locations and positions within the vessel wall could lead to an improvement in the uncertainties associated with damage trend curves and improved accuracy in the evaluation of damage gradients through the reactor vessel wall.

Because of this potential shift away from a threshold fluence toward an energy-dependent damage function for data correlation, ASTM E853 [17] recommends reporting displacements per iron atom along with fluence (E > 1.0 MeV) to provide a database for future reference. The energy-dependent dpa function to be used for this evaluation is specified in ASTM E693 [18]. The application of the dpa parameter to the assessment of embrittlement gradients through the thickness of the reactor vessel wall has been promulgated in Rev. 2 to Regulatory Guide 1.99 [1].

All of the calculations and dosimetry evaluations described in this section and in Appendix A were based on nuclear cross-section data derived from ENDF/B-VI. Furthermore, the neutron transport and dosimetry evaluation methodologies follow the guidance of Regulatory Guide 1.190 [8]. Additionally, the methods used to develop the calculated pressure vessel fluence are consistent with the NRC-approved methodology described in WCAP-18124-NP-A [19] and WCAP-18124-NP-A Supplement 1-NP-A [20].

6.2 DISCRETE ORDINATES ANALYSIS

The arrangement of the surveillance capsules in the reactor vessel is shown in Figure 4-1. Eight capsules were initially inserted into the reactor prior to plant startup. Capsules S, Y, T, and Z were originally loaded into 40-degree first octant equivalent (FOE) azimuthal locations, while Capsules V, U, W, and X were positioned at 4° FOE azimuthal locations. Capsule S was withdrawn for analysis at the conclusion of the first fuel cycle. At the end of Cycle 5, Capsule Y was withdrawn for analysis and Capsules T and Z were withdrawn and subsequently placed in storage for later analysis or reinsertion. Also, at the conclusion of Cycle 5, Capsule V was re-positioned from a 4° location to a 40° location, supplemental Capsule A was inserted into the now vacated 4° position, and supplemental Capsules B, C, and D were inserted into the vacant 40° holders. At the end of Cycle 25, Capsule B was withdrawn for analysis.

From a neutronic standpoint, the surveillance capsules and associated support structures are significant. The presence of these materials has a significant effect on both the spatial distribution of neutron exposure rate and the neutron spectrum in the vicinity of the capsules. However, the capsules are far enough apart that they do not interfere with one another. In order to determine the neutron environment at the test specimen location, the capsules themselves must be included in the analytical model.

In performing the fast neutron exposure evaluations for the reactor vessel and surveillance capsules, plant-specific 3D forward transport calculations were carried out to directly solve for the space- and energy-dependent neutron exposure rate, $\phi(r,\theta,z,E)$.

Plan and section views of the model of the reactor geometry used in the radiation transport calculations are shown in Figure 6-1 through Figure 6-4. The model contained a representation of the reactor core, the reactor internals, the pressure vessel cladding and vessel wall, the insulation external to the pressure vessel, and the primary biological shield wall. This model formed the basis for the calculated results. In developing this analytical model, nominal design dimensions were generally employed for the various structural components. In addition, water temperatures, and hence, coolant densities in the reactor core and downcomer regions of the reactor were taken to be representative of full-power operating conditions. The coolant densities were treated on a fuel-cycle-specific basis. The reactor core itself was treated as a mixture of fuel, cladding, water, and miscellaneous core structures, such as fuel assembly grids, guide tubes, etc.

Section views of the model are shown in Figure 6-3 and Figure 6-4. The model extends radially from the centerline of the reactor core out to a location interior to the primary biological shield and over an axial span from an elevation approximately five feet below the active fuel to more than five feet above the active fuel.

The RAPTOR-M3G model consisted of 227 radial, 205 azimuthal, and 420 axial meshes. Mesh sizes were chosen to ensure that proper convergence of the inner iterations was achieved on a pointwise basis. The pointwise inner iteration flux convergence criterion utilized in the calculations was set at a value of 0.001.

The core power distributions used in the plant-specific transport analysis included cycle-dependent fuel assembly initial enrichments, burnups, radial, and axial power distributions. Radiation exposure projections beyond Cycle 26 were based on Cycle 23 spatial power distributions, water temperatures, and reactor power level with and without a 10% bias on the peripheral and re-entrant corner relative powers as directed by Pacific Gas & Electric Company. The cycle-dependent fuel assembly initial enrichments, burnups, radial, and axial power distributions were used to develop spatial- and energy-dependent core source distributions averaged over each individual fuel cycle. Therefore, the results from the neutron transport calculations provided data in terms of fuel-cycle-averaged neutron exposure rates, which when multiplied by the appropriate fuel cycle lengths, generated the incremental neutron exposure for each fuel cycle. In constructing these core source distributions, the energy distribution of the source was based on an appropriate fission split for uranium and plutonium isotopes based on the initial enrichment and burnup history of individual fuel assemblies. From these assembly-dependent fission splits, composite values of energy release per fission, neutron yield per fission, and fission spectrum were determined.

All of the transport calculations supporting this analysis were carried out using the RAPTOR-M3G discrete ordinates code and the BUGLE-96 cross-section library [19, 20]. The BUGLE-96 library provides a coupled 47-neutron, 20-gamma-group cross-section data set produced specifically for light-water reactor (LWR) applications. In these analyses, anisotropic scattering was treated with a P_3 Legendre expansion, and angular discretization was modeled with an S_{16} order of angular quadrature. Energy- and space-dependent core power distributions, as well as system operating temperatures, were treated on a fuel-cycle-specific basis.

Results of the discrete ordinates transport analyses pertinent to the surveillance capsules are provided in Table 6-1 through Table 6-3. In Table 6-1, fast neutron (E > 1.0 MeV) fluence rates and iron atom displacement rates are provided at the geometric center of the surveillance capsules as a function of irradiation time. In Table 6-2, the fast neutron (E > 1.0 MeV) fluence for each of the surveillance capsules is presented as a function of irradiation time. Similar data presented in terms of iron atom displacements are presented in Table 6-3.

In Table 6-4, the lead factors associated with the surveillance capsules are presented as a function of operating time. The capsule lead factor is defined as the ratio of the fast neutron (E > 1.0 MeV) fluence at the geometric center of the surveillance capsule to the maximum fast neutron (E > 1.0 MeV) fluence at the clad/base metal interface.

Neutron exposure data pertinent to the pressure vessel clad/base metal interface are given in Table 6-5 and Table 6-6 for fast neutron (E > 1.0 MeV) fluence rate and fluence, respectively, and in Table 6-7 and Table 6-8 for iron atom displacement rate and displacements, respectively. In each case, the data are provided for each operating cycle of the reactor. Fast neutron (E > 1.0 MeV) fluence and iron atom displacements are also projected to future operating times extending to 54 EFPY. The vessel exposure data are presented in terms of the maximum exposure experienced by the pressure vessel at azimuthal angles of 0°, 15°, 30°, and 45° and at the azimuthal location providing the maximum exposure relative to the core cardinal axes. It is noted that the cycle operating times, in EFPY, identified in these tables may differ from other records based on the data set used to determine them (e.g., thermal generation versus cycle burnup data). However, any such differences are minor (34.87 EFPY at EOC 25 in this report versus 34.94 EFPY in other records).

In Table 6-9 and Table 6-10, maximum projected fluences and iron atom displacements of additional reactor pressure vessel (RPV) materials (welds and shells) are given.

6.3 NEUTRON DOSIMETRY

The validity of the calculated neutron exposures reported in Section 6.2 is demonstrated by a direct comparison against the measured sensor reaction rates and a least-squares evaluation performed for each of the capsule dosimetry sets. However, since the neutron dosimetry measurement data merely serve to validate the calculated results, only the direct comparison of measured-to-calculated results for the most recent surveillance capsule removed from the reactor is provided in this section of the report. For completeness, the assessment of all measured surveillance capsule dosimetry removed from the reactor to date based on both direct and least-squares evaluation comparisons is documented in Appendix A.

The direct comparison of measured versus calculated fast neutron threshold reaction rates for the sensors from Capsule B, which was withdrawn from the reactor at the conclusion of Cycle 25, is summarized below.

Reaction	Reaction Rate (rps/atom)		M/C
	Measured	Calculated	
^{63}Cu (n,α) ^{60}Co	2.94E-17	2.68E-17	1.10
^{54}Fe (n,p) ^{54}Mn	2.88E-15	2.85E-15	1.01
^{58}Ni (n,p) ^{58}Co	4.02E-15	3.91E-15	1.03
^{238}U(Cd) (n,f) ^{137}Cs	1.34E-14	1.38E-14	0.97
^{237}Np(Cd) (n,f) ^{137}Cs	1.05E-13	1.06E-13	0.99
^{59}Co (n,γ) ^{60}Co	2.03E-12	1.77E-12	1.15
^{59}Co(Cd) (n,γ) ^{60}Co	8.12E-13	8.31E-13	0.98
Average of M/C Results			1.02
Standard Deviation (%)			4.9

The measured-to-calculated (M/C) reaction rate ratios for the Capsule B threshold (i.e., non Co-59) reactions range from 0.97 to 1.03, and the average M/C ratio is 1.02 ± 4.9% (1σ). This direct comparison falls within the ± 20% criterion specified in Regulatory Guide 1.190. This comparison, along with the other plant-specific surveillance capsule dosimetry comparisons provided in Appendix A, validates the analytical results described in Section 6.2.

6.4 CALCULATIONAL UNCERTAINTIES

The uncertainty associated with the calculated neutron exposures of the surveillance capsules and reactor pressure vessel is based on the recommended approach provided in Regulatory Guide 1.190. In particular, the qualification of the neutron transport methodology used in the calculations was carried out in the following four stages:

1. **Simulator Benchmark Comparisons:** Comparisons of calculations with measurements from simulator benchmarks, including the Pool Critical Assembly (PCA) simulator at the Oak Ridge National Laboratory (ORNL) and the VENUS-1 Experiment.

2. **Operating Reactor and Calculational Benchmarks:** Comparisons of calculations with surveillance capsule and reactor cavity measurements from the H.B. Robinson power reactor benchmark experiment. Also considered are comparisons of calculations to results published in the USNRC fluence calculation benchmark.

3. **Analytic Uncertainty Analysis:** An analytical sensitivity study addressing the uncertainty components resulting from important input parameters applicable to the plant-specific transport calculations used in the neutron exposure assessments.

4. **Plant-Specific Benchmarking:** Comparisons of the plant-specific calculations with all available dosimetry results from the reactor vessel surveillance program.

The first phase of the methods qualification (simulator benchmark comparisons) addressed the adequacy of basic transport calculation and dosimetry evaluation techniques and associated cross-sections. This phase, however, did not test the accuracy of commercial core neutron source calculations nor did it address uncertainties in operational or geometric variables that impact power reactor calculations. The second phase of the qualification (operating reactor and calculational benchmark comparisons) addressed uncertainties in these additional areas that are primarily methods-related and would tend to apply generically to all fast neutron exposure evaluations. The third phase of the qualification (analytical sensitivity study) identified the potential uncertainties introduced into the overall evaluation due to calculational methods approximations, as well as to a lack of knowledge relative to various plant-specific input parameters. The overall calculational uncertainty applicable to the Diablo Canyon Unit 1 analysis was established from the results of these three phases of the methods qualification.

The fourth phase of the uncertainty assessment (comparisons with plant-specific measurements) was used solely to demonstrate the validity of the transport calculations and to confirm the uncertainty estimates associated with the analytical results. These comparisons were used only as a check and were not used in any way to modify the calculated surveillance capsule and pressure vessel neutron exposures described in Section 6.2. The validation of the analytical model based on the measured surveillance capsule dosimetry is completely described in Appendix A.

The following summarizes the uncertainties developed from the first three phases of the methodology qualification. Additional information pertinent to these evaluations is provided in Reference 19.

Description	**Capsule and Vessel IR**
Simulator Benchmark Comparisons	3%
Operating Reactor and Calculational Benchmarks	5%
Analytic Uncertainty Analysis	11%
Additional Uncertainty for Factors not Explicitly Evaluated	5%
Net Calculational Uncertainty	**13%**

The net calculational uncertainty was determined by combining the individual components in quadrature. Therefore, the resultant uncertainty was treated as random, and no systematic bias was applied to the analytical results. The plant-specific measurement comparisons described in Appendix A support these uncertainty assessments.

The USNRC safety evaluation in Section A of Reference 19 includes the following "Limitations and Conditions" associated with the application of RAPTOR-M3G and FERRET:

1. Applicability of WCAP-18124-NP, Revision 0 is limited to the RPV region near the active height of the core based on the uncertainty analysis performed and the measurement data provided. Additional justification should be provided via additional benchmarking, fluence sensitivity analysis to the response parameters of interest (e.g., pressure-temperature limits, material stress/strain), margin assessment, or a combination thereof, for applications of the method to components including, but not limited to, the RPV upper circumferential weld and the reactor coolant system inlet and outlet nozzles and reactor vessel internal components.
2. Least squares adjustment is acceptable if the adjustments to the M/C ratios and to the calculated spectra values are within the assigned uncertainties of the calculated spectra, the dosimetry measured reaction rates, and the dosimetry reaction cross sections. Should this not be the case, the user should re-examine both measured and calculated values for possible errors. If errors cannot be found, the particular values causing the discrepancy should be disqualified.

Limitation 1 was addressed in Reference 20, which provides the justification necessary to narrow this limitation and allow licensees to apply the RAPTOR-M3G method to the RPV extended beltline region on a generic basis. More specifically, the revised wording of Limitation 1 in Section 7 of Reference 20 provides the conditions under which the RAPTOR-M3G method may be applied to RPV extended beltline regions. With the exception of the lower shell to lower vessel head circumferential weld (whose fast neutron (E > 1.0 MeV) fluence exposures are significantly less than 1.0 E+17 n/cm^2), these conditions are met for the plant-specific neutron exposures provided in this report.

Limitation 2 applies in situations where the least-squares analysis is used to *adjust* the calculated values of neutron exposure. In this report, the least-squares analysis is provided only as a supplemental check on the results of the dosimetry evaluation. The least-squares analysis was *not* used to modify the calculated surveillance capsule or reactor pressure vessel neutron exposure. Therefore, Limitation 2 does not apply.

Table 6-1 Neutron Exposure Rates at the Center of the Surveillance Capsule Locations

Cycle	Cycle Length (EFPY)	Total Time (EFPY)	Fast Neutron (E > 1.0 MeV) Fluence Rate (n/cm^2-s)		Iron Atom Displacement Rate (dpa/s)	
			4°	40°	4°	40°
1	1.26	1.26	2.13E+10	7.37E+10	3.44E-11	1.25E-10
2	1.01	2.27	1.86E+10	6.17E+10	3.01E-11	1.04E-10
3	1.17	3.44	1.49E+10	6.31E+10	2.41E-11	1.07E-10
4	1.04	4.48	1.59E+10	5.01E+10	2.57E-11	8.44E-11
5	1.38	5.86	1.48E+10	4.23E+10	2.39E-11	7.13E-11
6	1.28	7.13	1.55E+10	4.25E+10	2.51E-11	7.17E-11
7	1.32	8.45	1.49E+10	4.19E+10	2.41E-11	7.07E-11
8	1.28	9.73	1.31E+10	3.76E+10	2.11E-11	6.34E-11
9	1.62	11.35	1.45E+10	3.95E+10	2.35E-11	6.66E-11
10	1.48	12.83	1.30E+10	3.86E+10	2.10E-11	6.51E-11
11	1.41	14.23	1.37E+10	3.48E+10	2.22E-11	5.86E-11
12	1.61	15.84	1.47E+10	3.99E+10	2.36E-11	6.72E-11
13	1.34	17.18	1.52E+10	4.15E+10	2.46E-11	7.00E-11
14	1.39	18.57	1.30E+10	3.96E+10	2.11E-11	6.68E-11
15	1.62	20.19	1.39E+10	4.07E+10	2.24E-11	6.87E-11
16	1.49	21.68	1.49E+10	3.89E+10	2.41E-11	6.55E-11
17	1.42	23.10	1.34E+10	3.81E+10	2.16E-11	6.43E-11
18	1.60	24.70	1.34E+10	3.92E+10	2.16E-11	6.60E-11
19	1.50	26.19	1.36E+10	3.75E+10	2.20E-11	6.31E-11
20	1.44	27.63	1.26E+10	3.69E+10	2.03E-11	6.22E-11
21	1.60	29.23	1.38E+10	4.34E+10	2.23E-11	7.31E-11
22	1.53	30.76	1.39E+10	3.98E+10	2.25E-11	6.71E-11
23	1.37	32.13	1.42E+10	4.00E+10	2.29E-11	6.74E-11
24	1.37	33.50	1.32E+10	3.88E+10	2.14E-11	6.53E-11
25	1.37	34.87	1.50E+10	4.09E+10	2.43E-11	6.89E-11
26	1.36	36.23	1.47E+10	4.03E+10	2.38E-11	6.79E-11
Proj.	no bias	--	1.42E+10	4.00E+10	2.29E-11	6.74E-11
Proj.	w/bias	--	1.58E+10	4.44E+10	2.54E-11	7.47E-11

Table 6-2 Fast Neutron (E > 1.0 MeV) Fluence at the Center of the Surveillance Capsules

Cycle	Total Time (EFPY)	Fast Neutron (E > 1.0 MeV) Fluence (n/cm^2)						
		S (40°)	Y / T / Z (40°)	V (4/40°)	U / W / X (4°)	A (4°)	B (40°)	C / D (40°)
1	1.26	2.93E+18	2.93E+18	8.47E+17	8.47E+17			
2	2.27		4.89E+18	1.44E+18	1.44E+18			
3	3.44		7.22E+18	1.99E+18	1.99E+18			
4	4.48		8.87E+18	2.51E+18	2.51E+18			
5	5.86		1.07E+19	3.16E+18	3.16E+18			
6	7.13			4.87E+18	3.78E+18	6.26E+17	1.72E+18	1.72E+18
7	8.45			6.61E+18	4.40E+18	1.25E+18	3.46E+18	3.46E+18
8	9.73			8.13E+18	4.93E+18	1.78E+18	4.98E+18	4.98E+18
9	11.35			1.01E+19	5.67E+18	2.52E+18	6.99E+18	6.99E+18
10	12.83			1.19E+19	6.28E+18	3.13E+18	8.79E+18	8.79E+18
11	14.23			1.35E+19	6.89E+18	3.73E+18	1.03E+19	1.03E+19
12	15.84				7.63E+18	4.48E+18	1.24E+19	1.24E+19
13	17.18				8.28E+18	5.12E+18	1.41E+19	
14	18.57				8.85E+18	5.69E+18	1.58E+19	
15	20.19				9.56E+18	6.41E+18	1.79E+19	
16	21.68				1.03E+19	7.11E+18	1.98E+19	
17	23.10				1.09E+19	7.71E+18	2.15E+19	
18	24.70				1.15E+19	8.38E+18	2.34E+19	
19	26.19				1.22E+19	9.02E+18	2.52E+19	
20	27.63				1.27E+19	9.59E+18	2.69E+19	
21	29.23				1.34E+19	1.03E+19	2.91E+19	
22	30.76				1.41E+19	1.10E+19	3.10E+19	
23	32.13				1.47E+19	1.16E+19	3.27E+19	
24	33.50				1.53E+19	1.22E+19	3.44E+19	
25	34.87				1.60E+19	1.28E+19	3.62E+19	
26	36.23				1.66E+19	1.34E+19		
Proj.	38				1.74E+19	1.42E+19		
	42				1.92E+19	1.60E+19		
	46				2.10E+19	1.78E+19		
	50				2.28E+19	1.96E+19		
	54				2.46E+19	2.14E+19		
Proj. with bias	38				1.75E+19	1.43E+19		
	42				1.95E+19	1.63E+19		
	46				2.14E+19	1.83E+19		
	50				2.34E+19	2.03E+19		
	54				2.54E+19	2.23E+19		

Table 6-3 Iron Atom Displacements at the Center of the Surveillance Capsules

Cycle	Total Time (EFPY)	Iron Atom Displacements (dpa)						
		S (40°)	Y / T / Z (40°)	V (4/40°)	U / W / X (4°)	A (4°)	B (40°)	C / D (40°)
1	1.26	4.97E-03	4.97E-03	1.37E-03	1.37E-03			
2	2.27		8.28E-03	2.33E-03	2.33E-03			
3	3.44		1.22E-02	3.21E-03	3.21E-03			
4	4.48		1.50E-02	4.06E-03	4.06E-03			
5	5.86		1.81E-02	5.10E-03	5.10E-03			
6	7.13			7.99E-03	6.11E-03	1.01E-03	2.89E-03	2.89E-03
7	8.45			1.09E-02	7.11E-03	2.01E-03	5.84E-03	5.84E-03
8	9.73			1.35E-02	7.96E-03	2.87E-03	8.39E-03	8.39E-03
9	11.35			1.69E-02	9.16E-03	4.06E-03	1.18E-02	1.18E-02
10	12.83			1.99E-02	1.01E-02	5.05E-03	1.48E-02	1.48E-02
11	14.23			2.25E-02	1.11E-02	6.03E-03	1.74E-02	1.74E-02
12	15.84				1.23E-02	7.23E-03	2.08E-02	2.08E-02
13	17.18				1.34E-02	8.27E-03	2.38E-02	
14	18.57				1.43E-02	9.19E-03	2.67E-02	
15	20.19				1.54E-02	1.03E-02	3.02E-02	
16	21.68				1.66E-02	1.15E-02	3.33E-02	
17	23.10				1.75E-02	1.24E-02	3.62E-02	
18	24.70				1.86E-02	1.35E-02	3.95E-02	
19	26.19				1.97E-02	1.46E-02	4.25E-02	
20	27.63				2.06E-02	1.55E-02	4.53E-02	
21	29.23				2.17E-02	1.66E-02	4.90E-02	
22	30.76				2.28E-02	1.77E-02	5.23E-02	
23	32.13				2.38E-02	1.87E-02	5.52E-02	
24	33.50				2.47E-02	1.96E-02	5.80E-02	
25	34.87				2.58E-02	2.07E-02	6.10E-02	
26	36.23				2.68E-02	2.17E-02		
Proj.	38				2.81E-02	2.30E-02		
	42				3.10E-02	2.59E-02		
	46				3.39E-02	2.88E-02		
	50				3.67E-02	3.16E-02		
	54				3.96E-02	3.45E-02		
Proj. with bias	38				2.82E-02	2.31E-02		
	42				3.14E-02	2.63E-02		
	46				3.46E-02	2.95E-02		
	50				3.78E-02	3.27E-02		
	54				4.10E-02	3.59E-02		

Table 6-4 Surveillance Capsule Lead Factors

Cycle	Total Time (EFPY)	Lead Factors						
		S (40°)	Y / T / Z (40°)	V (4/40°)	U / W / X (4°)	A (4°)	B (40°)	C / D (40°)
1	1.26	3.44	3.44	1.00	1.00			
2	2.27		3.44	1.01	1.01			
3	3.44		3.44	0.95	0.95			
4	4.48		3.43	0.97	0.97			
5	5.86		3.43	1.01	1.01			
6	7.13			1.34	1.04	0.17	0.47	0.47
7	8.45			1.60	1.07	0.30	0.84	0.84
8	9.73			1.78	1.08	0.39	1.09	1.09
9	11.35			1.96	1.10	0.49	1.35	1.35
10	12.83			2.10	1.10	0.55	1.55	1.55
11	14.23			2.20	1.12	0.61	1.68	1.68
12	15.84				1.13	0.67	1.84	1.84
13	17.18				1.14	0.71	1.95	
14	18.57				1.14	0.74	2.05	
15	20.19				1.14	0.77	2.15	
16	21.68				1.16	0.80	2.23	
17	23.10				1.16	0.82	2.29	
18	24.70				1.16	0.84	2.36	
19	26.19				1.16	0.86	2.41	
20	27.63				1.16	0.88	2.45	
21	29.23				1.16	0.89	2.51	
22	30.76				1.16	0.90	2.55	
23	32.13				1.16	0.91	2.58	
24	33.50				1.16	0.92	2.62	
25	34.87				1.17	0.94	2.65	
26	36.23				1.17	0.95		
Proj. / Proj. with bias	38				1.17 / 1.17	0.96 / 0.96		
	42				1.18 / 1.18	0.98 / 0.99		
	46				1.18 / 1.18	1.00 / 1.01		
	50				1.18 / 1.19	1.02 / 1.03		
	54				1.19 / 1.19	1.03 / 1.04		

Table 6-5 Fast Neutron (E > 1.0 MeV) Fluence Rate at the RPV Clad/Base Metal Interface

Cycle	Cycle Length (EFPY)	Total Time (EFPY)	Fast Neutron (E > 1.0 MeV) Fluence Rate (n/cm²-s)					Azimuth of Max. (°)	Axial Location of Max. (cm)
			0°	15°	30°	45°(1)	Maximum		
1	1.26	1.26	6.56E+09	1.09E+10	1.35E+10	2.14E+10	2.14E+10	45	-11
2	1.01	2.27	5.88E+09	8.61E+09	1.17E+10	1.80E+10	1.80E+10	45	-11
3	1.17	3.44	4.58E+09	7.80E+09	1.16E+10	1.83E+10	1.83E+10	45	-11
4	1.04	4.48	4.90E+09	7.83E+09	9.72E+09	1.50E+10	1.50E+10	45	39
5	1.38	5.86	4.57E+09	7.20E+09	8.85E+09	1.23E+10	1.23E+10	45	-7
6	1.28	7.13	4.80E+09	7.84E+09	8.94E+09	1.24E+10	1.24E+10	45	-11
7	1.32	8.45	4.61E+09	7.72E+09	9.04E+09	1.22E+10	1.22E+10	45	-11
8	1.28	9.73	4.14E+09	7.06E+09	8.37E+09	1.13E+10	1.13E+10	45	91
9	1.62	11.35	4.50E+09	7.14E+09	8.47E+09	1.15E+10	1.15E+10	45	-11
10	1.48	12.83	3.97E+09	7.41E+09	8.78E+09	1.12E+10	1.12E+10	45	-11
11	1.41	14.23	4.18E+09	8.06E+09	8.97E+09	1.01E+10	1.01E+10	45	-11
12	1.61	15.84	4.53E+09	7.20E+09	8.59E+09	1.16E+10	1.16E+10	45	-11
13	1.34	17.18	4.77E+09	7.61E+09	8.89E+09	1.21E+10	1.21E+10	45	-11
14	1.39	18.57	4.09E+09	6.74E+09	8.57E+09	1.16E+10	1.16E+10	45	-11
15	1.62	20.19	4.40E+09	6.66E+09	8.59E+09	1.19E+10	1.19E+10	45	-69
16	1.49	21.68	4.63E+09	7.34E+09	8.54E+09	1.14E+10	1.14E+10	45	43
17	1.42	23.10	4.21E+09	6.88E+09	8.28E+09	1.11E+10	1.11E+10	45	45
18	1.60	24.70	4.19E+09	6.89E+09	8.29E+09	1.15E+10	1.15E+10	45	43
19	1.50	26.19	4.27E+09	6.97E+09	8.20E+09	1.09E+10	1.09E+10	45	45
20	1.44	27.63	3.94E+09	6.81E+09	8.16E+09	1.08E+10	1.08E+10	45	45
21	1.60	29.23	4.35E+09	6.89E+09	8.53E+09	1.28E+10	1.28E+10	45	-69
22	1.53	30.76	4.36E+09	7.14E+09	8.59E+09	1.16E+10	1.16E+10	45	45
23	1.37	32.13	4.46E+09	6.94E+09	8.64E+09	1.16E+10	1.16E+10	45	43
24	1.37	33.50	4.19E+09	6.55E+09	8.26E+09	1.13E+10	1.13E+10	45	-11
25	1.37	34.87	4.74E+09	7.04E+09	8.68E+09	1.19E+10	1.19E+10	45	41
26	1.36	36.23	4.64E+09	7.15E+09	8.92E+09	1.18E+10	1.18E+10	45	41
Proj.	no bias	--	4.46E+09	6.94E+09	8.64E+09	1.16E+10	1.16E+10	45	43
Proj.	with bias	--	4.95E+09	7.70E+09	9.58E+09	1.29E+10	1.29E+10	45	43

Table 6-6 Fast Neutron (E > 1.0 MeV) Fluence at the Pressure Vessel Clad/Base Metal Interface

Cycle	Cycle Length (EFPY)	Total Time (EFPY)	Fast Neutron (E > 1.0 MeV) Fluence (n/cm²)					Azimuth of Max. (°)	Axial Location of Max. (cm)
			0°	15°	30°	45°	Maximum		
1	1.26	1.26	2.61E+17	4.32E+17	5.39E+17	8.51E+17	8.51E+17	45	-11
2	1.01	2.27	4.47E+17	7.05E+17	9.10E+17	1.42E+18	1.42E+18	45	-11
3	1.17	3.44	6.15E+17	9.94E+17	1.34E+18	2.10E+18	2.10E+18	45	-11
4	1.04	4.48	7.76E+17	1.25E+18	1.66E+18	2.59E+18	2.59E+18	45	-11
5	1.38	5.86	9.74E+17	1.56E+18	2.04E+18	3.12E+18	3.12E+18	45	-11
6	1.28	7.13	1.17E+18	1.88E+18	2.40E+18	3.63E+18	3.63E+18	45	-11
7	1.32	8.45	1.36E+18	2.20E+18	2.78E+18	4.13E+18	4.13E+18	45	-11
8	1.28	9.73	1.52E+18	2.48E+18	3.11E+18	4.58E+18	4.58E+18	45	-11
9	1.62	11.35	1.75E+18	2.84E+18	3.54E+18	5.17E+18	5.17E+18	45	-11
10	1.48	12.83	1.94E+18	3.19E+18	3.95E+18	5.69E+18	5.69E+18	45	-11
11	1.41	14.23	2.12E+18	3.55E+18	4.35E+18	6.14E+18	6.14E+18	45	-11
12	1.61	15.84	2.35E+18	3.91E+18	4.79E+18	6.73E+18	6.73E+18	45	-11
13	1.34	17.18	2.55E+18	4.23E+18	5.16E+18	7.24E+18	7.24E+18	45	-11
14	1.39	18.57	2.73E+18	4.53E+18	5.54E+18	7.75E+18	7.75E+18	45	-11
15	1.62	20.19	2.95E+18	4.87E+18	5.97E+18	8.35E+18	8.35E+18	45	-11
16	1.49	21.68	3.16E+18	5.21E+18	6.37E+18	8.88E+18	8.88E+18	45	-11
17	1.42	23.10	3.35E+18	5.51E+18	6.74E+18	9.38E+18	9.38E+18	45	-11
18	1.60	24.70	3.56E+18	5.86E+18	7.16E+18	9.96E+18	9.96E+18	45	-11
19	1.50	26.19	3.76E+18	6.19E+18	7.54E+18	1.05E+19	1.05E+19	45	-11
20	1.44	27.63	3.94E+18	6.49E+18	7.91E+18	1.10E+19	1.10E+19	45	-11
21	1.60	29.23	4.16E+18	6.84E+18	8.34E+18	1.16E+19	1.16E+19	45	-11
22	1.53	30.76	4.37E+18	7.18E+18	8.75E+18	1.22E+19	1.22E+19	45	-11
23	1.37	32.13	4.57E+18	7.48E+18	9.12E+18	1.27E+19	1.27E+19	45	-11
24	1.37	33.50	4.75E+18	7.76E+18	9.48E+18	1.32E+19	1.32E+19	45	-11
25	1.37	34.87	4.95E+18	8.06E+18	9.85E+18	1.37E+19	1.37E+19	45	-11
26	1.36	36.23	5.15E+18	8.37E+18	1.02E+19	1.42E+19	1.42E+19	45	-11

Table 6-6 Fast Neutron (E > 1.0 MeV) Fluence at the Pressure Vessel Clad/Base Metal Interface

Cycle	Cycle Length (EFPY)	Total Time (EFPY)	Fast Neutron (E > 1.0 MeV) Fluence (n/cm^2)					Azimuth of Max. (°)	Axial Location of Max. (cm)
			0°	15°	30°	45°	Maximum		
Projection with no bias on peripheral and re-entrant corner fuel assemblies									
		38	5.40E+18	8.76E+18	1.07E+19	1.48E+19	1.48E+19	45	-11
		42	5.96E+18	9.63E+18	1.18E+19	1.63E+19	1.63E+19	45	-11
		46	6.53E+18	1.05E+19	1.29E+19	1.78E+19	1.78E+19	45	-11
		50	7.09E+18	1.14E+19	1.40E+19	1.92E+19	1.92E+19	45	-11
		54	7.66E+18	1.23E+19	1.51E+19	2.07E+19	2.07E+19	45	-11
Projection with 10% positive bias on peripheral fuel and re-entrant corner assemblies									
		38	5.43E+18	8.80E+18	1.08E+19	1.49E+19	1.49E+19	45	-11
		42	6.05E+18	9.77E+18	1.20E+19	1.65E+19	1.65E+19	45	-11
		46	6.68E+18	1.07E+19	1.32E+19	1.81E+19	1.81E+19	45	-11
		50	7.30E+18	1.17E+19	1.44E+19	1.98E+19	1.98E+19	45	-11
		54	7.93E+18	1.27E+19	1.56E+19	2.14E+19	2.14E+19	45	-11

Table 6-7 Iron Atom Displacement Rate at the Pressure Vessel Clad/Base Metal Interface

Cycle	Cycle Length (EFPY)	Total Time (EFPY)	Iron Atom Displacement Rate (dpa/s)					Azimuth of Max. (°)	Axial Location of Max. (cm)
			0°	15°	30°	45°	Maximum		
1	1.26	1.26	1.06E-11	1.74E-11	2.19E-11	3.45E-11	3.45E-11	44	-11
2	1.01	2.27	9.42E-12	1.38E-11	1.88E-11	2.90E-11	2.91E-11	44	-11
3	1.17	3.44	7.40E-12	1.25E-11	1.87E-11	2.95E-11	2.96E-11	44	-11
4	1.04	4.48	7.92E-12	1.25E-11	1.57E-11	2.41E-11	2.41E-11	44	39
5	1.38	5.86	7.39E-12	1.15E-11	1.42E-11	1.99E-11	1.99E-11	44	-11
6	1.28	7.13	7.74E-12	1.25E-11	1.44E-11	2.00E-11	2.01E-11	44	-11
7	1.32	8.45	7.44E-12	1.23E-11	1.46E-11	1.97E-11	1.97E-11	44	-11
8	1.28	9.73	6.64E-12	1.13E-11	1.35E-11	1.82E-11	1.82E-11	44	93
9	1.62	11.35	7.27E-12	1.14E-11	1.36E-11	1.86E-11	1.86E-11	44	-11
10	1.48	12.83	6.43E-12	1.18E-11	1.41E-11	1.81E-11	1.81E-11	44	-11
11	1.41	14.23	6.77E-12	1.29E-11	1.44E-11	1.63E-11	1.63E-11	44	-11
12	1.61	15.84	7.32E-12	1.15E-11	1.38E-11	1.87E-11	1.88E-11	44	-11
13	1.34	17.18	7.66E-12	1.22E-11	1.43E-11	1.95E-11	1.95E-11	44	-11
14	1.39	18.57	6.57E-12	1.08E-11	1.38E-11	1.87E-11	1.87E-11	44	-11
15	1.62	20.19	7.04E-12	1.06E-11	1.38E-11	1.91E-11	1.91E-11	44	-11
16	1.49	21.68	7.48E-12	1.17E-11	1.38E-11	1.84E-11	1.84E-11	44	45
17	1.42	23.10	6.76E-12	1.10E-11	1.33E-11	1.79E-11	1.80E-11	44	45
18	1.60	24.70	6.72E-12	1.10E-11	1.33E-11	1.85E-11	1.85E-11	44	45
19	1.50	26.19	6.84E-12	1.11E-11	1.32E-11	1.76E-11	1.76E-11	44	45
20	1.44	27.63	6.33E-12	1.09E-11	1.31E-11	1.74E-11	1.74E-11	44	45
21	1.60	29.23	6.97E-12	1.10E-11	1.37E-11	2.06E-11	2.07E-11	44	43
22	1.53	30.76	6.99E-12	1.14E-11	1.38E-11	1.86E-11	1.87E-11	44	45
23	1.37	32.13	7.16E-12	1.11E-11	1.39E-11	1.88E-11	1.88E-11	44	45
24	1.37	33.50	6.71E-12	1.05E-11	1.33E-11	1.83E-11	1.83E-11	44	41
25	1.37	34.87	7.60E-12	1.13E-11	1.40E-11	1.92E-11	1.93E-11	44	41
26	1.36	36.23	7.44E-12	1.14E-11	1.43E-11	1.90E-11	1.90E-11	44	41
Proj.	no bias	--	7.16E-12	1.11E-11	1.39E-11	1.88E-11	1.88E-11	44	45
Proj.	with bias	--	7.94E-12	1.23E-11	1.54E-11	2.08E-11	2.09E-11	44	45

Table 6-8 Iron Atom Displacements at the Pressure Vessel Clad/Base Metal Interface

Cycle	Cycle Length (EFPY)	Total Time (EFPY)	Iron Atom Displacements (dpa)					Azimuth of Max. (°)	Axial Location of Max. (cm)
			0°	15°	30°	45°	Maximum		
1	1.26	1.26	4.22E-04	6.91E-04	8.69E-04	1.37E-03	1.37E-03	44	-11
2	1.01	2.27	7.21E-04	1.13E-03	1.47E-03	2.30E-03	2.30E-03	44	-11
3	1.17	3.44	9.94E-04	1.59E-03	2.16E-03	3.39E-03	3.39E-03	44	-11
4	1.04	4.48	1.25E-03	2.00E-03	2.67E-03	4.17E-03	4.18E-03	44	-11
5	1.38	5.86	1.57E-03	2.50E-03	3.29E-03	5.03E-03	5.04E-03	44	-11
6	1.28	7.13	1.89E-03	3.00E-03	3.87E-03	5.84E-03	5.85E-03	44	-11
7	1.32	8.45	2.20E-03	3.52E-03	4.48E-03	6.66E-03	6.67E-03	44	-11
8	1.28	9.73	2.46E-03	3.96E-03	5.01E-03	7.38E-03	7.39E-03	44	-11
9	1.62	11.35	2.83E-03	4.55E-03	5.70E-03	8.32E-03	8.34E-03	44	-11
10	1.48	12.83	3.13E-03	5.10E-03	6.37E-03	9.17E-03	9.18E-03	44	-11
11	1.41	14.23	3.43E-03	5.67E-03	7.01E-03	9.89E-03	9.91E-03	44	-11
12	1.61	15.84	3.80E-03	6.25E-03	7.71E-03	1.08E-02	1.09E-02	44	-11
13	1.34	17.18	4.13E-03	6.77E-03	8.31E-03	1.17E-02	1.17E-02	44	-11
14	1.39	18.57	4.41E-03	7.24E-03	8.91E-03	1.25E-02	1.25E-02	44	-11
15	1.62	20.19	4.77E-03	7.78E-03	9.62E-03	1.35E-02	1.35E-02	44	-11
16	1.49	21.68	5.12E-03	8.33E-03	1.03E-02	1.43E-02	1.43E-02	44	-11
17	1.42	23.10	5.42E-03	8.82E-03	1.09E-02	1.51E-02	1.51E-02	44	-11
18	1.60	24.70	5.75E-03	9.37E-03	1.15E-02	1.60E-02	1.61E-02	44	-11
19	1.50	26.19	6.07E-03	9.89E-03	1.21E-02	1.69E-02	1.69E-02	44	-11
20	1.44	27.63	6.36E-03	1.04E-02	1.27E-02	1.77E-02	1.77E-02	44	-11
21	1.60	29.23	6.71E-03	1.09E-02	1.34E-02	1.87E-02	1.87E-02	44	-11
22	1.53	30.76	7.04E-03	1.15E-02	1.41E-02	1.96E-02	1.96E-02	44	-11
23	1.37	32.13	7.35E-03	1.20E-02	1.47E-02	2.04E-02	2.04E-02	44	-11
24	1.37	33.50	7.64E-03	1.24E-02	1.53E-02	2.12E-02	2.12E-02	44	-11
25	1.37	34.87	7.96E-03	1.29E-02	1.59E-02	2.20E-02	2.21E-02	44	-11
26	1.36	36.23	8.28E-03	1.34E-02	1.65E-02	2.28E-02	2.29E-02	44	-11

Table 6-8 Iron Atom Displacements at the Pressure Vessel Clad/Base Metal Interface

Cycle	Cycle Length (EFPY)	Total Time (EFPY)	Iron Atom Displacements (dpa)					Azimuth of Max. (°)	Axial Location of Max. (cm)
			0°	15°	30°	45°	Maximum		
Projection with no bias on peripheral and re-entrant corner fuel assemblies									
		38	8.68E-03	1.40E-02	1.73E-02	2.39E-02	2.39E-02	44	-11
		42	9.58E-03	1.54E-02	1.90E-02	2.63E-02	2.63E-02	44	-11
		46	1.05E-02	1.68E-02	2.08E-02	2.86E-02	2.87E-02	44	-11
		50	1.14E-02	1.82E-02	2.25E-02	3.10E-02	3.10E-02	44	-11
		54	1.23E-02	1.96E-02	2.43E-02	3.33E-02	3.34E-02	44	-11
Projection with 10% positive bias on peripheral fuel and re-entrant corner assemblies									
		38	8.72E-03	1.41E-02	1.73E-02	2.40E-02	2.40E-02	44	-11
		42	9.72E-03	1.56E-02	1.93E-02	2.66E-02	2.67E-02	44	-11
		46	1.07E-02	1.72E-02	2.12E-02	2.92E-02	2.93E-02	44	-11
		50	1.17E-02	1.87E-02	2.32E-02	3.19E-02	3.19E-02	44	-11
		54	1.27E-02	2.03E-02	2.51E-02	3.45E-02	3.45E-02	44	-11

Table 6-9 Fast Neutron (E > 1.0 MeV) Neutron Fluence at Pressure Vessel Welds and Shells

Material	Fast Neutron (E > 1.0 MeV) Fluence (n/cm^2)				
	Projection with no bias on peripheral and re-entrant corner fuel assemblies[1]				
	38 EFPY	**42 EFPY**	**46 EFPY**	**50 EFPY**	**54 EFPY**
Upper Shell Plates (B4105-1, -2, -3)	1.60E+17	1.77E+17	1.94E+17	2.11E+17	2.28E+17
Intermediate Shell Plates (B4106-1, -2, -3)	1.48E+19	1.63E+19	1.78E+19	1.92E+19	2.07E+19
Lower Shell Plates (B4107-1, -2, -3)	1.47E+19	1.61E+19	1.76E+19	1.91E+19	2.05E+19
Inlet Nozzle Weld, lowest extent	2.03E+16	2.25E+16	2.46E+16	2.68E+16	2.90E+16
Outlet Nozzle Weld, lowest extent	1.50E+16	1.66E+16	1.82E+16	1.98E+16	2.14E+16
Upper Shell to Intermediate Shell Circumferential Weld (8-442)	1.82E+17	2.01E+17	2.20E+17	2.40E+17	2.59E+17
Upper Shell Longitudinal Weld (1-442A)	1.18E+17	1.31E+17	1.44E+17	1.56E+17	1.69E+17
Upper Shell Longitudinal Weld (1-442B)	7.54E+16	8.35E+16	9.16E+16	9.97E+16	1.08E+17
Upper Shell Longitudinal Weld (1-442C)	1.45E+17	1.61E+17	1.76E+17	1.92E+17	2.07E+17
Intermediate Shell to Lower Shell Circumferential Weld (9-442)	1.44E+19	1.58E+19	1.72E+19	1.87E+19	2.01E+19
Intermediate Shell Longitudinal Weld (2-442A, -B)	1.07E+19	1.18E+19	1.29E+19	1.40E+19	1.51E+19
Intermediate Shell Longitudinal Weld (2-442C)	5.37E+18	5.92E+18	6.48E+18	7.03E+18	7.59E+18
Lower Shell Longitudinal Weld (3-442A, -B)	8.72E+18	9.59E+18	1.05E+19	1.13E+19	1.22E+19
Lower Shell Longitudinal Weld (3-442C)	1.47E+19	1.61E+19	1.76E+19	1.91E+19	2.05E+19
Lower Shell to Lower Vessel Head Circumferential Weld (10-442)	3.70E+15	4.09E+15	4.47E+15	4.86E+15	5.25E+15

Table 6-9 Fast Neutron (E > 1.0 MeV) Neutron Fluence at Pressure Vessel Welds and Shells

Material	Fast Neutron (E > 1.0 MeV) Fluence (n/cm^2)				
	Projection with 10% positive bias on peripheral fuel and re-entrant corner assemblies[2]				
	38 EFPY	**42 EFPY**	**46 EFPY**	**50 EFPY**	**54 EFPY**
Upper Shell Plates (B4105-1, -2, -3)	1.61E+17	1.80E+17	1.98E+17	2.17E+17	2.36E+17
Intermediate Shell Plates (B4106-1, -2, -3)	1.49E+19	1.65E+19	1.81E+19	1.98E+19	2.14E+19
Lower Shell Plates (B4107-1, -2, -3)	1.47E+19	1.64E+19	1.80E+19	1.96E+19	2.12E+19
Inlet Nozzle Weld, lowest extent	2.04E+16	2.28E+16	2.52E+16	2.76E+16	3.00E+16
Outlet Nozzle Weld, lowest extent	1.51E+16	1.68E+16	1.86E+16	2.04E+16	2.21E+16
Upper Shell to Intermediate Shell Circumferential Weld (8-442)	1.83E+17	2.04E+17	2.26E+17	2.47E+17	2.68E+17
Upper Shell Longitudinal Weld (1-442A)	1.19E+17	1.33E+17	1.47E+17	1.61E+17	1.75E+17
Upper Shell Longitudinal Weld (1-442B)	7.58E+16	8.48E+16	9.37E+16	1.03E+17	1.12E+17
Upper Shell Longitudinal Weld (1-442C)	1.46E+17	1.63E+17	1.80E+17	1.98E+17	2.15E+17
Intermediate Shell to Lower Shell Circumferential Weld (9-442)	1.45E+19	1.60E+19	1.76E+19	1.92E+19	2.08E+19
Intermediate Shell Longitudinal Weld (2-442A, -B)	1.08E+19	1.20E+19	1.32E+19	1.44E+19	1.56E+19
Intermediate Shell Longitudinal Weld (2-442C)	5.39E+18	6.01E+18	6.63E+18	7.24E+18	7.86E+18
Lower Shell Longitudinal Weld (3-442A, -B)	8.76E+18	9.73E+18	1.07E+19	1.17E+19	1.26E+19
Lower Shell Longitudinal Weld (3-442C)	1.47E+19	1.64E+19	1.80E+19	1.96E+19	2.12E+19
Lower Shell to Lower Vessel Head Circumferential Weld (10-442)	3.72E+15	4.15E+15	4.58E+15	5.00E+15	5.43E+15

Note(s):

1. Values beyond Cycle 26 are based on core power distributions and reactor operating conditions of Cycle 23.
2. Values beyond Cycle 26 are based on core power distributions and reactor operating conditions of Cycle 23 but include a +10% bias on peripheral and re-entrant corner assembly relative powers.

Table 6-10 Iron Atom Displacements at Pressure Vessel Welds and Shells

Material	**Iron Atom Displacement (dpa)**				
	Projection with no bias on peripheral and re-entrant corner fuel assemblies[1]				
	38 EFPY	**42 EFPY**	**46 EFPY**	**50 EFPY**	**54 EFPY**
Upper Shell Plates (B4105-1, -2, -3)	2.79E-04	3.09E-04	3.38E-04	3.68E-04	3.98E-04
Intermediate Shell Plates (B4106-1, -2, -3)	2.39E-02	2.63E-02	2.87E-02	3.10E-02	3.34E-02
Lower Shell Plates (B4107-1, -2, -3)	2.36E-02	2.59E-02	2.83E-02	3.06E-02	3.30E-02
Inlet Nozzle Weld, lowest extent	1.01E-04	1.12E-04	1.22E-04	1.33E-04	1.44E-04
Outlet Nozzle Weld, lowest extent	8.87E-05	9.80E-05	1.07E-04	1.17E-04	1.26E-04
Upper Shell to Intermediate Shell Circumferential Weld (8-442)	3.15E-04	3.48E-04	3.82E-04	4.15E-04	4.48E-04
Upper Shell Longitudinal Weld (1-442A)	2.10E-04	2.33E-04	2.55E-04	2.77E-04	2.99E-04
Upper Shell Longitudinal Weld (1-442B)	1.34E-04	1.49E-04	1.63E-04	1.78E-04	1.92E-04
Upper Shell Longitudinal Weld (1-442C)	2.55E-04	2.82E-04	3.09E-04	3.37E-04	3.64E-04
Intermediate Shell to Lower Shell Circumferential Weld (9-442)	2.33E-02	2.56E-02	2.79E-02	3.03E-02	3.26E-02
Intermediate Shell Longitudinal Weld (2-442A, -B)	1.72E-02	1.90E-02	2.07E-02	2.25E-02	2.42E-02
Intermediate Shell Longitudinal Weld (2-442C)	8.68E-03	9.58E-03	1.05E-02	1.14E-02	1.23E-02
Lower Shell Longitudinal Weld (3-442A, -B)	1.39E-02	1.53E-02	1.67E-02	1.81E-02	1.95E-02
Lower Shell Longitudinal Weld (3-442C)	2.36E-02	2.59E-02	2.83E-02	3.06E-02	3.30E-02
Lower Shell to Lower Vessel Head Circumferential Weld (10-442)	2.40E-05	2.65E-05	2.90E-05	3.16E-05	3.41E-05

Table 6-10 Iron Atom Displacements at Pressure Vessel Welds and Shells

Material	**Iron Atom Displacement (dpa)**				
	Projection with 10% positive bias on peripheral fuel and re-entrant corner assemblies[2]				
	38 EFPY	**42 EFPY**	**46 EFPY**	**50 EFPY**	**54 EFPY**
Upper Shell Plates (B4105-1, -2, -3)	2.80E-04	3.13E-04	3.46E-04	3.79E-04	4.12E-04
Intermediate Shell Plates (B4106-1, -2, -3)	2.40E-02	2.67E-02	2.93E-02	3.19E-02	3.45E-02
Lower Shell Plates (B4107-1, -2, -3)	2.37E-02	2.63E-02	2.89E-02	3.15E-02	3.41E-02
Inlet Nozzle Weld, lowest extent	1.02E-04	1.14E-04	1.25E-04	1.37E-04	1.49E-04
Outlet Nozzle Weld, lowest extent	8.92E-05	9.95E-05	1.10E-04	1.20E-04	1.30E-04
Upper Shell to Intermediate Shell Circumferential Weld (8-442)	3.17E-04	3.54E-04	3.91E-04	4.28E-04	4.65E-04
Upper Shell Longitudinal Weld (1-442A)	2.11E-04	2.36E-04	2.61E-04	2.86E-04	3.10E-04
Upper Shell Longitudinal Weld (1-442B)	1.35E-04	1.51E-04	1.67E-04	1.83E-04	1.99E-04
Upper Shell Longitudinal Weld (1-442C)	2.56E-04	2.87E-04	3.17E-04	3.47E-04	3.77E-04
Intermediate Shell to Lower Shell Circumferential Weld (9-442)	2.34E-02	2.60E-02	2.86E-02	3.11E-02	3.37E-02
Intermediate Shell Longitudinal Weld (2-442A, -B)	1.73E-02	1.93E-02	2.12E-02	2.31E-02	2.51E-02
Intermediate Shell Longitudinal Weld (2-442C)	8.72E-03	9.72E-03	1.07E-02	1.17E-02	1.27E-02
Lower Shell Longitudinal Weld (3-442A, -B)	1.40E-02	1.56E-02	1.71E-02	1.87E-02	2.02E-02
Lower Shell Longitudinal Weld (3-442C)	2.37E-02	2.63E-02	2.89E-02	3.15E-02	3.41E-02
Lower Shell to Lower Vessel Head Circumferential Weld (10-442)	2.42E-05	2.69E-05	2.97E-05	3.25E-05	3.53E-05

Note(s):

1. Values beyond Cycle 26 are based on core power distributions and reactor operating conditions of Cycle 23.
2. Values beyond Cycle 26 are based on core power distributions and reactor operating conditions of Cycle 23 but include a +10% bias on peripheral and re-entrant corner assembly relative powers.

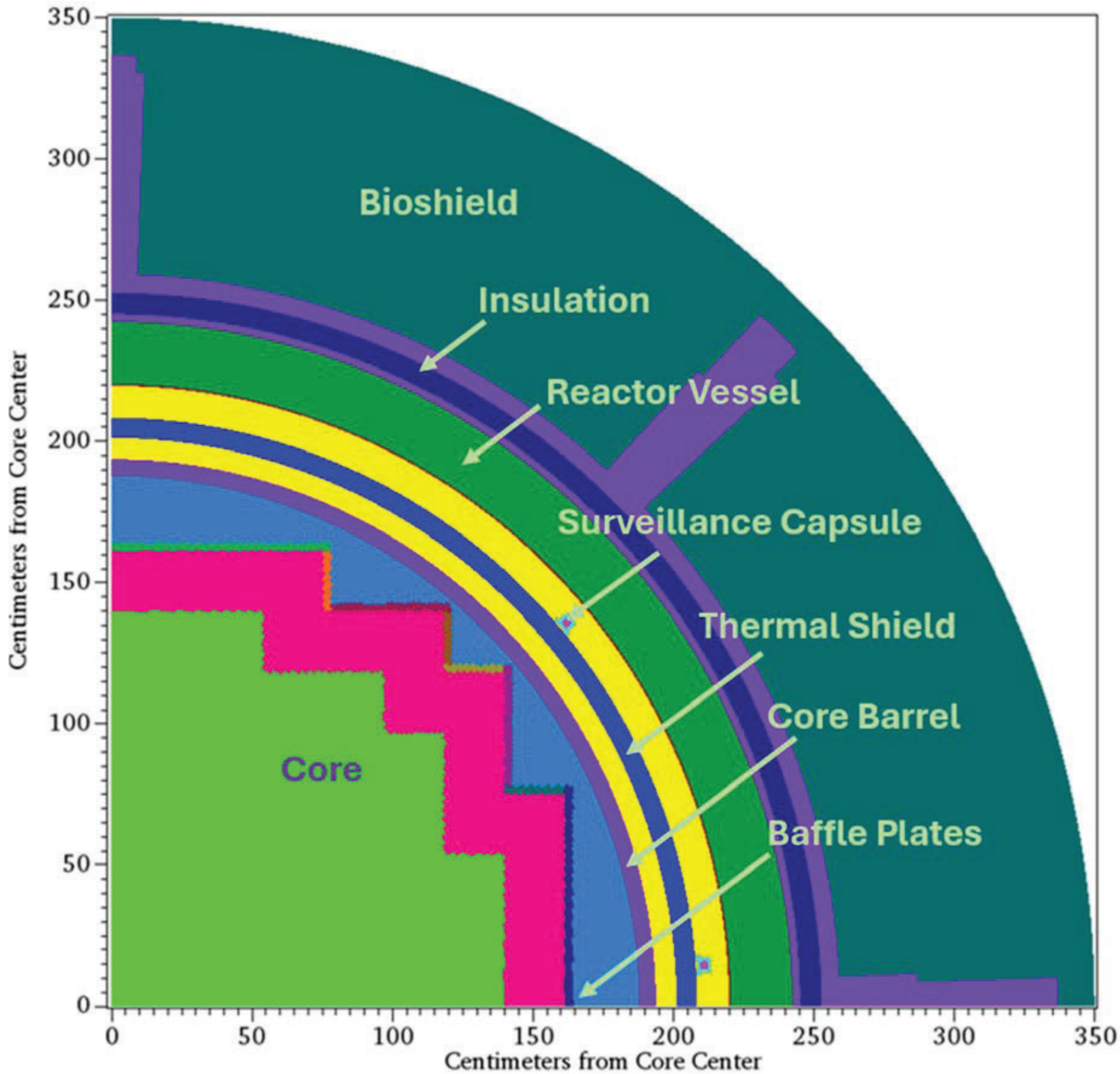

Figure 6-1 Plan View of the Reactor Geometry at the Core Centerline

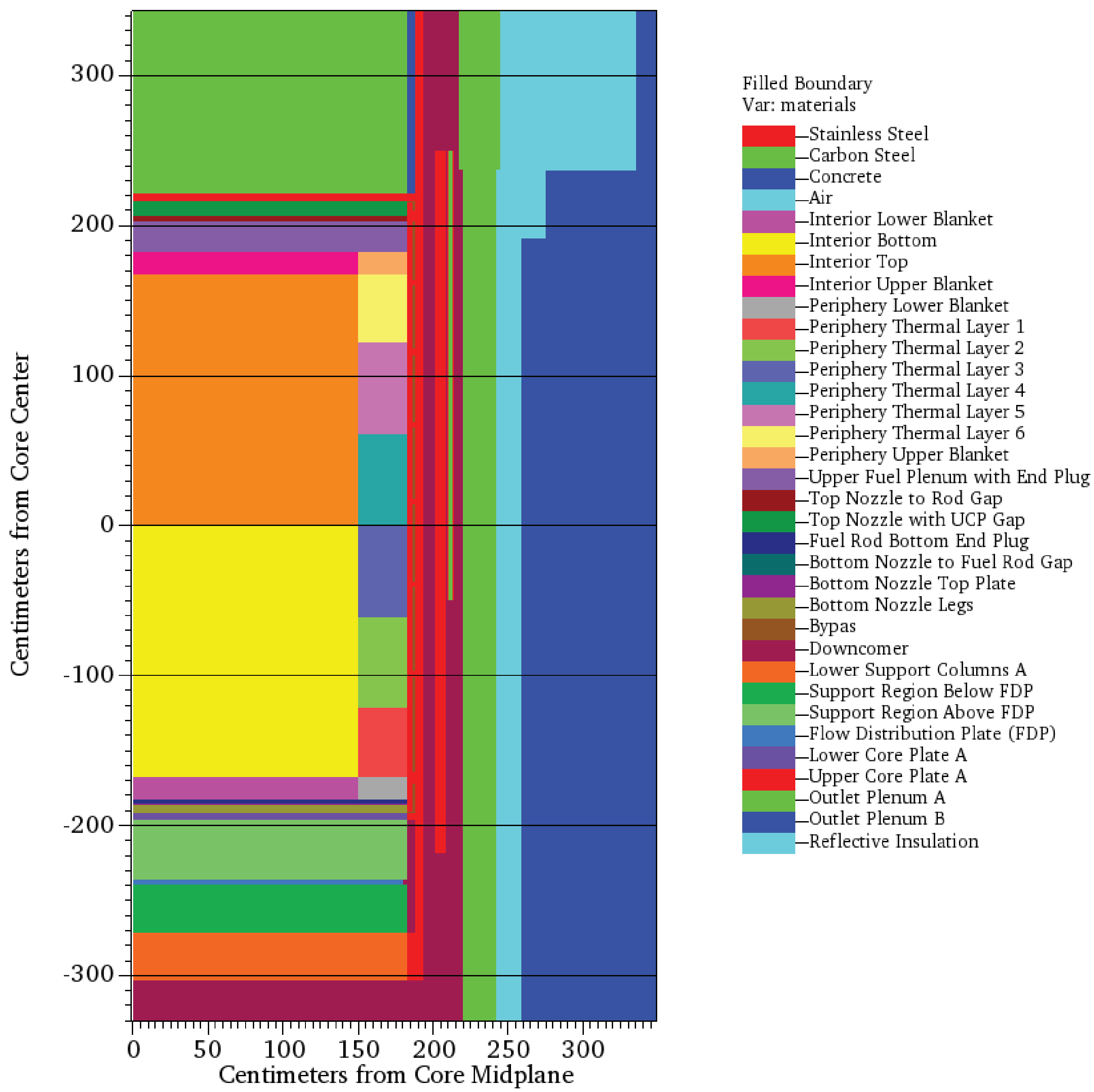

Figure 6-2 Section View of the Reactor Geometry at 40°

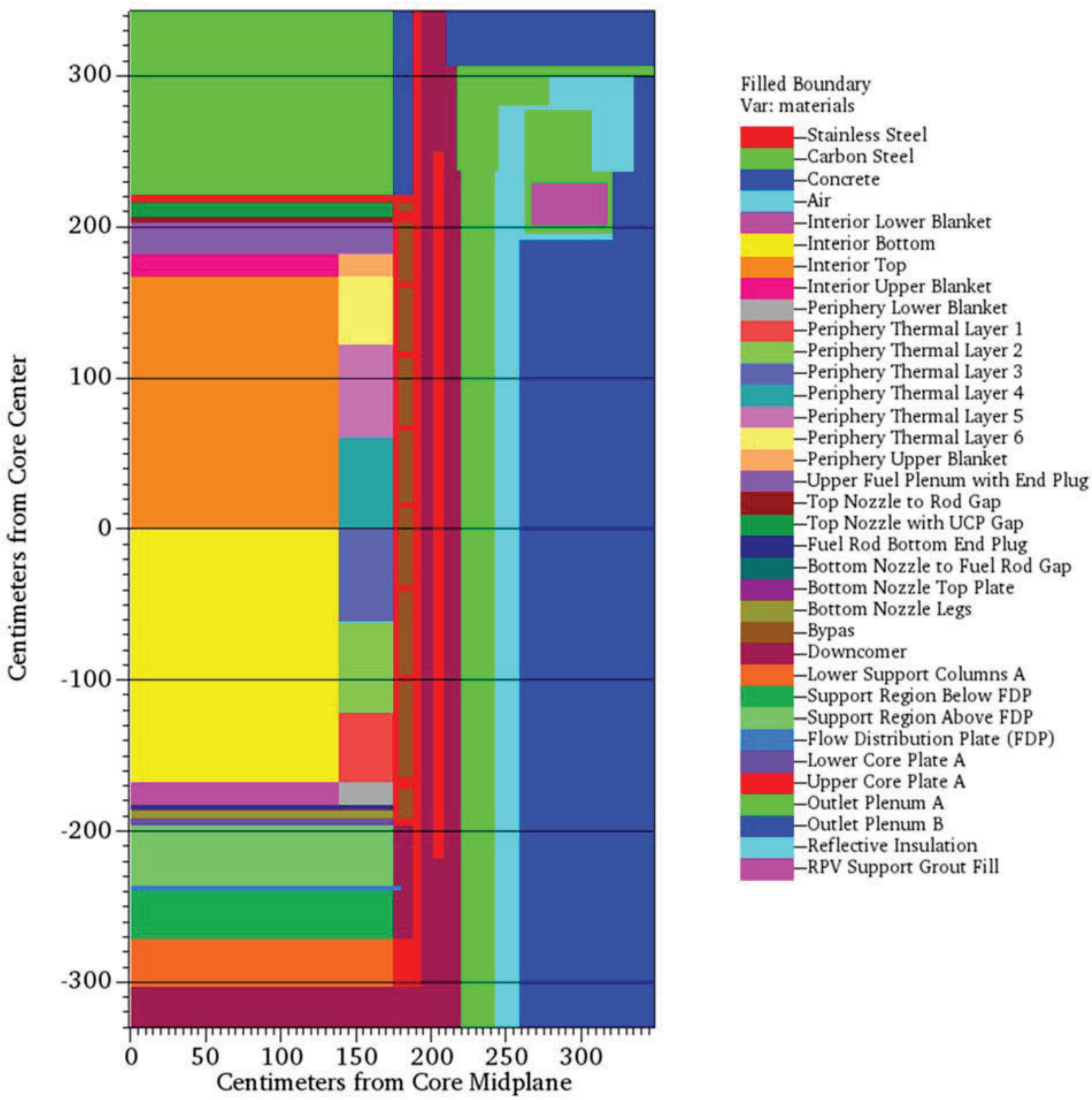

Figure 6-3 Section View of the Reactor Geometry at the Outlet Nozzle (22°)

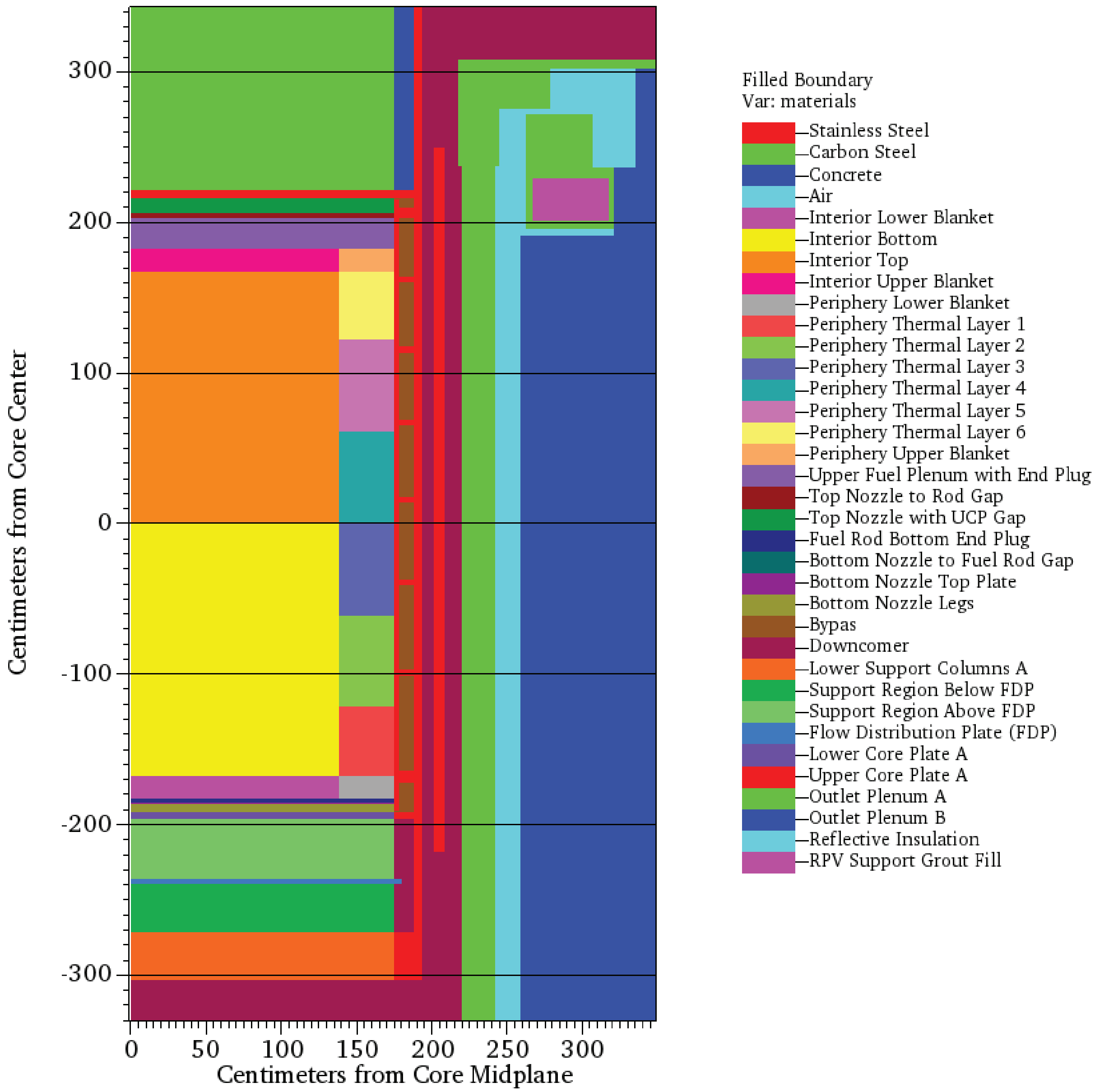

Figure 6-4 Section View of the Reactor Geometry at the Inlet Nozzle (67°)

7 SURVEILLANCE CAPSULE REMOVAL SCHEDULE

The following surveillance capsule removal schedule (Table 7-1) meets the requirements of ASTM E185-82 [10] with consideration of NUREG-1801 [7].

Table 7-1 Diablo Canyon Unit 1 Surveillance Capsule Withdrawal Schedule

Capsule(4)(5)	Capsule Location	Azimuthal Location	Lead Factor	Removal Time(1)	Capsule Fluence (n/cm^2, E > 1.0 MeV)
S	320°	40°	3.44	1.26 (Tested, EOC 1)	2.93×10^{18}
Y	40°	40°	3.43	5.86 (Tested, EOC 5)	1.07×10^{19}
T	140°	40°	3.43	5.86 (Removed, EOC 5)	1.07×10^{19}
Z	220°	40°	3.43	5.86 (Removed, EOC 5)	1.07×10^{19}
V	320° (184°)(2)	4° (40°)(2)	2.20	14.23 (Tested, EOC 11)	1.35×10^{19}
C(3)	140°	40°	1.84	15.84 (Removed, EOC 12)	1.24×10^{19}
D(3)	220°	40°	1.84	15.84 (Removed, EOC 12)	1.24×10^{19}
B(3)	40°	40°	2.65	34.87 (Tested, EOC 25)	3.62×10^{19}
A(3)	184°	4°	1.04	Standby	---
U	356°	4°	1.19	Standby	---
X	176°	4°	1.19	Standby	---
W	4°	4°	1.19	Standby	---

Notes:

1. Effective full power years (EFPY) from plant startup. End of Cycle (EOC) value given in parenthesis.
2. Capsule V was irradiated at the 184° (4°) location during Cycles 1-5, then relocated and irradiated at the 320° (40°) location for Cycles 6-11, prior to withdrawal after EOC 11 per WCAP-18924-NP [21].
3. Four (4) supplemental capsules (A, B, C, and D) were installed at 5.86 EFPY after EOC 5 per WCAP-13440 [16]. Capsules C, D, T and Z were removed from the reactor vessel and placed in the fuel pool.
4. Capsules T, U, W, X, and Z are Type 1 (base metal only).
5. Capsules S, V, and Y are Type 2 (base metal and weld).

8 REFERENCES

1. U.S. Nuclear Regulatory Commission, Office of Nuclear Regulatory Research, Regulatory Guide 1.99, Rev. 2, "Radiation Embrittlement of Reactor Vessel Materials," May 1988. *[Agencywide Documents Access and Management System (ADAMS) Accession Number ML003740284]*

2. Westinghouse Report, WCAP-8465, Rev. 0, "Pacific Gas and Electric Co. Diablo Canyon Unit No. 1 Reactor Vessel Radiation Surveillance Program," January 1975.

3. ASTM E185-70, "Standard Recommended Practice for Surveillance Tests for Nuclear Reactor Vessels," American Society for Testing and Materials, 1970.

4. Appendix G of the ASME Boiler and Pressure Vessel (B&PV) Code, Section XI, Division 1, Fracture Toughness Criteria for Protection Against Failure.

5. ASTM E208, Standard Test Method for Conducting Drop-Weight Test to Determine Nil-Ductility Transition Temperature of Ferritic Steels, ASTM.

6. ASTM International. ASTM E185-16 - Standard Practice for Design of Surveillance Programs for Light-Water Moderated Nuclear Power Reactor Vessels," American Society for Testing and Materials, 2016.

7. NUREG-1801, Rev. 2, "Generic Aging Lessons Learned (GALL) Report," December 2010, U.S. Nuclear Regulatory Commission Report. *[ADAMS Accession Number ML103490041]*

8. U.S. Nuclear Regulatory Commission, Office of Nuclear Regulatory Research, Regulatory Guide 1.190, "Calculational and Dosimetry Methods for Determining Pressure Vessel Neutron Fluence," March 2001. *[ADAMS Accession Number ML010890301]*

9. 10 CFR 50, Appendix H, "Reactor Vessel Material Surveillance Program Requirements," U.S. Nuclear Regulatory Commission, Federal Register.

10. ASTM E185-82, "Standard Practice for Conducting Surveillance Tests for Light-Water Cooled Nuclear Power Reactor Vessels," American Society for Testing and Materials, 1982.

11. ASTM E23-18, "Standard Test Methods for Notched Bar Impact Testing of Metallic Materials," American Society for Testing and Materials, 2018.

12. ASTM E2298-18, "Standard Test Method for Instrumented Impact Testing of Metallic Materials," American Society for Testing and Materials, 2018.

13. Westinghouse Report, WCAP-15958, Rev. 0, "Analysis of Capsule V from Pacific Gas and Electric Company Diablo Canyon Unit 1 Reactor Vessel Radiation Surveillance Program," January 2003.

14. ASTM E8/E8M-16a, Standard Test Methods for Tension Testing of Metallic Materials, 2016.

15. ASTM E21-17, Standard Test Methods for Elevated Temperature Tension Tests of Metallic Materials, 2017.

16. Westinghouse Report, WCAP-13440, Rev. 0, "Supplemental Reactor Vessel Radiation Surveillance Program for the Pacific Gas and Electric Company Diablo Canyon Unit No. 1," December 1992.

17. ASTM E853-23, Standard Practice for Analysis and Interpretation of Light-Water Reactor Surveillance Neutron Exposure Results, 2023.

18. ASTM E693-94, Standard Practice for Characterizing Neutron Exposures in Iron and Low Alloy Steels in Terms of Displacements Per Atom (DPA), 1994.

19. Westinghouse Report, WCAP-18124-NP-A, Rev. 0, "Fluence Determination with RAPTOR-M3G and FERRET," July 2018. *[ADAMS Accession Number ML18204A010]*

20. Westinghouse Report, WCAP-18124-NP-A Rev. 0 Supplement 1-NP, Rev. 0, "Fluence Determination with RAPTOR-M3G and FERRET – Supplement for Extended Beltline Materials," May 2022. *[ADAMS Accession Number ML22153A139]*

21. Westinghouse Report, WCAP-18924-NP, Revision 1, "Diablo Canyon Units 1 and 2 Initial License Renewal: Time-Limited Aging Analyses (TLAAs) on Reactor Vessel Integrity (RVI)," November 2024.

22. "Diablo Canyon Nuclear Power Plant, Units 1 and 2 – Safety Evaluation for the License Renewal Application (EPID No. L-2023-RNW-0021)," dated June 4, 2025 *[ADAMS Accession Number ML25139A612]*.

23. Westinghouse Report, WCAP-11567, Revision 0, "Analysis of Capsule S from the Pacific Gas and Electric Company Diablo Canyon Unit 1 Reactor Vessel Radiation Surveillance Program," December 1987.

24. Westinghouse Report, WCAP-13750, Revision 0, "Analysis of Capsule Y from the Pacific Gas and Electric Company Diablo Canyon Unit 1 Reactor Vessel Radiation Surveillance Program," July 1993.

25. Diablo Canyon Nuclear Power Plant, Units 1 and 2 – Issuance of Amendment Nos. 258 and 260 Re: Adoption of TSTF-585, "Revise LCO 3.0.3 to Require Managing Risk" (EPID L-2026-LLA-0011), May 19, 2026 *[ADAMS Accession Number ML26104A058]*

26. Diablo Canyon, Units 1 and 2, Pressure and Temperature Limits Report, *[ADAMS Accession Number ML25210A382]*

APPENDIX A VALIDATION OF THE RADIATION TRANSPORT MODELS BASED ON NEUTRON DOSIMETRY MEASUREMENTS

A.1 NEUTRON DOSIMETRY

This appendix provides comparisons of measured dosimetry results to both the calculated and least-squares adjusted values for the in-vessel surveillance capsules withdrawn from the reactor and analyzed to date. The sensor sets have been analyzed in accordance with the current dosimetry evaluation methodology described in Regulatory Guide 1.190 [A-1]. One of the main purposes for providing this material is to demonstrate that the overall measurements agree with the calculated and least-squares adjusted values to within ± 20% as specified by Regulatory Guide 1.190, thus serving to validate the calculated neutron exposures reported in Section 6.2.

A.1.1 Sensor Reaction Rate Determinations

In this section, the results of the evaluations of the surveillance capsules analyzed to date are presented. The capsule designations, locations within the reactor, and times of withdrawal are as follows:

Capsule	Azimuthal Location	Withdrawal Time	Irradiation Time (EFPY)
S	320°	End of Cycle 1	1.26
Y	40°	End of Cycle 5	5.86
T	140°	End of Cycle 5	5.86
Z	220°	End of Cycle 5	5.86
V[1]	184°/320°	End of Cycle 11	14.23
C[2]	140°	End of Cycle 12	15.84
D[2]	220°	End of Cycle 12	15.84
B[2]	40°	End of Cycle 25	34.87
A[2]	184°	Standby	-
U	356°	Standby	-
X	176°	Standby	-
W	4°	Standby	-

Note(s):

1. Capsule V was irradiated at the 184° (4°) location during Cycles 1–5, then relocated and irradiated at the 320° (40°) location for Cycles 6–11, prior to withdrawal after EOC 11 [21].
2. Supplemental capsules were installed at 5.86 EFPY following the completion of Cycle 5.

The passive neutron sensors included in these evaluations are summarized as follows:

Sensor Material	Reaction of Interest	Capsule S	Capsule Y	Capsule V	Capsule B
Copper	$^{63}Cu\ (n,\alpha)\ ^{60}Co$	X	X	X	X
Iron	$^{54}Fe\ (n,p)\ ^{54}Mn$	X	X	X	X
Nickel	$^{58}Ni\ (n,p)\ ^{58}Co$	X	X	X	X
Uranium-238	$^{238}U\ (Cd)\ (n,f)\ ^{137}Cs$	X	X	X	X
Neptunium-237	$^{237}Np\ (n,f)\ ^{137}Cs$	X	X	X	X
Cobalt-Aluminum	$^{59}Co(n,\gamma)\ ^{60}Co$	X	X	X	X
Cobalt (Cd covered)	$^{59}Co\ (Cd)\ (n,\gamma)\ ^{60}Co$	X	X	X	X

The design of the in-vessel surveillance capsules places the individual neutron sensors at several radial locations within the test specimen array. As a result of the various radial locations, gradient correction factors are applied to the measured reaction rates to index all of the neutron sensor measurements to a common geometric location (the center of the capsule) prior to use in the least-squares adjustment procedure. Pertinent physical and nuclear characteristics of the passive neutron sensors analyzed are listed in Table A-1.

The use of passive monitors does not yield a direct measure of the energy-dependent neutron exposure rate at the point of interest. Rather, the activation or fission process is a measure of the integrated effect that the time- and energy-dependent neutron exposure rate has on the target material over the course of the irradiation period. An accurate assessment of the average neutron exposure rate incident on the various monitors may be derived from the activation measurements only if the irradiation parameters are well known. In particular, the following variables are of interest:

- The measured specific activity of each monitor.
- The physical characteristics of each monitor.
- The operating history of the reactor.
- The energy response of each monitor.
- The neutron energy spectrum at the monitor location.

The radiometric counting of the sensors from Capsule B was carried out at the Westinghouse Analytical Services Laboratory at the Waltz Mill site. The radiometric counting followed established ASTM procedures. The previously withdrawn in-vessel Capsules S, Y and V were re-evaluated using the current calculational model.

The operating history of the reactor over the irradiation periods, which was based on monthly power generation from initial reactor criticality through the end of the dosimetry evaluation period, is summarized in Table A-2. For the sensor sets utilized in the surveillance capsules, the half-lives of the product isotopes are long enough that a monthly histogram describing reactor operation has proven to be an adequate representation for use in radioactive decay corrections for the reactions of interest in the exposure evaluations.

Having the measured specific activities, the physical characteristics of the sensors, and the operating history of the reactor, reaction rates referenced to full-power operation were determined from the following equation:

$$R = \frac{A}{N_0 F Y \sum \frac{P_j}{P_{ref}} C_j \left[1 - e^{-\lambda t_j}\right]\left[e^{-\lambda t_{d,j}}\right]}$$

where:

R	=	Reaction rate averaged over the irradiation period and referenced to operation at a core power level of P_{ref} (rps/nucleus).
A	=	Measured specific activity (dps/g).
N_0	=	Number of target element atoms per gram of sensor.
F	=	Atom fraction of the target isotope in the target element.
Y	=	Number of product atoms produced per reaction.
P_j	=	Average core power level during irradiation Period j (MW).
P_{ref}	=	Maximum or reference power level of the reactor (MW).
C_j	=	Calculated ratio of ϕ (E > 1.0 MeV) during irradiation Period j to the time weighted average ϕ (E > 1.0 MeV) over the entire irradiation period.
λ	=	Decay constant of the product isotope (1/sec).
t_j	=	Length of irradiation Period j (sec).
$t_{d,j}$	=	Decay time following irradiation Period j (sec).

The summation is carried out over the total number of monthly intervals comprising the irradiation period.

In the equation describing the reaction rate calculation, the ratio $[P_j]/[P_{ref}]$ accounts for month-by-month variation of reactor core power level within any given fuel cycle as well as over multiple fuel cycles. The ratio C_j, which was calculated for each fuel cycle using the transport methodology discussed in Section 6.2, accounts for the change in sensor reaction rates caused by variations in exposure rate level induced by changes in core spatial power distributions from fuel cycle to fuel cycle. For a single-cycle irradiation, C_j is normally taken to be 1.0. However, for multiple-cycle irradiations, the additional C_j term should be employed. The impact of changing exposure rate levels for constant power operation can be quite significant for sensor sets that have been irradiated for many cycles in a reactor that has transitioned from non-low-leakage to low-leakage fuel management or for sensor sets contained in surveillance capsules that have been moved from one capsule location to another. The fuel-cycle-specific neutron exposure rates are used to compute cycle-dependent values for C_j at the radial and azimuthal center of the respective capsules at the axial elevation of the core midplane.

Prior to using the measured reaction rates in the least-squares evaluations of the dosimetry sensor sets, additional corrections were made to the U-238 measurements to account for the presence of ^{235}U impurities in the sensors, as well as to adjust for the build-in of plutonium isotopes over the course of the irradiation. Corrections were also made to the U-238 and Np-237 sensor reaction rates to account for gamma-ray-induced fission reactions that occurred over the course of the surveillance capsule irradiations. The correction factors corresponding to the fission sensor reaction rates are summarized as follows:

Correction	Capsule S	Capsule Y	Capsule V	Capsule B
U-235 Impurity/Pu Build-in	0.873	0.843	0.831	0.755
U-238 (γ,f)	0.959	0.958	0.959	0.958
Net U-238 Correction	0.836	0.808	0.797	0.724
Np-237 (γ,f)	0.985	0.985	0.984	0.985

The correction factors were applied in a multiplicative fashion to the decay-corrected cadmium-covered fission sensor reaction rates.

Results of the sensor reaction rate determinations for the in-vessel capsules are given in Table A-3 through Table A-6, where the measured specific activities, decay-corrected saturated specific activities, and computed reaction rates for each sensor are listed.

A.1.2 Least-Squares Evaluation of Sensor Sets

Least-squares adjustment methods provide the capability of combining the measurement data with the corresponding neutron transport calculations, resulting in a best-estimate neutron energy spectrum with associated uncertainties. Best-estimates for key exposure parameters such as fast neutron (E > 1.0 MeV) fluence rate or dpa/s along with their uncertainties are then easily obtained from the adjusted spectrum. In general, the least-squares method, as applied to dosimetry evaluations, acts to reconcile the measured sensor reaction rate data, dosimetry reaction cross-sections, and the calculated neutron energy spectrum within their respective uncertainties. For example,

$$R_i \pm \delta_{R_i} = \sum_g (\sigma_{ig} \pm \delta_{\sigma_{ig}})(\varphi_g \pm \delta_{\varphi_g})$$

relates a set of measured reaction rates, R_i, to a single neutron spectrum, ϕ_g, through the multigroup dosimeter reaction cross-sections, σ_{ig}, each with an uncertainty δ. The primary objective of the least-squares evaluation is to produce unbiased estimates of the neutron exposure parameters at the location of the measurement.

For the least-squares evaluation, the FERRET code [A-2] was employed to combine the results of the plant-specific neutron transport calculations and sensor set reaction rate measurements to determine the best-estimate values of exposure parameters (fluence rate (E > 1.0 MeV) and dpa) and their associated uncertainties.

The application of the least-squares methodology requires the following input:

1. The calculated neutron energy spectrum and associated uncertainties at the measurement location.
2. The measured reaction rates and associated uncertainty for each sensor contained in the multiple sensor set.
3. The energy-dependent dosimetry reaction cross-sections and associated uncertainties for each sensor contained in the multiple sensor set.

The calculated neutron spectrum was obtained from the results of plant-specific neutron transport calculations described in Section 6.2. The sensor reaction rates were derived from the measured specific activities using the procedures described in Section A.1.1. The dosimetry reaction cross-sections and uncertainties were obtained from the SNLRML dosimetry cross-section library [A-3].

The uncertainties associated with the measured reaction rates, dosimetry cross-sections, and calculated neutron spectrum were input to the least-squares procedure in the form of variances and covariances. The assignment of the input uncertainties followed the guidance provided in ASTM E944 [A-4].

The following provides a summary of the uncertainties associated with the least-squares evaluation of the surveillance capsule sensor sets.

<u>Reaction Rate Uncertainties</u>

The overall uncertainty associated with the measured reaction rates includes components due to the basic measurement process, irradiation history corrections, and corrections for competing reactions. A high level of accuracy in the reaction rate determinations is ensured by utilizing laboratory procedures that conform to the ASTM International Consensus Standards for reaction rate determinations for each sensor type.

After combining all of these uncertainty components, the sensor reaction rates derived from the counting and data evaluation procedures were assigned the following net uncertainties for input to the least-squares evaluation:

Reaction	**Uncertainty (1σ)**
^{63}Cu (n,α) ^{60}Co	5%
^{54}Fe (n,p) ^{54}Mn	5%
^{58}Ni (n,p) ^{58}Co	5%
^{59}Co (n,γ) ^{60}Co	5%
^{59}Co (Cd) (n,γ) ^{60}Co	5%
^{238}U (n,f) FP	10%
^{237}Np (n,f) FP	10%

Dosimetry Cross-Section Uncertainties

The reaction rate cross-sections used in the least-squares evaluations were taken from the SNLRML library. This data library provides reaction cross-sections and associated uncertainties, including covariances, for 66 dosimetry sensors in common use. Both cross-sections and uncertainties are provided in a fine multigroup structure for use in least-squares adjustment applications. These cross-sections were compiled from recent cross-section evaluations, and they have been tested for accuracy and consistency for least-squares evaluations. Further, the library has been empirically tested for use in fission spectra determination, as well as in the fluence and energy characterization of 14 MeV neutron sources.

For sensors included in the surveillance program, the following uncertainties in the fission spectrum averaged cross-sections are provided in the SNLRML documentation package:

Reaction	Uncertainty
Cu-63 (n,α) Co-60	4.08–4.16%
Fe-54 (n,p) Mn-54	3.05–3.11%
Ni-58 (n,p) Co-58	4.49–4.56%
Co-59 (n,γ) Co-60	0.79–3.59%
U-238 (n,f)	0.54–0.64%
Np-237 (n,f)	10.32-10.97%

These tabulated ranges provide an indication of the dosimetry cross-section uncertainties associated with the sensor sets used in LWR irradiations.

Calculated Neutron Spectrum

The neutron spectra inputs to the least-squares adjustment procedure were obtained directly from the results of plant-specific transport calculations for each surveillance capsule irradiation period and location. The spectrum for each capsule was input in an absolute sense (rather than as simply a relative spectral shape). Therefore, within the constraints of the assigned uncertainties, the calculated data were treated equally with the measurements.

While the uncertainties associated with the reaction rates were obtained from the measurement procedures and counting benchmarks and the dosimetry cross-section uncertainties were supplied directly with the SNLRML library, the uncertainty matrix for the calculated spectrum was constructed from the following relationship:

$$M_{gg'} = R_n^2 + R_g * R_{g'} * P_{gg'}$$

where R_n specifies an overall fractional normalization uncertainty and the fractional uncertainties R_g and $R_{g'}$ specify additional random groupwise uncertainties that are correlated with a correlation matrix given by:

$$P_{gg'} = [1 - \theta]\delta_{gg'} + \theta\, e^{-H}$$

where:

$$H = \frac{(g - g')^2}{2\gamma^2}$$

The first term in the correlation matrix equation specifies purely random uncertainties, while the second term describes the short-range correlations over a group range γ (θ specifies the strength of the latter term). The value of δ is 1.0 when $g = g'$, and is 0.0 otherwise.

The set of parameters defining the input covariance matrix for the calculated spectra was as follows:

Exposure Rate Normalization Uncertainty (R_n)	15%
Exposure Rate Group Uncertainties (R_g, $R_{g'}$)	
(E > 0.0055 MeV)	15%
(0.68 eV < E < 0.0055 MeV)	25%
(E < 0.68 eV)	50%
Short Range Correlation (θ)	
(E > 0.0055 MeV)	0.9
(0.68 eV < E < 0.0055 MeV)	0.5
(E < 0.68 eV)	0.5
Exposure Rate Group Correlation Range (γ)	
(E > 0.0055 MeV)	6
(0.68 eV < E < 0.0055 MeV)	3
(E < 0.68 eV)	2

A.1.3 Comparisons of Measurements and Calculations

Results of the least-squares evaluations are provided in Table A-7 through Table A-10. In these tables, measured, calculated, and best-estimate values for sensor reaction rates are given. Also provided in these tabulations are ratios of the measured reaction rates to both the calculated and least-squares adjusted reaction rates. These ratios of measured-to-calculated (M/C) and measured-to-best-estimate (M/BE) illustrate the consistency of the fit of the calculated neutron energy spectra to the measured reaction rates both before and after adjustment. Additionally, comparisons of the calculated and best-estimate values of fast neutron (E > 1.0 MeV) fluence rate and iron atom displacement rate are tabulated along with the best-estimate-to-calculated (BE/C) ratios observed for each of the capsules.

The data comparisons provided in Table A-7 through Table A-10 show that the adjustments to the calculated spectra are relatively small and within the assigned uncertainties for the calculated spectra, measured sensor reaction rates, and dosimetry reaction cross-sections. Further, these results indicate that the use of the least-squares evaluation results in a reduction in the uncertainties associated with the exposure of the surveillance capsules. From Section 0, the calculational uncertainty is specified as 13% at the 1σ level.

Further comparisons of the measurement results with calculations are given in Table A-11 and Table A-12. In Table A-11, calculations of individual threshold sensor reaction rates are compared directly with the corresponding measurements. These threshold reaction rate comparisons provide a good evaluation of the accuracy of the fast neutron portion of the calculated energy spectra. In Table A-12, calculations of fast neutron exposure rates in terms of fast neutron (E > 1.0 MeV) fluence rate and dpa/s are compared with the best-estimate results obtained from the least-squares evaluation of the capsule dosimetry results. These comparisons yield consistent and similar results with all measurement-to-calculation comparisons falling within the 20% limits specified as the acceptance criteria in Regulatory Guide 1.190.

In the case of the direct comparison of the measured and calculated sensor reaction rates, for the individual threshold sensors considered in the least-squares analysis, the average M/C comparisons of the fast neutron threshold reactions range from 0.89 to 1.05. The overall average M/C ratio is 0.96 with an associated standard deviation of 9.7%.

In the case of the comparison of the best-estimate and calculated fast neutron exposure parameters, the BE/C comparisons are 0.94 for fast neutron (E > 1.0 MeV) fluence rate and 0.95 for iron atom displacement rate.

Based on these comparisons, it is concluded that the calculated fast neutron exposures provided in Section 6.2 are valid for use in the assessment of the condition of the materials comprising the beltline region of the reactor pressure vessel.

Table A-1 Nuclear Parameters Used in the Evaluation of Neutron Sensors

Reaction of Interest	Atomic Weight (g/g-atom)	Target Atom Fraction	Product Half-life (days)	Fission Yield (%)	90% Response Range[1] (MeV)
Cu-63 (n,α) Co-60	63.546	0.6915	1925.27	-	4.53–11.0
Fe-54 (n,p) Mn-54	55.845	0.05845	312.19	-	2.27–7.54
Ni-58 (n,p) Co-58	58.693	0.68077	70.85	-	1.98–7.51
Co-59 (n,γ) Co-60	58.933	0.0015	1925.27	-	Non-threshold
U-238 (n,f) Cs-137	238.051	1.00	10975.76	6.00	1.44–6.69
Np-237 (n,f) Cs-137	237.048	1.00	10975.76	6.21	0.68–5.61

Note:

1. Energies between which 90% of activity is produced (U-235 fission spectrum) [A-5].

Table A-2 Monthly Thermal Generation

Cycle 1		Cycle 2		Cycle 3		Cycle 4	
Month	**MW-h**	**Month**	**MW-h**	**Month**	**MW-h**	**Month**	**MW-h**
Nov-84	167071	Dec-86	48788	Jul-88	927368	Dec-89	818953
Dec-84	781228	Jan-87	1140482	Aug-88	2358057	Jan-90	2433618
Jan-85	84750	Feb-87	2028965	Sep-88	2068428	Feb-90	2037409
Feb-85	497207	Mar-87	2277945	Oct-88	2427826	Mar-90	2491017
Mar-85	1854601	Apr-87	2394500	Nov-88	2368095	Apr-90	2377992
Apr-85	0	May-87	2118322	Dec-88	2404073	May-90	2516299
May-85	1632108	Jun-87	2141394	Jan-89	2398489	Jun-90	1585625
Jun-85	2286901	Jul-87	2381703	Feb-89	2207286	Jul-90	2340515
Jul-85	2435846	Aug-87	2090122	Mar-89	2449786	Aug-90	2473468
Aug-85	2218873	Sep-87	2375321	Apr-89	2162399	Sep-90	2370556
Sep-85	2374552	Oct-87	2308588	May-89	2441421	Oct-90	2443130
Oct-85	2163216	Nov-87	2347282	Jun-89	2363360	Nov-90	2346761
Nov-85	1523963	Dec-87	1817741	Jul-89	2468579	Dec-90	1793532
Dec-85	1929994	Jan-88	2035485	Aug-89	2384230	Jan-91	2391971
Jan-86	2424269	Feb-88	1710575	Sep-89	2400292	Feb-91	27364
Feb-86	2102251	Mar-88	274544	Oct-89	439623		
Mar-86	2406348						
Apr-86	2132185						
May-86	2490682						
Jun-86	2163689						
Jul-86	1842336						
Aug-86	1366070						
Total	36878140	Total	29491757	Total	34269312	Total	30448210
EFPS	3.977E+07	EFPS	3.181E+07	EFPS	3.696E+07	EFPS	3.284E+07
EFPY	1.260	EFPY	1.008	EFPY	1.171	EFPY	1.041

Table A-2 Monthly Thermal Generation (cont.)

Cycle 5		Cycle 6		Cycle 7		Cycle 8	
Month	**MW-h**	**Month**	**MW-h**	**Month**	**MW-h**	**Month**	**MW-h**
Apr-91	1610788	Nov-92	1352555	May-94	546539	Oct-95	0
May-91	2161086	Dec-92	2428355	Jun-94	2383038	Nov-95	60824
Jun-91	2392176	Jan-93	2483047	Jul-94	2493803	Dec-95	1650488
Jul-91	2481053	Feb-93	2065992	Aug-94	2490277	Jan-96	2482638
Aug-91	2482327	Mar-93	2338926	Sep-94	2407121	Feb-96	2271956
Sep-91	2350718	Apr-93	2402015	Oct-94	2482344	Mar-96	2045407
Oct-91	2481357	May-93	2481334	Nov-94	2398894	Apr-96	2397718
Nov-91	2197143	Jun-93	2256675	Dec-94	2059217	May-96	2480874
Dec-91	2480444	Jul-93	2482118	Jan-95	2425927	Jun-96	2198496
Jan-92	2480772	Aug-93	2480942	Feb-95	2242278	Jul-96	2329842
Feb-92	2322063	Sep-93	2400588	Mar-95	2449140	Aug-96	1911123
Mar-92	2138149	Oct-93	2432353	Apr-95	2298107	Sep-96	2398306
Apr-92	2224782	Nov-93	2401678	May-95	2485576	Oct-96	2481168
May-92	2410682	Dec-93	1867363	Jun-95	2387434	Nov-96	1686924
Jun-92	2400268	Jan-94	2437616	Jul-95	2479699	Dec-96	2425633
Jul-92	2418213	Feb-94	2242952	Aug-95	2478524	Jan-97	2470296
Aug-92	2381626	Mar-94	872868	Sep-95	2070677	Feb-97	2215833
Sep-92	835392					Mar-97	2479111
						Apr-97	1429228
Total	40249039	Total	37427377	Total	38578595	Total	37415865
EFPS	4.341E+07	EFPS	4.037E+07	EFPS	4.161E+07	EFPS	4.035E+07
EFPY	1.376	EFPY	1.279	EFPY	1.318	EFPY	1.279

Table A-2 Monthly Thermal Generation (cont.)

Cycle 9		Cycle 10		Cycle 11		Cycle 12	
Month	**MW-h**	**Month**	**MW-h**	**Month**	**MW-h**	**Month**	**MW-h**
May-97	0	Mar-99	1098455	Nov-00	695918	May-02	124310
Jun-97	2072263	Apr-99	2396984	Dec-00	2449052	Jun-02	2142727
Jul-97	2480639	May-99	2480081	Jan-01	2385664	Jul-02	2430715
Aug-97	2466623	Jun-99	2396014	Feb-01	2291938	Aug-02	2286881
Sep-97	2394045	Jul-99	2473999	Mar-01	2537268	Sep-02	2404322
Oct-97	2361899	Aug-99	2474498	Apr-01	2447550	Oct-02	1521032
Nov-97	2389197	Sep-99	2136320	May-01	2537285	Nov-02	0
Dec-97	2468651	Oct-99	2214363	Jun-01	2381547	Dec-02	1425096
Jan-98	2404594	Nov-99	2224383	Jul-01	2533658	Jan-03	2531694
Feb-98	2188679	Dec-99	2464655	Aug-01	2536196	Feb-03	2291449
Mar-98	2414420	Jan-00	2377796	Sep-01	2455470	Mar-03	2531129
Apr-98	2336535	Feb-00	2298401	Oct-01	2537982	Apr-03	2451585
May-98	2469944	Mar-00	2469797	Nov-01	2177067	May-03	2537039
Jun-98	2360812	Apr-00	2352203	Dec-01	2506152	Jun-03	2291703
Jul-98	2414420	May-00	1311575	Jan-02	2537285	Jul-03	2529491
Aug-98	2414420	Jun-00	2400627	Feb-02	2260855	Aug-03	2537129
Sep-98	2336535	Jul-00	2481168	Mar-02	2530637	Sep-03	2455168
Oct-98	2414420	Aug-00	2479288	Apr-02	2213606	Oct-03	2540310
Nov-98	2336535	Sep-00	2391812			Nov-03	2455446
Dec-98	1572621	Oct-00	400560			Dec-03	2425713
Jan-99	2474763					Jan-04	2449232
Feb-99	500553					Feb-04	2218484
						Mar-04	1473297
Total	47272568	Total	43322979	Total	42015130	Total	48053952
EFPS	5.098E+07	EFPS	4.672E+07	EFPS	4.434E+07	EFPS	5.072E+07
EFPY	1.615	EFPY	1.480	EFPY	1.405	EFPY	1.607

Table A-2 Monthly Thermal Generation (cont.)

Cycle 13		Cycle 14		Cycle 15		Cycle 16	
Month	**MW-h**	**Month**	**MW-h**	**Month**	**MW-h**	**Month**	**MW-h**
Jun-04	1530101	Dec-05	2116500	May-07	76436	Mar-09	400144
Jul-04	2321782	Jan-06	2521526	Jun-07	2434753	Apr-09	2451447
Aug-04	2537017	Feb-06	2287068	Jul-07	2535584	May-09	2532951
Sep-04	2455012	Mar-06	2536133	Aug-07	1899267	Jun-09	2451390
Oct-04	2539666	Apr-06	2448949	Sep-07	2452935	Jul-09	2533459
Nov-04	2454979	May-06	2534272	Oct-07	2534618	Aug-09	2494344
Dec-04	2521495	Jun-06	2443057	Nov-07	2457079	Sep-09	2055798
Jan-05	2492317	Jul-06	2535459	Dec-07	2444306	Oct-09	2481393
Feb-05	2104803	Aug-06	2534682	Jan-08	2506416	Nov-09	2447122
Mar-05	2536534	Sep-06	2452381	Feb-08	2370997	Dec-09	2532403
Apr-05	2451062	Oct-06	2538014	Mar-08	2531759	Jan-10	2375542
May-05	2531688	Nov-06	2308976	Apr-08	2453606	Feb-10	2134658
Jun-05	2401356	Dec-06	2534198	May-08	2398192	Mar-10	2528503
Jul-05	2536256	Jan-07	2534853	Jun-08	2447965	Apr-10	2449853
Aug-05	2534700	Feb-07	2288436	Jul-08	2530099	May-10	2532659
Sep-05	2342994	Mar-07	2530032	Aug-08	2535076	Jun-10	2450140
Oct-05	1793481	Apr-07	2362967	Sep-08	2451666	Jul-10	2531218
				Oct-08	2476274	Aug-10	2530408
				Nov-08	2455817	Sep-10	2445146
				Dec-08	2532489	Oct-10	129461
				Jan-09	1981900		
Total	40085243	Total	41507503	Total	48507234	Total	44488039
EFPS	4.231E+07	EFPS	4.381E+07	EFPS	5.119E+07	EFPS	4.695E+07
EFPY	1.341	EFPY	1.388	EFPY	1.622	EFPY	1.488

Table A-2 Monthly Thermal Generation (cont.)

Cycle 17		Cycle 18		Cycle 19		Cycle 20	
Month	**MW-h**	**Month**	**MW-h**	**Month**	**MW-h**	**Month**	**MW-h**
Nov-10	1303872	May-12	0	Mar-14	471171	Nov-15	1709351
Dec-10	2528484	Jun-12	961436	Apr-14	2453542	Dec-15	2383260
Jan-11	2531137	Jul-12	2534305	May-14	2488842	Jan-16	2535542
Feb-11	2286486	Aug-12	2534312	Jun-14	2452920	Feb-16	2372405
Mar-11	2518000	Sep-12	2436347	Jul-14	2535546	Mar-16	2532207
Apr-11	2430313	Oct-12	2534968	Aug-14	2535350	Apr-16	2451992
May-11	2531267	Nov-12	2456528	Sep-14	2407158	May-16	2535428
Jun-11	2449510	Dec-12	2247036	Oct-14	2535202	Jun-16	2453523
Jul-11	2533093	Jan-13	2535239	Nov-14	2456721	Jul-16	2535338
Aug-11	2532397	Feb-13	2289876	Dec-14	2169432	Aug-16	2535501
Sep-11	2233291	Mar-13	2531856	Jan-15	2191101	Sep-16	2453777
Oct-11	2491236	Apr-13	2453358	Feb-15	2290321	Oct-16	2336982
Nov-11	2454281	May-13	2530147	Mar-15	2532244	Nov-16	2457037
Dec-11	2532929	Jun-13	2047296	Apr-15	2454009	Dec-16	2535305
Jan-12	2532856	Jul-13	2350946	May-15	2533581	Jan-17	2481815
Feb-12	2367801	Aug-13	2535329	Jun-15	2453960	Feb-17	2289772
Mar-12	2527668	Sep-13	2453432	Jul-15	2535513	Mar-17	2531840
Apr-12	1665400	Oct-13	2292438	Aug-15	2531780	Apr-17	1779713
		Nov-13	2369210	Sep-15	2453583		
		Dec-13	2535189	Oct-15	226462		
		Jan-14	2535108				
		Feb-14	642952				
Total	42450021	Total	47807308	Total	44708438	Total	42910788
EFPS	4.480E+07	EFPS	5.046E+07	EFPS	4.719E+07	EFPS	4.529E+07
EFPY	1.420	EFPY	1.599	EFPY	1.495	EFPY	1.435

Table A-2 Monthly Thermal Generation (cont.)

Cycle 21		Cycle 22		Cycle 23		Cycle 24	
Month	**MW-h**	**Month**	**MW-h**	**Month**	**MW-h**	**Month**	**MW-h**
May-17	0	Mar-19	943265	Nov-20	2159076	Apr-22	241932
Jun-17	509772	Apr-19	2453138	Dec-20	2534550	May-22	2534789
Jul-17	2433570	May-19	2535273	Jan-21	2535122	Jun-22	2453010
Aug-17	2535246	Jun-19	2453589	Feb-21	2289966	Jul-22	2534935
Sep-17	2453603	Jul-19	2535426	Mar-21	2531554	Aug-22	2535239
Oct-17	2535279	Aug-19	2532841	Apr-21	2406147	Sep-22	2453440
Nov-17	2456969	Sep-19	2453474	May-21	2486252	Oct-22	2534936
Dec-17	2532864	Oct-19	2535297	Jun-21	2453340	Nov-22	2453334
Jan-18	2535418	Nov-19	2456775	Jul-21	2534617	Dec-22	2535108
Feb-18	2290110	Dec-19	2448906	Aug-21	2535165	Jan-23	2426523
Mar-18	2532059	Jan-20	2535166	Sep-21	2453318	Feb-23	2289557
Apr-18	2218782	Feb-20	2371503	Oct-21	2458950	Mar-23	2249885
May-18	2502558	Mar-20	2531497	Nov-21	2456414	Apr-23	2453448
Jun-18	2453201	Apr-20	2453392	Dec-21	2535018	May-23	2535198
Jul-18	2535267	May-20	2304991	Jan-22	2534740	Jun-23	2453342
Aug-18	2535295	Jun-20	2453458	Feb-22	2204803	Jul-23	2535231
Sep-18	2453570	Jul-20	2535191	Mar-22	1912098	Aug-23	2535214
Oct-18	2535304	Aug-20	2534698			Sep-23	2342784
Nov-18	2380598	Sep-20	2409239				
Dec-18	2317527	Oct-20	193020				
Jan-19	2535140						
Feb-19	703219						
Total	47985351	Total	45670139	Total	41021131	Total	42016123
EFPS	5.064E+07	EFPS	4.820E+07	EFPS	4.329E+07	EFPS	4.443E+07
EFPY	1.605	EFPY	1.527	EFPY	1.372	EFPY	1.408

Table A-2 Monthly Thermal Generation (cont.)

Cycle 25	
Month	**MW-h**
Oct-23	0
Nov-23	1249359
Dec-23	1764013
Jan-24	2534256
Feb-24	2371331
Mar-24	2535247
Apr-24	2453489
May-24	2535304
Jun-24	2453473
Jul-24	2535255
Aug-24	2490786
Sep-24	2217141
Oct-24	2441752
Nov-24	2453464
Dec-24	2535220
Jan-25	2534756
Feb-25	2289819
Mar-25	2535132
Apr-25	972331
Total	40902130
EFPS	4.317E+07
EFPY	1.368

Table A-3 Measured Sensor Activities and Reaction Rates for Surveillance Capsule S

Sample ID	Reaction	Measured Activity (Bq/g)	Radially Corrected Saturated Activity (dps/g)	Reaction Rate (rps/atom)	Average Reaction Rate (rps/atom)	Corrected Average Reaction Rate (rps/atom)
0808	^{63}Cu (n,α) ^{60}Co	4.47E+04	3.27E+05	4.99E-17	4.90E-17	4.90E-17
0814	^{63}Cu (n,α) ^{60}Co	4.29E+04	3.14E+05	4.79E-17		
W-3	^{54}Fe (n,p) ^{54}Mn	1.13E+06	2.83E+06	4.49E-15	4.76E-15	4.76E-15
W-4	^{54}Fe (n,p) ^{54}Mn	1.13E+06	2.83E+06	4.49E-15		
W-3	^{54}Fe (n,p) ^{54}Mn	1.15E+06	2.88E+06	4.57E-15		
W-4	^{54}Fe (n,p) ^{54}Mn	1.33E+06	2.76E+06	4.35E-15		
W-8	^{54}Fe (n,p) ^{54}Mn	1.35E+06	2.80E+06	4.41E-15		
1078	^{58}Ni (n,p) ^{58}Co	8.20E+06	4.99E+07	7.15E-15	7.15E-15	7.15E-15
0811	^{238}U(Cd) (n,f) ^{137}Cs	1.31E+05	4.63E+06	3.04E-14	3.04E-14	2.55E-14
0804	^{237}Np(Cd) (n,f) ^{137}Cs	9.97E+05	3.52E+07	2.21E-13	2.21E-13	2.20E-13
0805	^{59}Co (n,γ) ^{60}Co	7.56E+06	5.10E+07	3.33E-12	3.43E-12	3.43E-12
0807	^{59}Co (n,γ) ^{60}Co	7.35E+06	4.96E+07	3.23E-12		
0810	^{59}Co (n,γ) ^{60}Co	7.87E+06	5.31E+07	3.46E-12		
0813	^{59}Co(Cd) (n,γ) ^{60}Co	4.03E+06	2.45E+07	1.60E-12	1.60E-12	1.60E-12
0806	^{59}Co(Cd) (n,γ) ^{60}Co	3.98E+06	2.42E+07	1.58E-12		
0809	^{59}Co(Cd) (n,γ) ^{60}Co	4.05E+06	2.47E+07	1.61E-12		

Table A-4 Measured Sensor Activities and Reaction Rates for Surveillance Capsule Y

<table>
<tr><th>Sample ID</th><th>Reaction</th><th>Measured Activity (Bq/g)</th><th>Radially Corrected Saturated Activity (dps/g)</th><th>Reaction Rate (rps/atom)</th><th>Average Reaction Rate (rps/atom)</th><th>Corrected Average Reaction Rate (rps/atom)</th></tr>
<tr><td>0118</td><td>^{63}Cu (n,α) ^{60}Co</td><td>1.15E+05</td><td>2.55E+05</td><td>3.73E-17</td><td rowspan="2">3.68E-17</td><td rowspan="2">3.68E-17</td></tr>
<tr><td>0124</td><td>^{63}Cu (n,α) ^{60}Co</td><td>1.12E+05</td><td>2.49E+05</td><td>3.63E-17</td></tr>
<tr><td>W-17</td><td>^{54}Fe (n,p) ^{54}Mn</td><td>1.11E+06</td><td>2.17E+06</td><td>3.29E-15</td><td rowspan="4">3.44E-15</td><td rowspan="4">3.44E-15</td></tr>
<tr><td>W-20</td><td>^{54}Fe (n,p) ^{54}Mn</td><td>1.15E+06</td><td>2.25E+06</td><td>3.41E-15</td></tr>
<tr><td>W-24</td><td>^{54}Fe (n,p) ^{54}Mn</td><td>1.22E+06</td><td>2.39E+06</td><td>3.61E-15</td></tr>
<tr><td>E-60</td><td>^{54}Fe (n,p) ^{54}Mn</td><td>9.64E+05</td><td>1.89E+06</td><td>3.44E-15</td></tr>
<tr><td>0121</td><td>^{58}Ni (n,p) ^{58}Co</td><td>7.02E+06</td><td>3.82E+07</td><td>5.23E-15</td><td>5.23E-15</td><td>5.23E-15</td></tr>
<tr><td>0114</td><td>^{238}U(Cd) (n,f) ^{137}Cs</td><td>4.20E+05</td><td>3.44E+06</td><td>2.26E-14</td><td>2.26E-14</td><td>1.83E-14</td></tr>
<tr><td>0115</td><td>^{237}Np(Cd) (n,f) ^{137}Cs</td><td>2.41E+06</td><td>1.97E+07</td><td>1.25E-13</td><td>1.25E-13</td><td>1.23E-13</td></tr>
<tr><td>0116</td><td>^{59}Co (n,γ) ^{60}Co</td><td>1.66E+07</td><td>3.68E+07</td><td>2.33E-12</td><td rowspan="3">2.35E-12</td><td rowspan="3">2.35E-12</td></tr>
<tr><td>0119</td><td>^{59}Co (n,γ) ^{60}Co</td><td>1.61E+07</td><td>3.57E+07</td><td>2.26E-12</td></tr>
<tr><td>0122</td><td>^{59}Co (n,γ) ^{60}Co</td><td>1.74E+07</td><td>3.86E+07</td><td>2.45E-12</td></tr>
<tr><td>0117</td><td>^{59}Co(Cd) (n,γ) ^{60}Co</td><td>6.82E+06</td><td>1.51E+07</td><td>1.14E-12</td><td rowspan="3">1.15E-12</td><td rowspan="3">1.15E-12</td></tr>
<tr><td>0120</td><td>^{59}Co(Cd) (n,γ) ^{60}Co</td><td>6.79E+06</td><td>1.51E+07</td><td>1.14E-12</td></tr>
<tr><td>0123</td><td>^{59}Co(Cd) (n,γ) ^{60}Co</td><td>7.05E+06</td><td>1.56E+07</td><td>1.18E-12</td></tr>
</table>

Table A-5 Measured Sensor Activities and Reaction Rates for Surveillance Capsule V

Sample ID	Reaction	Measured Activity (Bq/g)	Radially Corrected Saturated Activity (dps/g)	Reaction Rate (rps/atom)	Average Reaction Rate (rps/atom)	Corrected Average Reaction Rate (rps/atom)
0432	$^{63}Cu\ (n,\alpha)\ ^{60}Co$	1.23E+05	1.46E+05	2.22E-17	2.27E-17	2.27E-17
0438	$^{63}Cu\ (n,\alpha)\ ^{60}Co$	1.28E+05	1.52E+05	2.31E-17		
W-9	$^{54}Fe\ (n,p)\ ^{54}Mn$	1.02E+06	1.13E+06	1.79E-15	1.88E-15	1.88E-15
W-16	$^{54}Fe\ (n,p)\ ^{54}Mn$	1.05E+06	1.16E+06	1.84E-15		
E-49	$^{54}Fe\ (n,p)\ ^{54}Mn$	8.87E+05	1.17E+06	1.86E-15		
E-56	$^{54}Fe\ (n,p)\ ^{54}Mn$	9.03E+05	1.19E+06	1.90E-15		
0435	$^{58}Ni\ (n,p)\ ^{58}Co$	9.58E+06	2.12E+07	3.03E-15	3.03E-15	3.03E-15
0428	$^{238}U(Cd)\ (n,f)\ ^{137}Cs$	4.68E+05	1.68E+06	1.10E-14	1.10E-14	8.80E-15
0429	$^{237}Np(Cd)\ (n,f)\ ^{137}Cs$	3.44E+06	1.23E+07	7.77E-14	7.77E-14	7.65E-14
0460	$^{59}Co\ (n,\gamma)\ ^{60}Co$	1.38E+07	1.49E+07	9.72E-13	9.93E-12	9.93E-12
0433	$^{59}Co\ (n,\gamma)\ ^{60}Co$	1.46E+07	1.58E+07	1.03E-12		
0436	$^{59}Co\ (n,\gamma)\ ^{60}Co$	1.39E+07	1.50E+07	9.79E-13		
0431	$^{59}Co(Cd)\ (n,\gamma)\ ^{60}Co$	6.53E+06	8.42E+06	5.49E-13	5.70E-13	5.70E-13
0434	$^{59}Co(Cd)\ (n,\gamma)\ ^{60}Co$	7.42E+06	9.57E+06	6.24E-13		
0437	$^{59}Co(Cd)\ (n,\gamma)\ ^{60}Co$	6.37E+06	8.21E+06	5.36E-13		

Table A-6 Measured Sensor Activities and Reaction Rates for Surveillance Capsule B

Sample ID	Reaction	Measured Activity (Bq/g)	Radially Corrected Saturated Activity (dps/g)	Reaction Rate (rps/atom)	Average Reaction Rate (rps/atom)	Corrected Average Reaction Rate (rps/atom)
9211005	^{63}Cu (n,α) ^{60}Co	1.72E+05	1.99E+05	3.04E-17	2.94E-17	2.94E-17
9211010	^{63}Cu (n,α) ^{60}Co	1.69E+05	1.96E+05	2.99E-17		
9211015	^{63}Cu (n,α) ^{60}Co	1.59E+05	1.84E+05	2.81E-17		
9211007	^{54}Fe (n,p) ^{54}Mn	1.40E+06	1.88E+06	2.98E-15	2.88E-15	2.88E-15
9211012	^{54}Fe (n,p) ^{54}Mn	1.35E+06	1.81E+06	2.88E-15		
9211017	^{54}Fe (n,p) ^{54}Mn	1.30E+06	1.75E+06	2.77E-15		
9211006	^{58}Ni (n,p) ^{58}Co	1.14E+07	2.92E+07	4.18E-15	4.03E-15	4.03E-15
9211011	^{58}Ni (n,p) ^{58}Co	1.10E+07	2.82E+07	4.04E-15		
9211016	^{58}Ni (n,p) ^{58}Co	1.05E+07	2.69E+07	3.85E-15		
9211001	^{238}U(Cd) (n,f) ^{137}Cs	1.32E+06	2.80E+06	1.85E-14	1.85E-14	1.34E-14
9211002	^{237}Np(Cd) (n,f) ^{137}Cs	7.93E+06	1.68E+07	1.07E-13	1.07E-13	1.05E-13
9211003	^{59}Co (n,γ) ^{60}Co	2.76E+07	3.12E+07	2.04E-12	2.03E-12	2.03E-12
9211008	^{59}Co (n,γ) ^{60}Co	2.74E+07	3.10E+07	2.02E-12		
9211013	^{59}Co (n,γ) ^{60}Co	2.77E+07	3.13E+07	2.04E-12		
9211004	^{59}Co(Cd) (n,γ) ^{60}Co	1.23E+07	1.25E+07	8.18E-13	8.12E-13	8.12E-13
9211009	^{59}Co(Cd) (n,γ) ^{60}Co	1.21E+07	1.23E+07	8.05E-13		
9211014	^{59}Co(Cd) (n,γ) ^{60}Co	1.22E+07	1.24E+07	8.12E-13		

Table A-7 Least-Squares Evaluation of Dosimetry in Surveillance Capsule S (40° Position, Irradiated During Cycle 1)

Reaction	Reaction Rate (rps/atom)			M/C	M/BE	BE/C
	Measured (M)	Calculated (C)	Best-Estimate (BE)			
^{63}Cu (n,α) ^{60}Co	4.90E-17	4.50E-17	4.70E-17	1.09	1.04	1.04
^{54}Fe (n,p) ^{54}Mn	4.47E-15	5.07E-15	4.88E-15	0.88	0.92	0.96
^{58}Ni (n,p) ^{58}Co	7.14E-15	6.99E-15	6.97E-15	1.02	1.02	1.00
^{238}U (n,f) ^{137}Cs	2.55E-14	2.53E-14	2.49E-14	1.01	1.02	0.98
^{237}Np (n,f) ^{137}Cs	2.20E-13	1.99E-13	2.09E-13	1.11	1.05	1.05
^{59}Co (n,γ) ^{60}Co	3.44E-12	3.39E-12	3.44E-12	1.01	1.00	1.01
^{59}Co(Cd) (n,γ) ^{60}Co	1.60E-12	1.59E-12	1.60E-12	1.00	1.00	1.01
Fast Reaction Threshold Foil Average				1.02	1.01	1.01
Standard deviation				8.8%	5.3%	3.8%

	C	BE	%Unc.	BE/C	
Fluence Rate (E>1.0 MeV) (n/cm^2-s)	7.34E+10	7.26E+10	6.0	0.99	
Fluence Rate (E>0.1 MeV) (n/cm^2-s)	2.46E+11	2.51E+11	10.0	1.02	χ^2/DOF
DPA/s	1.22E-10	1.23E-10	7.0	1.01	0.580

Table A-8 Least-Squares Evaluation of Dosimetry in Surveillance Capsule Y (40° Position, Irradiated During Cycles 1– 5)

Reaction	Reaction Rate (rps/atom) Measured (M)	Reaction Rate (rps/atom) Calculated (C)	Reaction Rate (rps/atom) Best-Estimate (BE)	M/C	M/BE	BE/C
^{63}Cu (n,α) ^{60}Co	3.68E-17	3.73E-17	3.58E-17	0.99	1.03	0.96
^{54}Fe (n,p) ^{54}Mn	3.44E-15	4.07E-15	3.63E-15	0.84	0.94	0.89
^{58}Ni (n,p) ^{58}Co	5.23E-15	5.61E-15	5.10E-15	0.93	1.02	0.91
^{238}U (n,f) ^{137}Cs	1.83E-14	2.00E-14	1.76E-14	0.91	1.03	0.88
^{237}Np (n,f) ^{137}Cs	1.23E-13	1.55E-13	1.30E-13	0.79	0.95	0.83
^{59}Co (n,γ) ^{60}Co	2.35E-12	2.62E-12	2.35E-12	0.89	1.00	0.90
^{59}Co(Cd) (n,γ) ^{60}Co	1.15E-12	1.23E-12	1.15E-12	0.94	1.00	0.94
Fast Reaction Threshold Foil Average				0.89	1.00	0.89
Standard deviation				8.8%	4.4%	5.3%

	C	BE	%Unc.	BE/C		
Fluence Rate (E>1.0 MeV) (n/cm^2-s)	5.78E+10	5.04E+10	6.0	0.87		
Fluence Rate (E>0.1 MeV) (n/cm^2-s)	1.92E+11	1.68E+11	10.0	0.87		χ^2/DOF
DPA/s	9.58E-11	8.41E-11	7.0	0.88		0.294

Table A-9 Least-Squares Evaluation of Dosimetry in Surveillance Capsule V (Irradiated at 4° Position Cycles 1-5, 40° Position Cycles 6–11)

Reaction	Reaction Rate (rps/atom)			M/C	M/BE	BE/C
	Measured (M)	Calculated (C)	Best-Estimate (BE)			
^{63}Cu (n,α) ^{60}Co	2.27E-17	2.27E-17	2.20E-17	1.00	1.03	0.97
^{54}Fe (n,p) ^{54}Mn	1.88E-15	2.28E-15	2.03E-15	0.82	0.93	0.89
^{58}Ni (n,p) ^{58}Co	3.03E-15	3.11E-15	2.89E-15	0.97	1.05	0.93
^{238}U (n,f) ^{137}Cs	8.80E-15	1.07E-14	9.51E-15	0.83	0.93	0.89
^{237}Np (n,f) ^{137}Cs	7.65E-14	7.96E-14	7.38E-14	0.96	1.04	0.93
^{59}Co (n,γ) ^{60}Co	9.93E-13	1.27E-12	1.00E-12	0.78	0.99	0.79
^{59}Co(Cd) (n,γ) ^{60}Co	5.70E-13	5.97E-13	5.66E-13	0.95	1.01	0.95
Fast Reaction Threshold Foil Average				0.92	1.00	0.92
Standard deviation				9.2%	6.4%	3.6%

	C	BE	%Unc.	BE/C	
Fluence Rate (E>1.0 MeV) (n/cm^2-s)	3.01E+10	2.68E+10	6.0	0.89	
Fluence Rate (E>0.1 MeV) (n/cm^2-s)	9.64E+10	8.79E+10	10.0	0.91	χ^2/DOF
DPA/s	4.93E-11	4.45E-11	7.0	0.90	0.650

Table A-10 Least-Squares Evaluation of Dosimetry in Surveillance Capsule B (40° Position, Irradiated During Cycles 6–25)

Reaction	Reaction Rate (rps/atom)			M/C	M/BE	BE/C
	Measured (M)	Calculated (C)	Best-Estimate (BE)			
^{63}Cu (n,α) ^{60}Co	2.94E-17	2.68E-17	2.88E-17	1.10	1.02	1.08
^{54}Fe (n,p) ^{54}Mn	2.88E-15	2.85E-15	2.92E-15	1.01	0.99	1.02
^{58}Ni (n,p) ^{58}Co	4.02E-15	3.91E-15	4.01E-15	1.03	1.00	1.03
^{238}U (n,f) ^{137}Cs	1.34E-14	1.38E-14	1.39E-14	0.97	0.96	1.00
^{237}Np (n,f) ^{137}Cs	1.05E-13	1.06E-13	1.05E-13	0.99	1.00	0.99
^{59}Co (n,γ) ^{60}Co	2.03E-12	1.77E-12	2.03E-12	1.15	1.00	1.14
^{59}Co(Cd) (n,γ) ^{60}Co	8.12E-13	8.31E-13	8.15E-13	0.98	1.00	0.98
Fast Reaction Threshold Foil Average				1.02	0.99	1.02
Standard deviation				4.9%	2.2%	3.4%

	C	BE	%Unc.	BE/C	
Fluence Rate (E>1.0 MeV) (n/cm^2-s)	3.96E+10	3.94E+10	6	0.99	
Fluence Rate (E>0.1 MeV) (n/cm^2-s)	1.30E+11	1.29E+11	10	0.99	χ^2/DOF
DPA/s	6.55E-11	6.53E-11	7	1.00	0.055

Table A-11 Measured-to-Calculated (M/C) Reaction Rates – In-Vessel Capsules

Reaction	Capsule				Reaction Average	Reaction Std. Dev.
	S	Y	V	B		
$^{63}Cu\ (n,\alpha)\ ^{60}Co$	1.09	0.99	1.00	1.10	1.05	5.6%
$^{54}Fe\ (n,p)\ ^{54}Mn$	0.88	0.84	0.82	1.01	0.89	9.6%
$^{58}Ni\ (n,p)\ ^{58}Co$	1.02	0.93	0.97	1.03	0.99	4.7%
$^{238}U(Cd)\ (n,f)\ ^{137}Cs$	1.01	0.91	0.83	0.97	0.93	8.4%
$^{237}Np(Cd)\ (n,f)\ ^{137}Cs$	1.11	0.79	0.96	0.99	0.96	13.7%
Average of M/C Results					**0.96**	**9.7%**

Table A-12 Best-Estimate-to-Calculated (BE/C) Exposure Rates – In-Vessel Capsules

Capsule	Fast (E > 1.0 MeV) Fluence Rate		Iron Atom Displacement Rate	
	BE/C	Std. Dev.	BE/C	Std. Dev.
S	0.99	6%	1.01	7%
Y	0.87	6%	0.88	7%
V	0.89	6%	0.90	7%
B	0.99	6%	1.00	7%
Average	0.94	6.8%	0.95	7.1%

A.2 REFERENCES

A-1 U.S. Nuclear Regulatory Commission Regulatory Guide 1.190, "Calculational and Dosimetry Methods for Determining Pressure Vessel Neutron Fluence," March 2001. *[ADAMS Accession Number ML010890301]*

A-2 A. Schmittroth, FERRET Data Analysis Core, HEDL-TME 79-40, Hanford Engineering Development Laboratory, Richland, WA, September 1979.

A-3 RSICC Data Library Collection DLC-178, SNLRML Recommended Dosimetry Cross-Section Compendium, July 1994.

A-4 ASTM Standard E944-19, Standard Guide for Application of Neutron Spectrum Adjustment Methods in Reactor Surveillance, 2019.

A-5 ASTM Standard E844-25, Standard Guide for Sensor Set Design and Irradiation for Reactor Surveillance, 2025.

APPENDIX B LOAD-TIME RECORDS FOR CHARPY SPECIMEN TESTS FROM CAPSULE B

- "ATXX, BTXX, CTXX" denotes Lower Shell Plate B4107-1
- "DTXX, ETXX" denotes Correlation Monitor Material Plate HSST02
- "SWXX" denotes Surrogate Weld
- "WXX" denotes Reconstituted Surveillance Weld

Note that the instrumented Charpy data is not required per ASTM Standards E185-82 or E23-18.

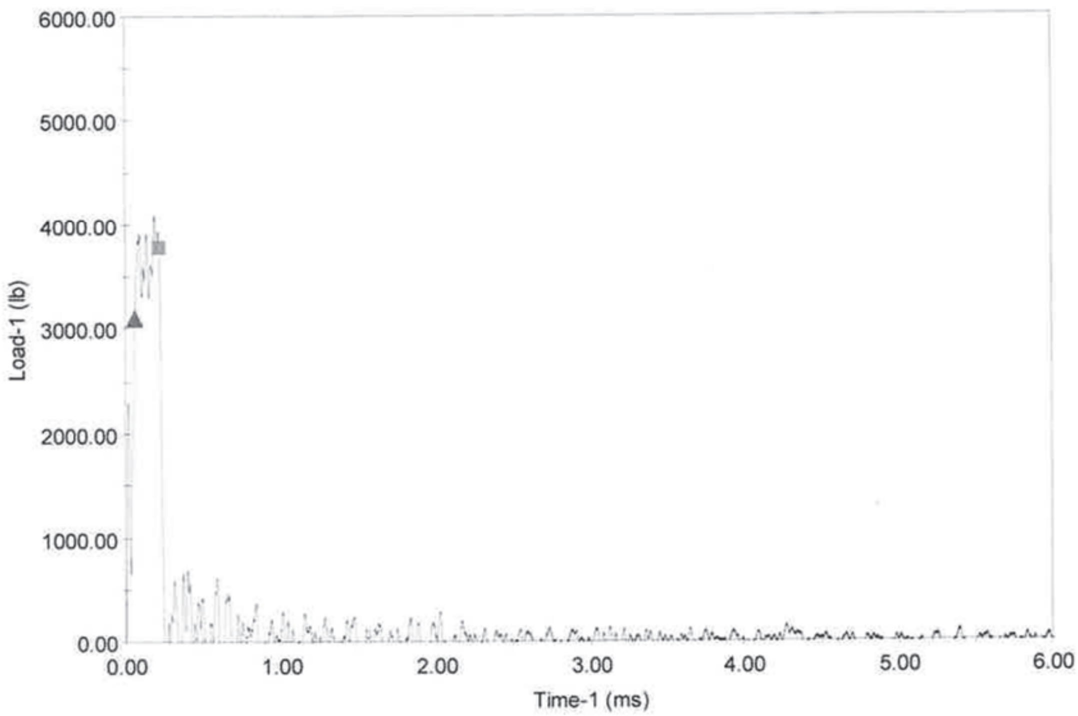

AT106, 74°F

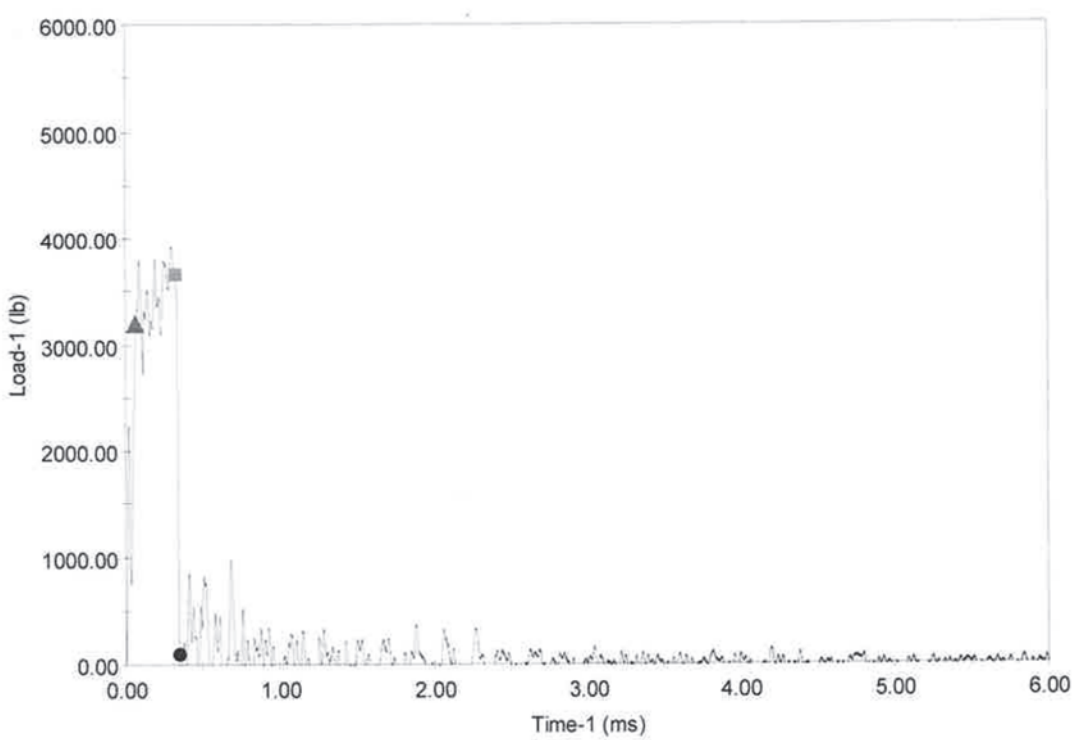

BT140, 100°F

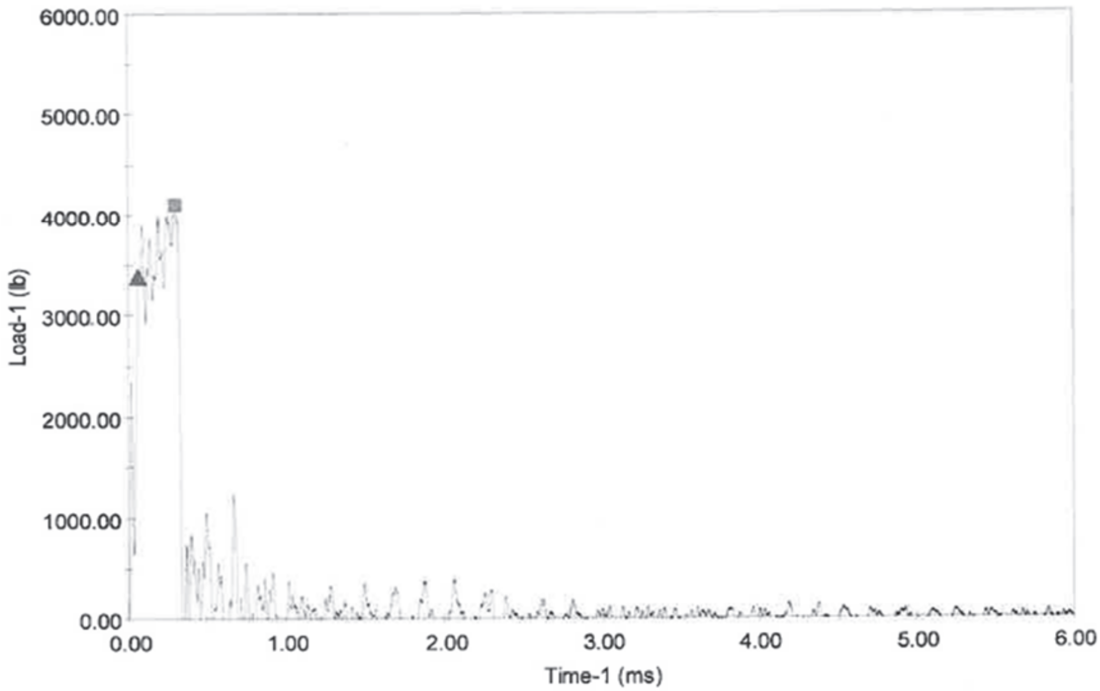

AT107, 125°F

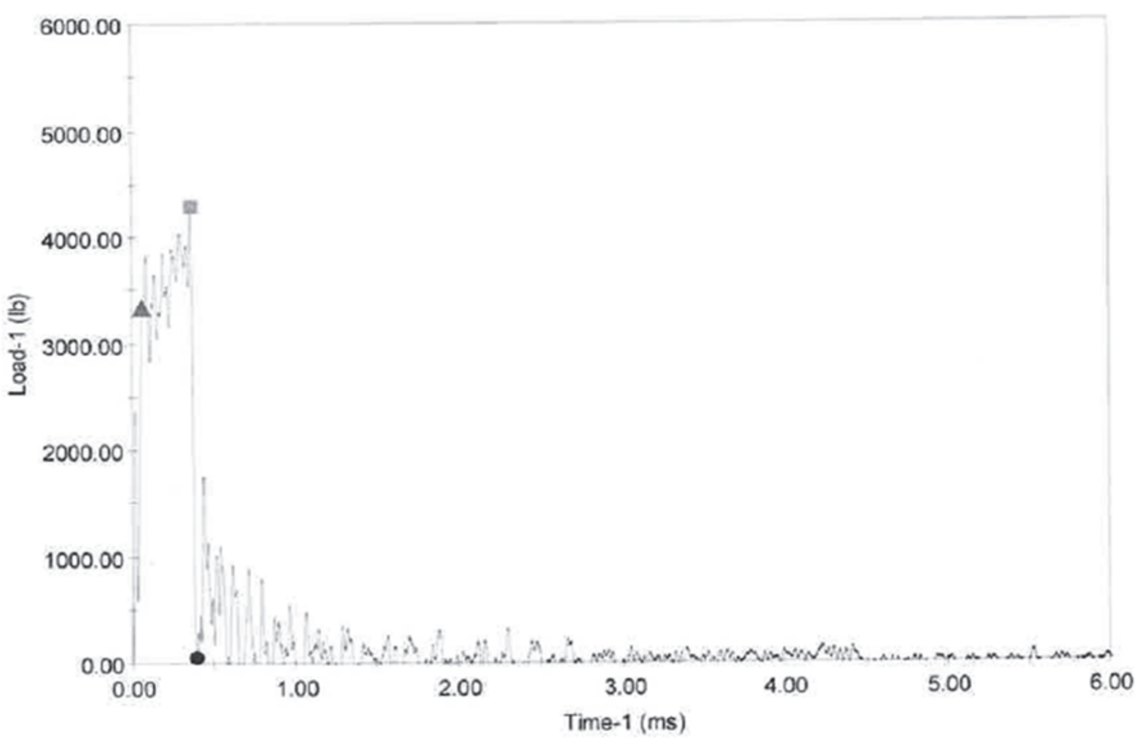

AT109, 150°F

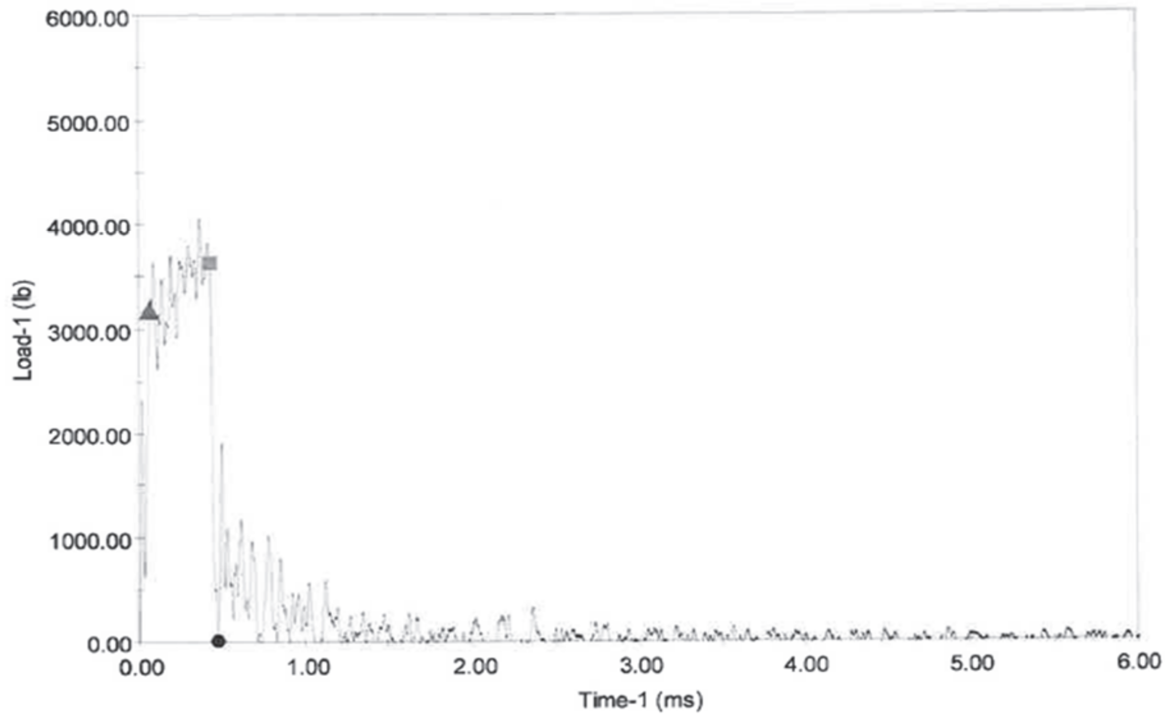

CT170, 160°F

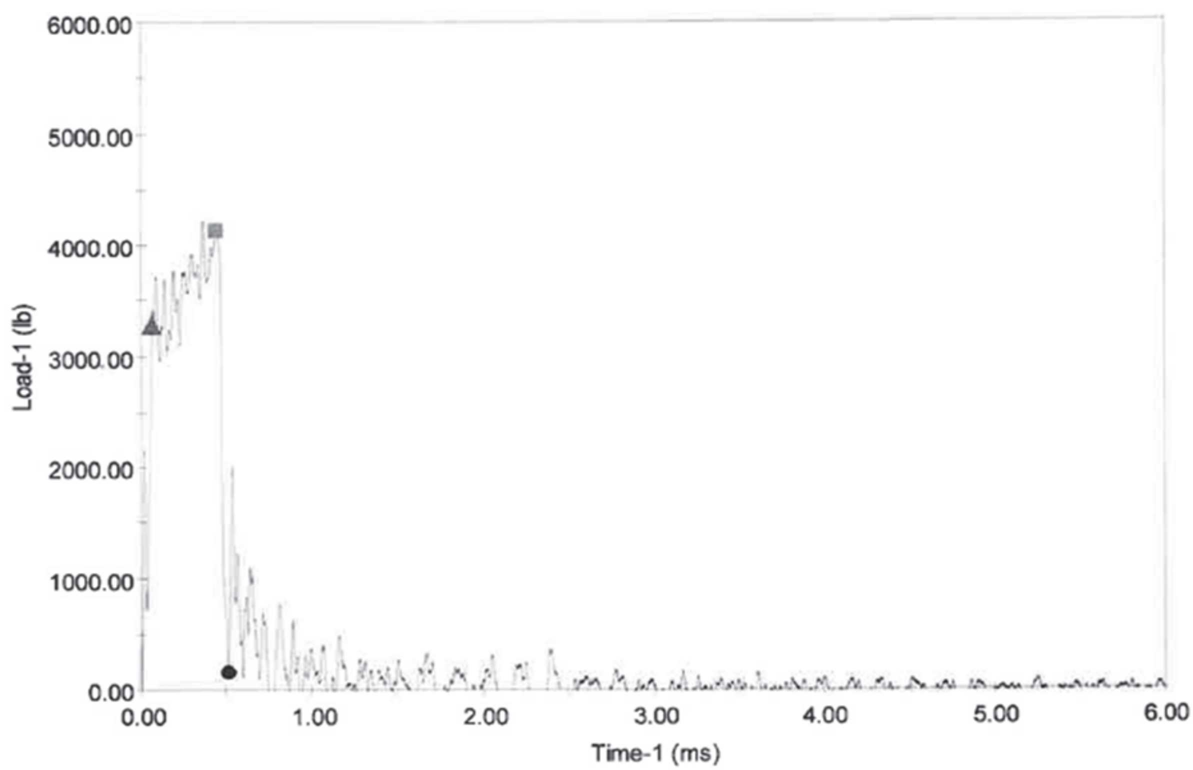

AT110, 180°F

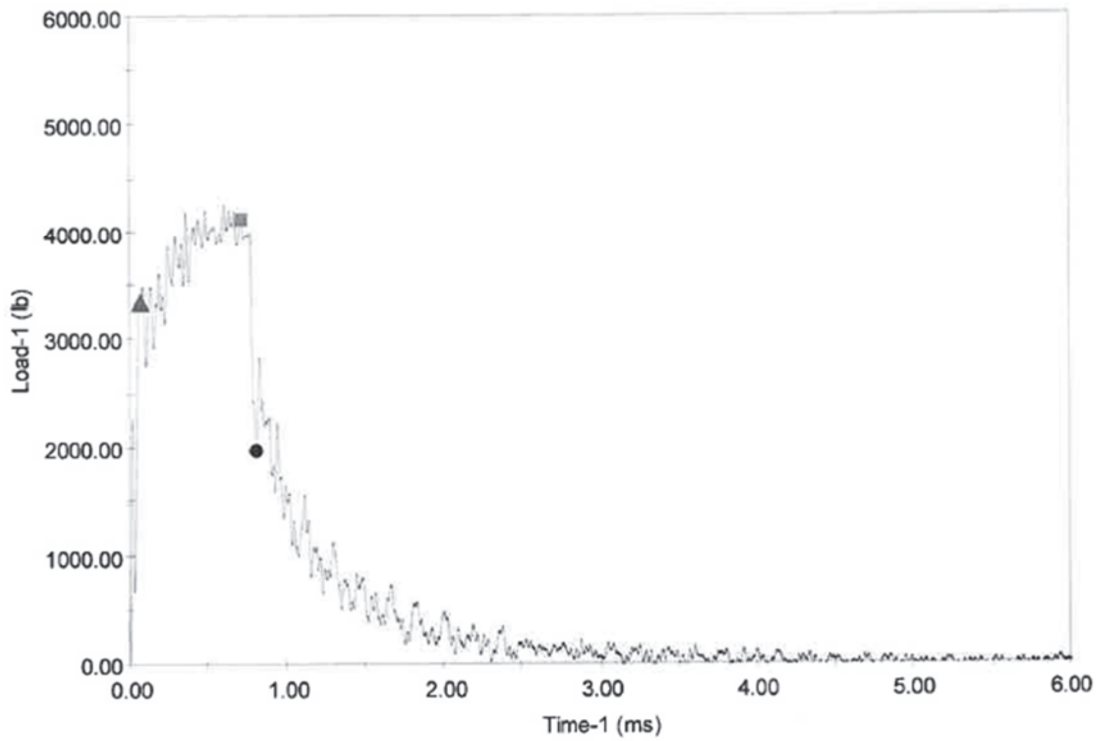

CT166, 190°F

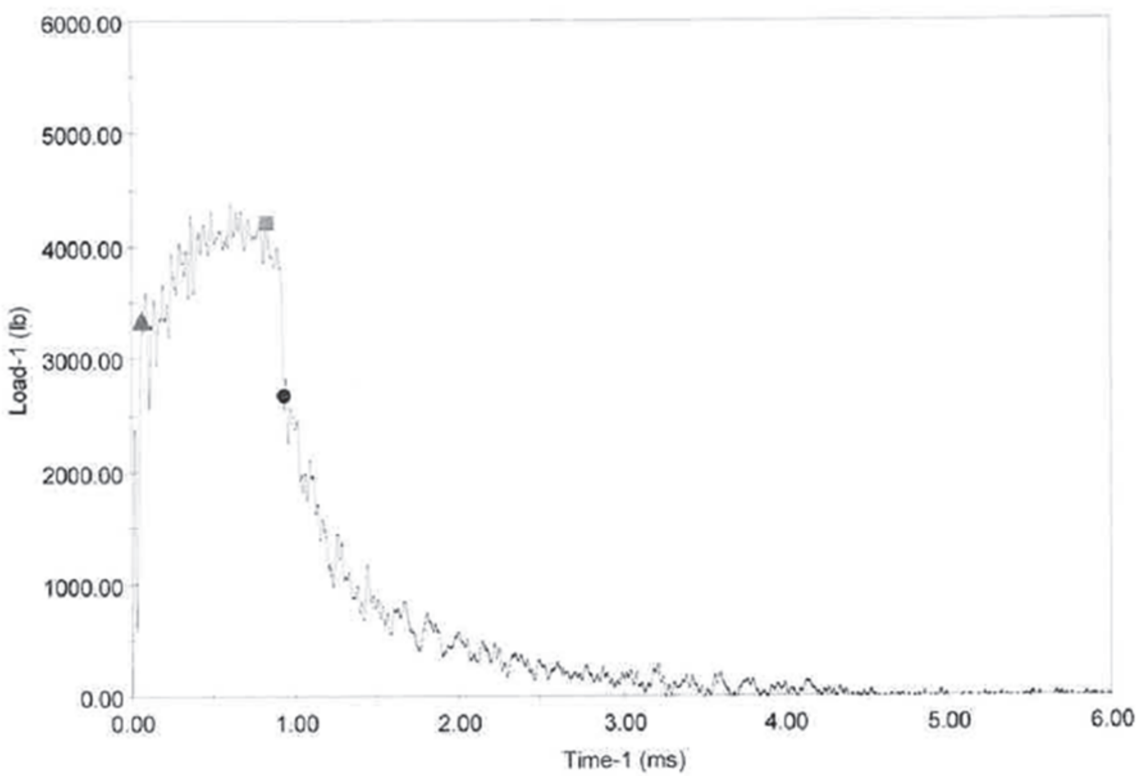

BT137, 190°F

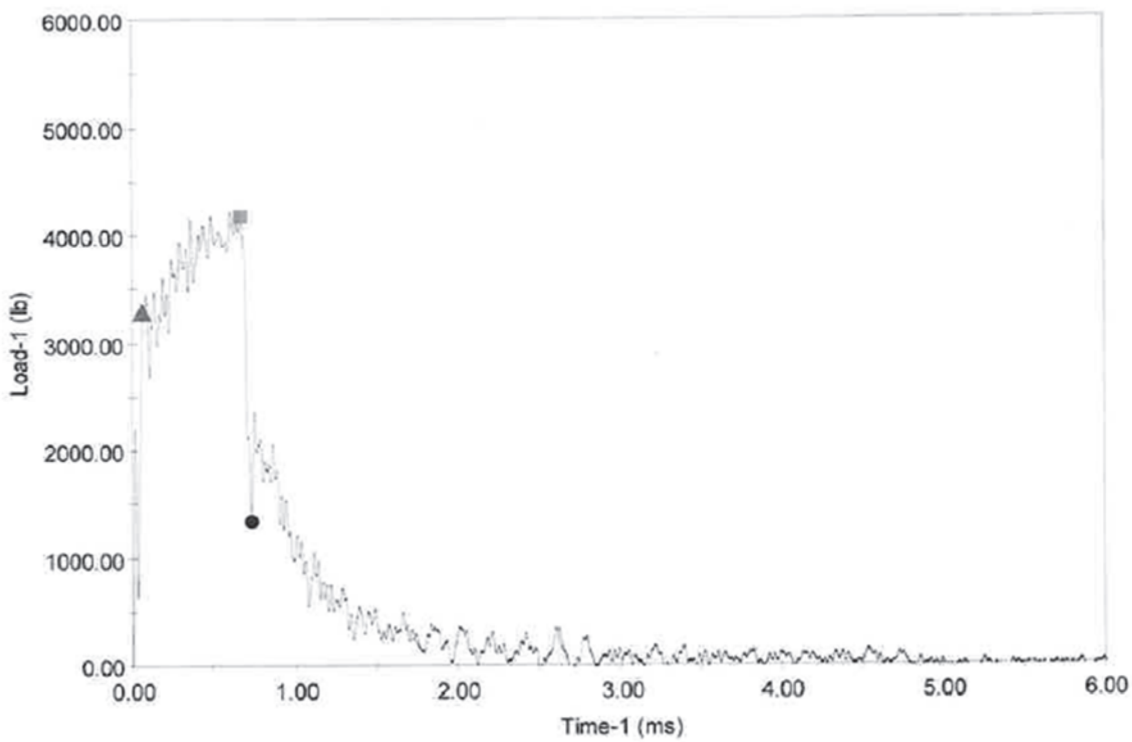

BT139, 200°F

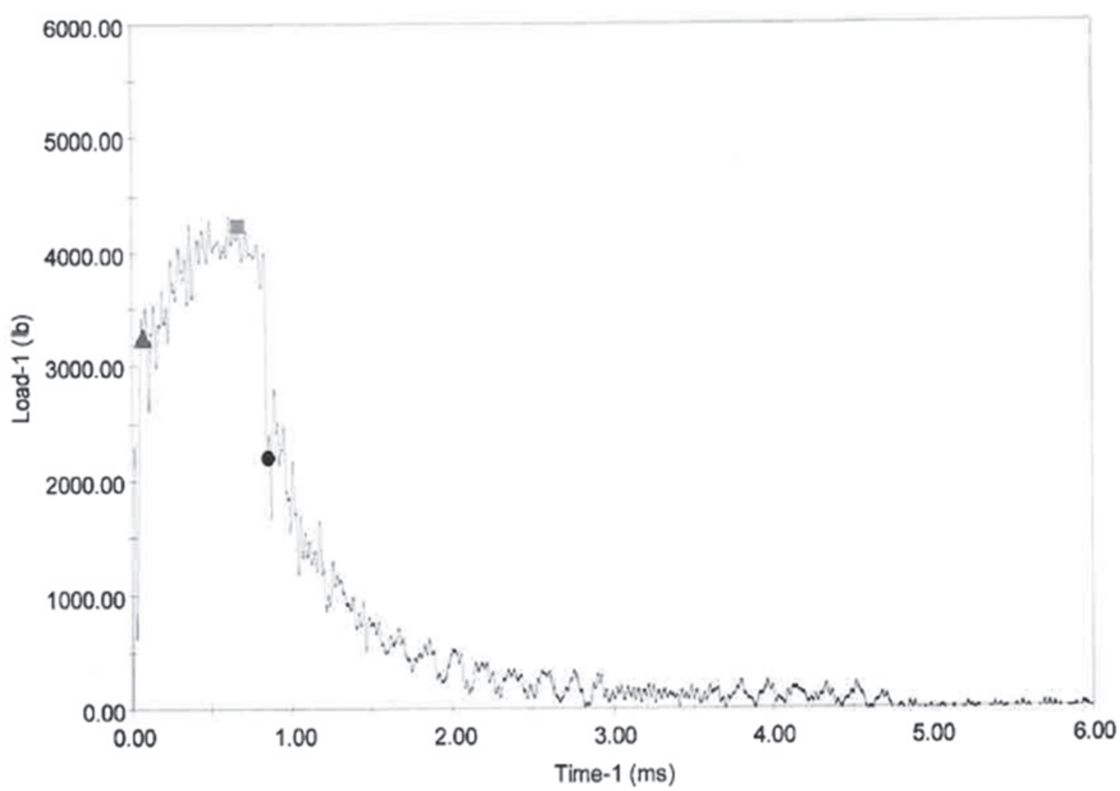

BT136, 210°F

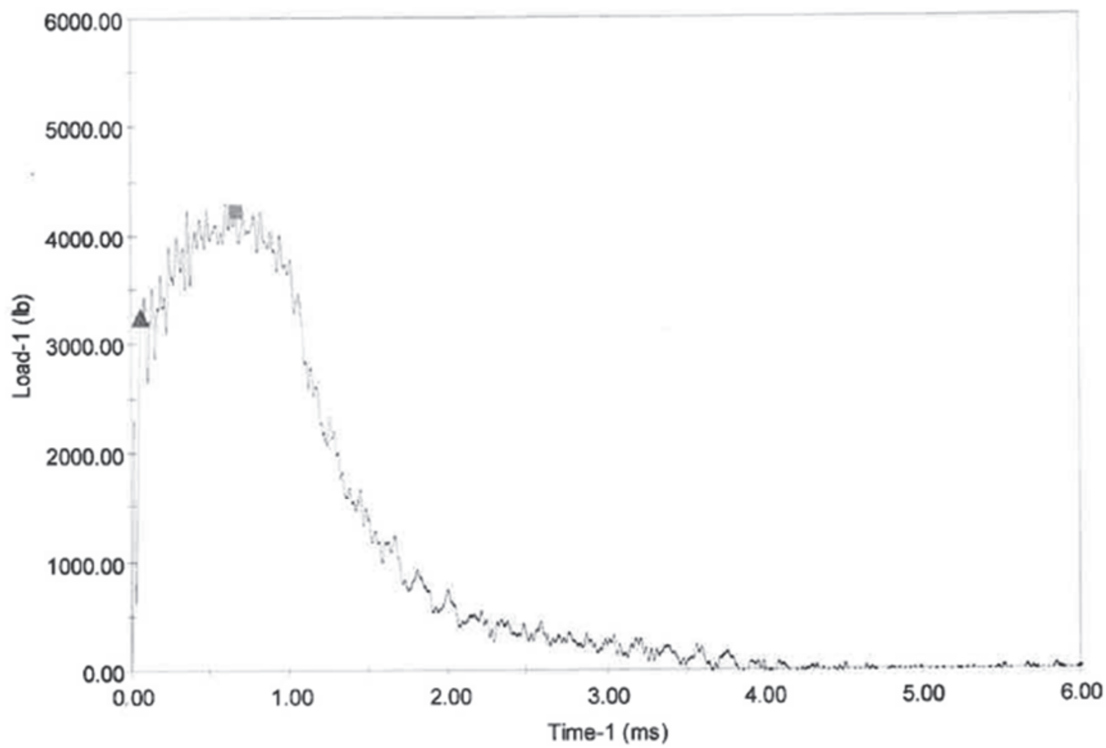

CT169, 225°F

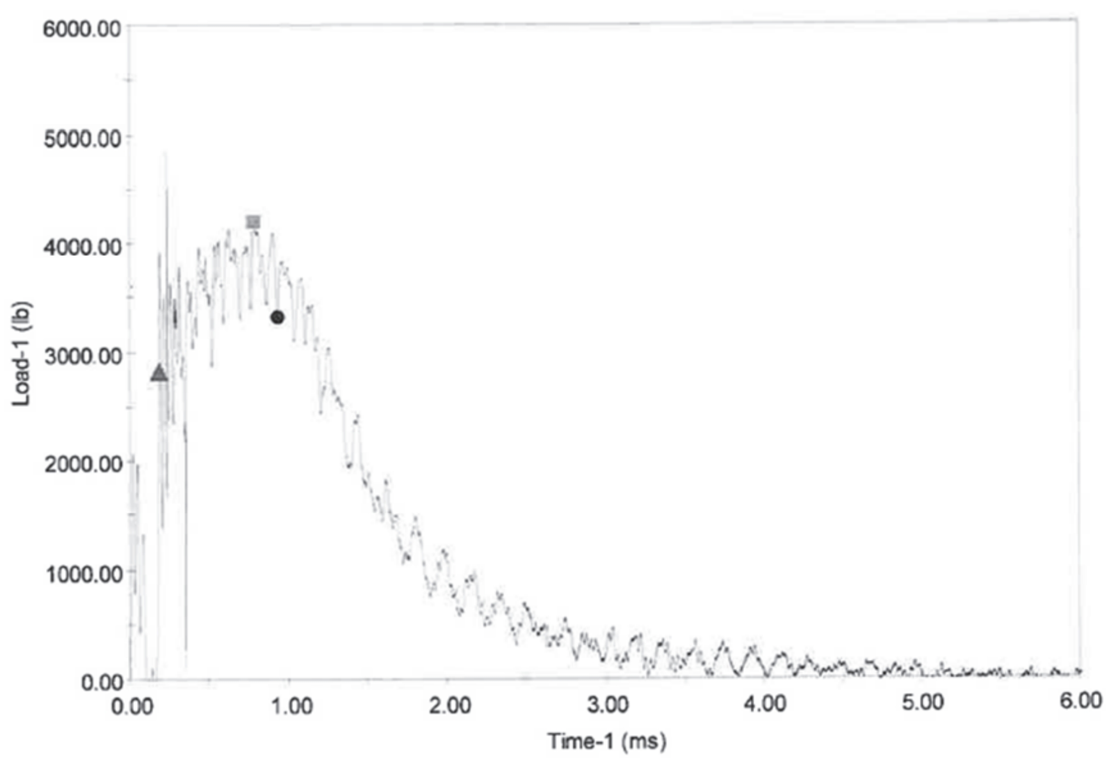

CT167, 250°F

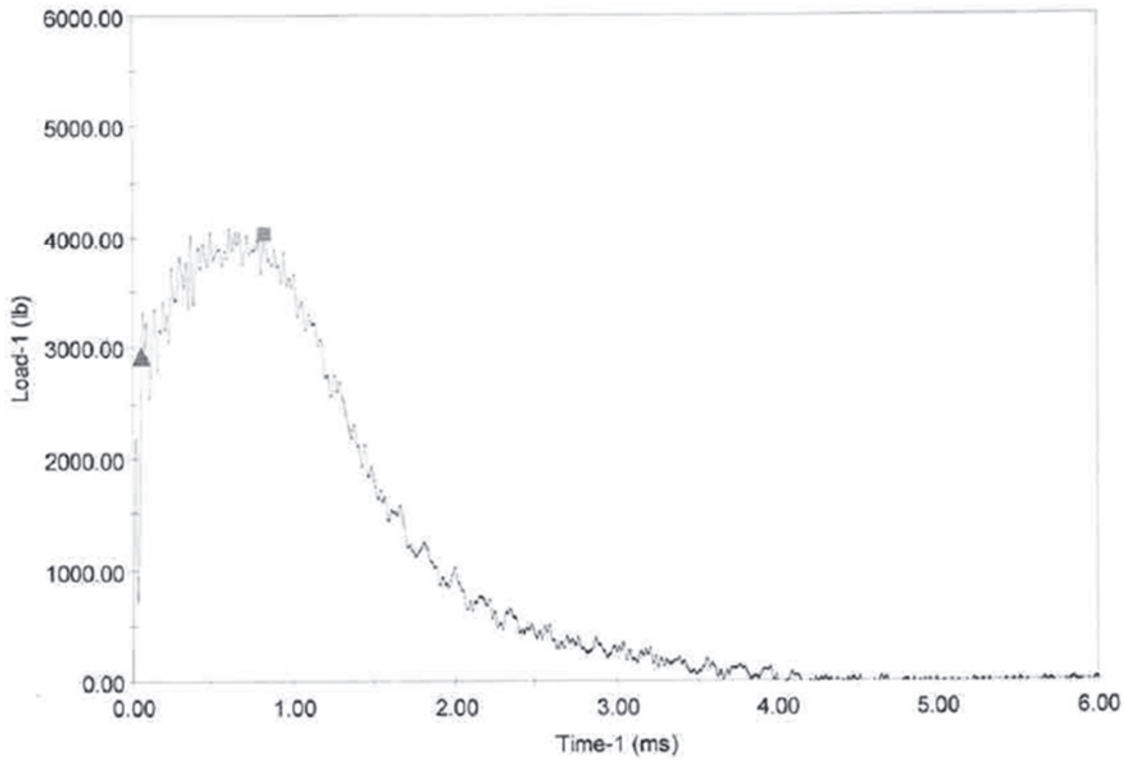

BT138, 300°F

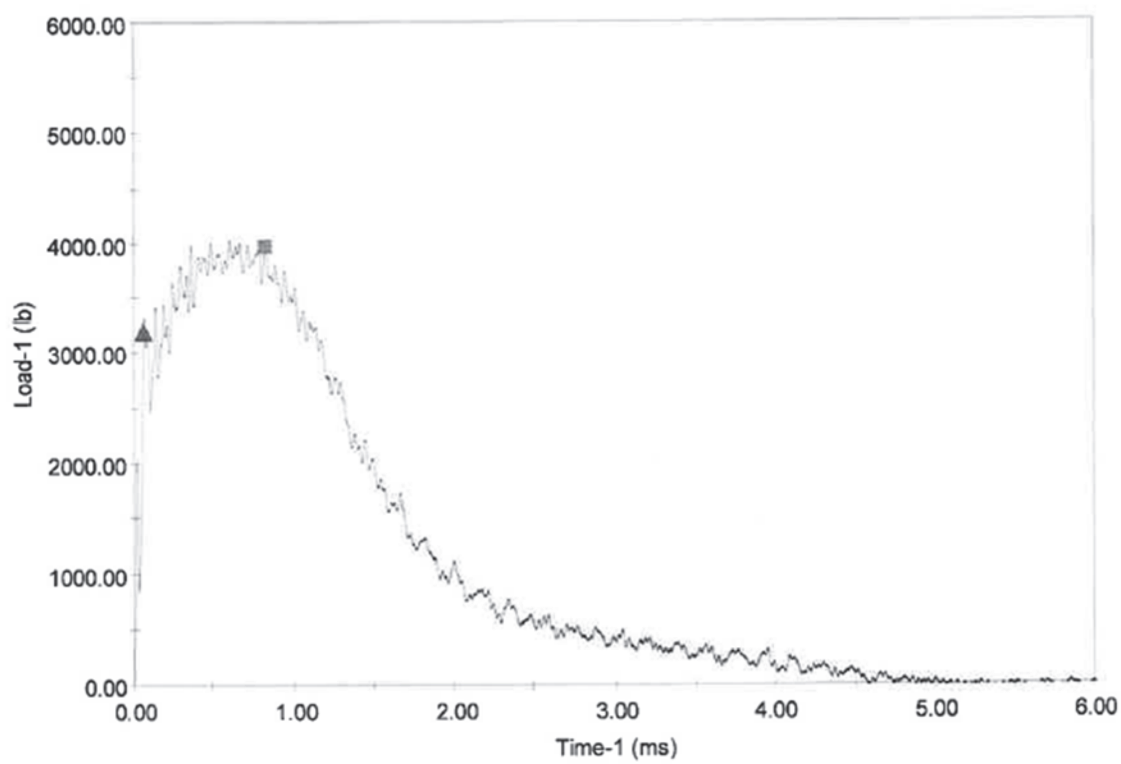

CT168, 350°F

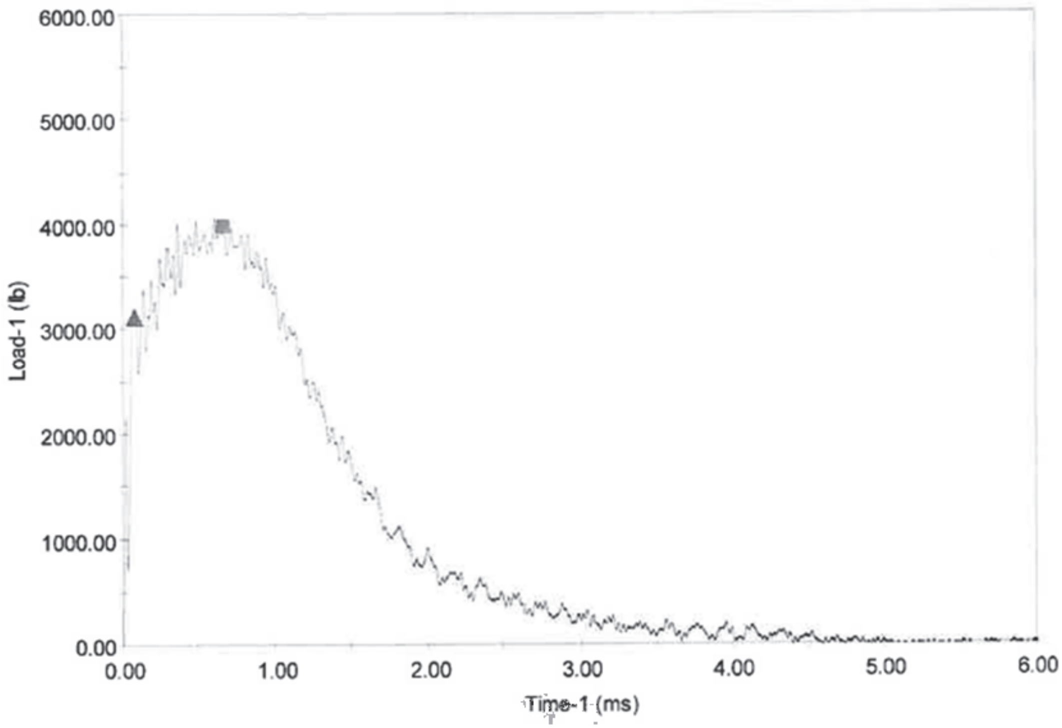
6000.00
5000.00
4000.00
3000.00
2000.00
1000.00
0.00
Load-1 (lb)
0.00
1.00
2.00
3.00
4.00
5.00
6.00
Time-1 (ms)

AT108, 375°F

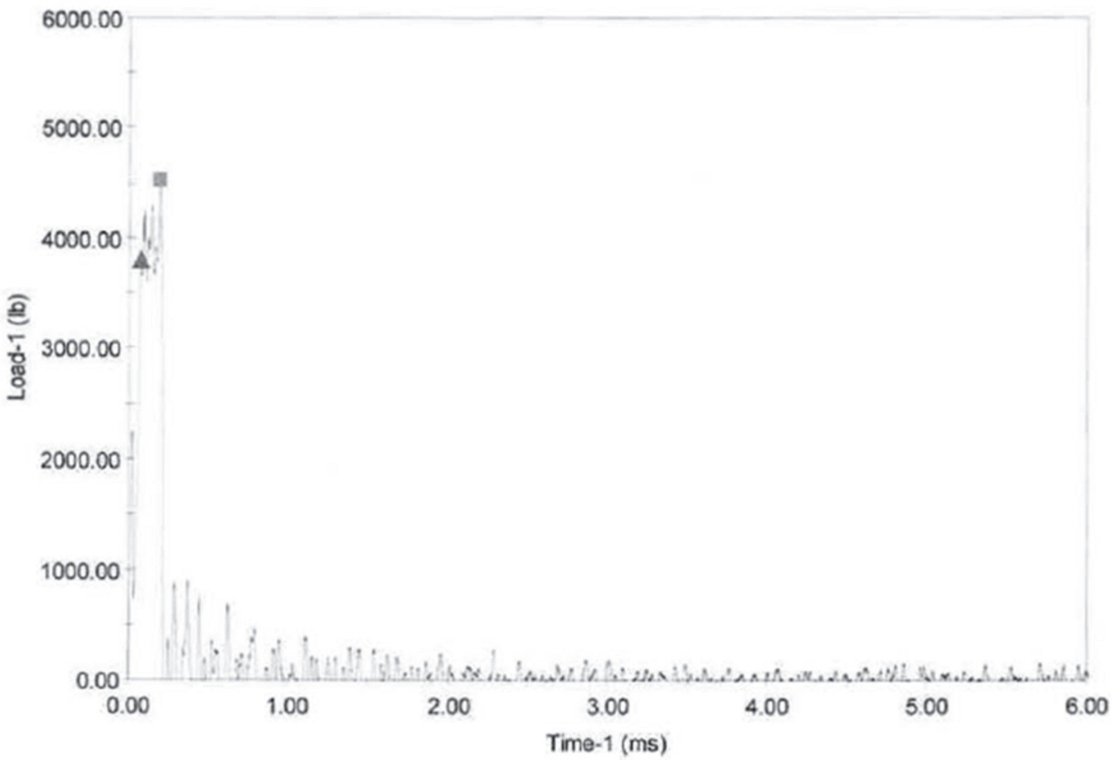

SW027, 125°F

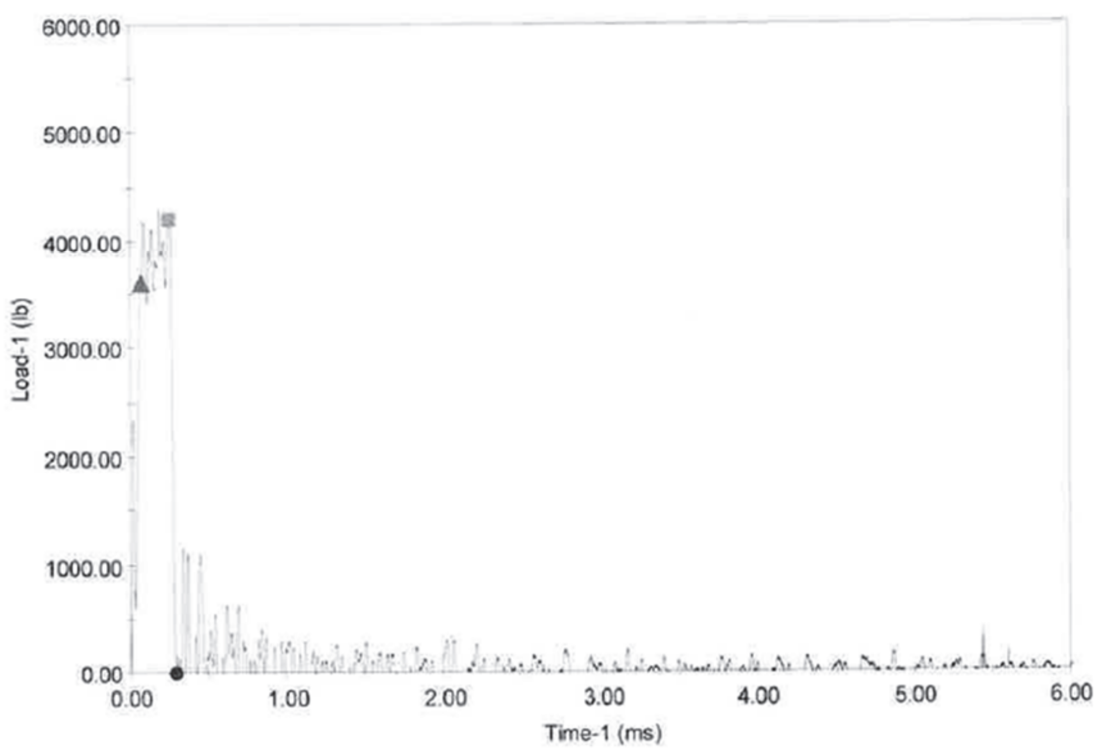

SW031, 150°F

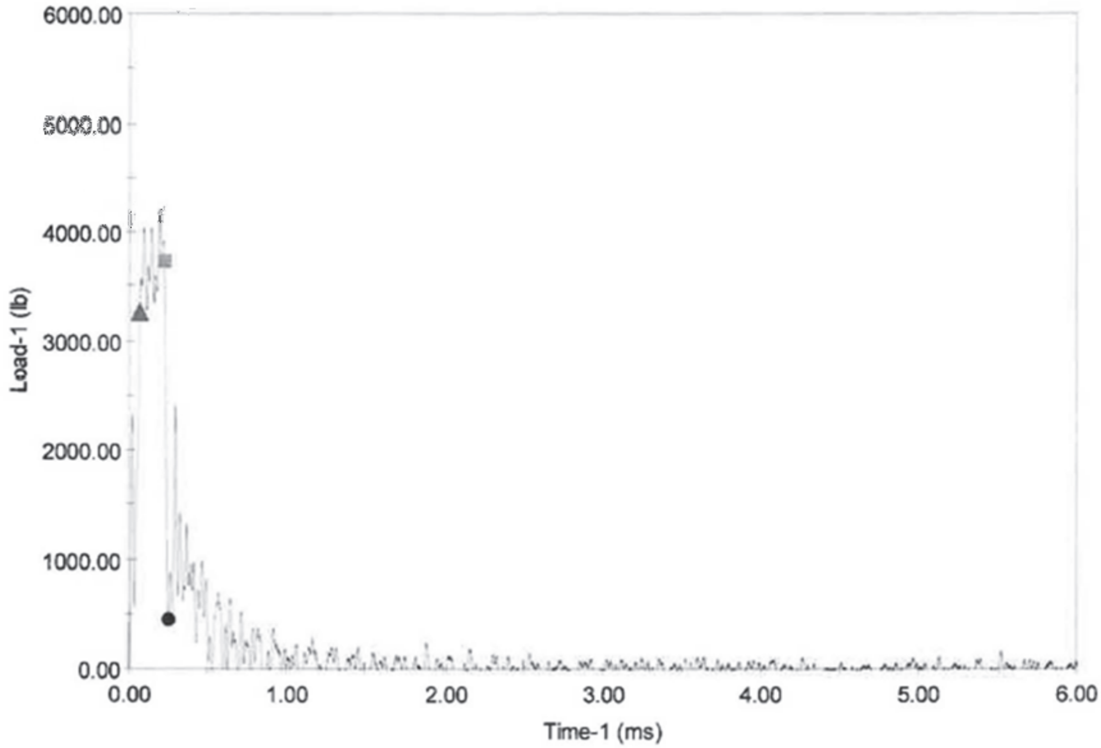

SW019, 180°F

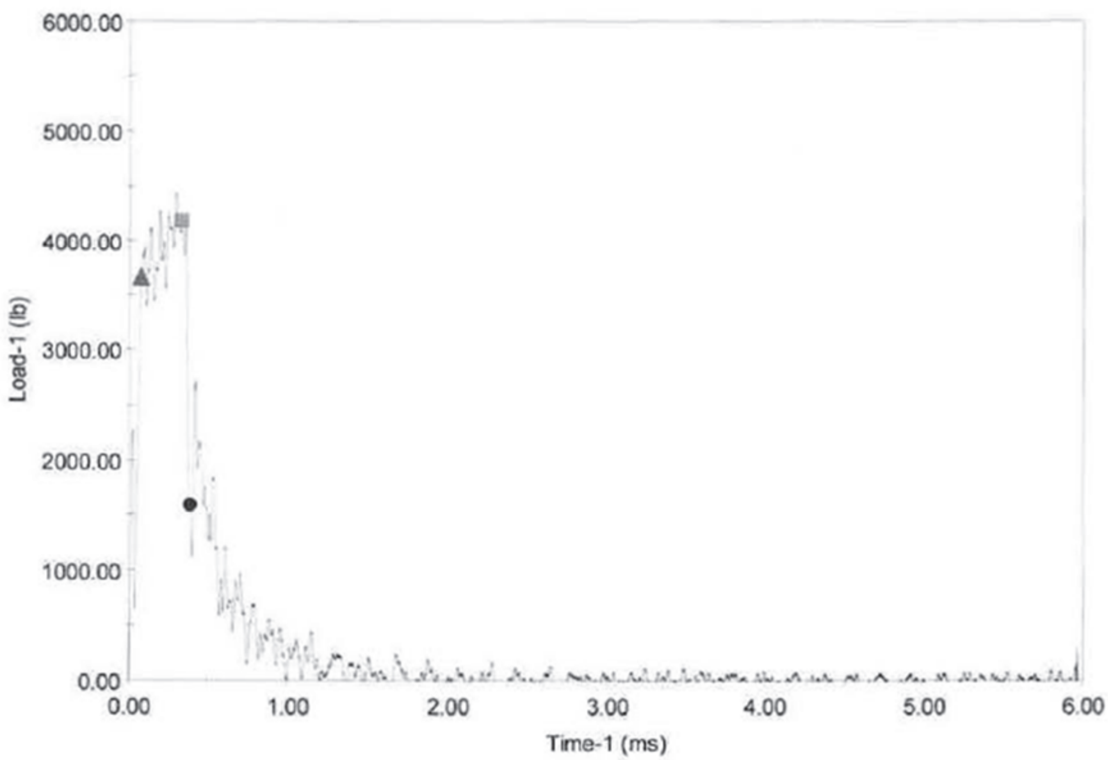

SW033, 190°F

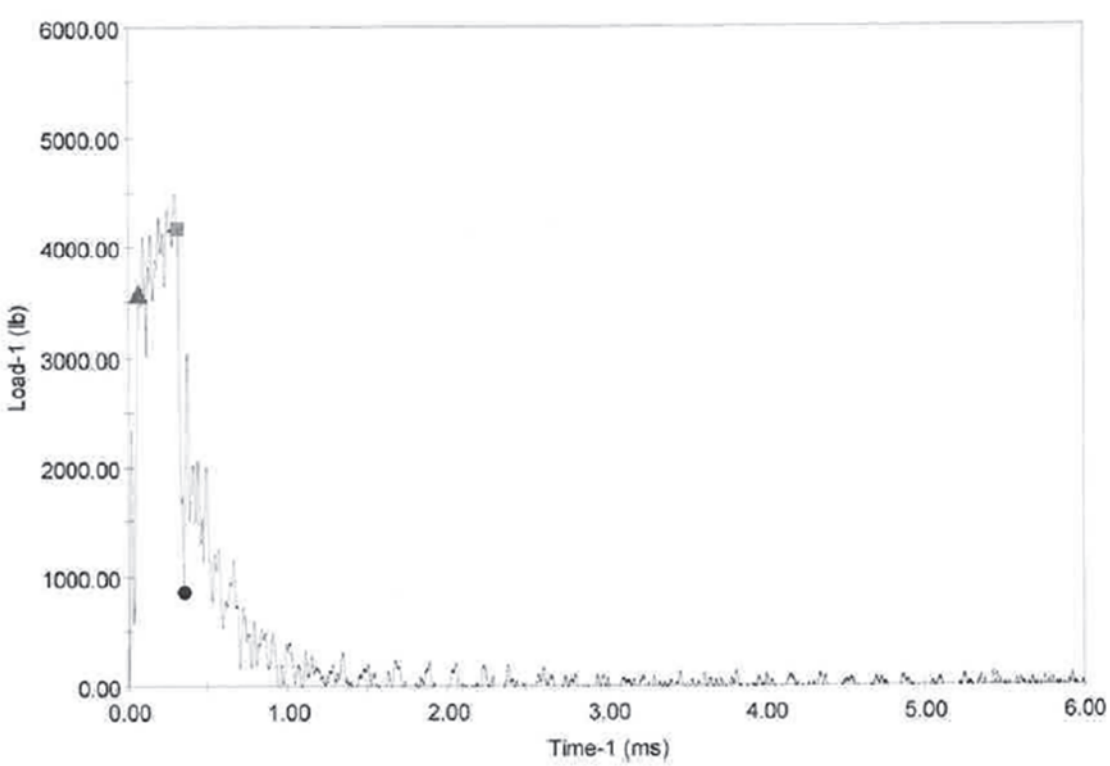

SW025, 200°F

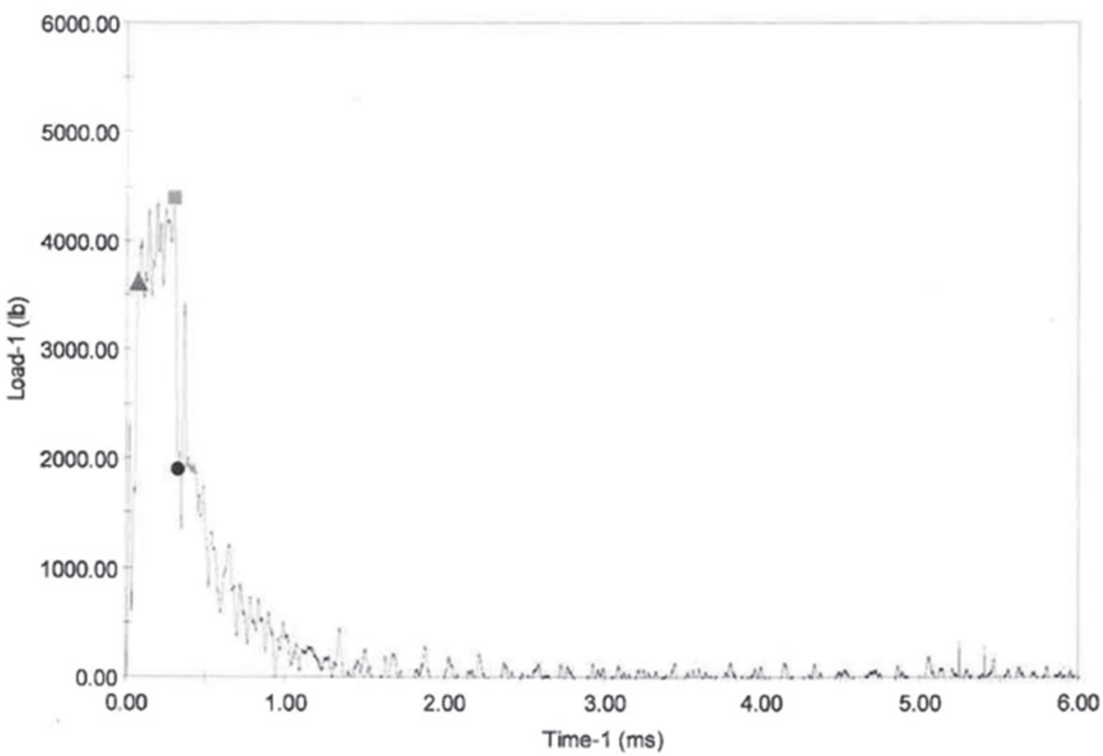

SW022, 210°F

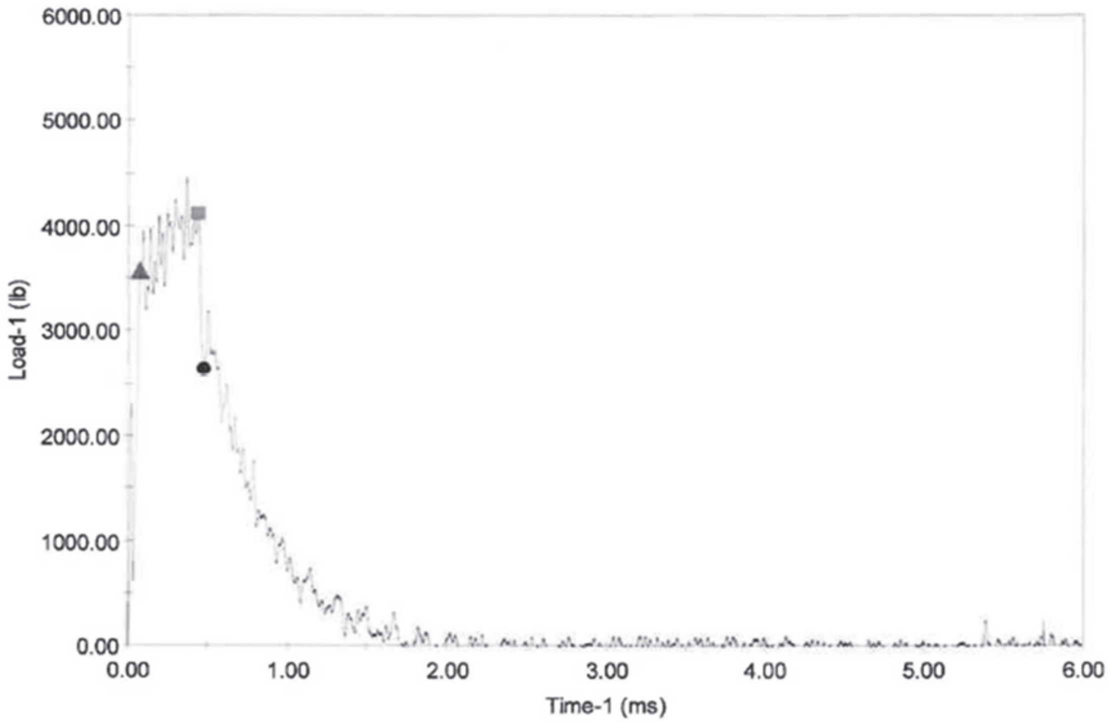

SW030, 225°F

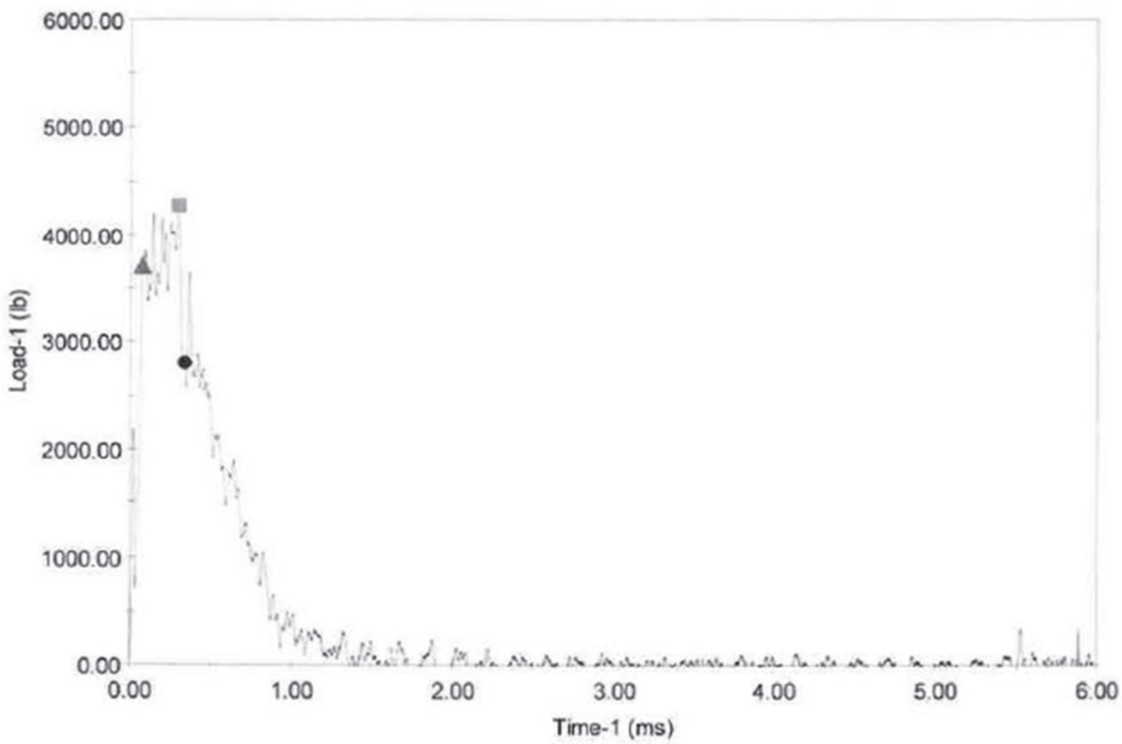

SW026, 225°F

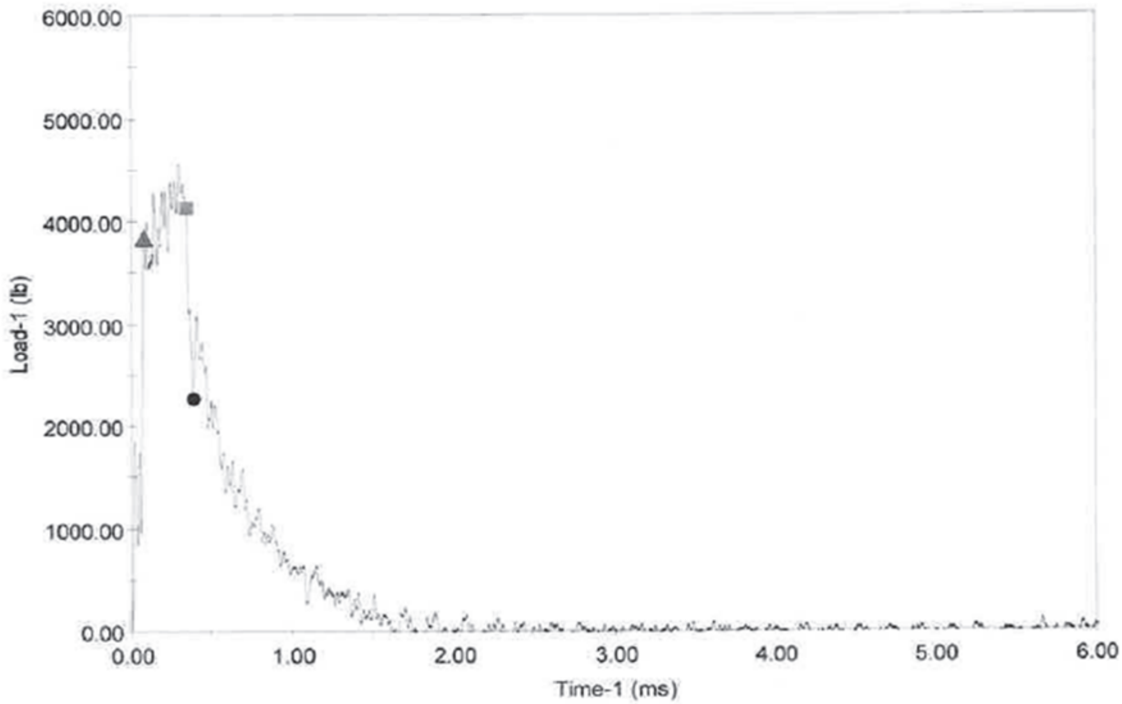

SW023, 250°F

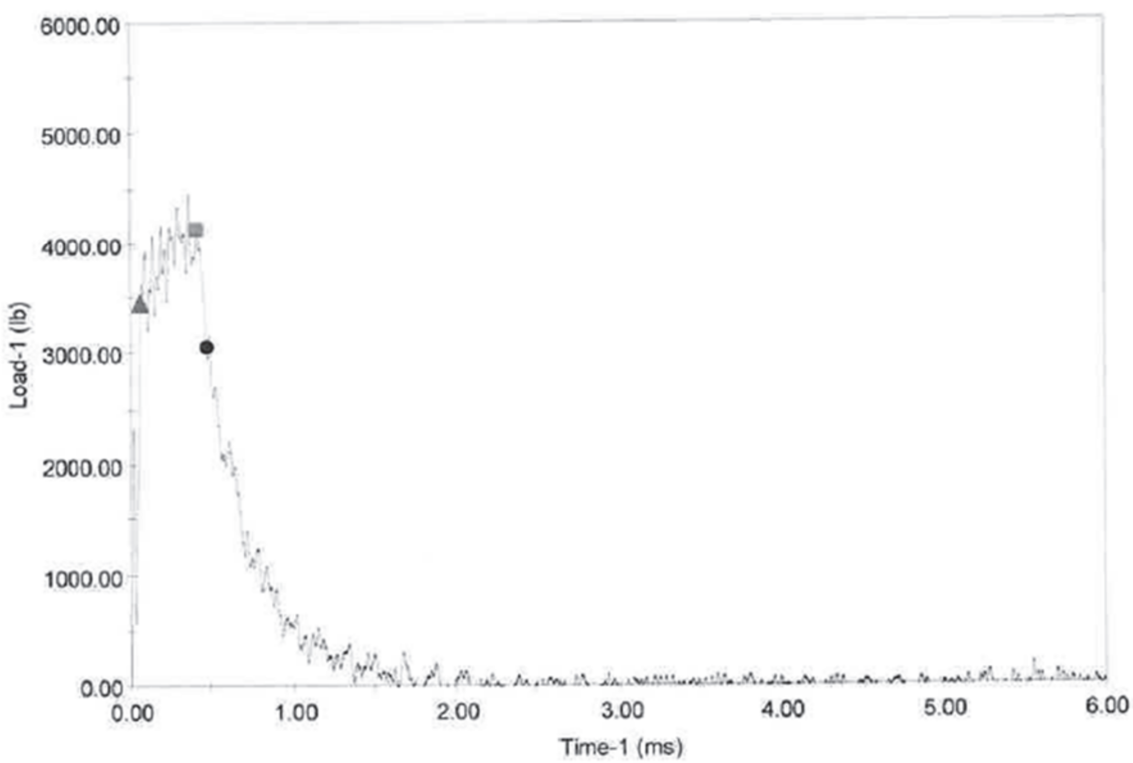

SW028, 275°F

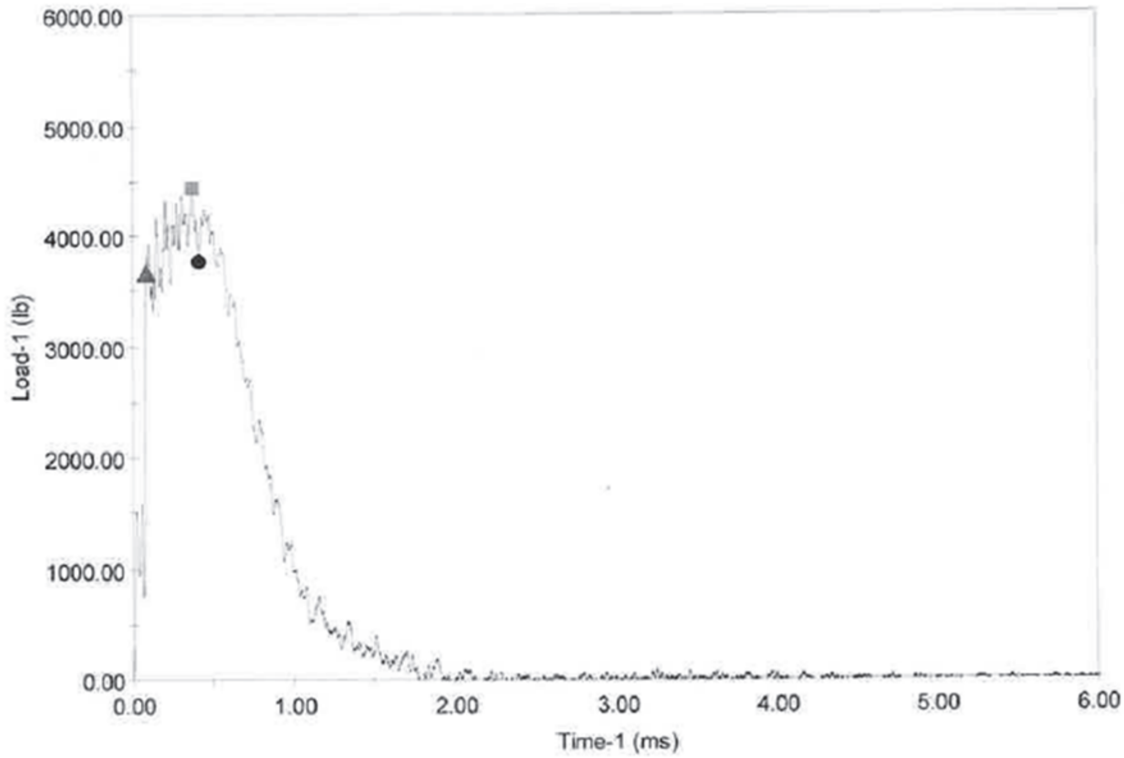

SW024, 300°F

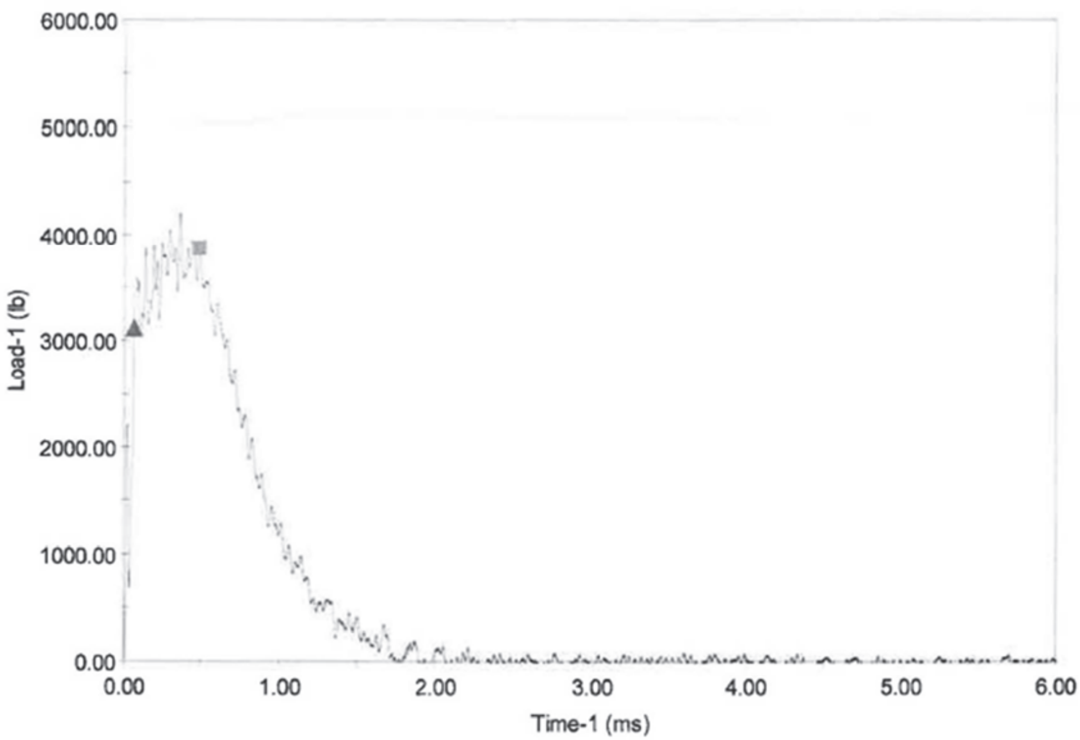

SW018, 325°F

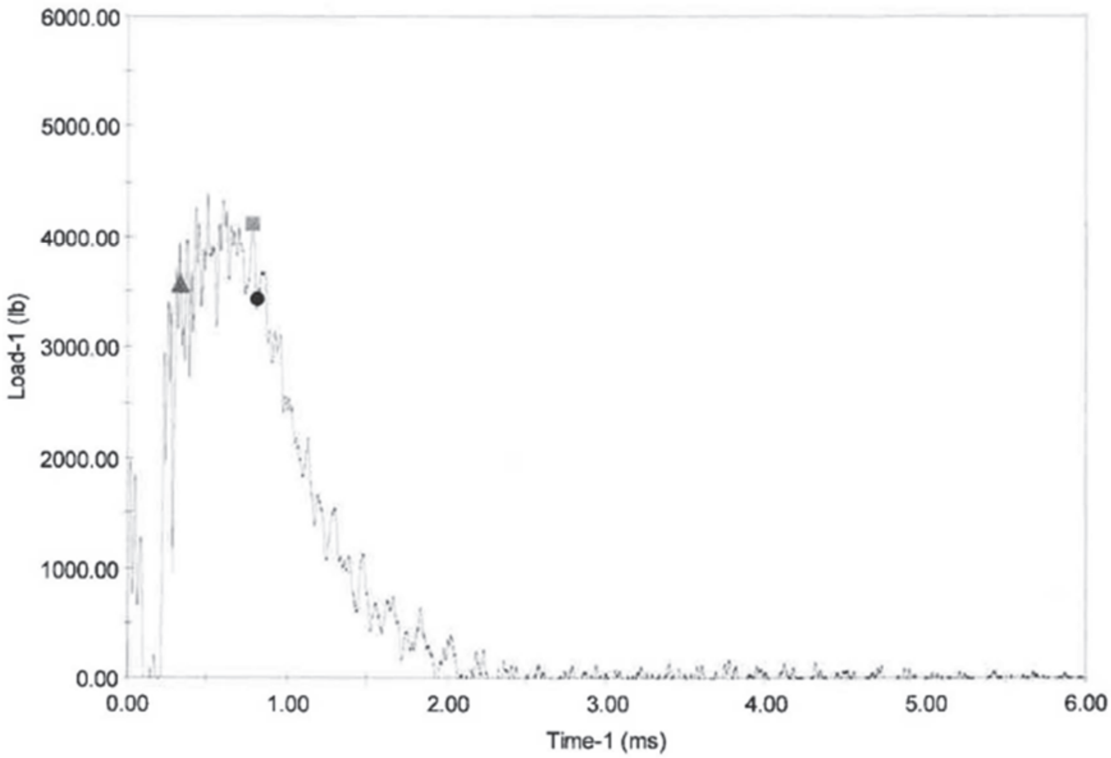

SW029, 350°F

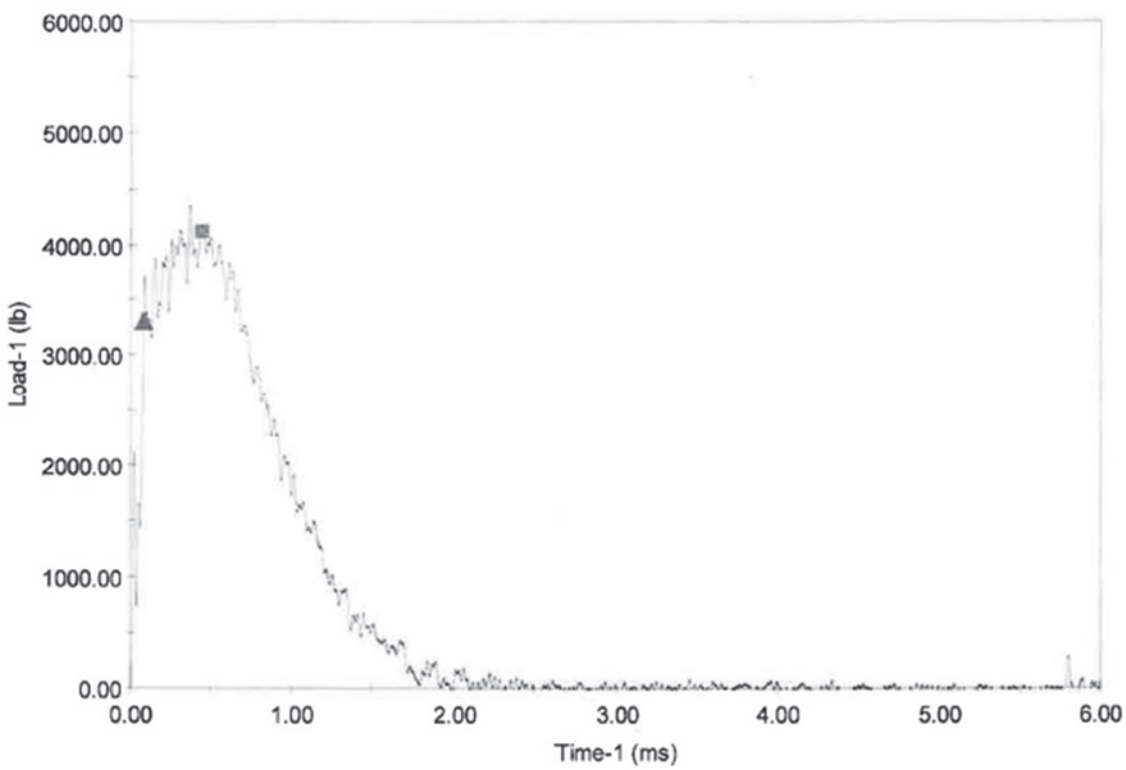

SW032, 375°F

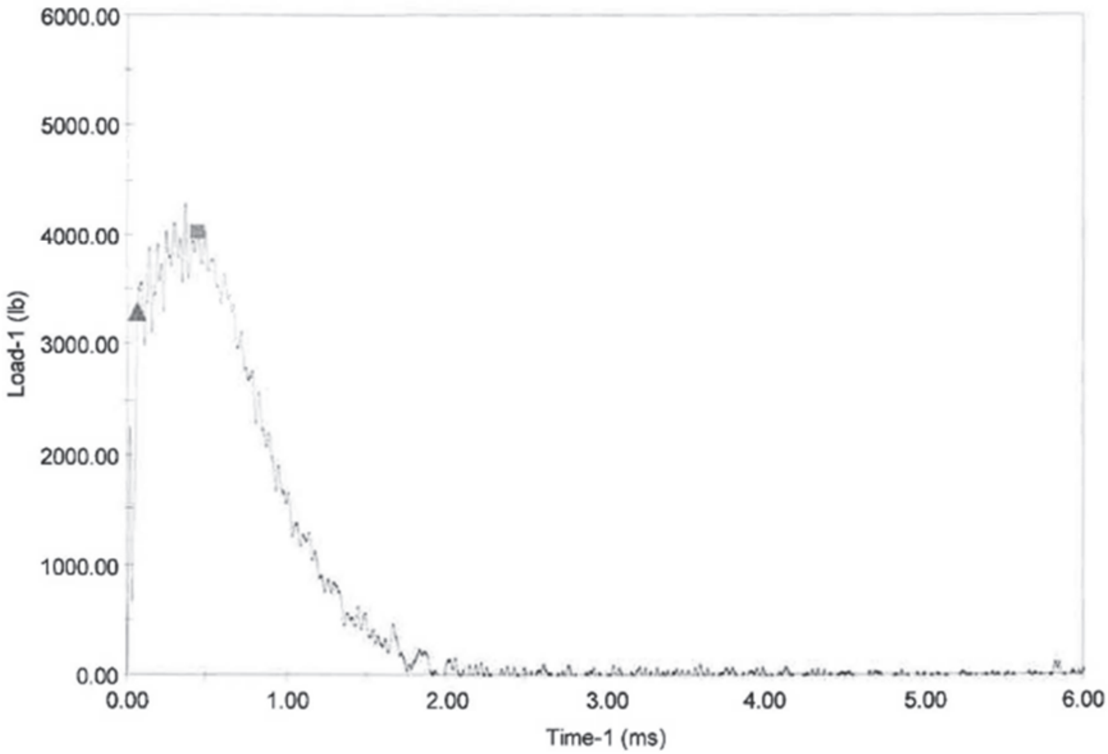
6000.00
5000.00
4000.00
3000.00
2000.00
1000.00
0.00
Load-1 (lb)
0.00
1.00
2.00
3.00
4.00
5.00
6.00
Time-1 (ms)

SW021, 400°F

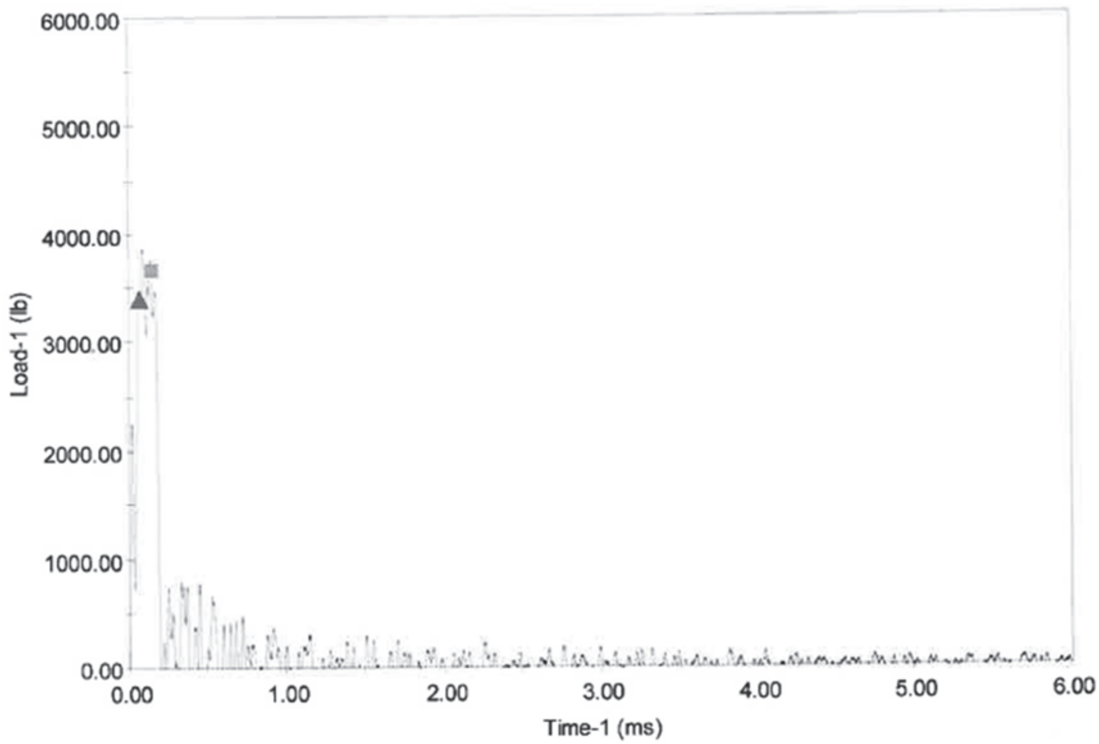

DT08, 160°F

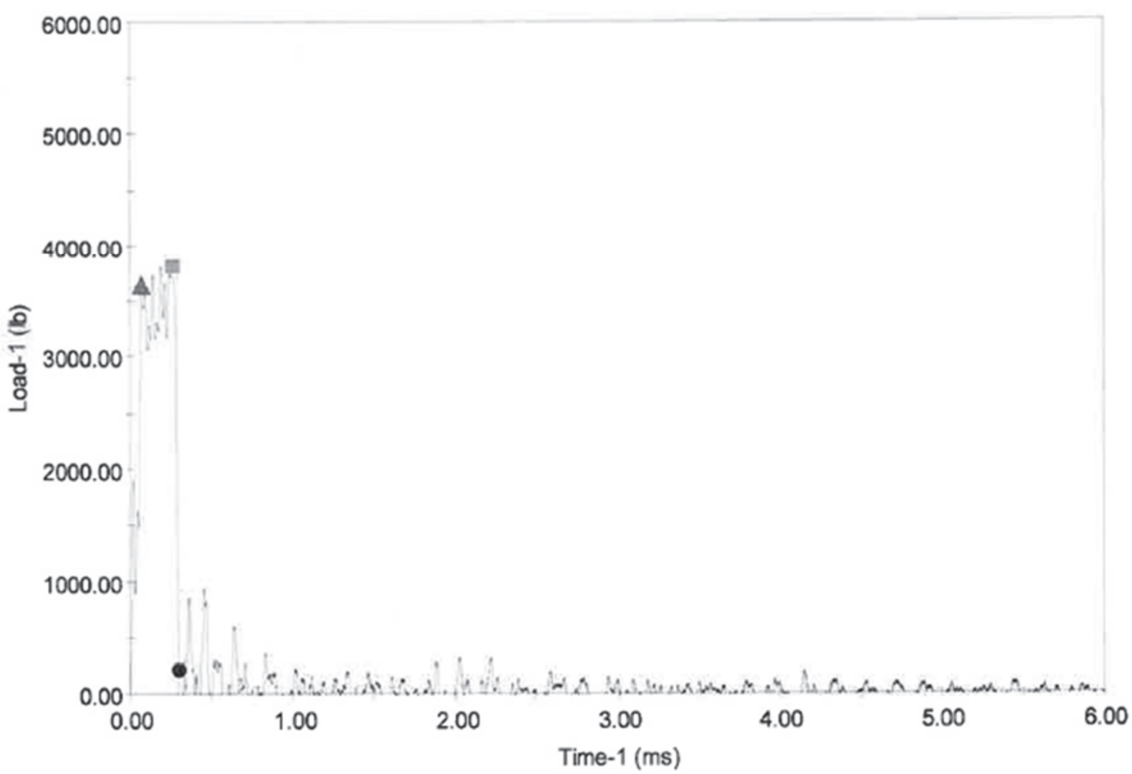

ET17, 180°F

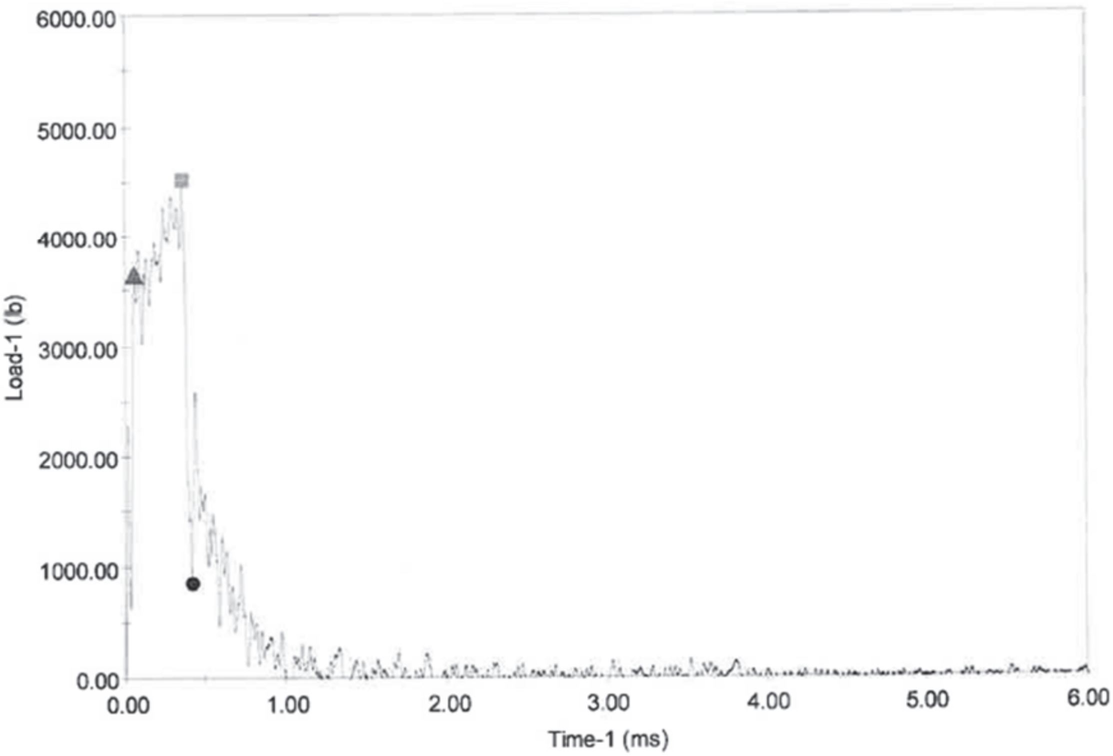

ET19, 200°F

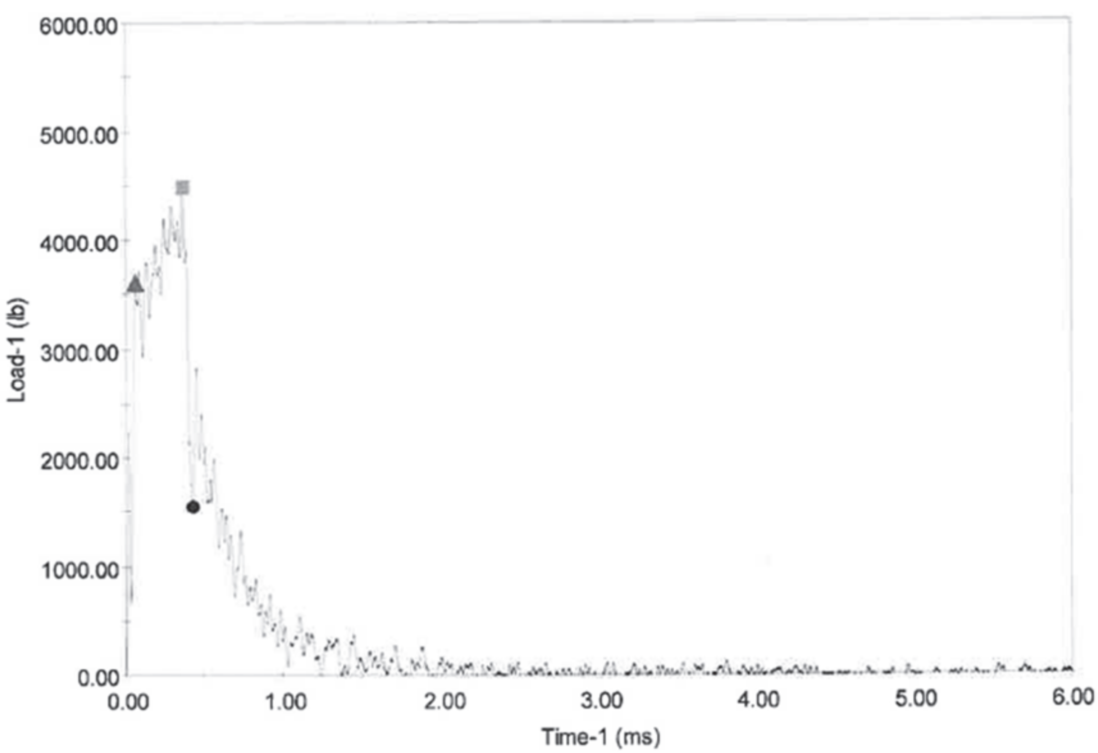

ET20, 225°F

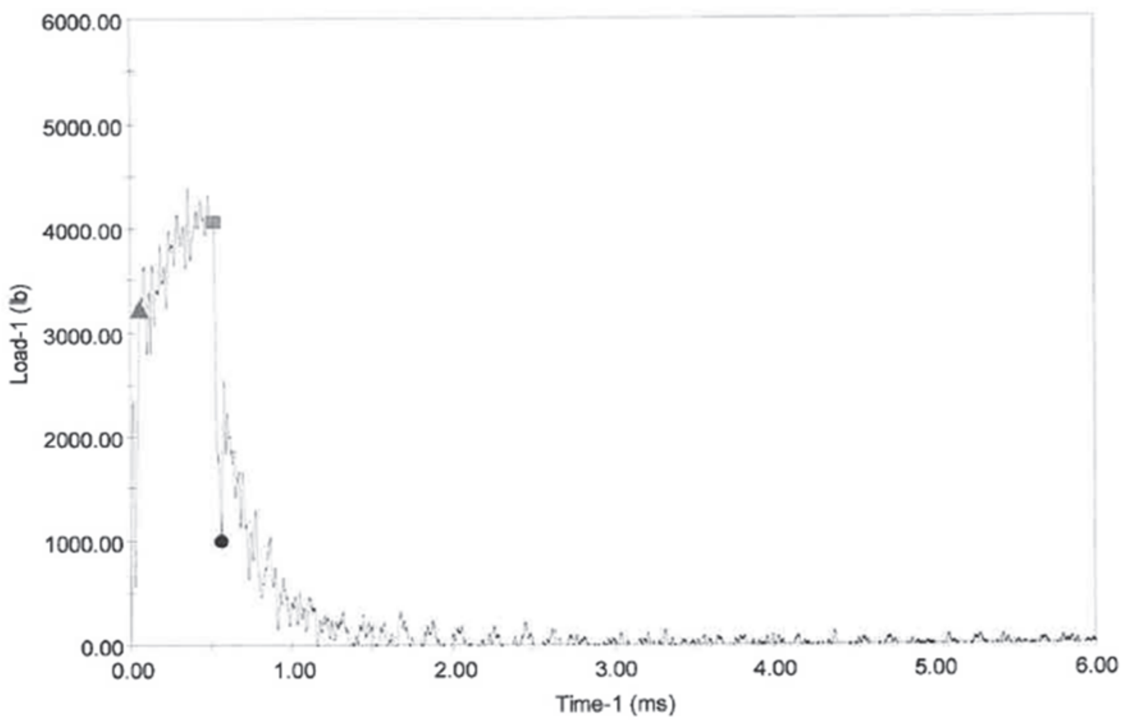

DT09, 250°F

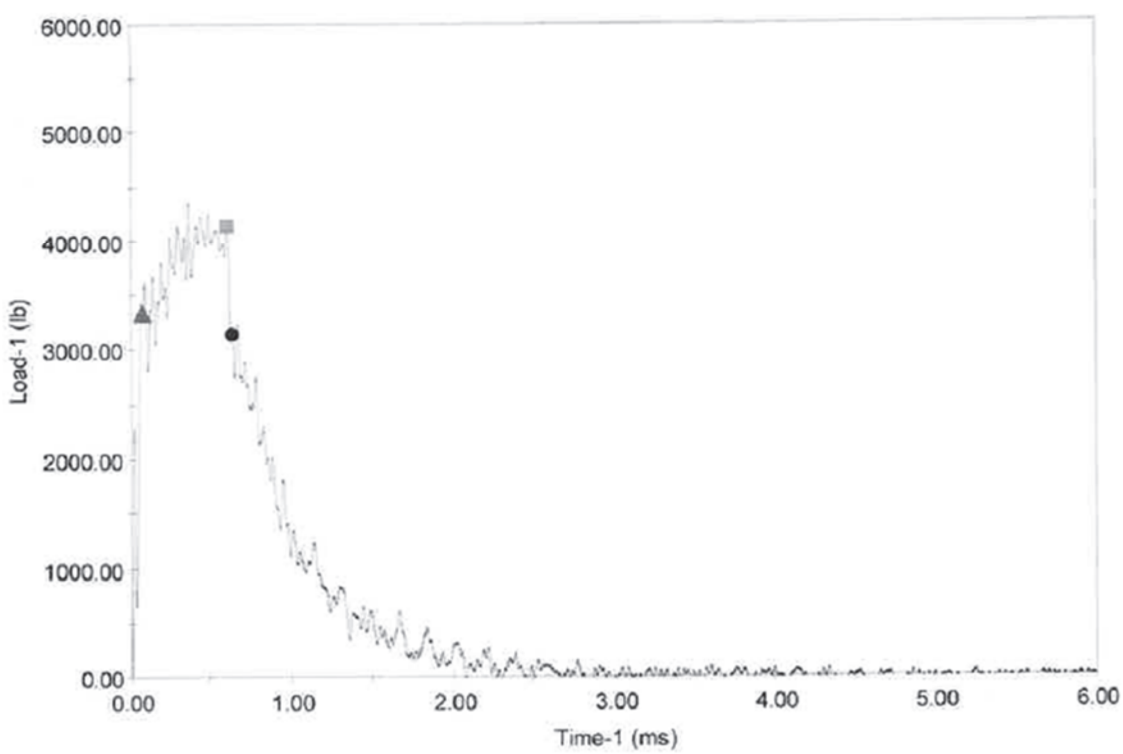

ET18, 275°F

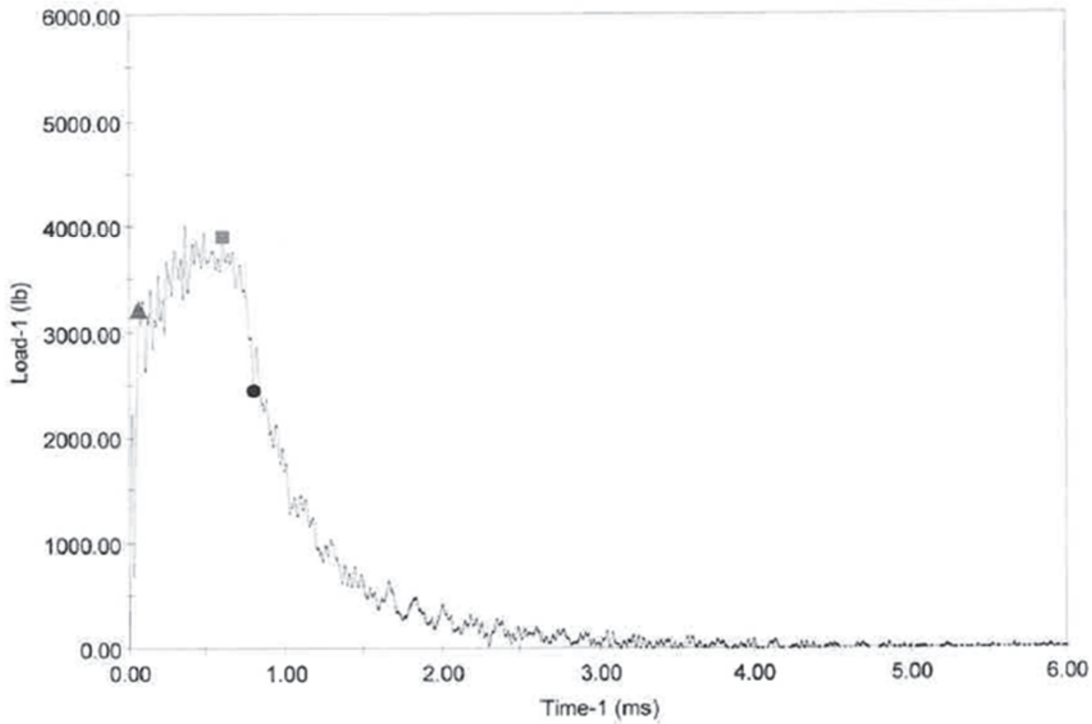

DT07, 300°F

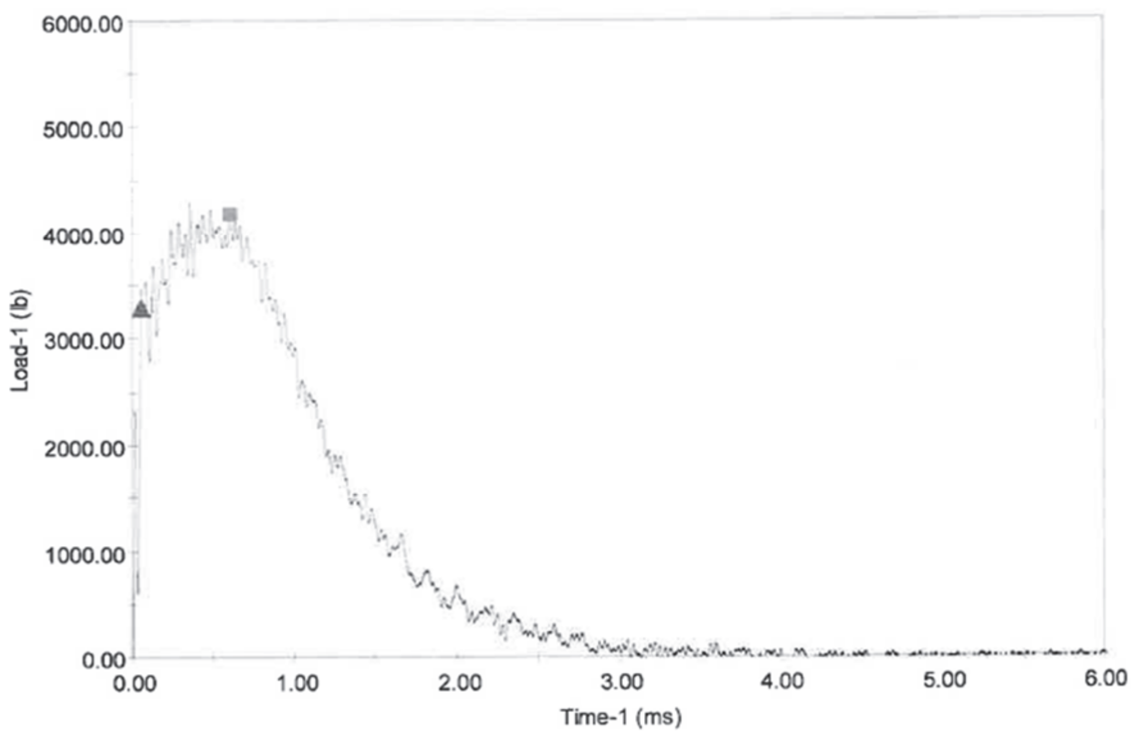

DT10, 350°F

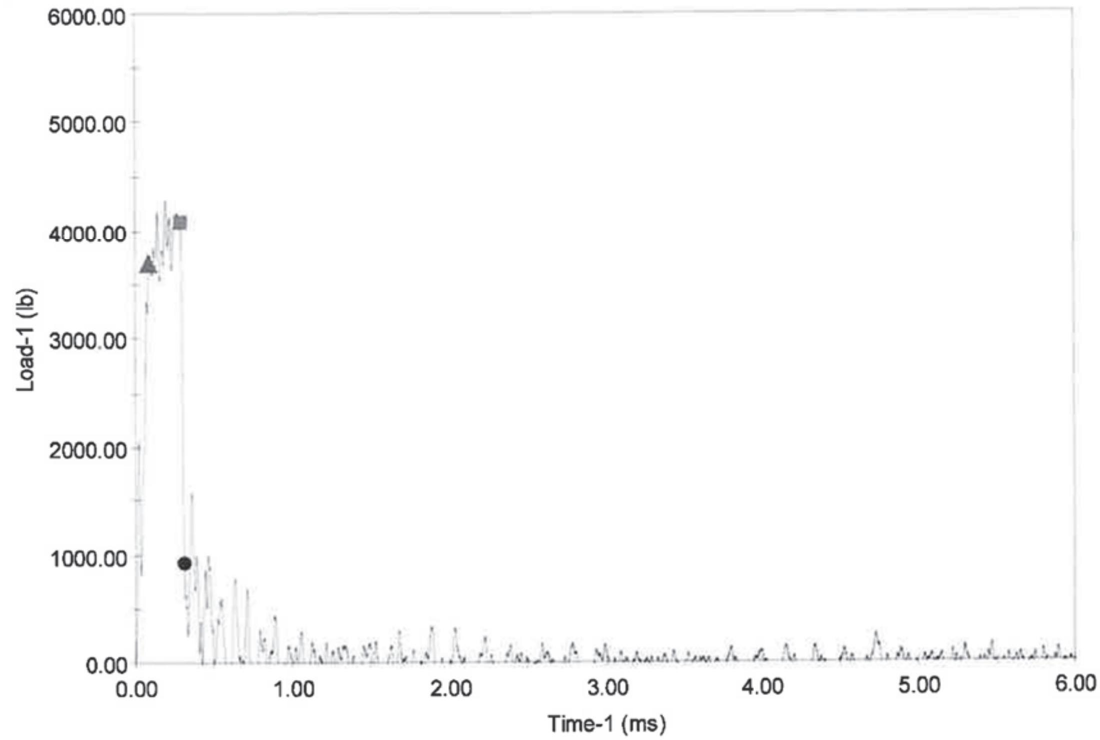

W11, 180°F

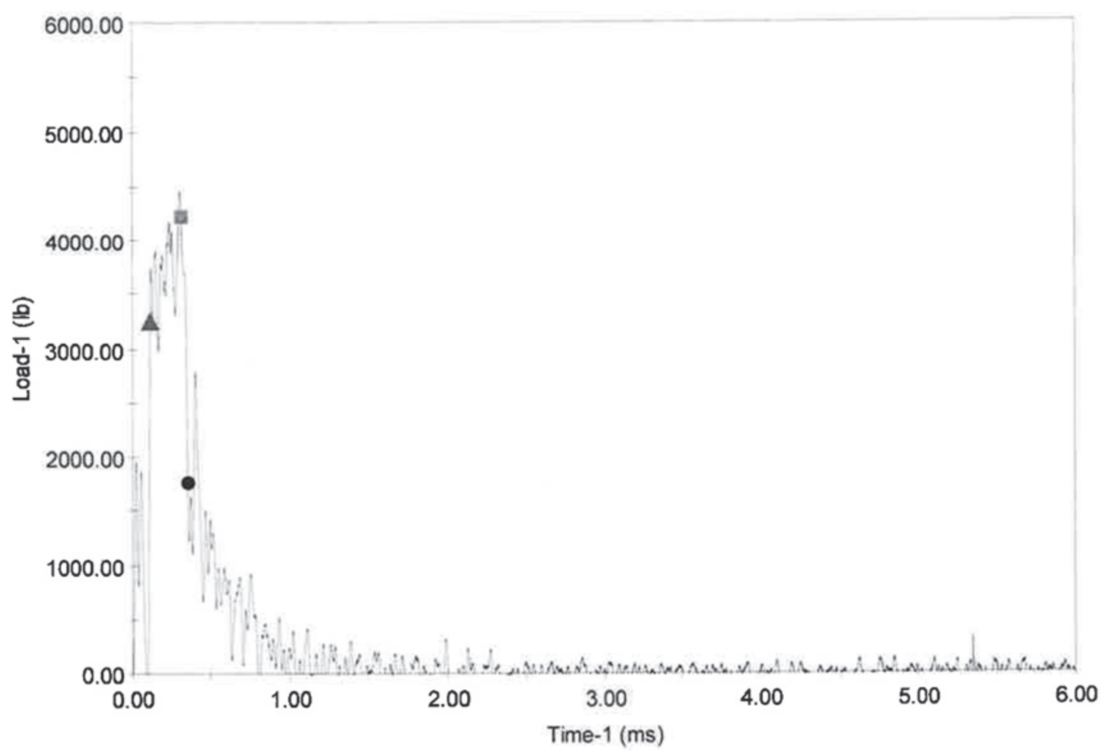

W4, 210°F

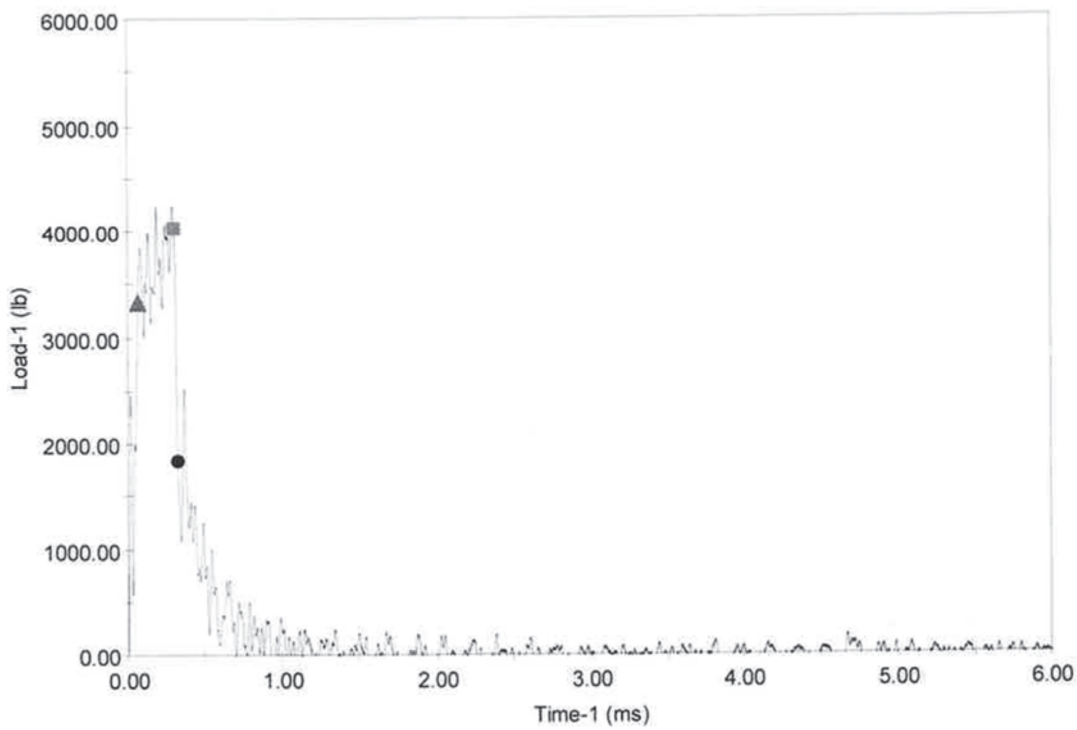

W5, 240°F

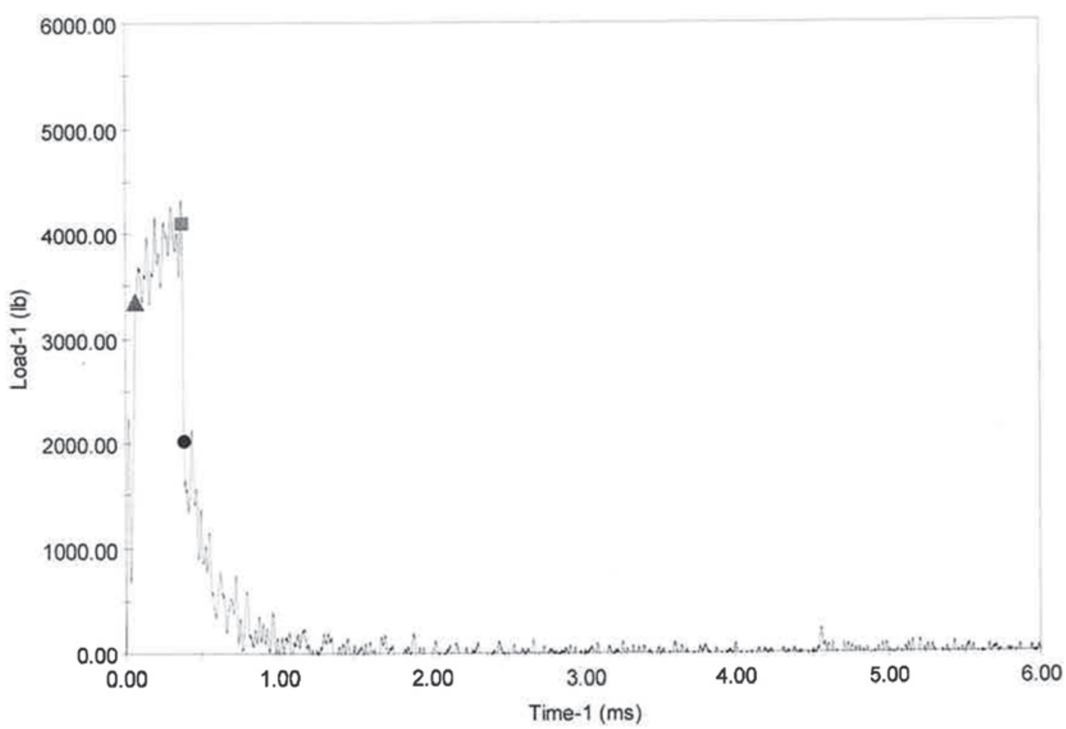

W22, 250°F

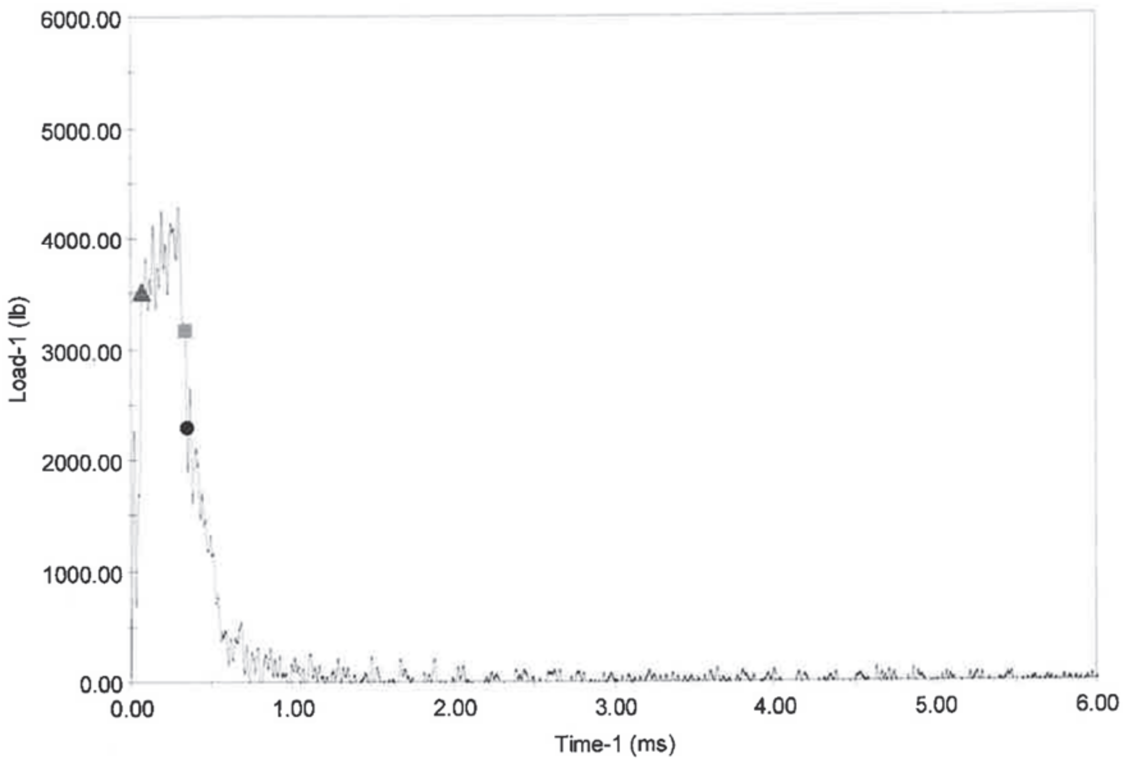

W12, 260°F

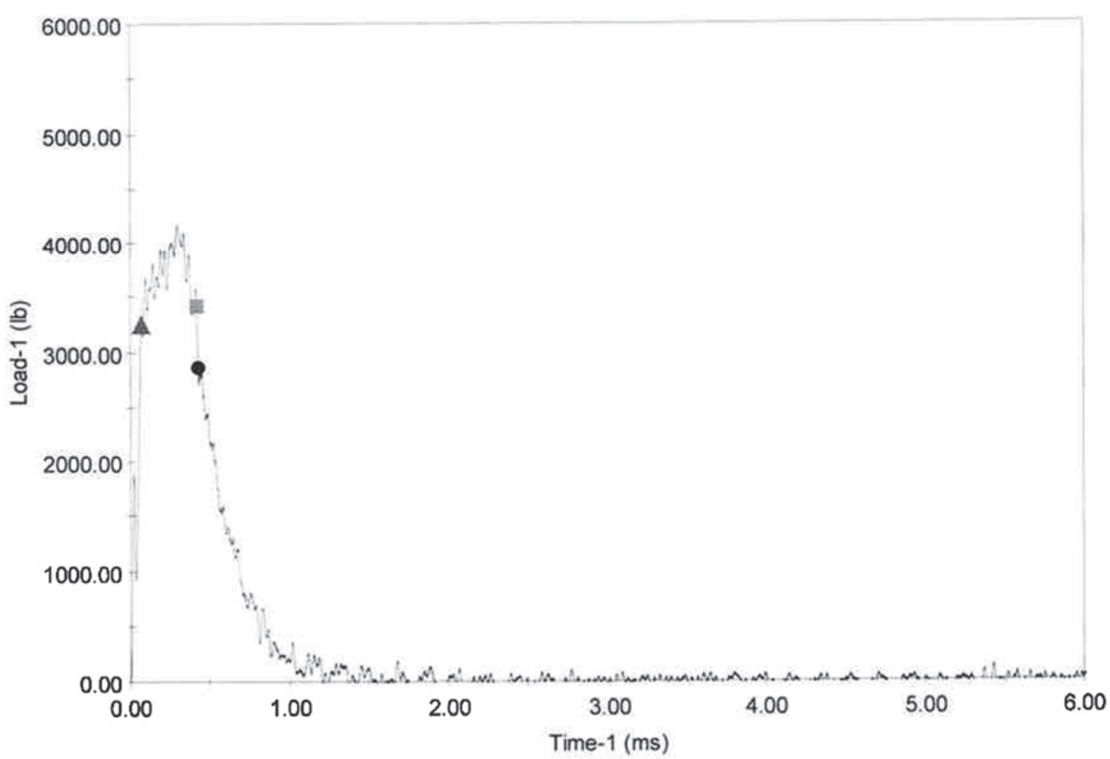

W21, 280°F

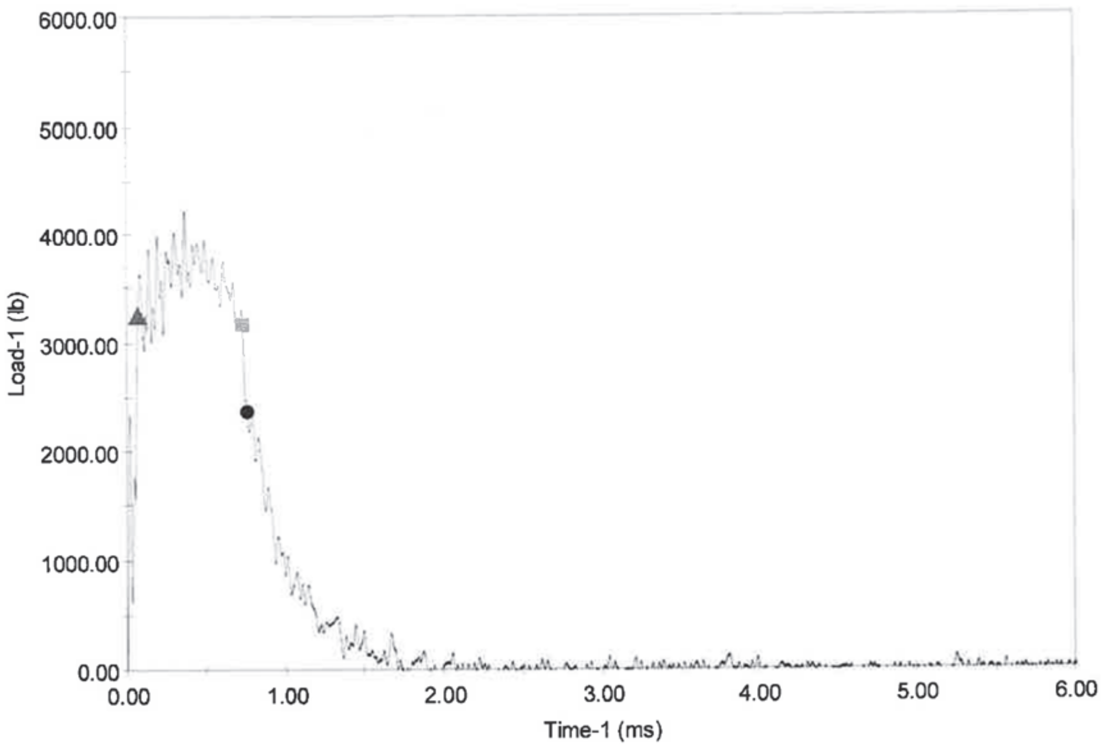

W7, 300°F

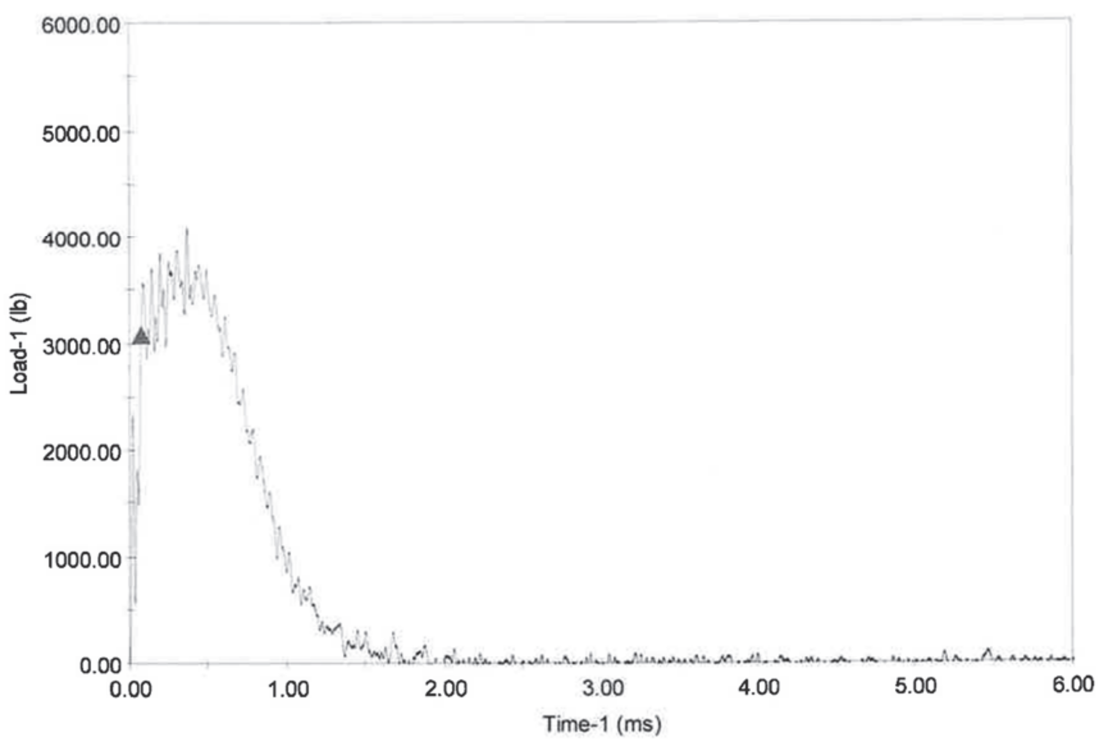

W2, 375°F

APPENDIX C CHARPY V-NOTCH PLOTS FOR EACH CAPSULE INCLUDING BASELINE DATA USING SYMMETRIC HYPERBOLIC TANGENT CURVE-FITTING METHOD

C.1 METHODOLOGY

Contained in Table C-1 are the upper-shelf energy (USE) values that are used as input for the generation of the Charpy V-notch plots using CVGRAPH, Version 6.02. The definition for USE is given in ASTM E185-82 [C-1], Section 4.18, and reads as follows:

> "*upper shelf energy level* – the average energy value for all Charpy specimens (normally three) whose test temperature is above the upper end of the transition region. For specimens tested in sets of three at each test temperature, the set having the highest average may be regarded as defining the upper shelf energy."

Westinghouse reports the average of all Charpy data (≥ 95% shear) as the USE, excluding any values that are deemed outliers using engineering judgment. No outliers were identified in the Capsule B data set; thus all data points were considered. Hence, the Capsule B USE values reported in Table C-1 were determined by applying this methodology to the Charpy data tabulated in Table 5-1 through Table 5-4 of this report. The surveillance weld and CMM USE values documented in Table C-1 for the unirradiated materials, as well as for Capsules S, Y, and V, were determined by applying the methodology described above to the Charpy impact data reported in WCAP-8465 [C-2] and WCAP-15958 [C-3]. The Lower Shell Plate B4107-1 and surrogate weld USE values, documented in Table C-1 for unirradiated materials, were determined in a similar manner from the Charpy impact data reported in WCAP-13440 [C-4]. These USE values were used in the generation of the Charpy V-notch curves.

The lower-shelf energy values were fixed at 2.2 ft-lb for all cases. The lower-shelf lateral expansion values were fixed at 1.0 mil to be consistent with the previous capsule analysis. Similarly, the upper-shelf energy must also be fixed for curve-fitting the Charpy V-notch (CVN) Energy data using the values reported in Table C-1. However, the upper-shelf lateral expansion is not fixed in CVGRAPH.

Table C-1 Upper-Shelf Energy Values Fixed in CVGRAPH(1)

Material	Unirradiated (ft-lb)	Capsule S (ft-lb)	Capsule Y (ft-lb)	Capsule V (ft-lb)	Capsule B (ft-lb)
Lower Shell Plate B4107-1 (Transverse Orientation)	112.6	---(2)	---(2)	---(2)	98.0
Surrogate Weld (Heat # 27204)	104.3	---	---	---	58.6
Surveillance Welds (Heat # 27204)	87.6	80.5	60.3	65.7	50.0
Correlation Monitor Material HSST02	120.4	120.0	107.7	117.0	83.0

Note:
1. These values are calculated as an average of all in-family data points with a shear ⩾ 95%, consistent with ASTM E185-82 [C-1], unless otherwise noted.
2. Per WCAP-13440 [C-3], Capsules S, Y, and V contained Intermediate Shell Plate B4106-3, while Supplemental Surveillance Program Capsule B contained Lower Shell Plate B4107-1.

CVGRAPH, Version 6.02 plots of all surveillance data are provided in this appendix, on the pages following the reference list.

C.2 REFERENCES

C-1 ASTM E185-82, "Standard Practice for Conducting Surveillance Tests for Light-Water Cooled Nuclear Power Reactor Vessels," American Society for Testing and Materials, 1982.

C-2 Westinghouse Report, WCAP-8465, Rev. 0, "Pacific Gas and Electric Co. Diablo Canyon Unit No. 1 Reactor Vessel Radiation Surveillance Program," January 1975.

C-3 Westinghouse Report, WCAP-15958, Rev. 0, "Analysis of Capsule V from Pacific Gas and Electric Company Diablo Canyon Unit 1 Reactor Vessel Radiation Surveillance Program," January 2003.

C-4 Westinghouse Report, WCAP-13440, Rev. 0, "Supplemental Reactor Vessel Radiation Surveillance Program for the Pacific Gas and Electric Company Diablo Canyon Unit No. 1," December 1992.

C.3 CVGRAPH VERSION 6.02 INDIVIDUAL PLOTS

C.3.1 Lower Shell Plate B4107-1

Unirradiated Lower Shell Plate B4107-1

CVGraph 6.02: Hyperbolic Tangent Curve Printed on 6/10/2026 7:32 AM

A = 57.40 B = 55.20 C = 108.43 T0 = 77.25 D = 0.00

Equation is A + B * [Tanh((T-T0)/(C+DT))]

Upper Shelf Energy = 112.60 (Fixed) Lower Shelf Energy = 2.20 (Fixed)

Temp@30 ft-lbs= 18.30° F Temp@35 ft-lbs= 30.60° F Temp@50 ft-lbs= 62.70° F

Plant: **Diablo Canyon 1** Material: **SA533B1** Heat: **C3121-1**

Orientation: **TL** Capsule: **Unirrad** Fluence: **0.00E+000 n/cm²**

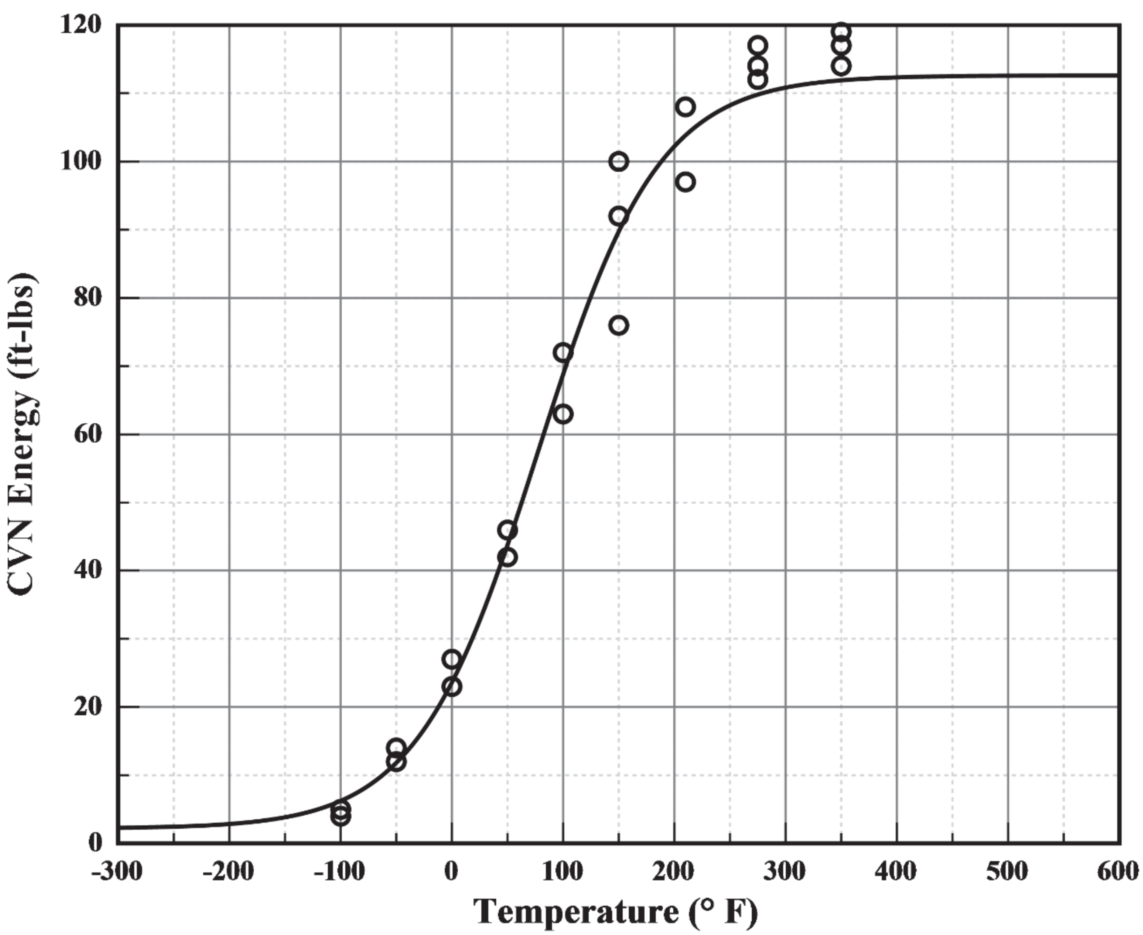

CVGraph 6.02 06/10/2026 Page 1/2

Plant: **Diablo Canyon 1** Material: **SA533B1** Heat: **C3121-1**
Orientation: **TL** Capsule: **Unirrad** Fluence: **0.00E+000 n/cm²**

Unirradiated Lower Shell Plate B4107-1

Charpy V-Notch Data

Temperature (° F)	Input CVN	Computed CVN	Differential
-100	5.0	6.2	-1.24
-100	4.0	6.2	-2.24
-50	14.0	11.8	2.16
-50	12.0	11.8	0.16
0	27.0	23.6	3.39
0	23.0	23.6	-0.61
50	42.0	43.8	-1.81
50	46.0	43.8	2.19
100	72.0	68.8	3.19
100	63.0	68.8	-5.81
150	92.0	89.7	2.27
150	100.0	89.7	10.27
150	76.0	89.7	-13.73
210	97.0	103.8	-6.82
210	108.0	103.8	4.18
275	112.0	109.8	2.20
275	114.0	109.8	4.20
275	117.0	109.8	7.20
350	114.0	111.9	2.12
350	117.0	111.9	5.12
350	119.0	111.9	7.12

CVGraph 6.02 06/10/2026 Page 2/2

Capsule B Lower Shell Plate B4107-1

CVGraph 6.02: Hyperbolic Tangent Curve Printed on 5/18/2026 3:12 PM

A = 50.10 B = 47.90 C = 50.94 T0 = 177.92 D = 0.00

Equation is A + B * [Tanh((T-T0)/(C+DT))]

Upper Shelf Energy = 98.00 (Fixed) Lower Shelf Energy = 2.20 (Fixed)

Temp@30 ft-lbs=155.20° F Temp@35 ft-lbs=161.30° F Temp@50 ft-lbs=177.90° F

Plant: **Diablo Canyon 1** Material: **SA533B1** Heat: **C3121-1**

Orientation: **TL** Capsule: **B** Fluence: **3.62E+019 n/cm²**

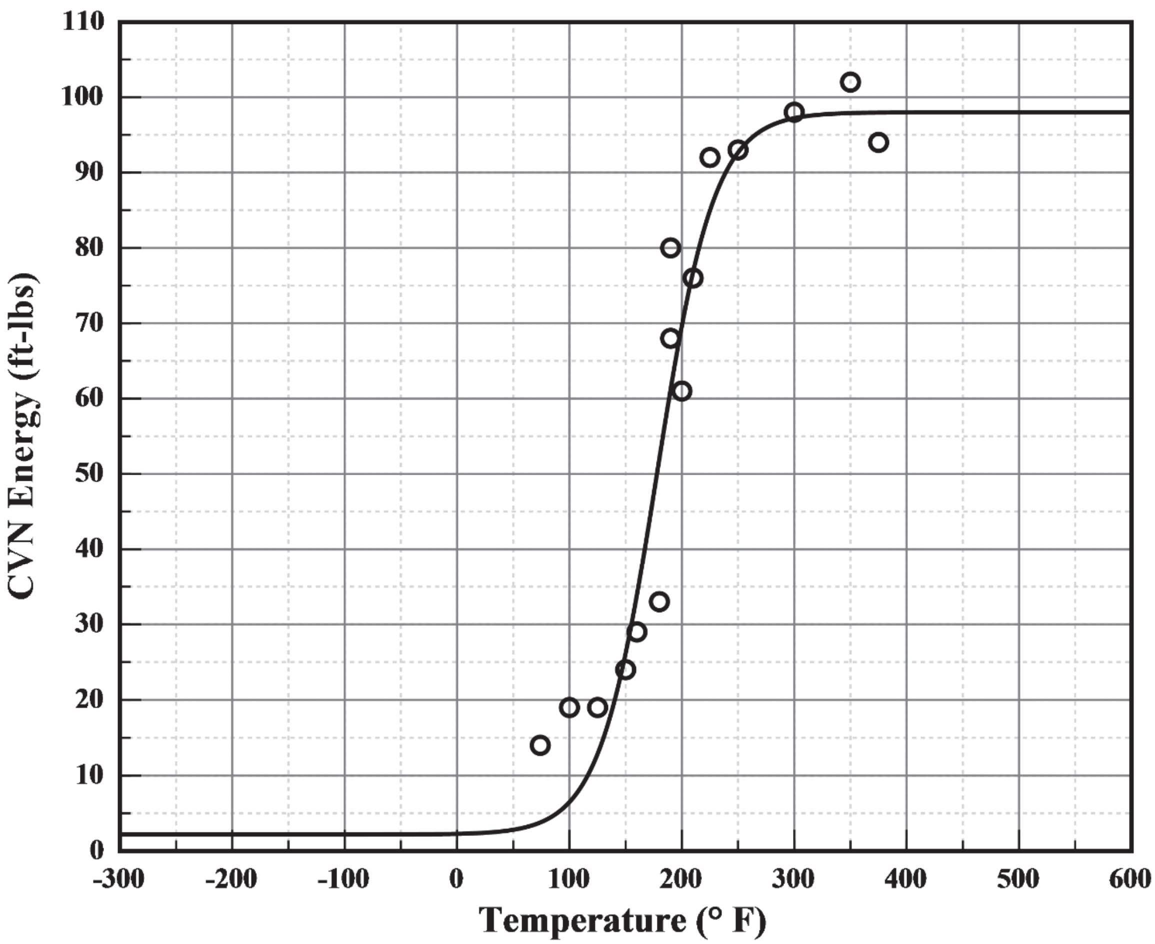

CVGraph 6.02 05/18/2026 Page 1/2

Plant: **Diablo Canyon 1** Material: **SA533B1** Heat: **C3121-1**
Orientation: **TL** Capsule: **B** Fluence: **3.62E+019 n/cm²**

Capsule B Lower Shell Plate B4107-1

Charpy V-Notch Data

Temperature (° F)	Input CVN	Computed CVN	Differential
74	14.0	3.8	10.21
100	19.0	6.5	12.51
125	19.0	12.9	6.14
150	24.0	26.2	-2.19
160	29.0	33.9	-4.91
180	33.0	52.1	-19.05
190	68.0	61.2	6.75
190	80.0	61.2	18.75
200	61.0	69.7	-8.65
210	76.0	76.8	-0.82
225	92.0	85.0	7.04
250	93.0	92.7	0.34
300	98.0	97.2	0.79
350	102.0	97.9	4.11
375	94.0	98.0	-3.96

CVGraph 6.02 05/18/2026 Page 2/2

Unirradiated Lower Shell Plate B4107-1

CVGraph 6.02: Hyperbolic Tangent Curve Printed on 5/18/2026 2:49 PM

A = 41.94 B = 40.94 C = 109.04 T0 = 56.71 D = 0.00

Equation is A + B * [Tanh((T-T0)/(C+DT))]

Upper Shelf L.E. = 82.88 Lower Shelf L.E. = 1.00 (Fixed)

Temp@35 mils= 38.10° F

Plant: **Diablo Canyon 1** Material: **SA533B1** Heat: **C3121-1**
Orientation: **TL** Capsule: **Unirrad** Fluence: **0.00E+000 n/cm²**

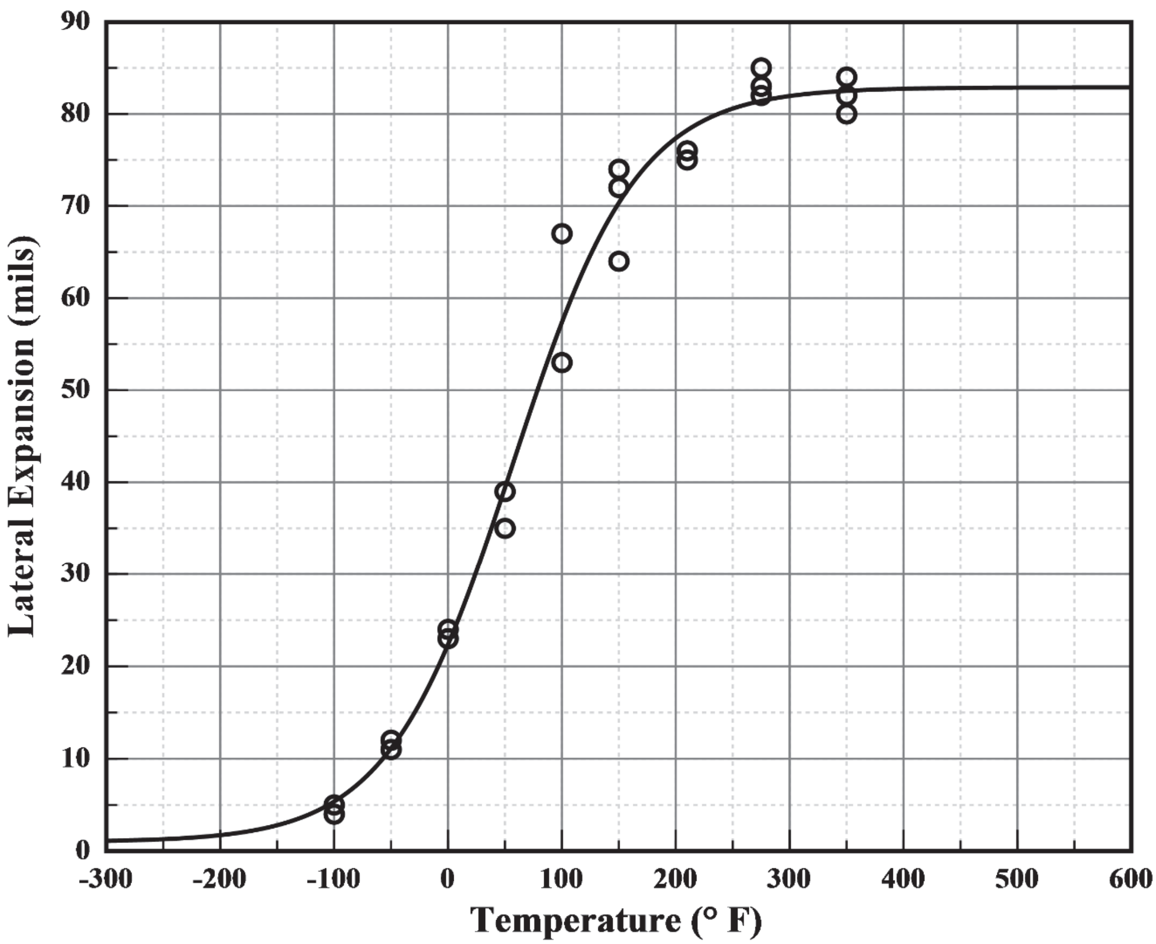

CVGraph 6.02 05/18/2026 Page 1/2

Plant: **Diablo Canyon 1** Material: **SA533B1** Heat: **C3121-1**
Orientation: **TL** Capsule: **Unirrad** Fluence: **0.00E+000 n/cm²**

Unirradiated Lower Shell Plate B4107-1

Charpy V-Notch Data

Temperature (° F)	Input L. E.	Computed L. E.	Differential
-100	5.0	5.4	-0.38
-100	4.0	5.4	-1.38
-50	11.0	11.1	-0.13
-50	12.0	11.1	0.87
0	24.0	22.4	1.62
0	23.0	22.4	0.62
50	35.0	39.4	-4.42
50	39.0	39.4	-0.42
100	67.0	57.4	9.61
100	53.0	57.4	-4.39
150	74.0	70.4	3.65
150	72.0	70.4	1.65
150	64.0	70.4	-6.35
210	75.0	78.2	-3.24
210	76.0	78.2	-2.24
275	83.0	81.4	1.59
275	82.0	81.4	0.59
275	85.0	81.4	3.59
350	80.0	82.5	-2.50
350	84.0	82.5	1.50
350	82.0	82.5	-0.50

CVGraph 6.02 05/18/2026 Page 2/2

Capsule B Lower Shell Plate B4107-1 (Transverse)

CVGraph 6.02: Hyperbolic Tangent Curve Printed on 5/18/2026 3:13 PM

A = 40.66 B = 39.66 C = 83.22 T0 = 178.73 D = 0.00

Equation is A + B * [Tanh((T-T0)/(C+DT))]

Upper Shelf L.E. = 80.33 Lower Shelf L.E. = 1.00 (Fixed)

Temp@35 mils=166.80° F

Plant: **Diablo Canyon 1** Material: **SA533B1** Heat: **C3121-1**

Orientation: **TL** Capsule: **B** Fluence: **3.62E+019 n/cm²**

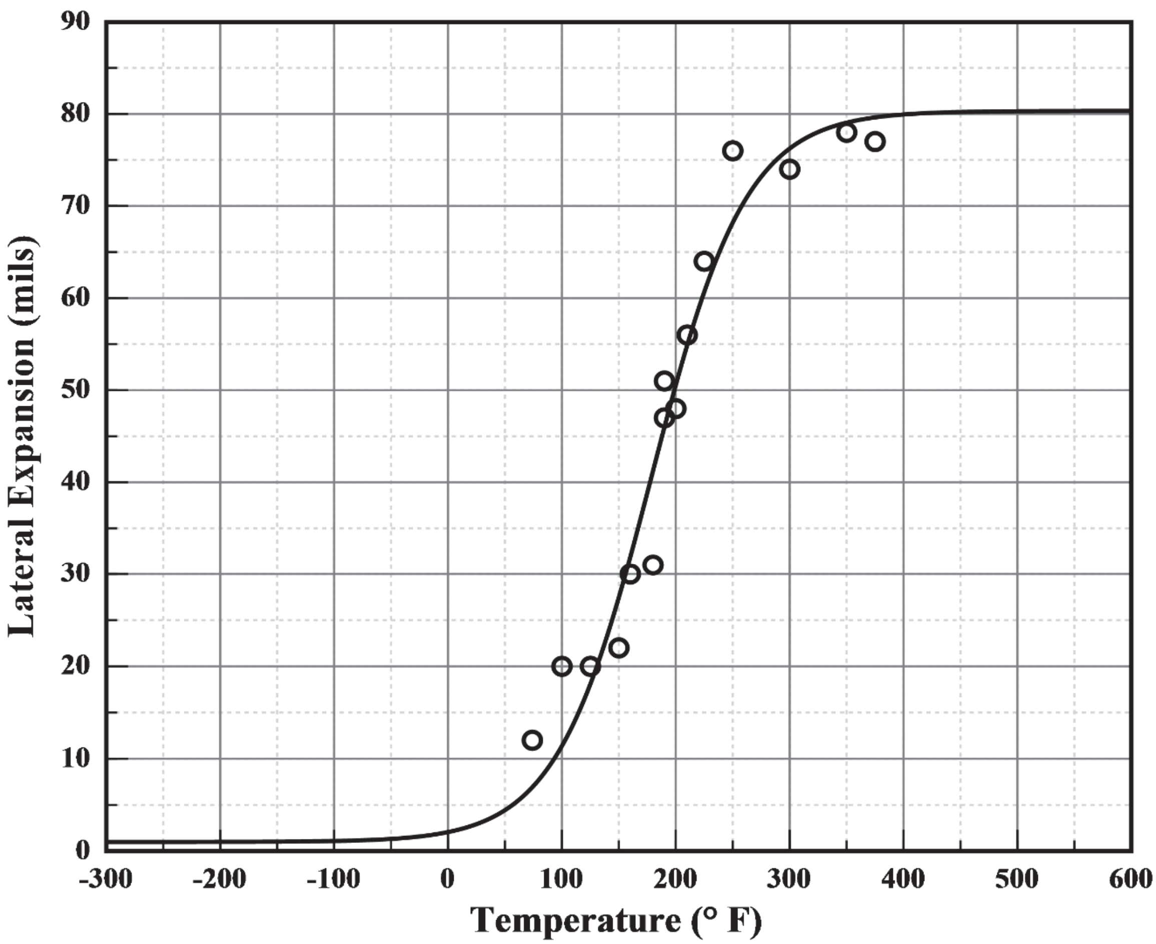

CVGraph 6.02 05/18/2026 Page 1/2

Plant: **Diablo Canyon 1** Material: **SA533B1** Heat: **C3121-1**
Orientation: **TL** Capsule: **B** Fluence: **3.62E+019 n/cm²**

Capsule B Lower Shell Plate B4107-1 (Transverse)

Charpy V-Notch Data

Temperature (° F)	Input L. E.	Computed L. E.	Differential
74	12.0	6.9	5.08
100	20.0	11.4	8.61
125	20.0	18.1	1.90
150	22.0	27.5	-5.49
160	30.0	31.9	-1.88
180	31.0	41.3	-10.27
190	47.0	46.0	1.00
190	51.0	46.0	5.00
200	48.0	50.6	-2.58
210	56.0	54.9	1.10
225	64.0	60.7	3.31
250	76.0	68.2	7.80
300	74.0	76.2	-2.25
350	78.0	79.1	-1.05
375	77.0	79.6	-2.62

CVGraph 6.02 05/18/2026 Page 2/2

Unirradiated Lower Shell Plate B4107-1

CVGraph 6.02: Hyperbolic Tangent Curve Printed on 5/18/2026 2:50 PM

A = 50.00 B = 50.00 C = 98.17 T0 = 69.06 D = 0.00

Equation is A + B * [Tanh((T-T0)/(C+DT))]

Upper Shelf %Shear = 100.00 (Fixed) Lower Shelf %Shear = 0.00 (Fixed)

Temperature at 50% Shear = 69.10

Plant: **Diablo Canyon 1** Material: **SA533B1** Heat: **C3121-1**

Orientation: **TL** Capsule: **Unirrad** Fluence: **0.00E+000 n/cm²**

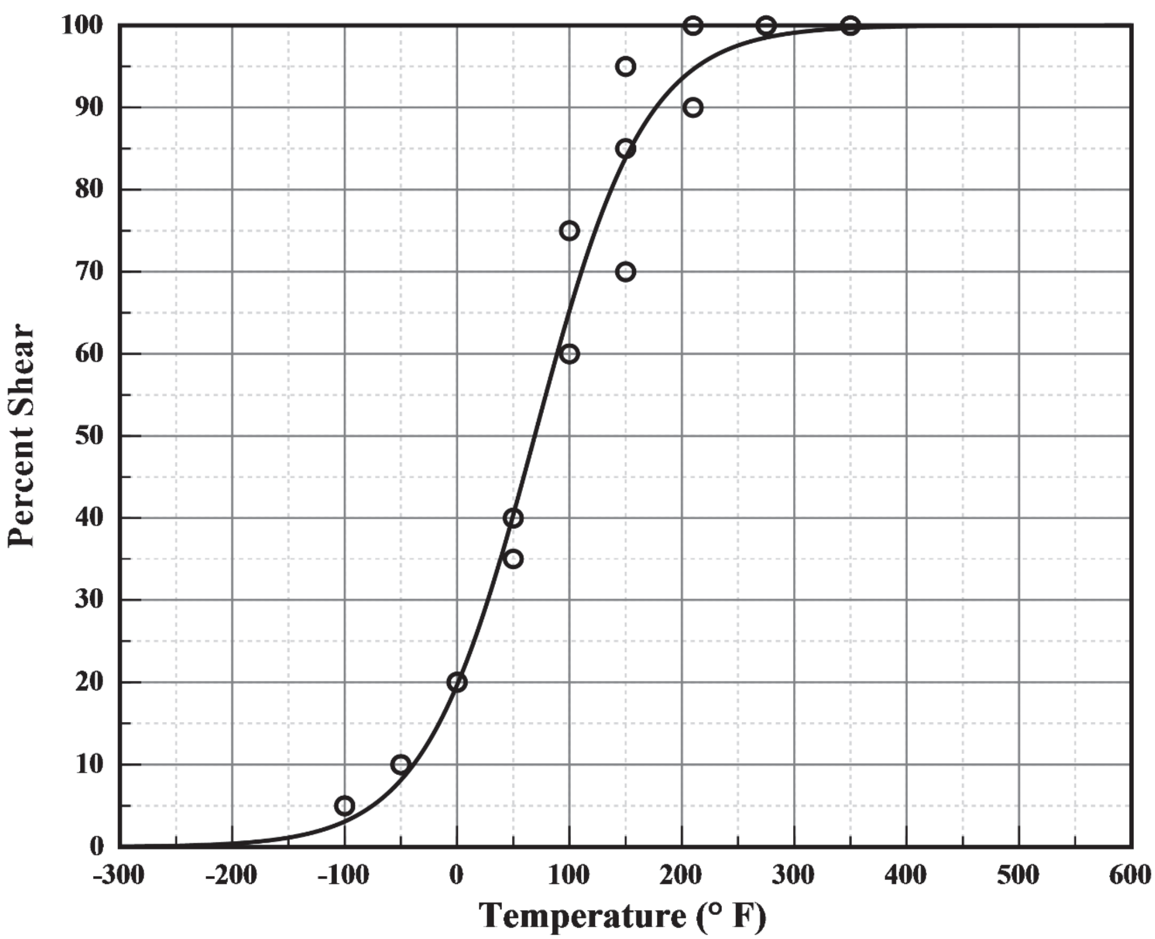

CVGraph 6.02 05/18/2026 Page 1/2

Plant: **Diablo Canyon 1** Material: **SA533B1** Heat: **C3121-1**
Orientation: **TL** Capsule: **Unirrad** Fluence: **0.00E+000 n/cm²**

Unirradiated Lower Shell Plate B4107-1
Charpy V-Notch Data

Temperature (° F)	Input %Shear	Computed %Shear	Differential
-100	5.0	3.1	1.91
-100	5.0	3.1	1.91
-50	10.0	8.1	1.88
-50	10.0	8.1	1.88
0	20.0	19.7	0.33
0	20.0	19.7	0.33
50	40.0	40.4	-0.41
50	35.0	40.4	-5.41
100	75.0	65.3	9.75
100	60.0	65.3	-5.25
150	85.0	83.9	1.13
150	95.0	83.9	11.13
150	70.0	83.9	-13.87
210	90.0	94.6	-4.64
210	100.0	94.6	5.36
275	100.0	98.5	1.48
275	100.0	98.5	1.48
275	100.0	98.5	1.48
350	100.0	99.7	0.33
350	100.0	99.7	0.33
350	100.0	99.7	0.33

CVGraph 6.02 05/18/2026 Page 2/2

Capsule B Lower Shell Plate B4107-1

CVGraph 6.02: Hyperbolic Tangent Curve Printed on 5/18/2026 3:14 PM

A = 50.00 B = 50.00 C = 55.10 T0 = 201.17 D = 0.00

Equation is A + B * [Tanh((T-T0)/(C+DT))]

Upper Shelf %Shear = 100.00 (Fixed) Lower Shelf %Shear = 0.00 (Fixed)

Temperature at 50% Shear = 201.20

Plant: **Diablo Canyon 1** Material: **SA533B1** Heat: **C3121-1**

Orientation: **TL** Capsule: **B** Fluence: **3.62E+019 n/cm²**

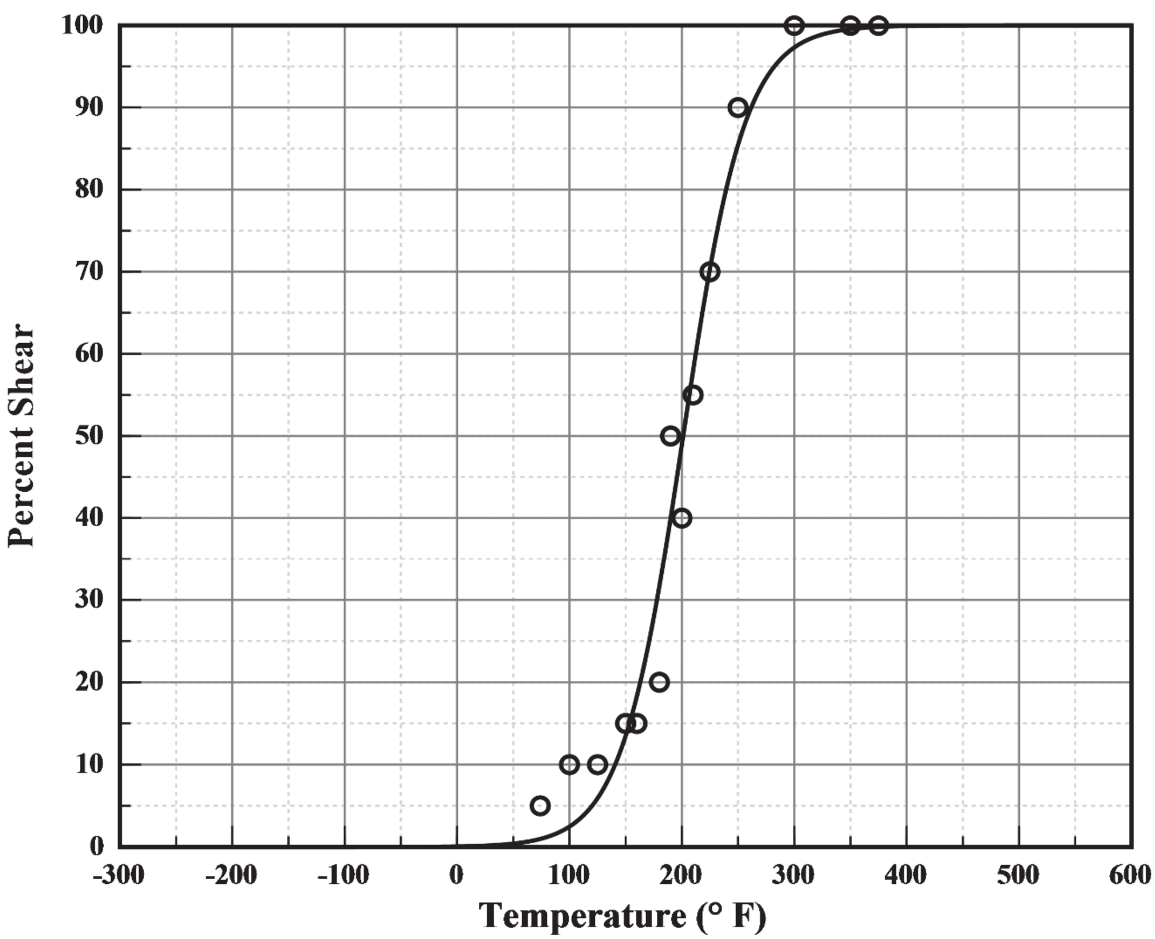

CVGraph 6.02 05/18/2026 Page 1/2

Plant: **Diablo Canyon 1** Material: **SA533B1** Heat: **C3121-1**
Orientation: **TL** Capsule: **B** Fluence: **3.62E+019 n/cm²**

Capsule B Lower Shell Plate B4107-1
Charpy V-Notch Data

Temperature (° F)	Input %Shear	Computed %Shear	Differential
74	5.0	1.0	4.02
100	10.0	2.5	7.52
125	10.0	5.9	4.07
150	15.0	13.5	1.50
160	15.0	18.3	-3.33
180	20.0	31.7	-11.68
190	50.0	40.0	10.00
190	50.0	40.0	10.00
200	40.0	48.9	-8.94
210	55.0	57.9	-2.95
225	70.0	70.4	-0.37
250	90.0	85.5	4.52
300	100.0	97.3	2.69
350	100.0	99.6	0.45
375	100.0	99.8	0.18

CVGraph 6.02 05/18/2026 Page 2/2

C.3.2 Surrogate Weld

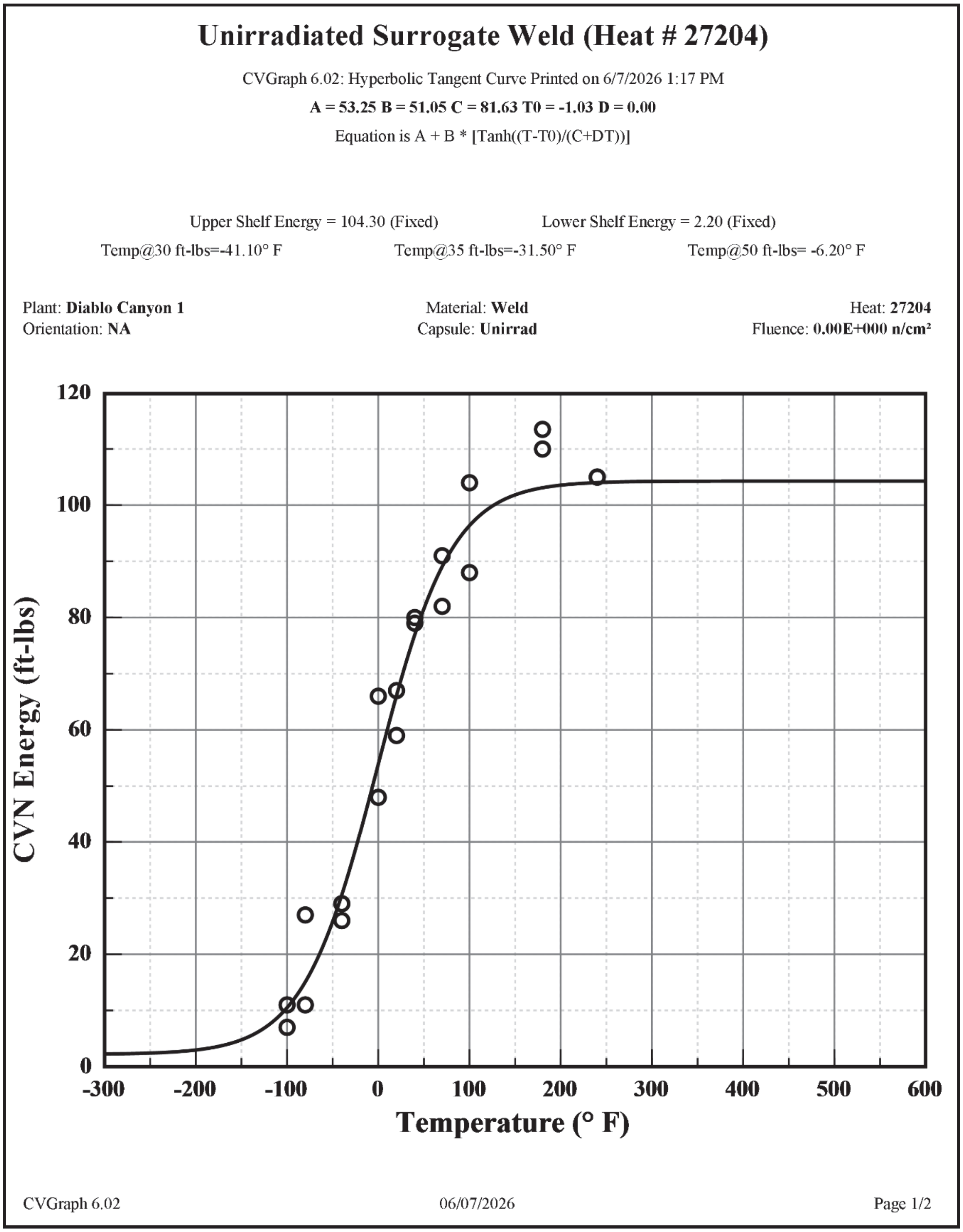

Plant: **Diablo Canyon 1** Material: **Weld** Heat: **27204**
Orientation: **NA** Capsule: **Unirrad** Fluence: **0.00E+000 n/cm²**

Unirradiated Surrogate Weld (Heat # 27204)

Charpy V-Notch Data

Temperature (° F)	Input CVN	Computed CVN	Differential
-100	7.0	10.5	-3.50
-100	11.0	10.5	0.50
-80	11.0	15.1	-4.09
-80	27.0	15.1	11.91
-40	26.0	30.6	-4.58
-40	29.0	30.6	-1.58
0	66.0	53.9	12.11
0	48.0	53.9	-5.89
20	59.0	66.1	-7.12
20	67.0	66.1	0.88
40	79.0	76.9	2.05
40	80.0	76.9	3.05
70	82.0	89.1	-7.06
70	91.0	89.1	1.94
100	104.0	96.4	7.62
100	88.0	96.4	-8.38
180	110.0	103.1	6.90
180	113.5	103.1	10.40
240	105.0	104.0	0.98
240	105.0	104.0	0.98

CVGraph 6.02 06/07/2026 Page 2/2

Capsule B Surrogate Weld (Heat # 27204)

CVGraph 6.02: Hyperbolic Tangent Curve Printed on 5/18/2026 3:32 PM

A = 30.40 B = 28.20 C = 93.07 T0 = 202.82 D = 0.00

Equation is A + B * [Tanh((T-T0)/(C+DT))]

Upper Shelf Energy = 58.60 (Fixed) Lower Shelf Energy = 2.20 (Fixed)

Temp@30 ft-lbs=201.50° F Temp@35 ft-lbs=218.20° F Temp@50 ft-lbs=282.70° F

Plant: **Diablo Canyon 1** Material: **Weld** Heat: **27204**
Orientation: **NA** Capsule: **B** Fluence: **3.62E+019 n/cm²**

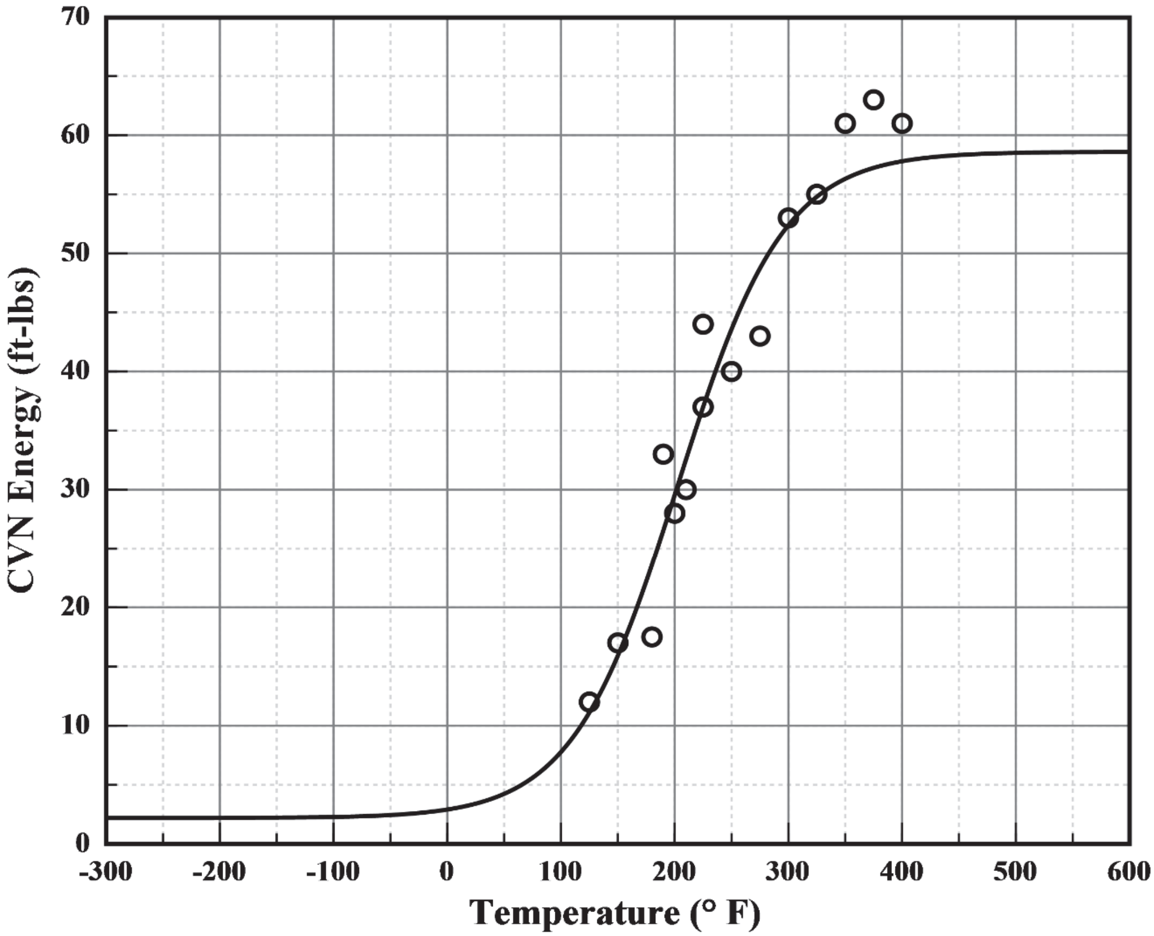

CVGraph 6.02 05/18/2026 Page 1/2

Plant: **Diablo Canyon 1** Material: **Weld** Heat: **27204**
Orientation: **NA** Capsule: **B** Fluence: **3.62E+019 n/cm²**

Capsule B Surrogate Weld (Heat # 27204)
Charpy V-Notch Data

Temperature (° F)	Input CVN	Computed CVN	Differential
125	12.0	11.1	0.88
150	17.0	15.9	1.08
180	17.5	23.6	-6.12
190	33.0	26.5	6.46
200	28.0	29.5	-1.55
210	30.0	32.6	-2.57
225	44.0	37.0	7.00
225	37.0	37.0	0.00
250	40.0	43.6	-3.58
275	43.0	48.7	-5.73
300	53.0	52.4	0.62
325	55.0	54.8	0.21
350	61.0	56.3	4.69
375	63.0	57.2	5.76
400	61.0	57.8	3.20

CVGraph 6.02 05/18/2026 Page 2/2

Unirradiated Surrogate Weld (Heat # 27204)

CVGraph 6.02: Hyperbolic Tangent Curve Printed on 6/7/2026 1:18 PM

A = 47.20 B = 46.20 C = 86.82 T0 = -16.12 D = 0.00

Equation is A + B * [Tanh((T-T0)/(C+DT))]

Upper Shelf L.E. = 93.39 Lower Shelf L.E. = 1.00 (Fixed)

Temp@35 mils=-39.60° F

Plant: **Diablo Canyon 1**	Material: **Weld**	Heat: **27204**
Orientation: **NA**	Capsule: **Unirrad**	Fluence: **0.00E+000 n/cm²**

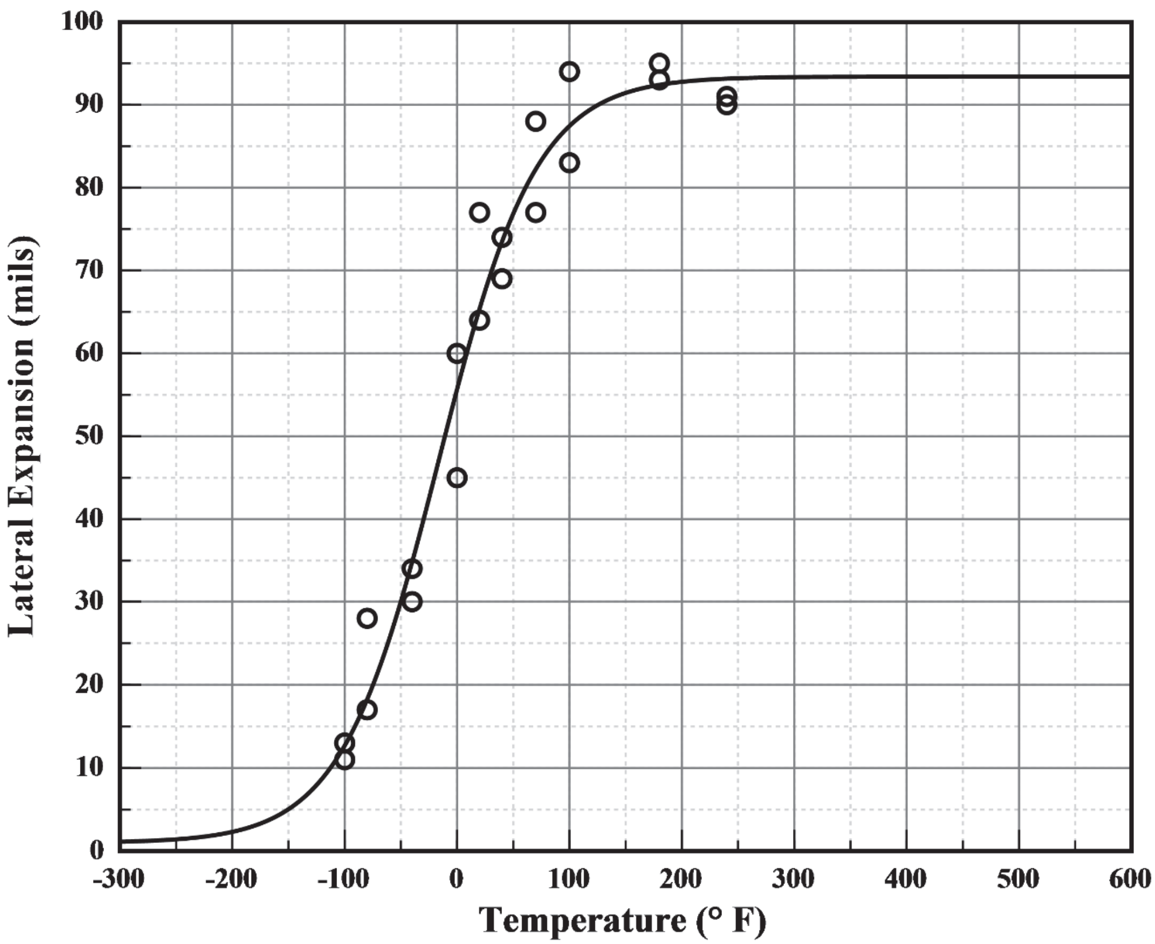

CVGraph 6.02 06/07/2026 Page 1/2

Plant: **Diablo Canyon 1** Material: **Weld** Heat: **27204**
Orientation: **NA** Capsule: **Unirrad** Fluence: **0.00E+000 n/cm²**

Unirradiated Surrogate Weld (Heat # 27204)
Charpy V-Notch Data

Temperature (° F)	Input L. E.	Computed L. E.	Differential
-100	11.0	12.7	-1.69
-100	13.0	12.7	0.31
-80	17.0	18.3	-1.25
-80	28.0	18.3	9.75
-40	30.0	34.8	-4.80
-40	34.0	34.8	-0.80
0	60.0	55.7	4.32
0	45.0	55.7	-10.68
20	64.0	65.4	-1.38
20	77.0	65.4	11.62
40	69.0	73.5	-4.49
40	74.0	73.5	0.51
70	77.0	82.2	-5.22
70	88.0	82.2	5.78
100	94.0	87.4	6.56
100	83.0	87.4	-4.44
180	93.0	92.4	0.60
180	95.0	92.4	2.60
240	90.0	93.1	-3.14
240	91.0	93.1	-2.14

CVGraph 6.02 06/07/2026 Page 2/2

Capsule B Surrogate Weld (Heat # 27204)

CVGraph 6.02: Hyperbolic Tangent Curve Printed on 5/18/2026 3:33 PM

A = 26.00 B = 25.00 C = 115.26 T0 = 211.85 D = 0.00

Equation is A + B * [Tanh((T-T0)/(C+DT))]

Upper Shelf L.E. = 51.00 Lower Shelf L.E. = 1.00 (Fixed)

Temp@35 mils=255.30° F

Plant: **Diablo Canyon 1** Material: **Weld** Heat: **27204**

Orientation: **NA** Capsule: **B** Fluence: **3.62E+019 n/cm²**

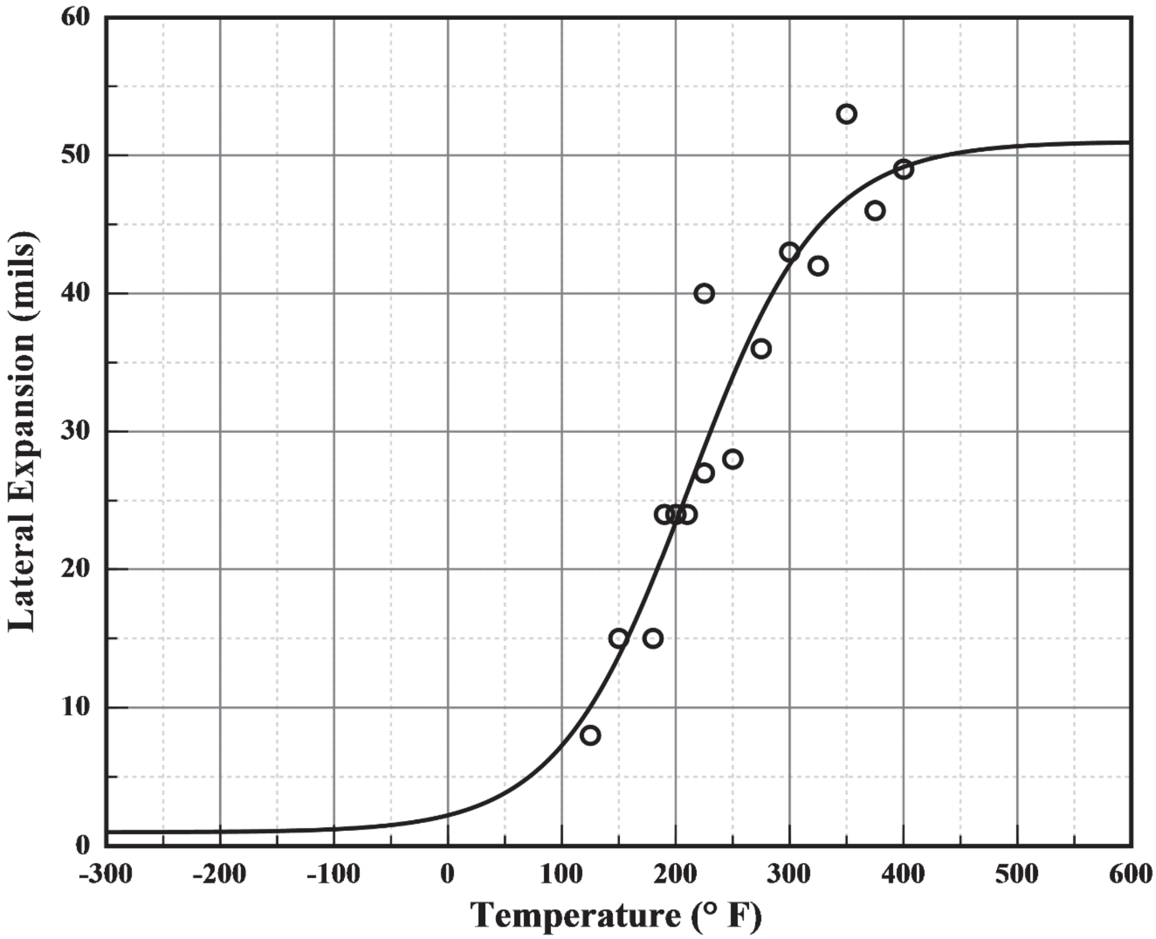

CVGraph 6.02 05/18/2026 Page 1/2

Plant: **Diablo Canyon 1** Material: **Weld** Heat: **27204**
Orientation: **NA** Capsule: **B** Fluence: **3.62E+019 n/cm²**

Capsule B Surrogate Weld (Heat # 27204)
Charpy V-Notch Data

Temperature (° F)	Input L. E.	Computed L. E.	Differential
125	8.0	10.1	-2.07
150	15.0	13.7	1.26
180	15.0	19.3	-4.26
190	24.0	21.3	2.68
200	24.0	23.4	0.56
210	24.0	25.6	-1.60
225	40.0	28.8	11.16
225	27.0	28.8	-1.84
250	28.0	34.0	-5.98
275	36.0	38.5	-2.47
300	43.0	42.1	0.90
325	42.0	44.8	-2.84
350	53.0	46.8	6.17
375	46.0	48.2	-2.21
400	49.0	49.2	-0.16

CVGraph 6.02 05/18/2026 Page 2/2

Unirradiated Surrogate Weld (Heat # 27204)

CVGraph 6.02: Hyperbolic Tangent Curve Printed on 6/7/2026 1:20 PM

A = 50.00 B = 50.00 C = 68.64 T0 = -0.17 D = 0.00

Equation is A + B * [Tanh((T-T0)/(C+DT))]

Upper Shelf %Shear = 100.00 (Fixed)   Lower Shelf %Shear = 0.00 (Fixed)

Temperature at 50% Shear = -0.10

Plant: **Diablo Canyon 1**   Material: **Weld**   Heat: **27204**

Orientation: **NA**   Capsule: **Unirrad**   Fluence: **0.00E+000 n/cm²**

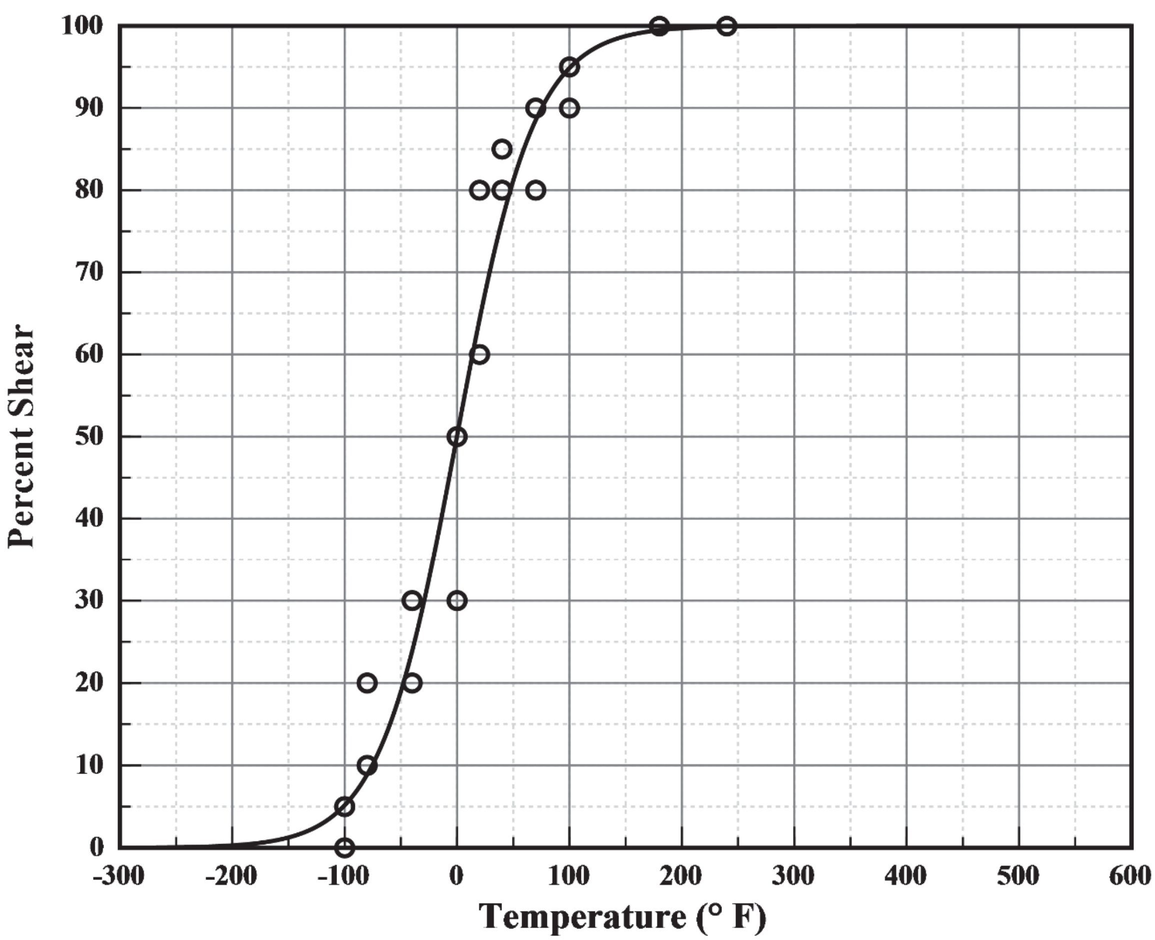

CVGraph 6.02   06/07/2026   Page 1/2

Plant: **Diablo Canyon 1** Material: **Weld** Heat: **27204**
Orientation: **NA** Capsule: **Unirrad** Fluence: **0.00E+000 n/cm²**

Unirradiated Surrogate Weld (Heat # 27204)
Charpy V-Notch Data

Temperature (° F)	Input %Shear	Computed %Shear	Differential
-100	0.0	5.2	-5.17
-100	5.0	5.2	-0.17
-80	10.0	8.9	1.10
-80	20.0	8.9	11.10
-40	30.0	23.9	6.14
-40	20.0	23.9	-3.86
0	50.0	50.1	-0.12
0	30.0	50.1	-20.12
20	60.0	64.3	-4.28
20	80.0	64.3	15.72
40	80.0	76.3	3.68
40	85.0	76.3	8.68
70	90.0	88.5	1.46
70	80.0	88.5	-8.54
100	90.0	94.9	-4.87
100	95.0	94.9	0.13
180	100.0	99.5	0.52
180	100.0	99.5	0.52
240	100.0	99.9	0.09
240	100.0	99.9	0.09

CVGraph 6.02 06/07/2026 Page 2/2

Capsule B Surrogate Weld (Heat # 27204)

CVGraph 6.02: Hyperbolic Tangent Curve Printed on 5/18/2026 3:34 PM

A = 50.00 B = 50.00 C = 54.79 T0 = 192.51 D = 0.00

Equation is A + B * [Tanh((T-T0)/(C+DT))]

Upper Shelf %Shear = 100.00 (Fixed) Lower Shelf %Shear = 0.00 (Fixed)

Temperature at 50% Shear = 192.60

Plant: **Diablo Canyon 1** Material: **Weld** Heat: **27204**

Orientation: **NA** Capsule: **B** Fluence: **3.62E+019 n/cm²**

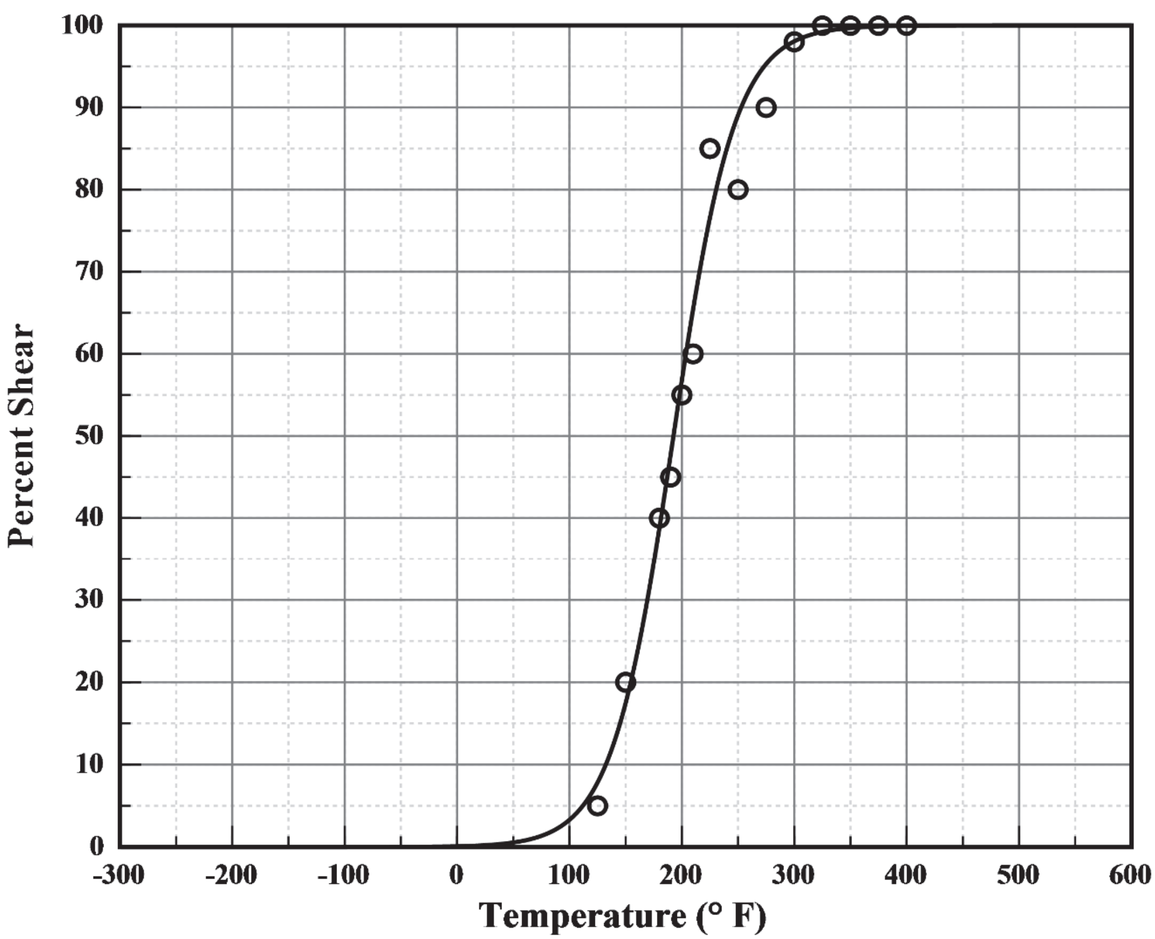

CVGraph 6.02 05/18/2026 Page 1/2

Plant: **Diablo Canyon 1** Material: **Weld** Heat: **27204**
Orientation: **NA** Capsule: **B** Fluence: **3.62E+019 n/cm²**

Capsule B Surrogate Weld (Heat # 27204)
Charpy V-Notch Data

Temperature (° F)	Input %Shear	Computed %Shear	Differential
125	5.0	7.8	-2.84
150	20.0	17.5	2.52
180	40.0	38.8	1.22
190	45.0	47.7	-2.71
200	55.0	56.8	-1.79
210	60.0	65.4	-5.44
225	85.0	76.6	8.40
225	85.0	76.6	8.40
250	80.0	89.1	-9.08
275	90.0	95.3	-5.31
300	98.0	98.1	-0.06
325	100.0	99.2	0.79
350	100.0	99.7	0.32
375	100.0	99.9	0.13
400	100.0	99.9	0.05

CVGraph 6.02 05/18/2026 Page 2/2

C.3.3 Surveillance Weld

Unirradiated Weld Metal

CVGraph 6.02: Hyperbolic Tangent Curve Printed on 6/8/2026 10:30 AM

A = 44.90 B = 42.70 C = 82.66 T0 = -34.94 D = 0.00

Equation is A + B * [Tanh((T-T0)/(C+DT))]

Upper Shelf Energy = 87.60 (Fixed) Lower Shelf Energy = 2.20 (Fixed)

Temp@30 ft-lbs=-65.00° F Temp@35 ft-lbs=-54.40° F Temp@50 ft-lbs=-25.00° F

Plant: **Diablo Canyon 1** Material: **Weld** Heat: **27204**

Orientation: **NA** Capsule: **Unirrad** Fluence: **0.00E+000 n/cm²**

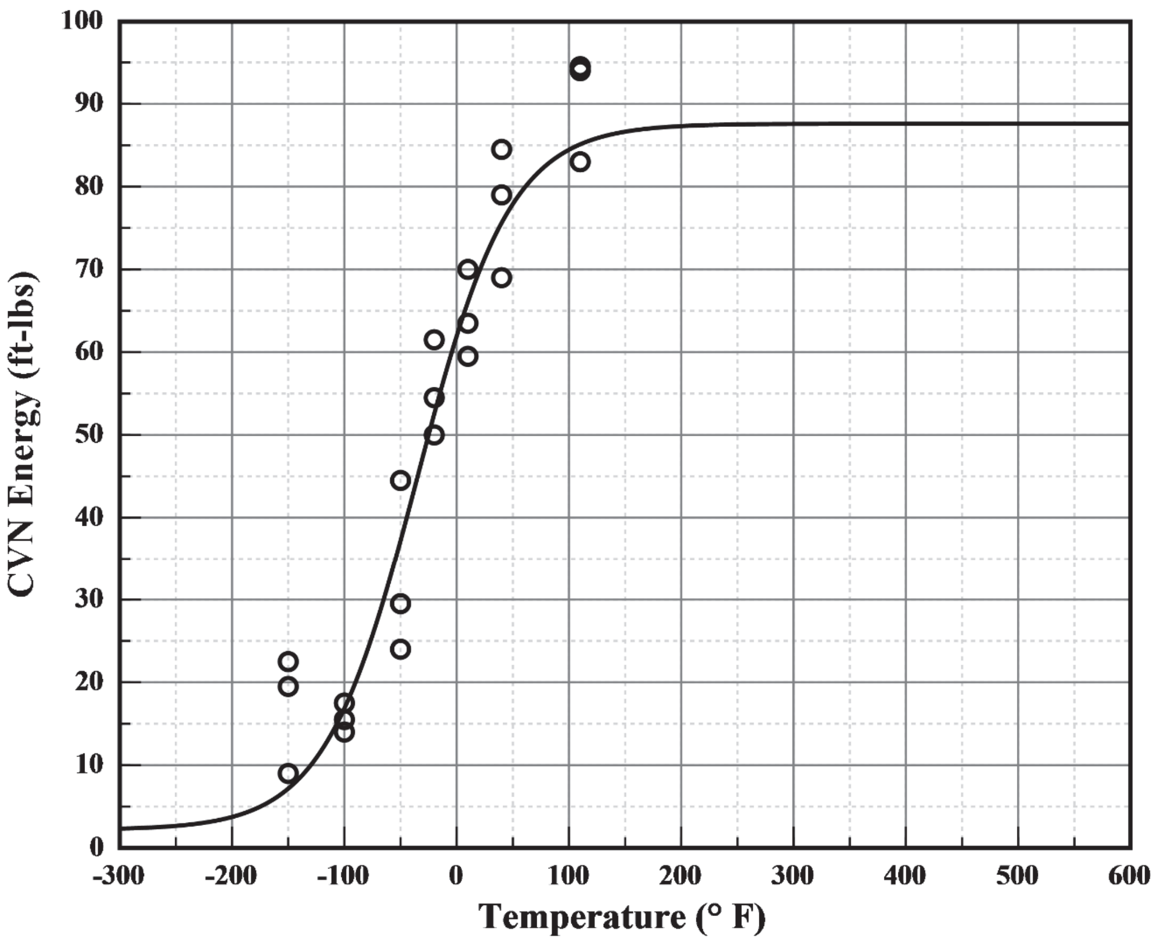

CVGraph 6.02 06/08/2026 Page 1/2

Plant: **Diablo Canyon 1** Material: **Weld** Heat: **27204**
Orientation: **NA** Capsule: **Unirrad** Fluence: **0.00E+000 n/cm²**

Unirradiated Weld Metal
Charpy V-Notch Data

Temperature (° F)	Input CVN	Computed CVN	Differential
-150	9.0	7.2	1.83
-150	22.5	7.2	15.33
-150	19.5	7.2	12.33
-100	17.5	16.9	0.64
-100	14.0	16.9	-2.86
-100	15.5	16.9	-1.36
-50	24.0	37.2	-13.21
-50	29.5	37.2	-7.71
-50	44.5	37.2	7.29
-20	61.5	52.5	8.96
-20	54.5	52.5	1.96
-20	50.0	52.5	-2.54
10	59.5	66.1	-6.57
10	70.0	66.1	3.93
10	63.5	66.1	-2.57
40	84.5	75.6	8.88
40	79.0	75.6	3.38
40	69.0	75.6	-6.62
110	94.5	85.1	9.39
110	94.0	85.1	8.89
110	83.0	85.1	-2.11

CVGraph 6.02 06/08/2026 Page 2/2

Capsule S Weld Metal

CVGraph 6.02: Hyperbolic Tangent Curve Printed on 5/29/2026 1:49 PM

A = 41.35 B = 39.15 C = 143.17 T0 = 87.77 D = 0.00

Equation is A + B * [Tanh((T-T0)/(C+DT))]

Upper Shelf Energy = 80.50 (Fixed) Lower Shelf Energy = 2.20 (Fixed)

Temp@30 ft-lbs= 45.10° F Temp@35 ft-lbs= 64.40° F Temp@50 ft-lbs=120.00° F

Plant: **Diablo Canyon 1** Material: **Weld** Heat: **27204**

Orientation: **NA** Capsule: **S** Fluence: **2.93E+018 n/cm²**

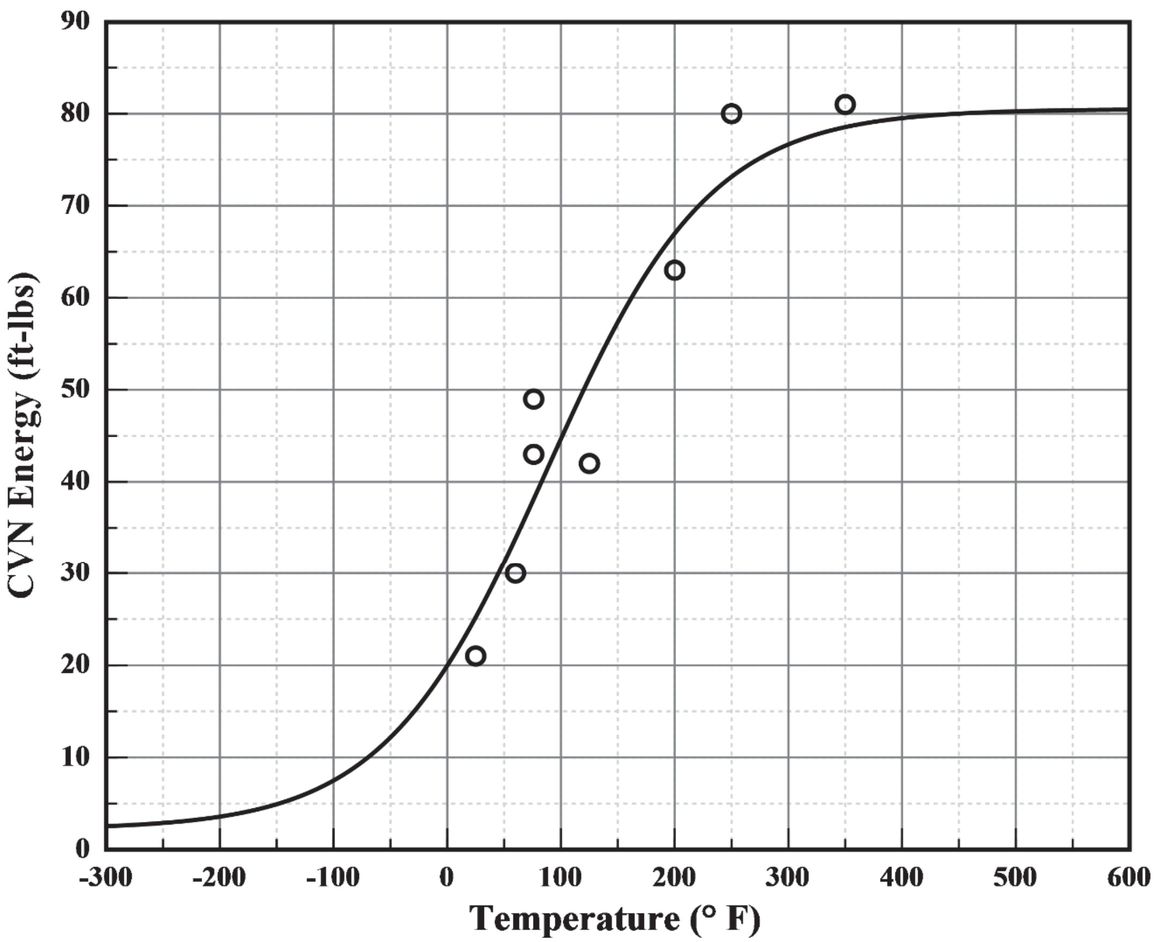

CVGraph 6.02 05/29/2026 Page 1/2

Note: This is a replot of data from a previously tested capsule.

Plant: **Diablo Canyon 1** Material: **Weld** Heat: **27204**
Orientation: **NA** Capsule: **S** Fluence: **2.93E+018 n/cm²**

Capsule S Weld Metal
Charpy V-Notch Data

Temperature (° F)	Input CVN	Computed CVN	Differential
25	21.0	25.2	-4.21
60	30.0	33.9	-3.85
76	43.0	38.1	4.86
76	49.0	38.1	10.86
125	42.0	51.3	-9.31
200	63.0	67.0	-3.99
250	80.0	73.1	6.86
350	81.0	78.5	2.46

CVGraph 6.02 05/29/2026 Page 2/2

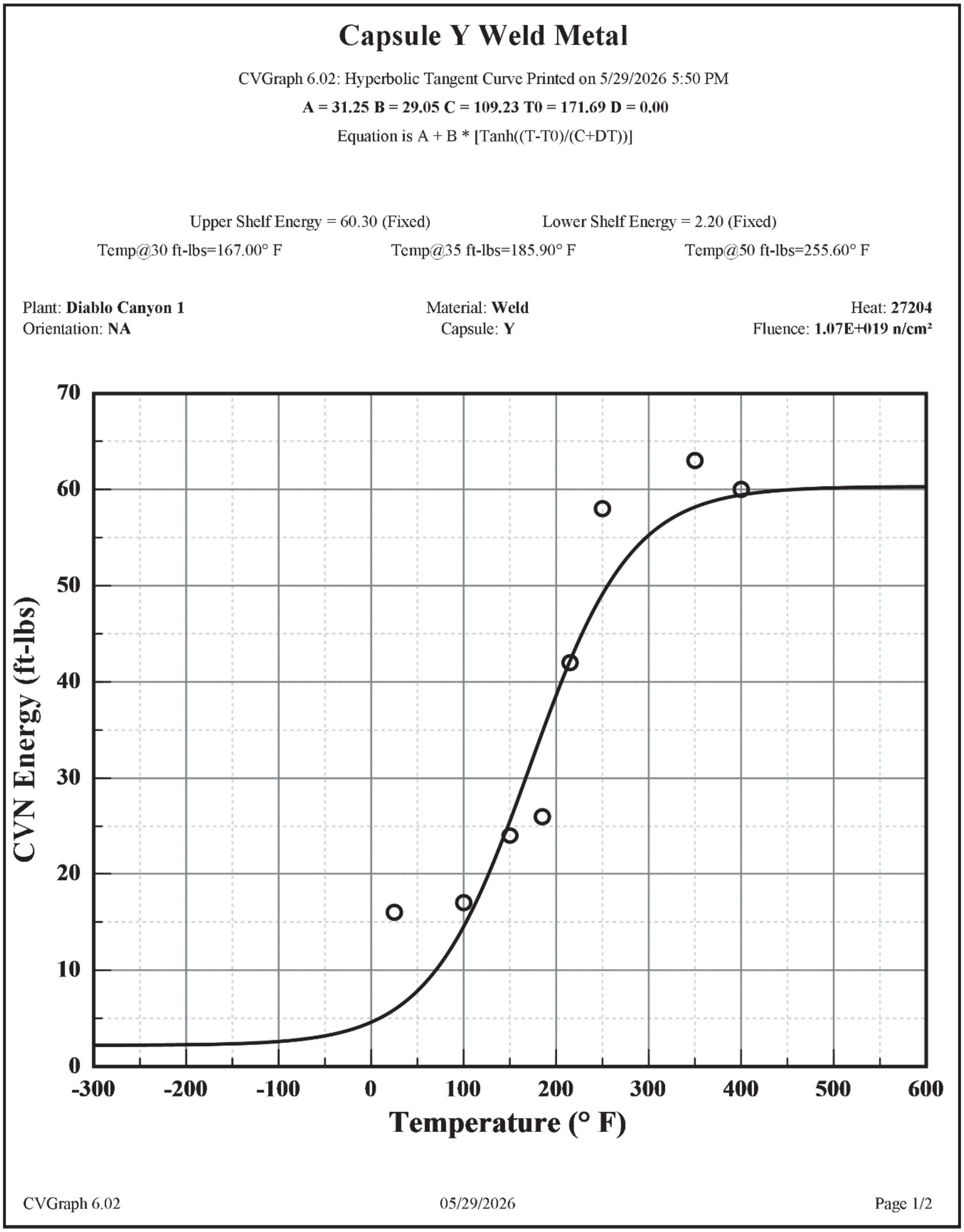

Note: This is a replot of data from a previously tested capsule.

Plant: **Diablo Canyon 1** Material: **Weld** Heat: **27204**
Orientation: **NA** Capsule: **Y** Fluence: **1.07E+019 n/cm²**

Capsule Y Weld Metal
Charpy V-Notch Data

Temperature (° F)	Input CVN	Computed CVN	Differential
25	16.0	5.9	10.09
100	17.0	14.5	2.48
150	24.0	25.6	-1.56
185	26.0	34.8	-8.77
215	42.0	42.2	-0.20
250	58.0	49.1	8.88
350	63.0	58.2	4.84
400	60.0	59.4	0.58

CVGraph 6.02 05/29/2026 Page 2/2

Capsule V Weld Metal

CVGraph 6.02: Hyperbolic Tangent Curve Printed on 5/29/2026 5:54 PM

A = 33.95 B = 31.75 C = 123.38 T0 = 150.60 D = 0.00

Equation is A + B * [Tanh((T-T0)/(C+DT))]

Upper Shelf Energy = 65.70 (Fixed) Lower Shelf Energy = 2.20 (Fixed)

Temp@30 ft-lbs=135.20° F Temp@35 ft-lbs=154.70° F Temp@50 ft-lbs=219.30° F

Plant: **Diablo Canyon 1** Material: **Weld** Heat: **27204**

Orientation: **NA** Capsule: **V** Fluence: **1.35E+019 n/cm²**

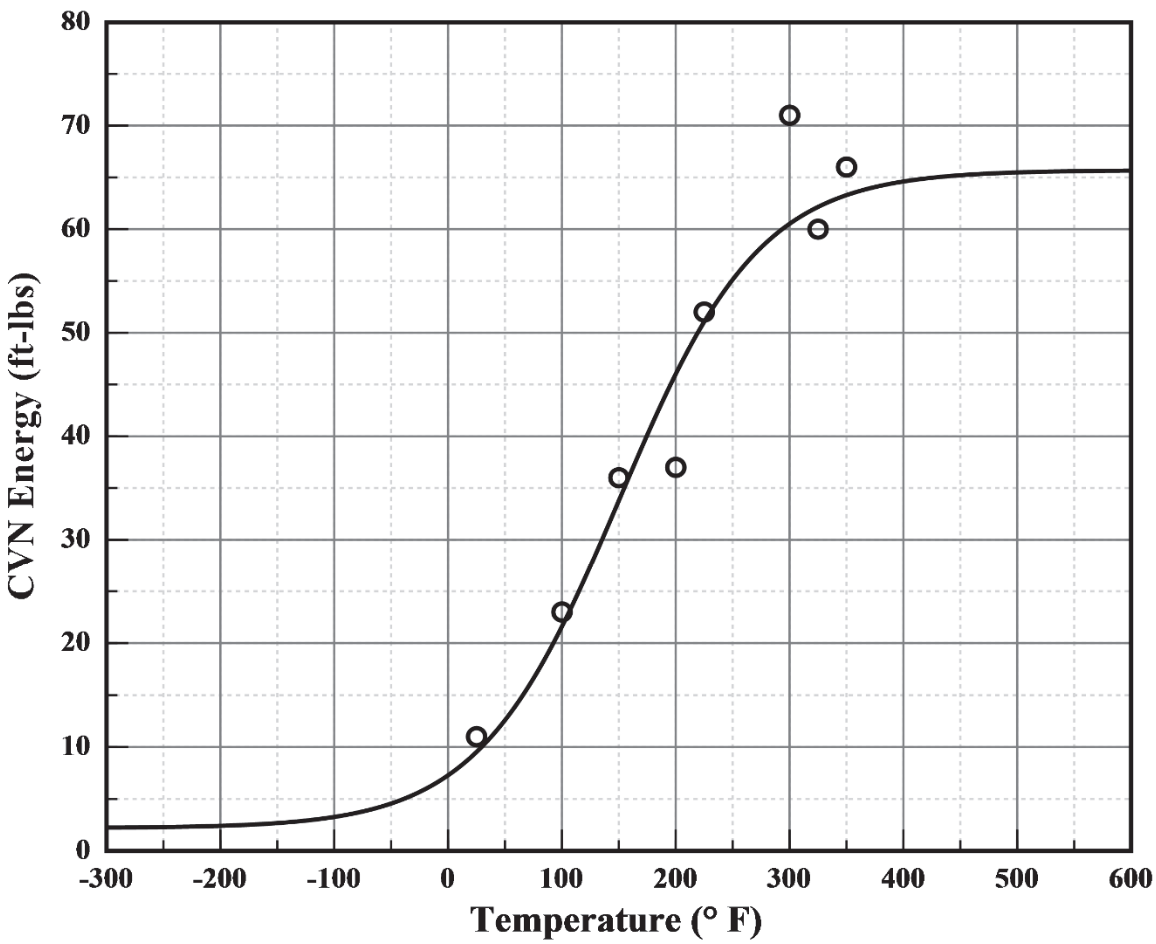

CVGraph 6.02 05/29/2026 Page 1/2

Note: This is a replot of data from a previously tested capsule.

Plant: **Diablo Canyon 1** Material: **Weld** Heat: **27204**
Orientation: **NA** Capsule: **V** Fluence: **1.35E+019 n/cm²**

Capsule V Weld Metal
Charpy V-Notch Data

Temperature (° F)	Input CVN	Computed CVN	Differential
25	11.0	9.5	1.47
100	23.0	21.6	1.39
150	36.0	33.8	2.20
200	37.0	46.0	-9.02
225	52.0	51.1	0.93
300	71.0	60.5	10.48
325	60.0	62.2	-2.15
350	66.0	63.3	2.71

CVGraph 6.02 05/29/2026 Page 2/2

Capsule B Reconstituted Weld

CVGraph 6.02: Hyperbolic Tangent Curve Printed on 5/18/2026 4:18 PM

A = 26.10 B = 23.90 C = 102.48 T0 = 226.82 D = 0.00

Equation is A + B * [Tanh((T-T0)/(C+DT))]

Upper Shelf Energy = 50.00 (Fixed) Lower Shelf Energy = 2.20 (Fixed)

Temp@30 ft-lbs=243.70° F Temp@35 ft-lbs=267.00° F Temp@50 ft-lbs= 0.00° F

Plant: **Diablo Canyon 1** Material: **Weld** Heat: **27204**

Orientation: **NA** Capsule: **B** Fluence: **3.62E+019 n/cm²**

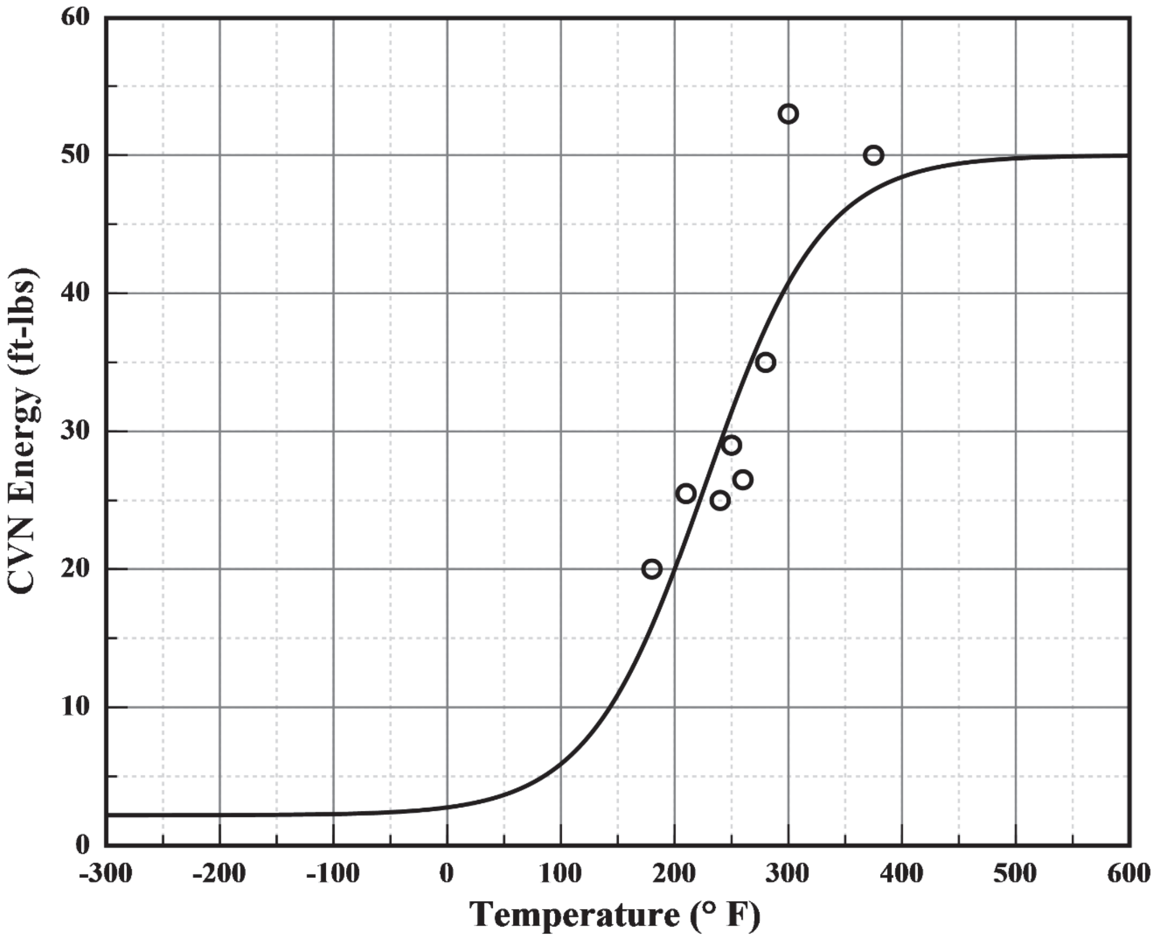

CVGraph 6.02 05/18/2026 Page 1/2

Plant: **Diablo Canyon 1** Material: **Weld** Heat: **27204**
Orientation: **NA** Capsule: **B** Fluence: **3.62E+019 n/cm²**

Capsule B Reconstituted Weld
Charpy V-Notch Data

Temperature (° F)	Input CVN	Computed CVN	Differential
180	20.0	15.9	4.12
210	25.5	22.2	3.29
240	25.0	29.2	-4.16
250	29.0	31.4	-2.42
260	26.5	33.6	-7.08
280	35.0	37.5	-2.50
300	53.0	40.8	12.24
375 (1)	50.0(2)	47.5	2.51

Note:
1. The fitted Charpy energy curve did not attain the 50 ft lb energy level within the evaluated temperature range; therefore, the irradiated 50 ft lb transition temperature was set to the highest temperature which achieved a measurement of 50 ft-lb.
2. Only one specimen exhibited a fracture appearance of ≥95% shear. Consistent with the USE determination methodology, the USE was therefore based on this single data point and is equal to 50 ft-lb.

CVGraph 6.02 05/18/2026 Page 2/2

Unirradiated Weld Metal

CVGraph 6.02: Hyperbolic Tangent Curve Printed on 6/8/2026 10:31 AM

A = 44.60 B = 43.60 C = 94.90 T0 = -25.15 D = 0.00

Equation is A + B * [Tanh((T-T0)/(C+DT))]

Upper Shelf L.E. = 88.20 Lower Shelf L.E. = 1.00 (Fixed)

Temp@35 mils=-46.30° F

Plant: **Diablo Canyon 1** Material: **Weld** Heat: **27204**

Orientation: **NA** Capsule: **Unirrad** Fluence: **0.00E+000 n/cm²**

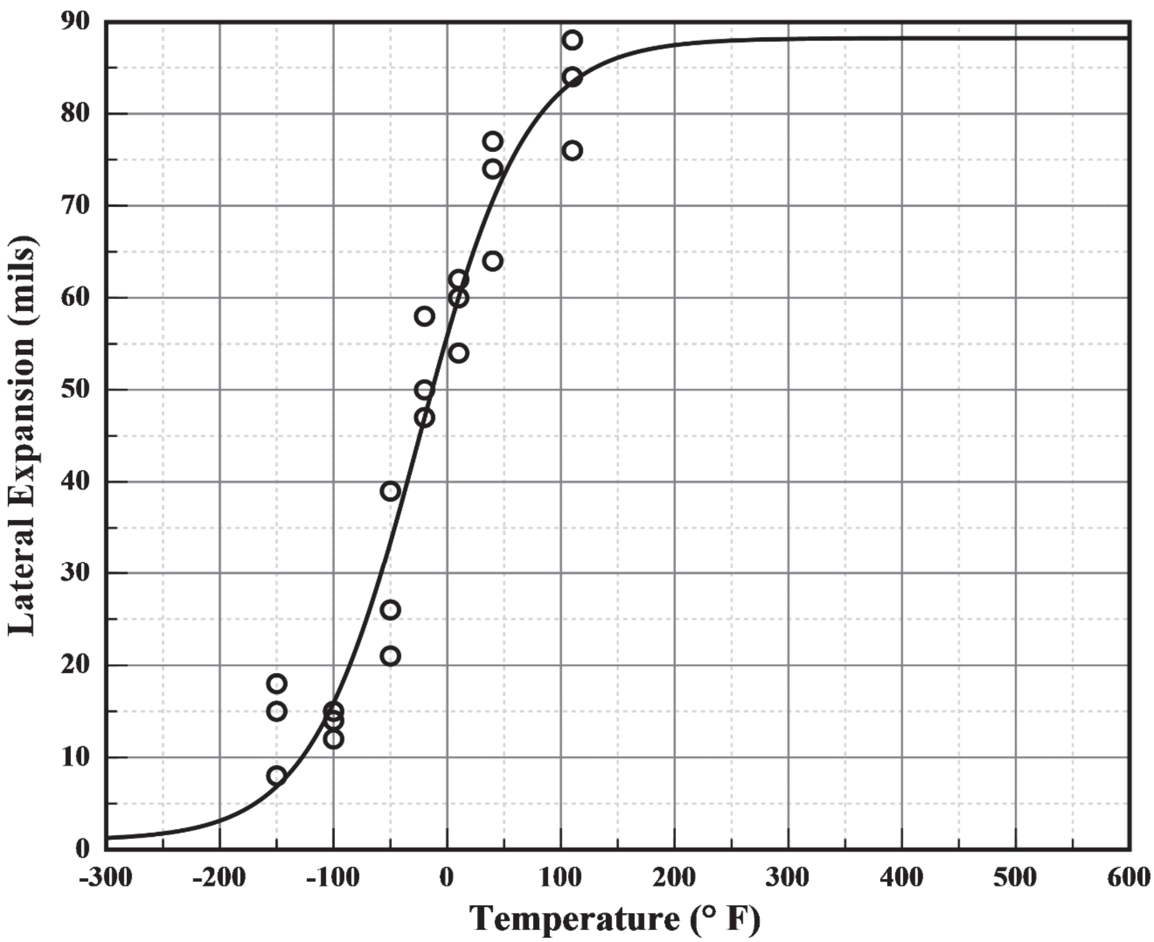

CVGraph 6.02 06/08/2026 Page 1/2

Plant: **Diablo Canyon 1** Material: **Weld** Heat: **27204**
Orientation: **NA** Capsule: **Unirrad** Fluence: **0.00E+000 n/cm²**

Unirradiated Weld Metal
Charpy V-Notch Data

Temperature (° F)	Input L. E.	Computed L. E.	Differential
-150	8.0	6.9	1.14
-150	18.0	6.9	11.14
-150	15.0	6.9	8.14
-100	15.0	15.9	-0.92
-100	14.0	15.9	-1.92
-100	12.0	15.9	-3.92
-50	21.0	33.4	-12.44
-50	26.0	33.4	-7.44
-50	39.0	33.4	5.56
-20	58.0	47.0	11.04
-20	50.0	47.0	3.04
-20	47.0	47.0	0.04
10	54.0	60.0	-6.05
10	62.0	60.0	1.95
10	60.0	60.0	-0.05
40	77.0	70.6	6.43
40	74.0	70.6	3.43
40	64.0	70.6	-6.57
110	88.0	83.4	4.58
110	84.0	83.4	0.58
110	76.0	83.4	-7.42

CVGraph 6.02 06/08/2026 Page 2/2

Capsule S Weld Metal

CVGraph 6.02: Hyperbolic Tangent Curve Printed on 5/29/2026 1:50 PM

A = 37.43 B = 36.43 C = 151.94 T0 = 105.64 D = 0.00

Equation is A + B * [Tanh((T-T0)/(C+DT))]

Upper Shelf L.E. = 73.86 Lower Shelf L.E. = 1.00 (Fixed)

Temp@35 mils= 95.50° F

Plant: **Diablo Canyon 1** Material: **Weld** Heat: **27204**

Orientation: **NA** Capsule: **S** Fluence: **2.93E+018 n/cm²**

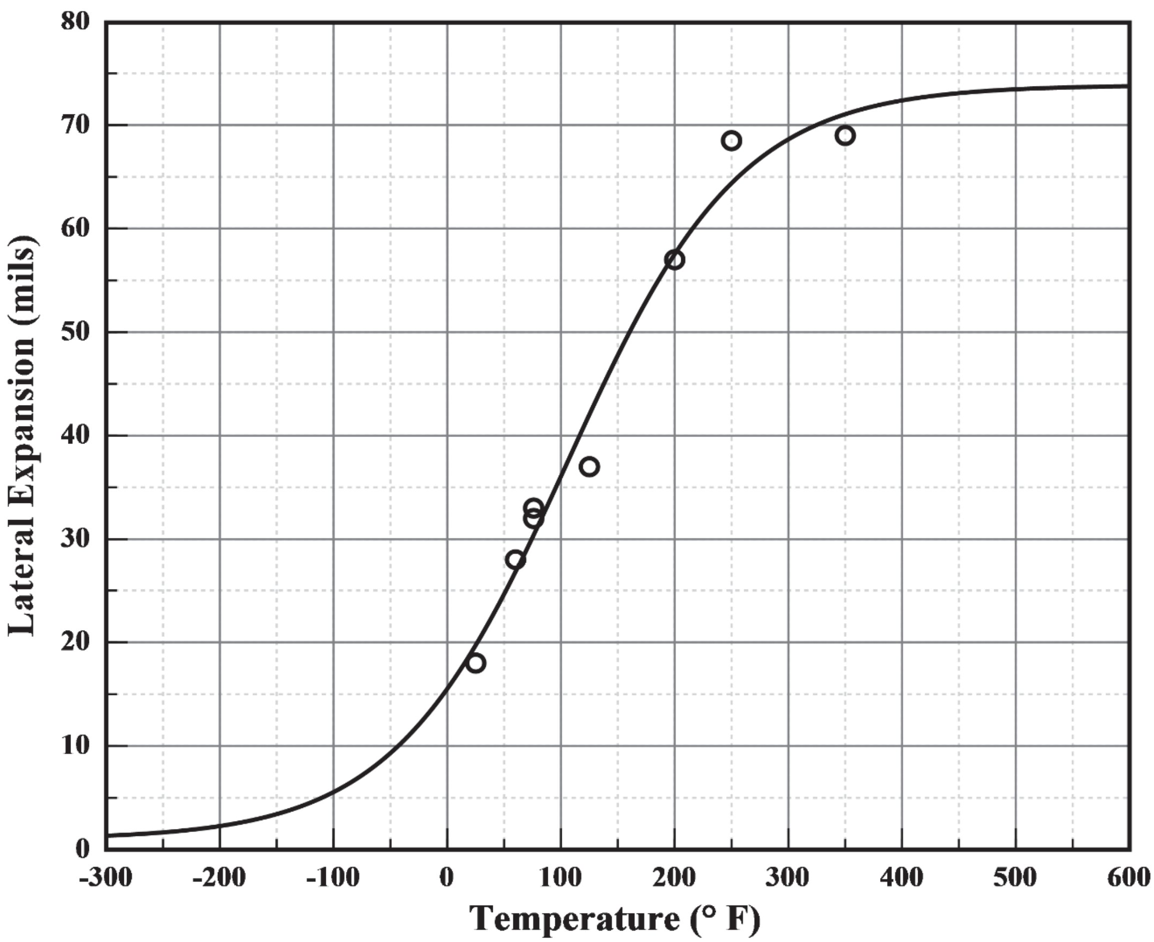

CVGraph 6.02 05/29/2026 Page 1/2

Note: This is a replot of data from a previously tested capsule.

Plant: **Diablo Canyon 1** Material: **Weld** Heat: **27204**
Orientation: **NA** Capsule: **S** Fluence: **2.93E+018 n/cm²**

Capsule S Weld Metal
Charpy V-Notch Data

Temperature (° F)	Input L. E.	Computed L. E.	Differential
25	18.0	19.7	-1.73
60	28.0	26.8	1.19
76	32.0	30.4	1.59
76	33.0	30.4	2.59
125	37.0	42.1	-5.05
200	57.0	57.5	-0.54
250	68.5	64.4	4.11
350	69.0	71.1	-2.06

CVGraph 6.02 05/29/2026 Page 2/2

Capsule Y Weld Metal

CVGraph 6.02: Hyperbolic Tangent Curve Printed on 5/29/2026 5:52 PM

A = 31.10 B = 30.10 C = 117.03 T0 = 178.63 D = 0.00

Equation is A + B * [Tanh((T-T0)/(C+DT))]

Upper Shelf L.E. = 61.20 Lower Shelf L.E. = 1.00 (Fixed)

Temp@35 mils=193.90° F

Plant: **Diablo Canyon 1** Material: **Weld** Heat: **27204**
Orientation: **NA** Capsule: **Y** Fluence: **1.07E+019 n/cm²**

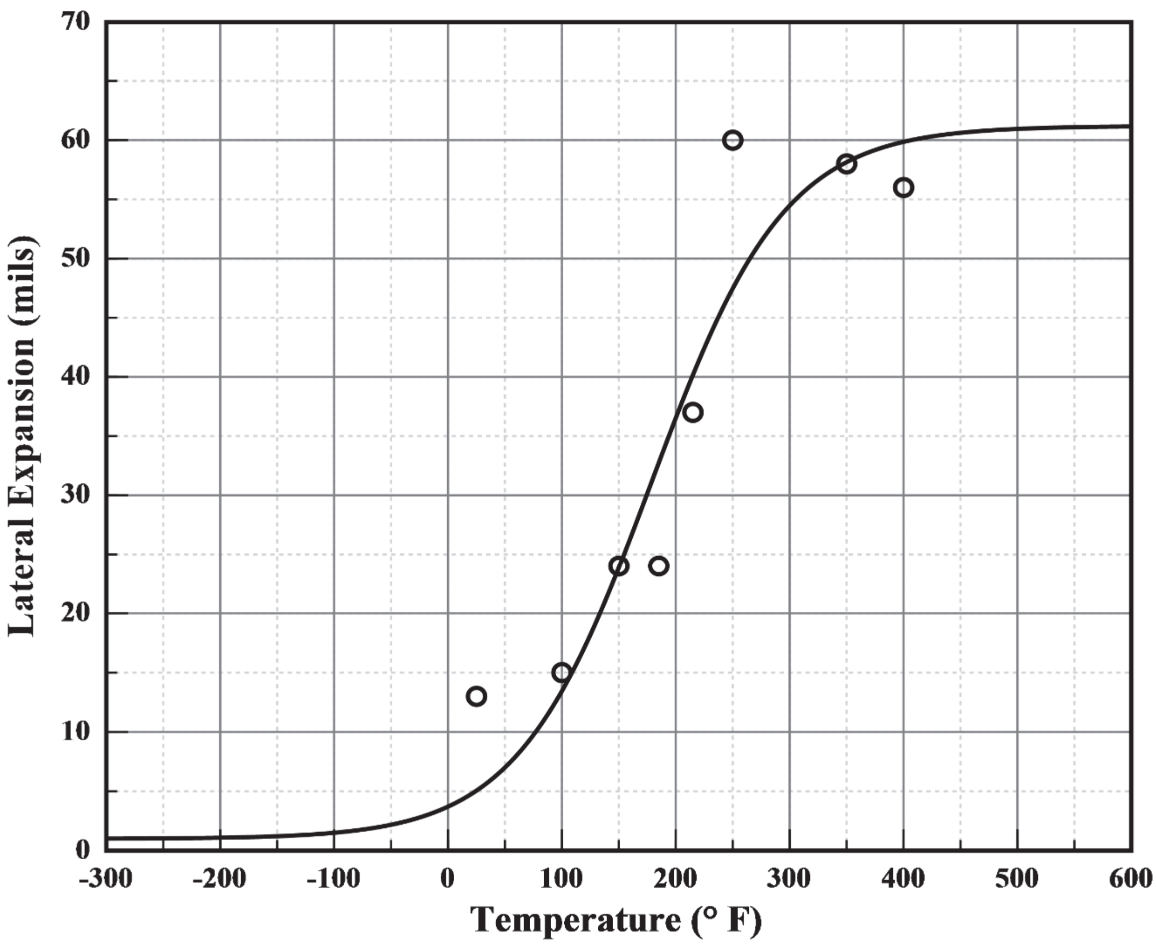

CVGraph 6.02 05/29/2026 Page 1/2

Note: This is a replot of data from a previously tested capsule.

Plant: **Diablo Canyon 1** Material: **Weld** Heat: **27204**
Orientation: **NA** Capsule: **Y** Fluence: **1.07E+019 n/cm²**

Capsule Y Weld Metal
Charpy V-Notch Data

Temperature (° F)	Input L. E.	Computed L. E.	Differential
25	13.0	5.1	7.94
100	15.0	13.5	1.55
150	24.0	23.9	0.12
185	24.0	32.7	-8.74
215	37.0	40.2	-3.16
250	60.0	47.5	12.53
350	58.0	58.1	-0.14
400	56.0	59.9	-3.86

CVGraph 6.02 05/29/2026 Page 2/2

Capsule V Weld Metal

CVGraph 6.02: Hyperbolic Tangent Curve Printed on 5/29/2026 5:55 PM

A = 27.72 B = 26.72 C = 124.18 T0 = 185.84 D = 0.00

Equation is A + B * [Tanh((T-T0)/(C+DT))]

Upper Shelf L.E. = 54.43 Lower Shelf L.E. = 1.00 (Fixed)

Temp@35 mils=220.60° F

Plant: **Diablo Canyon 1** Material: **Weld** Heat: **27204**

Orientation: **NA** Capsule: **V** Fluence: **1.35E+019 n/cm²**

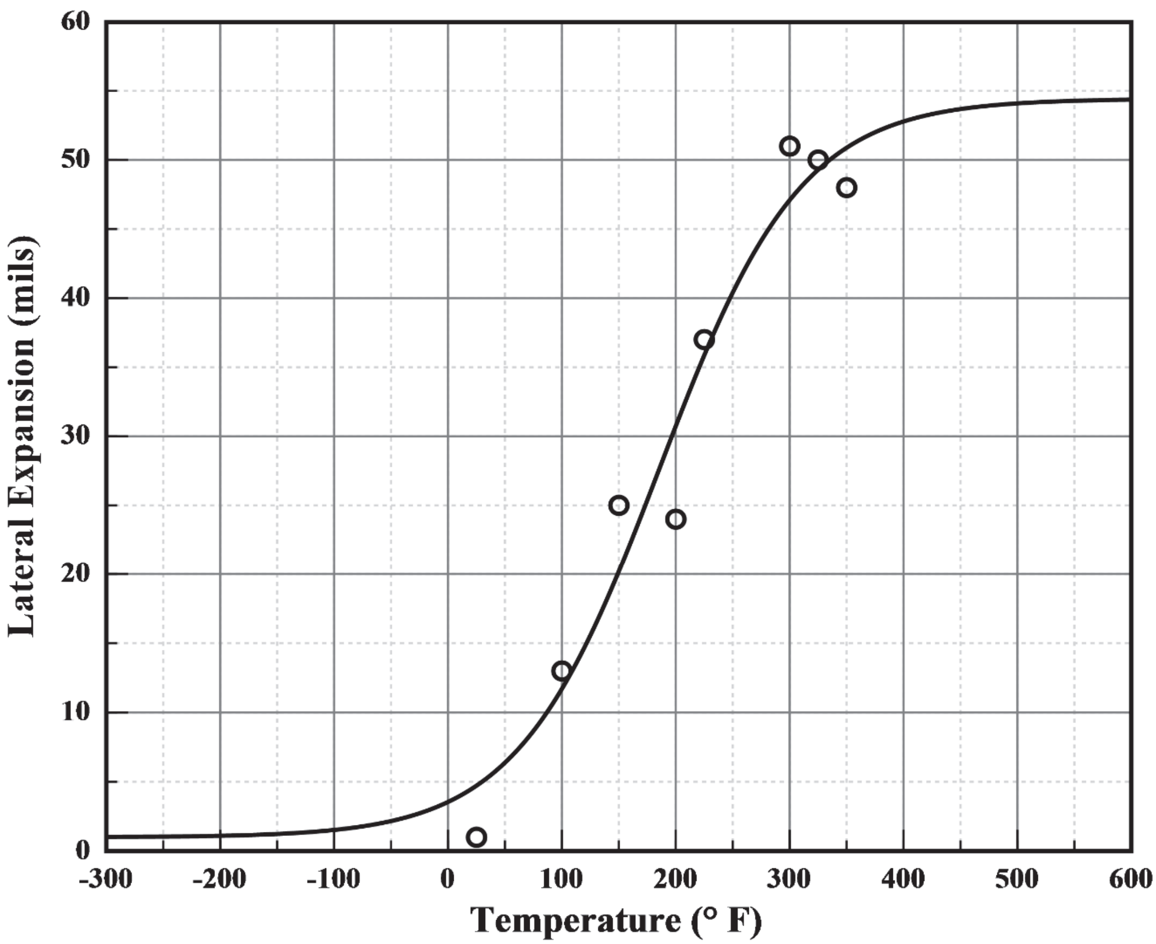

CVGraph 6.02 05/29/2026 Page 1/2

Note: This is a replot of data from a previously tested capsule.

Plant: **Diablo Canyon 1** Material: **Weld** Heat: **27204**
Orientation: **NA** Capsule: **V** Fluence: **1.35E+019 n/cm²**

Capsule V Weld Metal
Charpy V-Notch Data

Temperature (° F)	Input L. E.	Computed L. E.	Differential
25	1.0	4.7	-3.73
100	13.0	11.7	1.28
150	25.0	20.2	4.79
200	24.0	30.7	-6.75
225	37.0	35.9	1.13
300	51.0	47.1	3.90
325	50.0	49.3	0.70
350	48.0	50.9	-2.89

CVGraph 6.02 05/29/2026 Page 2/2

Capsule B Reconstituted Weld

CVGraph 6.02: Hyperbolic Tangent Curve Printed on 5/18/2026 4:19 PM

A = 27.88 B = 26.88 C = 98.56 T0 = 267.10 D = 0.00

Equation is A + B * [Tanh((T-T0)/(C+DT))]

Upper Shelf L.E. = 54.75 Lower Shelf L.E. = 1.00 (Fixed)

Temp@35 mils=293.90° F

Plant: **Diablo Canyon 1** Material: **Weld** Heat: **27204**

Orientation: **NA** Capsule: **B** Fluence: **3.62E+019 n/cm²**

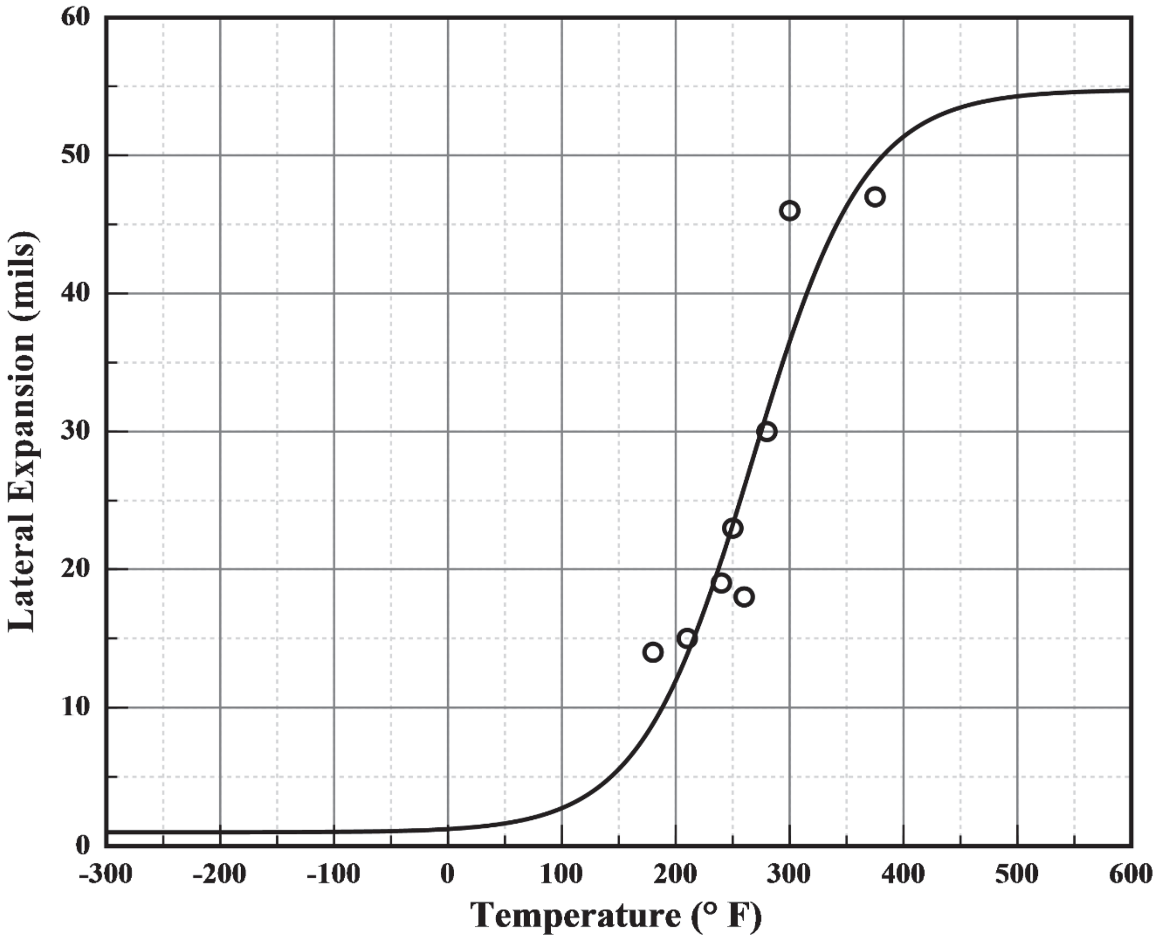

CVGraph 6.02 05/18/2026 Page 1/2

Plant: **Diablo Canyon 1** Material: **Weld** Heat: **27204**
Orientation: **NA** Capsule: **B** Fluence: **3.91E+019 n/cm²**

Capsule B Reconstituted Weld
Charpy V-Notch Data

Temperature (° F)	Input L. E.	Computed L. E.	Differential
180	14.0	8.8	5.16
210	15.0	13.8	1.16
240	19.0	20.7	-1.67
250	23.0	23.3	-0.26
260	18.0	25.9	-7.94
280	30.0	31.4	-1.38
300	46.0	36.5	9.47
375	47.0	49.3	-2.34

CVGraph 6.02 05/18/2026 Page 2/2

Unirradiated Weld Metal

CVGraph 6.02: Hyperbolic Tangent Curve Printed on 6/8/2026 10:32 AM

A = 50.00 B = 50.00 C = 75.77 T0 = -16.11 D = 0.00

Equation is A + B * [Tanh((T-T0)/(C+DT))]

Upper Shelf %Shear = 100.00 (Fixed) Lower Shelf %Shear = 0.00 (Fixed)

Temperature at 50% Shear = -16.10

Plant: **Diablo Canyon 1** Material: **Weld** Heat: **27204**

Orientation: **NA** Capsule: **Unirrad** Fluence: **0.00E+000 n/cm²**

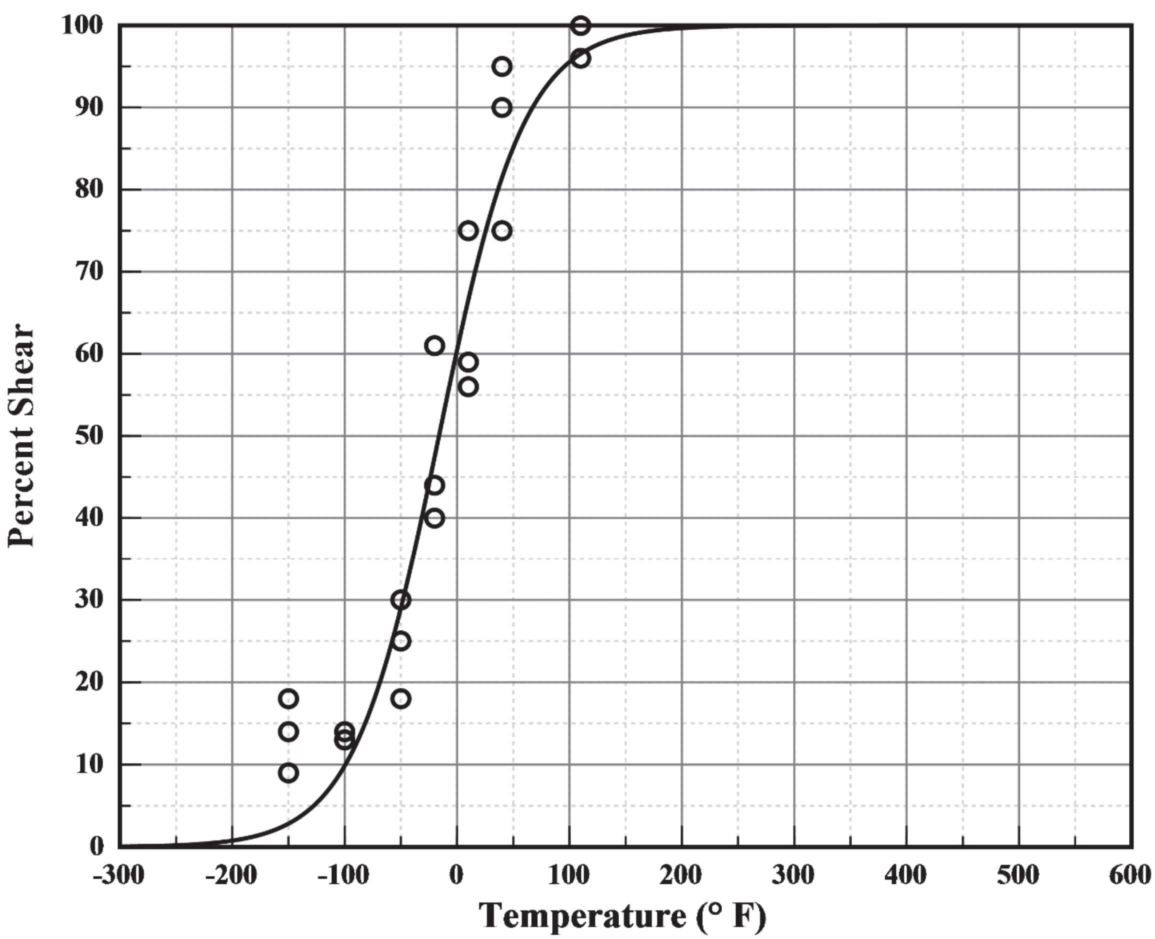

CVGraph 6.02 06/08/2026 Page 1/2

Plant: **Diablo Canyon 1**
Orientation: **NA**

Material: **Weld**
Capsule: **Unirrad**

Heat: **27204**
Fluence: **0.00E+000 n/cm²**

Unirradiated Weld Metal
Charpy V-Notch Data

Temperature (° F)	Input %Shear	Computed %Shear	Differential
-150	9.0	2.8	6.16
-150	14.0	2.8	11.16
-150	18.0	2.8	15.16
-100	13.0	9.8	3.15
-100	13.0	9.8	3.15
-100	14.0	9.8	4.15
-50	18.0	29.0	-11.02
-50	25.0	29.0	-4.02
-50	30.0	29.0	0.98
-20	61.0	47.4	13.56
-20	44.0	47.4	-3.44
-20	40.0	47.4	-7.44
10	59.0	66.6	-7.58
10	75.0	66.6	8.42
10	56.0	66.6	-10.58
40	90.0	81.5	8.53
40	95.0	81.5	13.53
40	75.0	81.5	-6.47
110	100.0	96.5	3.46
110	100.0	96.5	3.46
110	96.0	96.5	-0.54

CVGraph 6.02 06/08/2026 Page 2/2

Capsule S Weld Metal

CVGraph 6.02: Hyperbolic Tangent Curve Printed on 5/29/2026 1:51 PM

A = 50.00 B = 50.00 C = 109.95 T0 = 110.92 D = 0.00

Equation is A + B * [Tanh((T-T0)/(C+DT))]

Upper Shelf %Shear = 100.00 (Fixed) Lower Shelf %Shear = 0.00 (Fixed)

Temperature at 50% Shear = 111.00

Plant: **Diablo Canyon 1** Material: **Weld** Heat: **27204**

Orientation: **NA** Capsule: **S** Fluence: **2.93E+018 n/cm²**

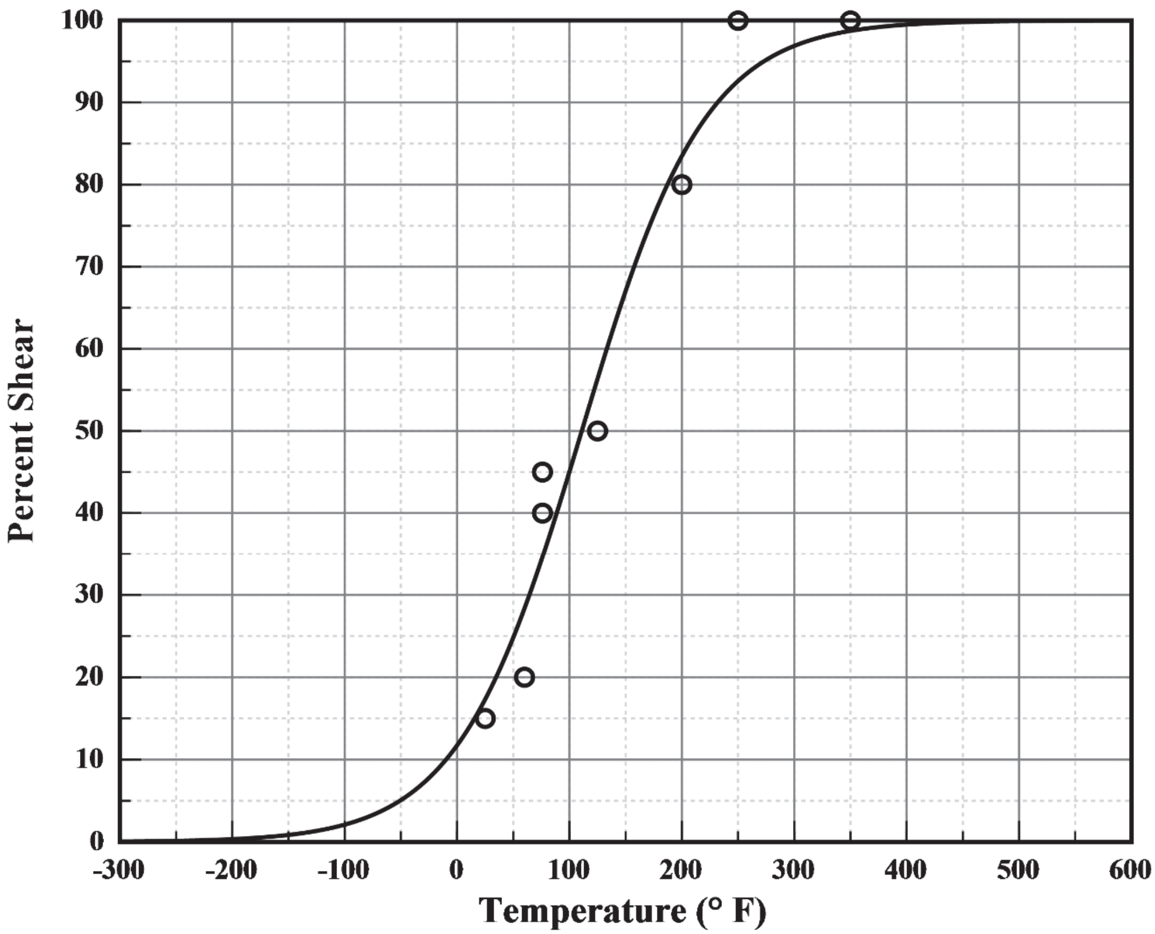

CVGraph 6.02 05/29/2026 Page 1/2

Note: This is a replot of data from a previously tested capsule.

Plant: **Diablo Canyon 1** Material: **Weld** Heat: **27204**
Orientation: **NA** Capsule: **S** Fluence: **2.93E+018 n/cm²**

Capsule S Weld Metal
Charpy V-Notch Data

Temperature (° F)	Input %Shear	Computed %Shear	Differential
25	15.0	17.3	-2.32
60	20.0	28.4	-8.37
76	40.0	34.6	5.36
76	45.0	34.6	10.36
125	50.0	56.4	-6.37
200	80.0	83.5	-3.49
250	100.0	92.6	7.38
350	100.0	98.7	1.28

CVGraph 6.02 05/29/2026 Page 2/2

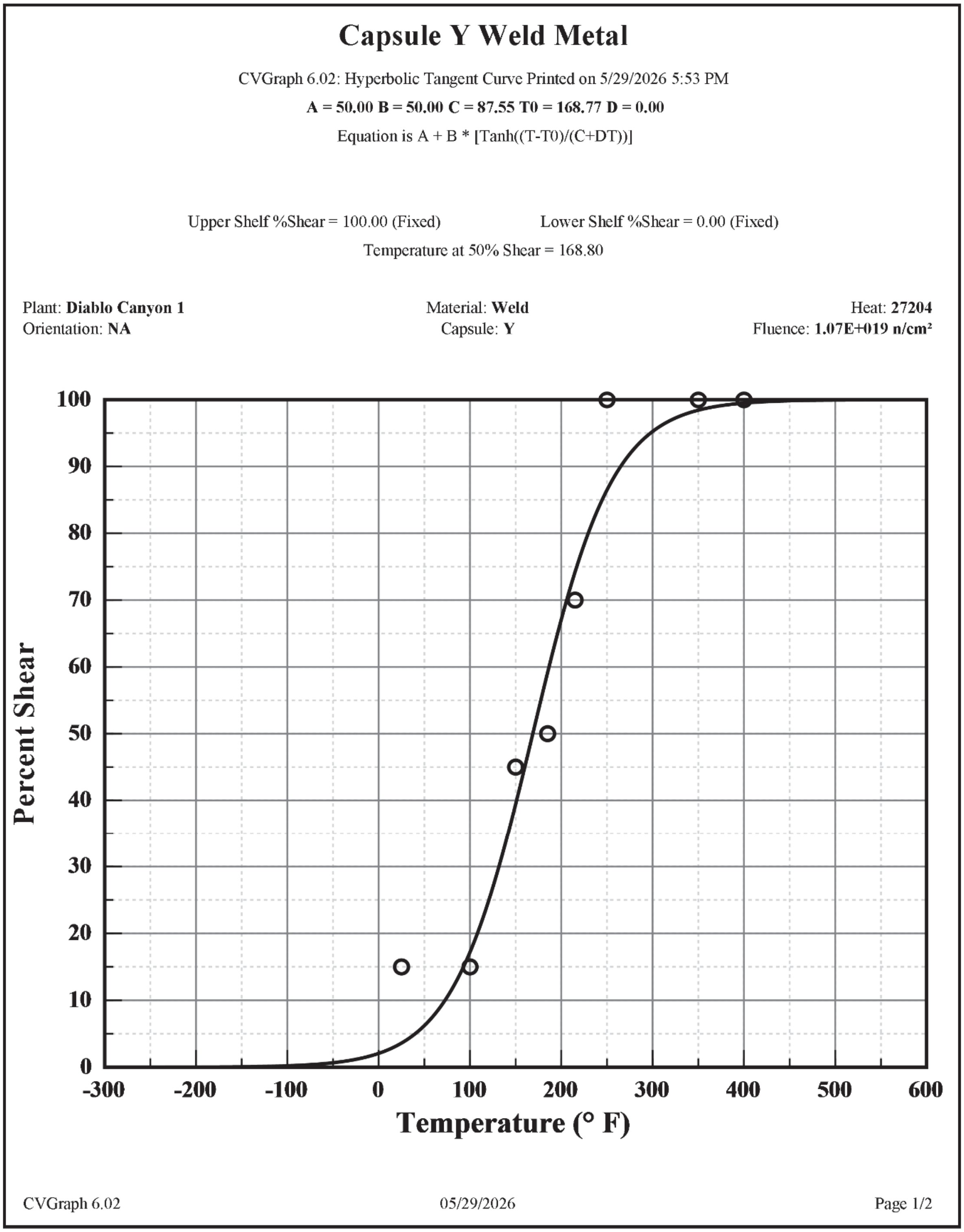

Note: This is a replot of data from a previously tested capsule.

Plant: **Diablo Canyon 1** Material: **Weld** Heat: **27204**
Orientation: **NA** Capsule: **Y** Fluence: **1.07E+019 n/cm²**

Capsule Y Weld Metal
Charpy V-Notch Data

Temperature (° F)	Input %Shear	Computed %Shear	Differential
25	15.0	3.6	11.39
100	15.0	17.2	-2.21
150	45.0	39.4	5.56
185	50.0	59.2	-9.16
215	70.0	74.2	-4.19
250	100.0	86.5	13.52
350	100.0	98.4	1.57
400	100.0	99.5	0.51

CVGraph 6.02 05/29/2026 Page 2/2

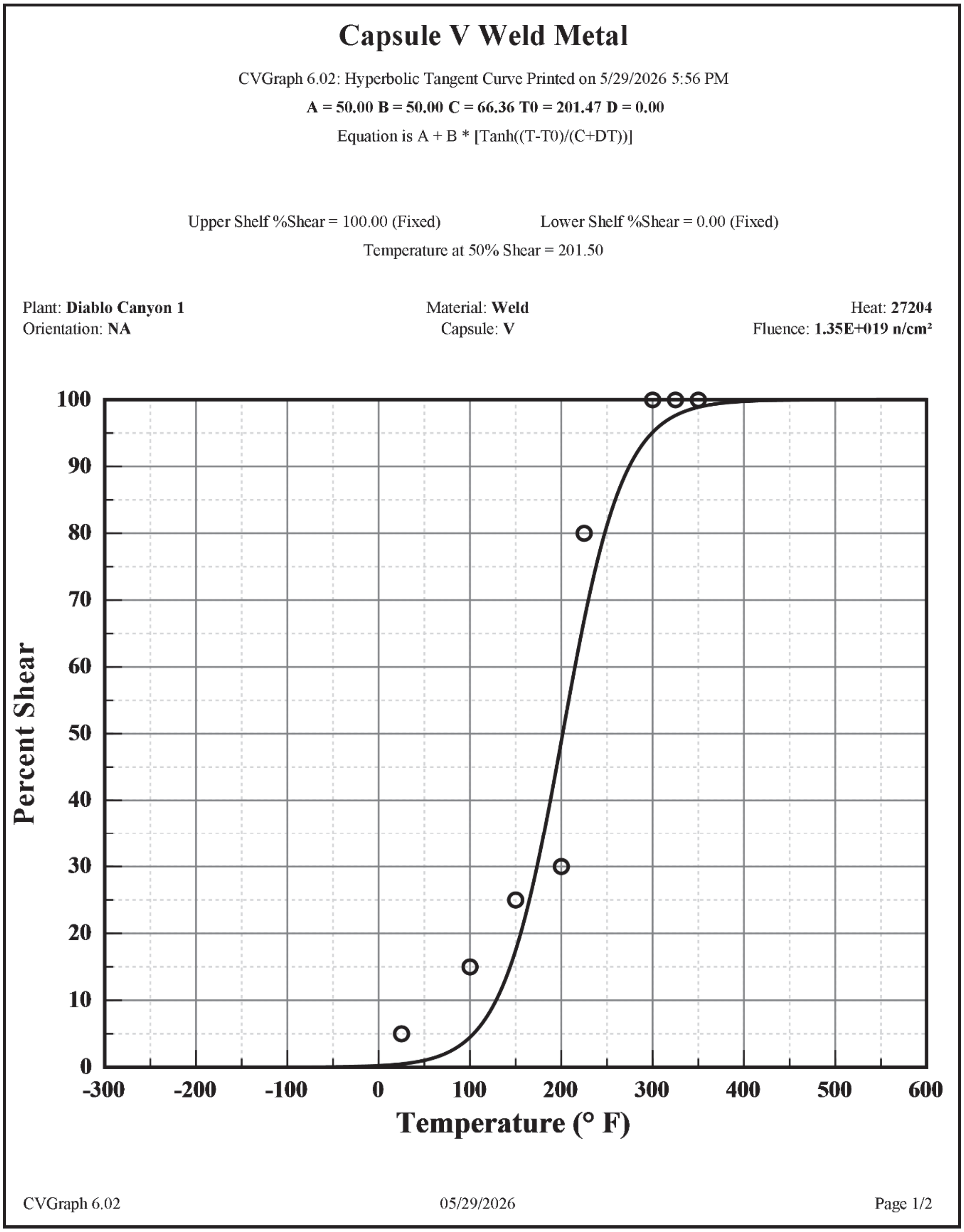

Note: This is a replot of data from a previously tested capsule.

Plant: **Diablo Canyon 1** Material: **Weld** Heat: **27204**
Orientation: **NA** Capsule: **V** Fluence: **1.35E+019 n/cm²**

Capsule V Weld Metal
Charpy V-Notch Data

Temperature (° F)	Input %Shear	Computed %Shear	Differential
25	5.0	0.5	4.51
100	15.0	4.5	10.51
150	25.0	17.5	7.51
200	30.0	48.9	-18.89
225	80.0	67.0	12.98
300	100.0	95.1	4.88
325	100.0	97.6	2.36
350	100.0	98.9	1.12

CVGraph 6.02 05/29/2026 Page 2/2

Capsule B Reconstituted Weld

CVGraph 6.02: Hyperbolic Tangent Curve Printed on 5/18/2026 4:25 PM

A = 50.00 B = 50.00 C = 95.81 T0 = 239.78 D = 0.00

Equation is A + B * [Tanh((T-T0)/(C+DT))]

Upper Shelf %Shear = 100.00 (Fixed) Lower Shelf %Shear = 0.00 (Fixed)

Temperature at 50% Shear = 239.80

Plant: **Diablo Canyon 1** Material: **Weld** Heat: **27204**
Orientation: **NA** Capsule: **B** Fluence: **3.62E+019 n/cm²**

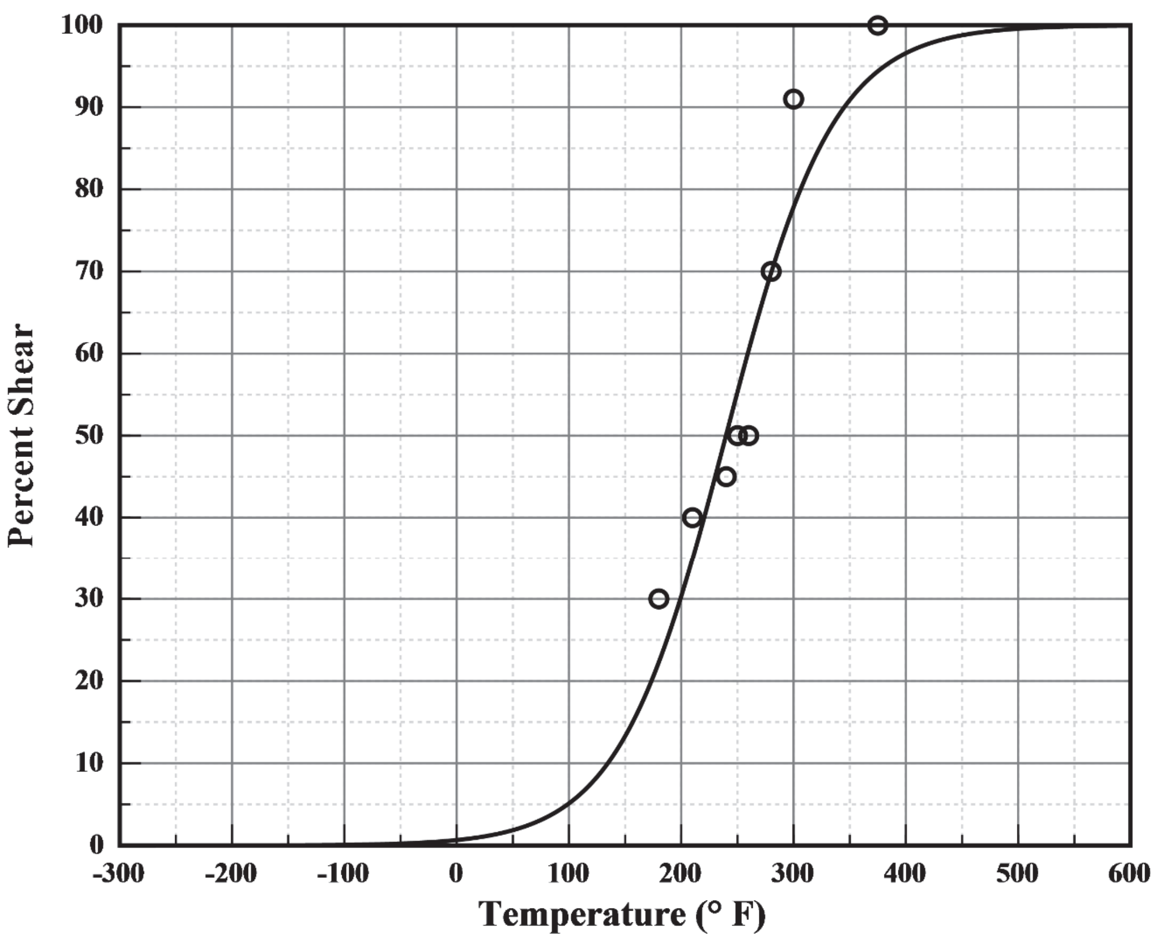

CVGraph 6.02 05/18/2026 Page 1/2

Plant: **Diablo Canyon 1** Material: **Weld** Heat: **27204**
Orientation: **NA** Capsule: **B** Fluence: **3.91E+019 n/cm²**

Capsule B Reconstituted Weld
Charpy V-Notch Data

Temperature (° F)	Input %Shear	Computed %Shear	Differential
180	30.0	22.3	7.69
210	40.0	34.9	5.06
240	45.0	50.1	-5.12
250	50.0	55.3	-5.31
260	50.0	60.4	-10.40
280	70.0	69.8	0.16
300	91.0	77.9	13.15
375	100.0	94.4	5.61

CVGraph 6.02 05/18/2026 Page 2/2

C.3.4 Correlation Monitor Material

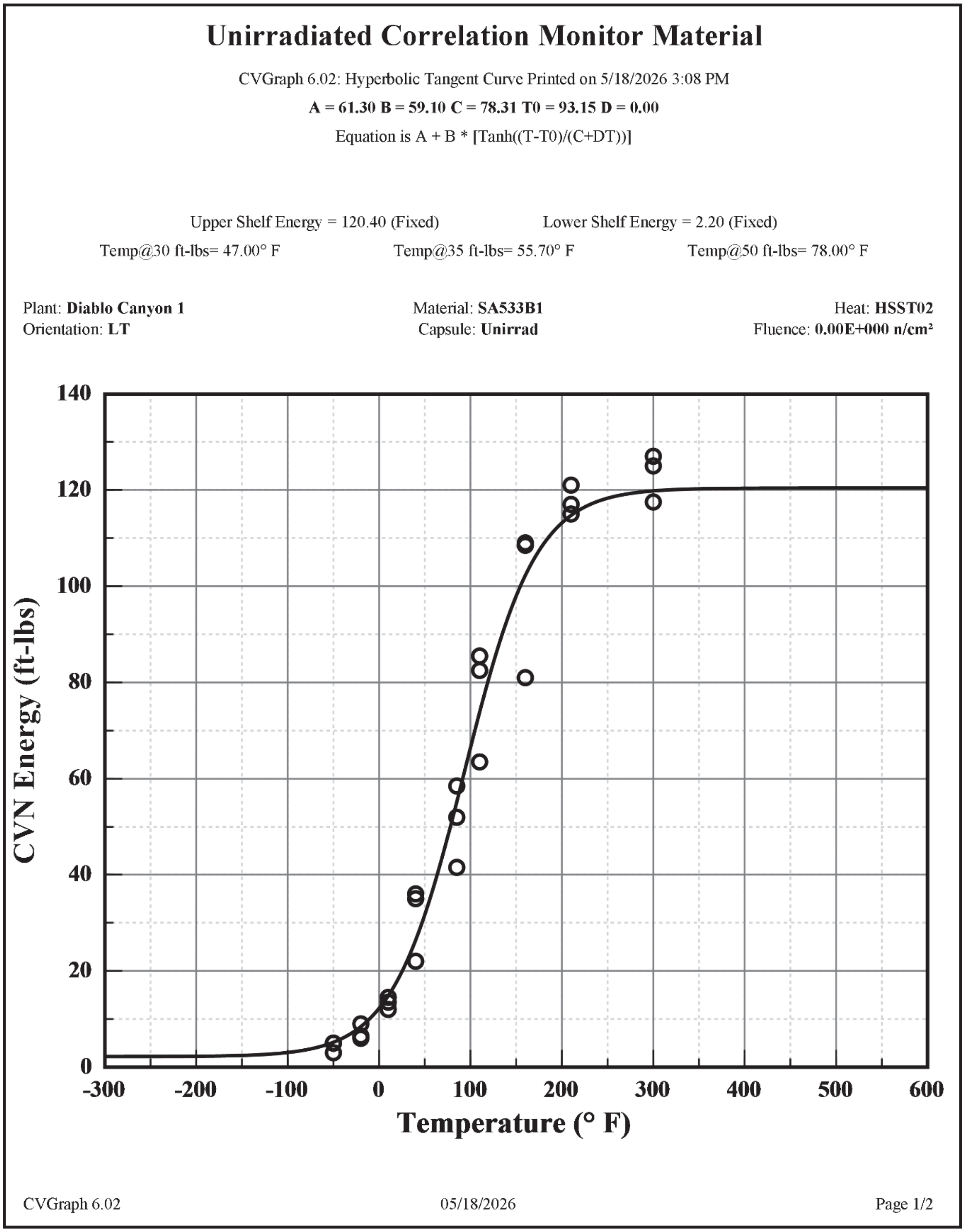

Plant: **Diablo Canyon 1** Material: **SA533B1** Heat: **HSST02**
Orientation: **LT** Capsule: **Unirrad** Fluence: **0.00E+000 n/cm²**

Unirradiated Correlation Monitor Material
Charpy V-Notch Data

Temperature (° F)	Input CVN	Computed CVN	Differential
-50	5.0	5.2	-0.18
-50	5.0	5.2	-0.18
-50	3.0	5.2	-2.18
-20	6.5	8.4	-1.93
-20	9.0	8.4	0.57
-20	6.0	8.4	-2.43
10	12.0	14.8	-2.83
10	14.5	14.8	-0.33
10	13.5	14.8	-1.33
40	22.0	26.4	-4.39
40	36.0	26.4	9.61
40	35.0	26.4	8.61
85	58.5	55.2	3.32
85	41.5	55.2	-13.68
85	52.0	55.2	-3.18
110	82.5	73.8	8.67
110	85.5	73.8	11.67
110	63.5	73.8	-10.33
160	108.5	102.3	6.24
160	81.0	102.3	-21.26
160	109.0	102.3	6.74
210	117.0	114.7	2.29
210	115.0	114.7	0.29
210	121.0	114.7	6.29
300	125.0	119.8	5.20
300	117.5	119.8	-2.30
300	127.0	119.8	7.20

CVGraph 6.02 05/18/2026 Page 2/2

Capsule S Correlation Monitor Material

CVGraph 6.02: Hyperbolic Tangent Curve Printed on 5/28/2026 1:27 PM

A = 61.10 B = 58.90 C = 78.96 T0 = 158.60 D = 0.00

Equation is A + B * [Tanh((T-T0)/(C+DT))]

Upper Shelf Energy = 120.00 (Fixed) Lower Shelf Energy = 2.20 (Fixed)

Temp@30 ft-lbs=112.30° F Temp@35 ft-lbs=121.10° F Temp@50 ft-lbs=143.60° F

Plant: **Diablo Canyon 1** Material: **SA533B1** Heat: **HSST02**

Orientation: **NA** Capsule: **S** Fluence: **2.93E+018 n/cm²**

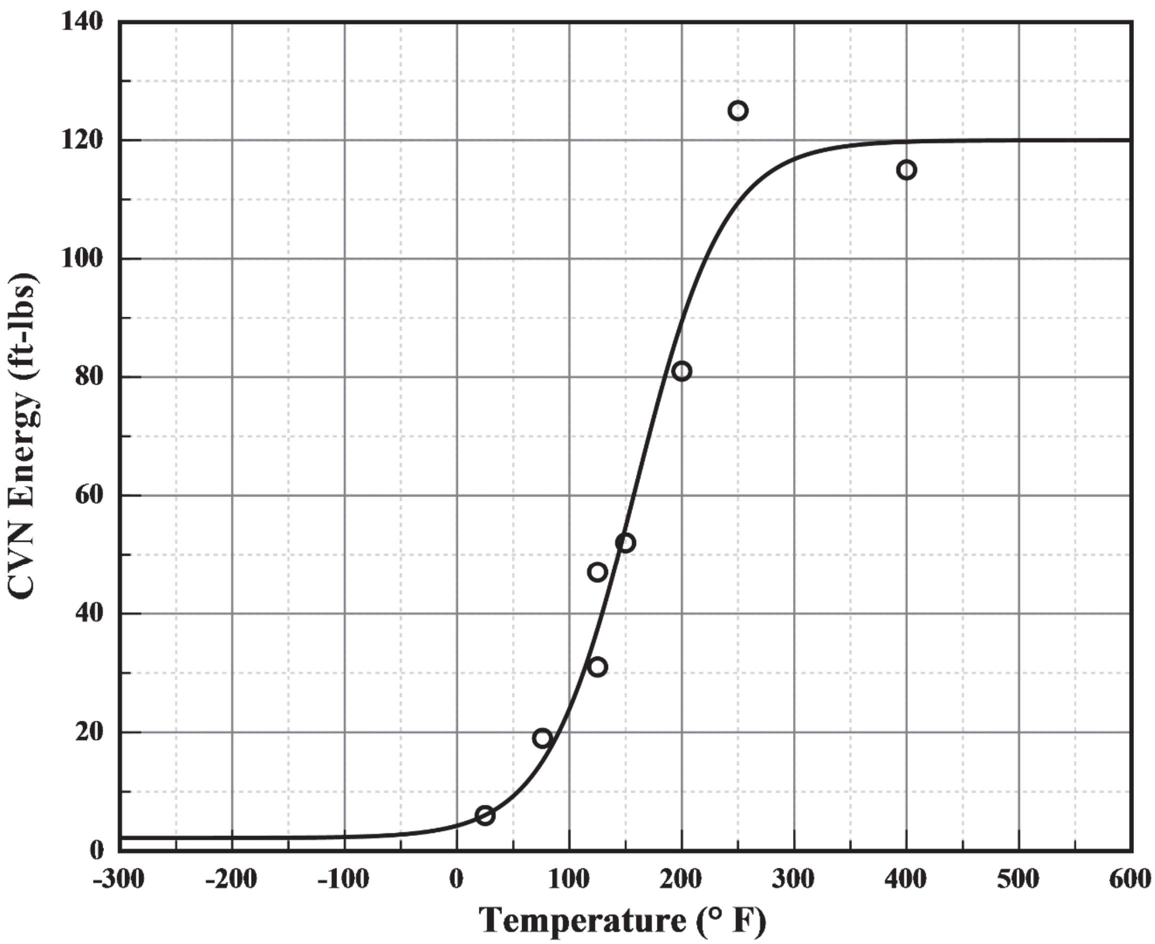

CVGraph 6.02 05/28/2026 Page 1/2

Note: This is a replot of data from a previously tested capsule.

Plant: **Diablo Canyon 1** Material: **SA533B1** Heat: **HSST02**
Orientation: **NA** Capsule: **S** Fluence: **2.93E+018 n/cm²**

Capsule S Correlation Monitor Material

Charpy V-Notch Data

Temperature (° F)	Input CVN	Computed CVN	Differential
25	6.0	6.1	-0.06
76	19.0	15.1	3.86
125	47.0	37.4	9.55
125	31.0	37.4	-6.45
150	52.0	54.7	-2.71
200	81.0	89.4	-8.43
250	125.0	109.4	15.59
400	115.0	119.7	-4.74

CVGraph 6.02 05/28/2026 Page 2/2

Capsule Y Correlation Monitor Material

CVGraph 6.02: Hyperbolic Tangent Curve Printed on 5/28/2026 1:35 PM

A = 54.95 B = 52.75 C = 60.05 T0 = 194.01 D = 0.00

Equation is A + B * [Tanh((T-T0)/(C+DT))]

Upper Shelf Energy = 107.70 (Fixed) Lower Shelf Energy = 2.20 (Fixed)

Temp@30 ft-lbs=163.20° F Temp@35 ft-lbs=170.20° F Temp@50 ft-lbs=188.40° F

Plant: **Diablo Canyon 1** Material: **SA533B1** Heat: **HSST02**

Orientation: **NA** Capsule: **Y** Fluence: **1.07E+019 n/cm²**

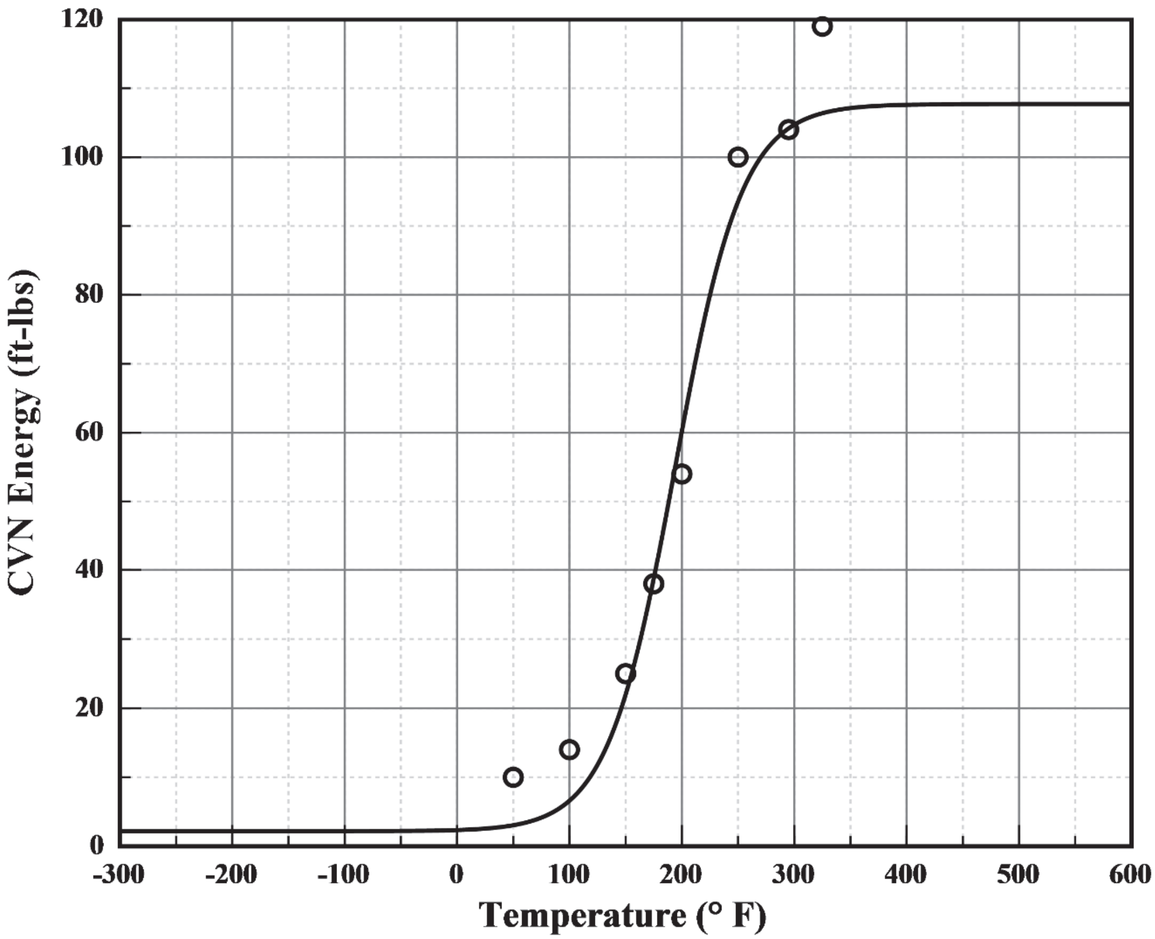

CVGraph 6.02 05/28/2026 Page 1/2

Note: This is a replot of data from a previously tested capsule.

Plant: **Diablo Canyon 1** Material: **SA533B1** Heat: **HSST02**
Orientation: **NA** Capsule: **Y** Fluence: **1.07E+019 n/cm²**

Capsule Y Correlation Monitor Material
Charpy V-Notch Data

Temperature (° F)	Input CVN	Computed CVN	Differential
50	10.0	3.1	6.94
100	14.0	6.6	7.39
150	25.0	22.0	3.01
175	38.0	38.8	-0.79
200	54.0	60.2	-6.20
250	100.0	93.5	6.45
295	104.0	104.2	-0.17
325	119.0	106.4	12.63

CVGraph 6.02 05/28/2026 Page 2/2

Capsule V Correlation Monitor Material

CVGraph 6.02: Hyperbolic Tangent Curve Printed on 5/29/2026 7:17 AM

A = 59.60 B = 57.40 C = 85.27 T0 = 211.97 D = 0.00

Equation is A + B * [Tanh((T-T0)/(C+DT))]

Upper Shelf Energy = 117.00 (Fixed) Lower Shelf Energy = 2.20 (Fixed)

Temp@30 ft-lbs=163.40° F Temp@35 ft-lbs=173.00° F Temp@50 ft-lbs=197.60° F

Plant: **Diablo Canyon 1** Material: **SA533B1** Heat: **HSST02**

Orientation: **NA** Capsule: **V** Fluence: **1.35E+019 n/cm²**

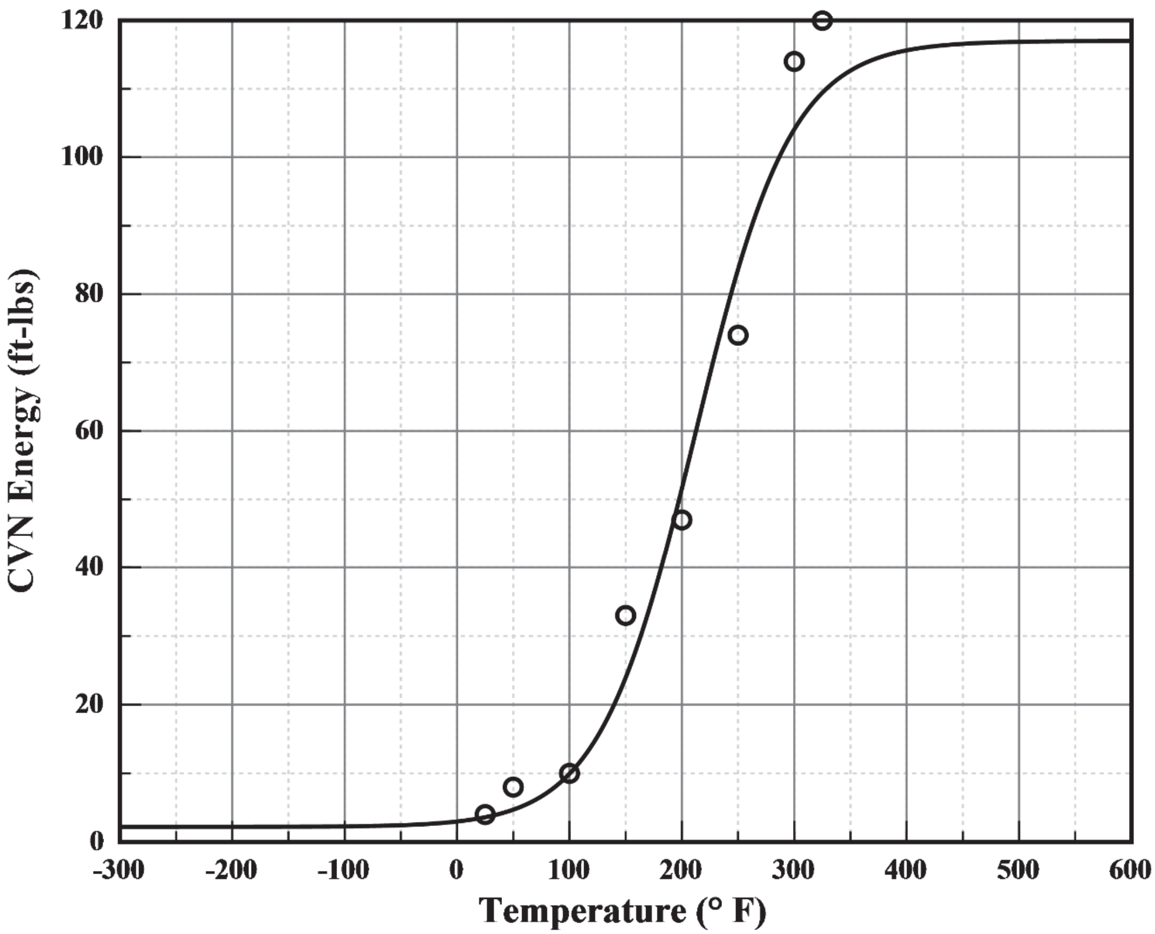

CVGraph 6.02 05/29/2026 Page 1/2

Note: This is a replot of data from a previously tested capsule.

Plant: **Diablo Canyon 1** Material: **SA533B1** Heat: **HSST02**
Orientation: **NA** Capsule: **V** Fluence: **1.35E+019 n/cm²**

Capsule V Correlation Monitor Material
Charpy V-Notch Data

Temperature (° F)	Input CVN	Computed CVN	Differential
25	4.0	3.6	0.39
50	8.0	4.7	3.29
100	10.0	9.9	0.06
150	33.0	23.9	9.05
200	47.0	51.6	-4.59
250	74.0	83.6	-9.63
300	114.0	104.1	9.92
325	120.0	109.4	10.57

CVGraph 6.02 05/29/2026 Page 2/2

Capsule B Correlation Monitor Material

CVGraph 6.02: Hyperbolic Tangent Curve Printed on 5/18/2026 4:07 PM

A = 42.60 B = 40.40 C = 84.52 T0 = 238.01 D = 0.00

Equation is A + B * [Tanh((T-T0)/(C+DT))]

Upper Shelf Energy = 83.00 (Fixed) Lower Shelf Energy = 2.20 (Fixed)

Temp@30 ft-lbs=210.80° F Temp@35 ft-lbs=222.00° F Temp@50 ft-lbs=253.70° F

Plant: **Diablo Canyon 1** Material: **SA533B1** Heat: **HSST02**
Orientation: **NA** Capsule: **B** Fluence: **3.62E+019 n/cm²**

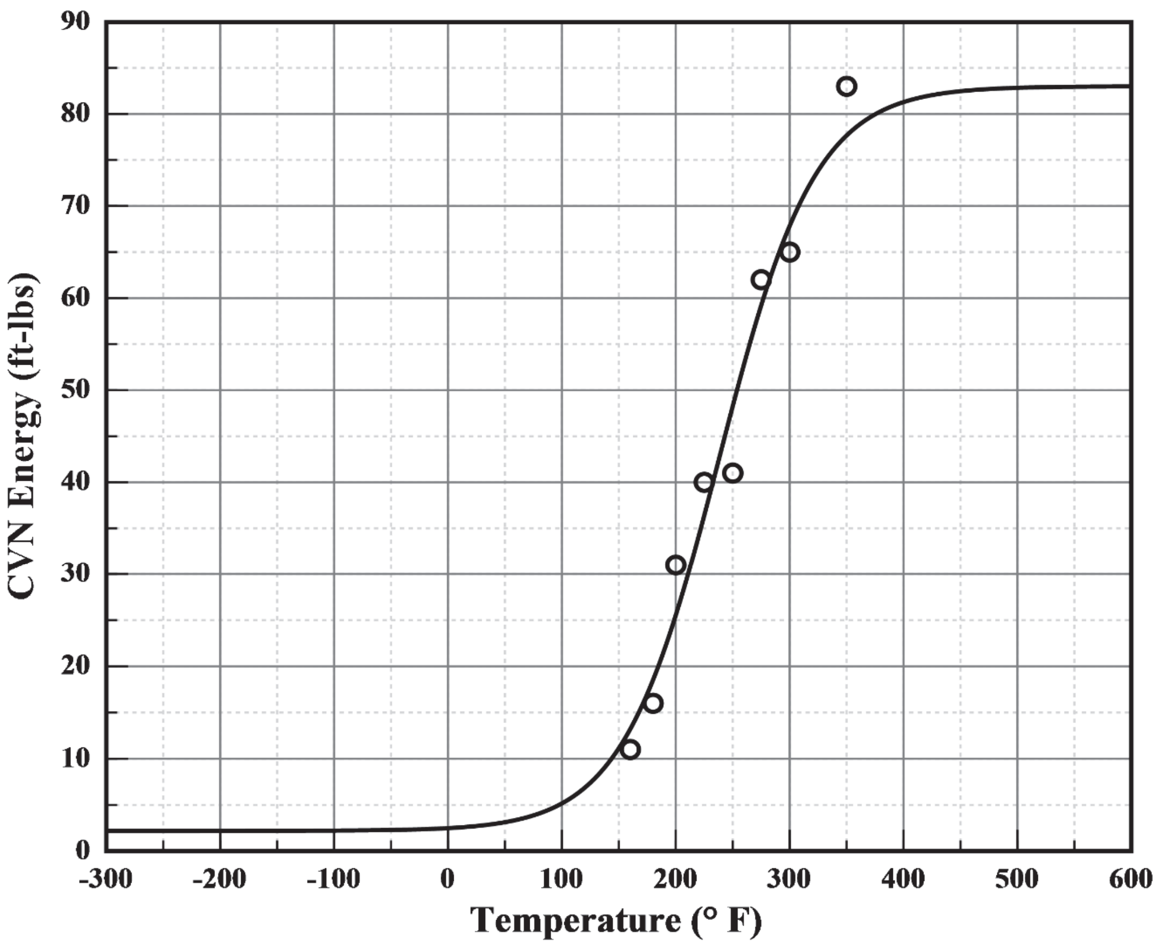

CVGraph 6.02 05/18/2026 Page 1/2

Note: This is a replot of data from a previously tested capsule.

Plant: **Diablo Canyon 1** Material: **SA533B1** Heat: **HSST02**
Orientation: **NA** Capsule: **B** Fluence: **3.62E+019 n/cm²**

Capsule B Correlation Monitor Material
Charpy V-Notch Data

Temperature (° F)	Input CVN	Computed CVN	Differential
160	11.0	13.2	-2.22
180	16.0	18.5	-2.54
200	31.0	25.6	5.43
225	40.0	36.4	3.57
250	41.0	48.3	-7.29
275	62.0	59.2	2.77
300	65.0	67.9	-2.86
350	83.0	77.7	5.33

CVGraph 6.02 05/18/2026 Page 2/2

Unirradiated Correlation Monitor Material

CVGraph 6.02: Hyperbolic Tangent Curve Printed on 5/18/2026 3:09 PM

A = 43.69 B = 42.69 C = 84.29 T0 = 76.48 D = 0.00

Equation is A + B * [Tanh((T-T0)/(C+DT))]

Upper Shelf L.E. = 86.37 Lower Shelf L.E. = 1.00 (Fixed)

Temp@35 mils= 59.10° F

Plant: **Diablo Canyon 1** Material: **SA533B1** Heat: **HSST02**

Orientation: **LT** Capsule: **Unirrad** Fluence: **0.00E+000 n/cm²**

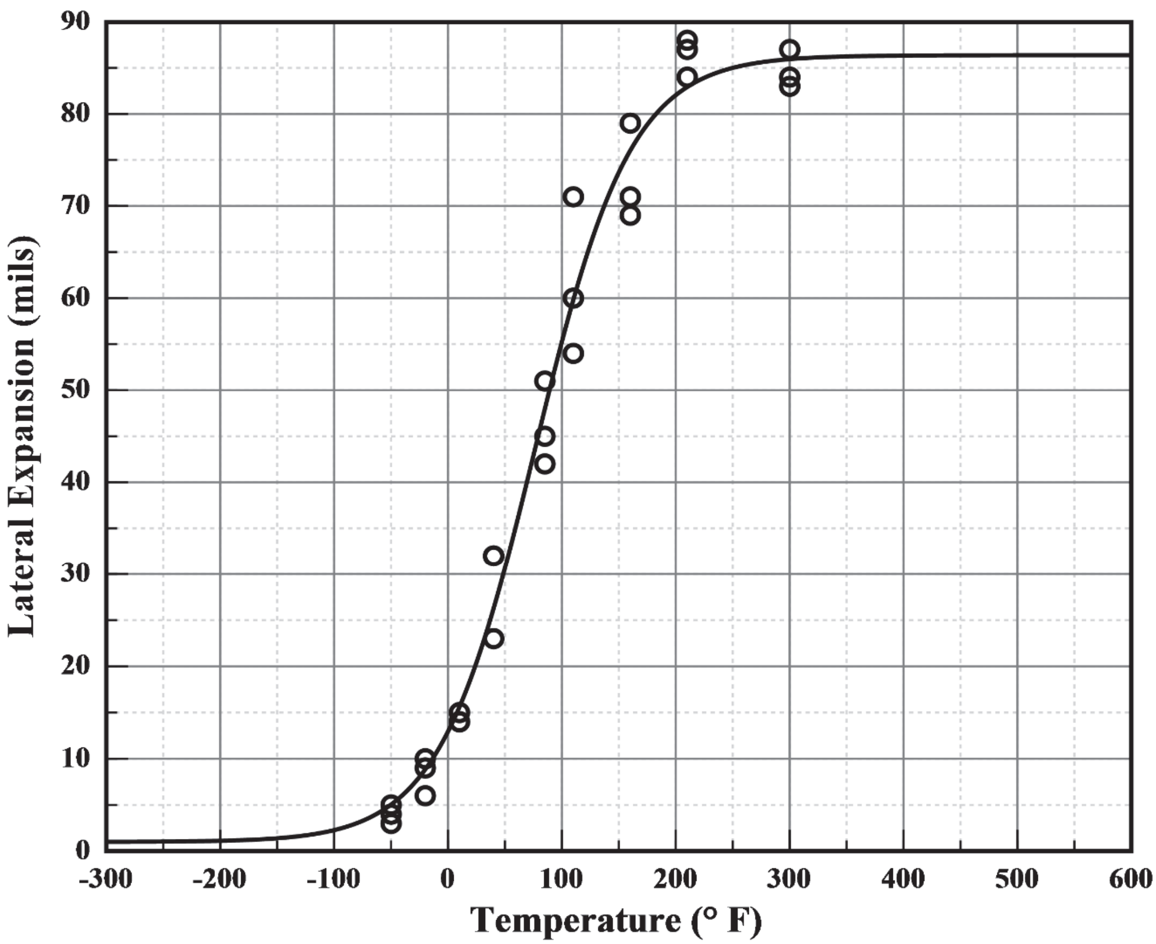

CVGraph 6.02 05/18/2026 Page 1/2

Plant: **Diablo Canyon 1** Material: **SA533B1** Heat: **HSST02**
Orientation: **LT** Capsule: **Unirrad** Fluence: **0.00E+000 n/cm²**

Unirradiated Correlation Monitor Material
Charpy V-Notch Data

Temperature (° F)	Input L. E.	Computed L. E.	Differential
-50	3.0	5.0	-2.05
-50	5.0	5.0	-0.05
-50	4.0	5.0	-1.05
-20	6.0	8.9	-2.86
-20	10.0	8.9	1.14
-20	9.0	8.9	0.14
10	15.0	15.6	-0.61
10	14.0	15.6	-1.61
10	14.0	15.6	-1.61
40	23.0	26.3	-3.29
40	32.0	26.3	5.71
40	32.0	26.3	5.71
85	51.0	48.0	3.01
85	42.0	48.0	-5.99
85	45.0	48.0	-2.99
110	60.0	59.8	0.18
110	71.0	59.8	11.18
110	54.0	59.8	-5.82
160	71.0	76.0	-5.03
160	69.0	76.0	-7.03
160	79.0	76.0	2.97
210	84.0	82.9	1.08
210	88.0	82.9	5.08
210	87.0	82.9	4.08
300	87.0	85.9	1.05
300	83.0	85.9	-2.95
300	84.0	85.9	-1.95

CVGraph 6.02 05/18/2026 Page 2/2

Capsule S Correlation Monitor Material

CVGraph 6.02: Hyperbolic Tangent Curve Printed on 5/28/2026 1:28 PM

A = 43.49 B = 42.49 C = 100.63 T0 = 144.83 D = 0.00

Equation is A + B * [Tanh((T-T0)/(C+DT))]

Upper Shelf L.E. = 85.98 Lower Shelf L.E. = 1.00 (Fixed)

Temp@35 mils=124.50° F

Plant: **Diablo Canyon 1** Material: **SA533B1** Heat: **HSST02**

Orientation: **NA** Capsule: **S** Fluence: **2.93E+018 n/cm²**

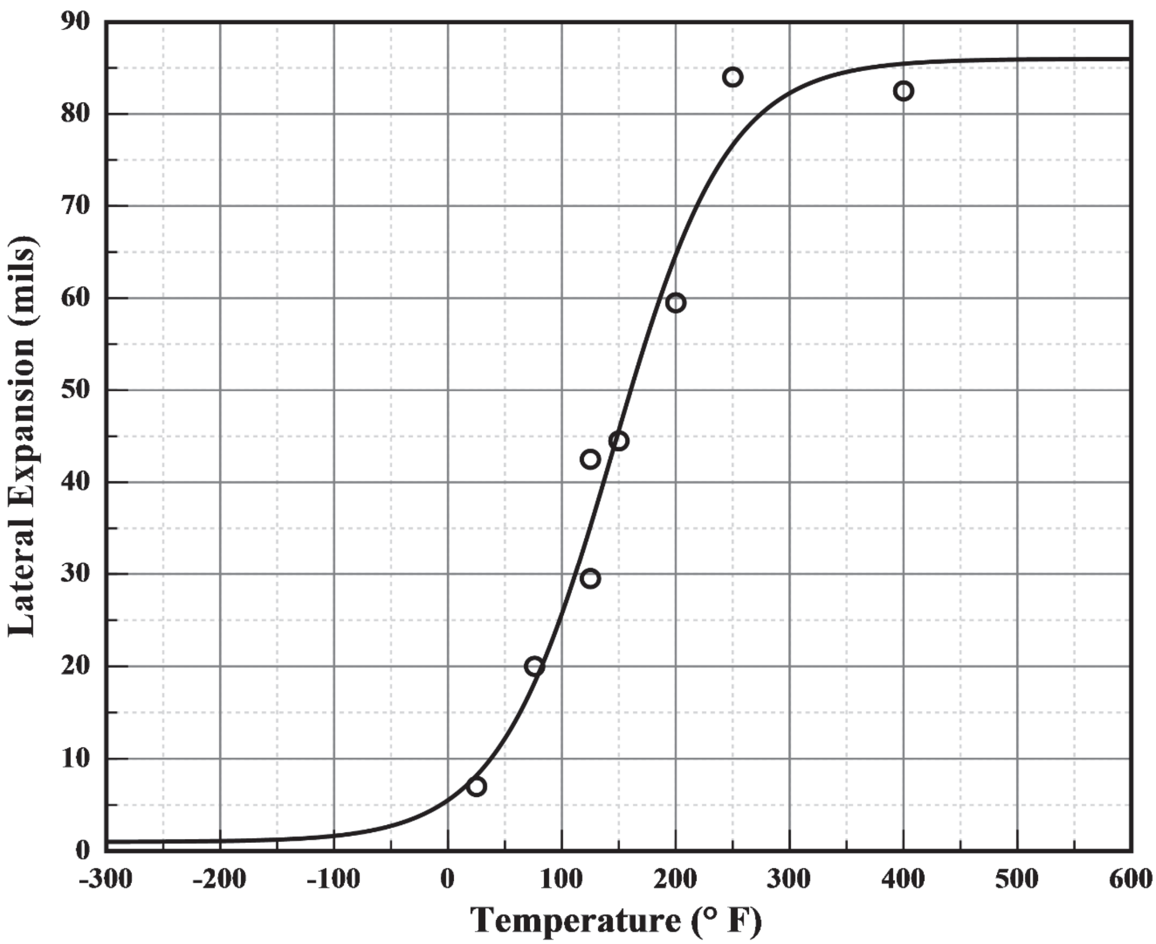

CVGraph 6.02 05/28/2026 Page 1/2

Note: This is a replot of data from a previously tested capsule.

Plant: **Diablo Canyon 1** Material: **SA533B1** Heat: **HSST02**
Orientation: **NA** Capsule: **S** Fluence: **2.93E+018 n/cm²**

Capsule S Correlation Monitor Material

Charpy V-Notch Data

Temperature (° F)	Input L. E.	Computed L. E.	Differential
25	7.0	8.2	-1.19
76	20.0	18.2	1.75
125	42.5	35.2	7.28
125	29.5	35.2	-5.72
150	44.5	45.7	-1.17
200	59.5	64.7	-5.20
250	84.0	76.6	7.37
400	82.5	85.4	-2.95

CVGraph 6.02 05/28/2026 Page 2/2

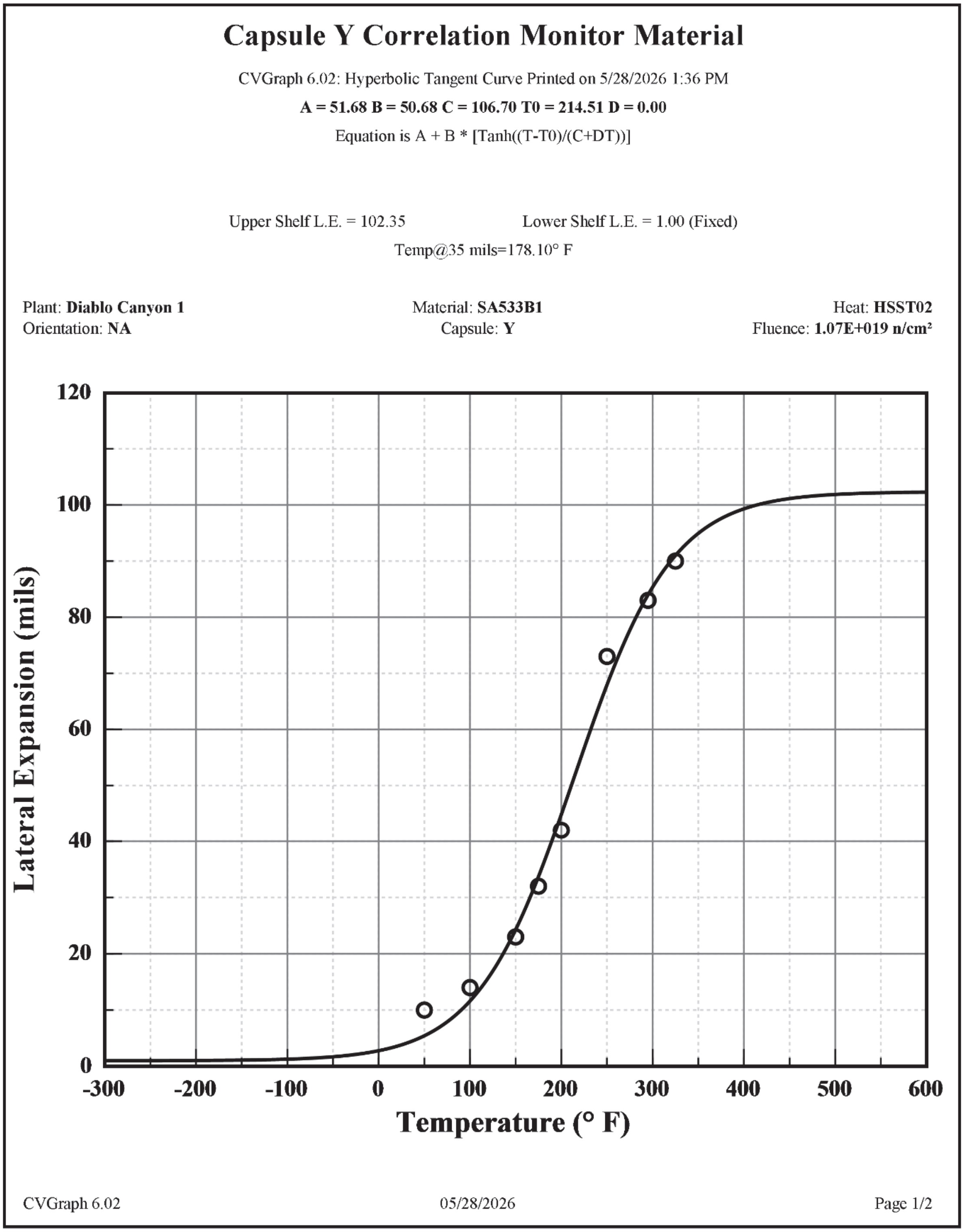

Note: This is a replot of data from a previously tested capsule.

Plant: **Diablo Canyon 1** Material: **SA533B1** Heat: **HSST02**
Orientation: **NA** Capsule: **Y** Fluence: **1.07E+019 n/cm²**

Capsule Y Correlation Monitor Material
Charpy V-Notch Data

Temperature (° F)	Input L. E.	Computed L. E.	Differential
50	10.0	5.4	4.56
100	14.0	11.6	2.39
150	23.0	24.3	-1.30
175	32.0	33.7	-1.73
200	42.0	44.8	-2.83
250	73.0	67.9	5.06
295	83.0	84.0	-1.00
325	90.0	91.0	-1.01

CVGraph 6.02 05/28/2026 Page 2/2

Capsule V Correlation Monitor Material

CVGraph 6.02: Hyperbolic Tangent Curve Printed on 5/29/2026 7:18 AM

A = 52.26 B = 51.26 C = 116.93 T0 = 254.43 D = 0.00

Equation is A + B * [Tanh((T-T0)/(C+DT))]

Upper Shelf L.E. = 103.52 Lower Shelf L.E. = 1.00 (Fixed)

Temp@35 mils=213.50° F

Plant: **Diablo Canyon 1** Material: **SA533B1** Heat: **HSST02**

Orientation: **NA** Capsule: **V** Fluence: **1.35E+019 n/cm²**

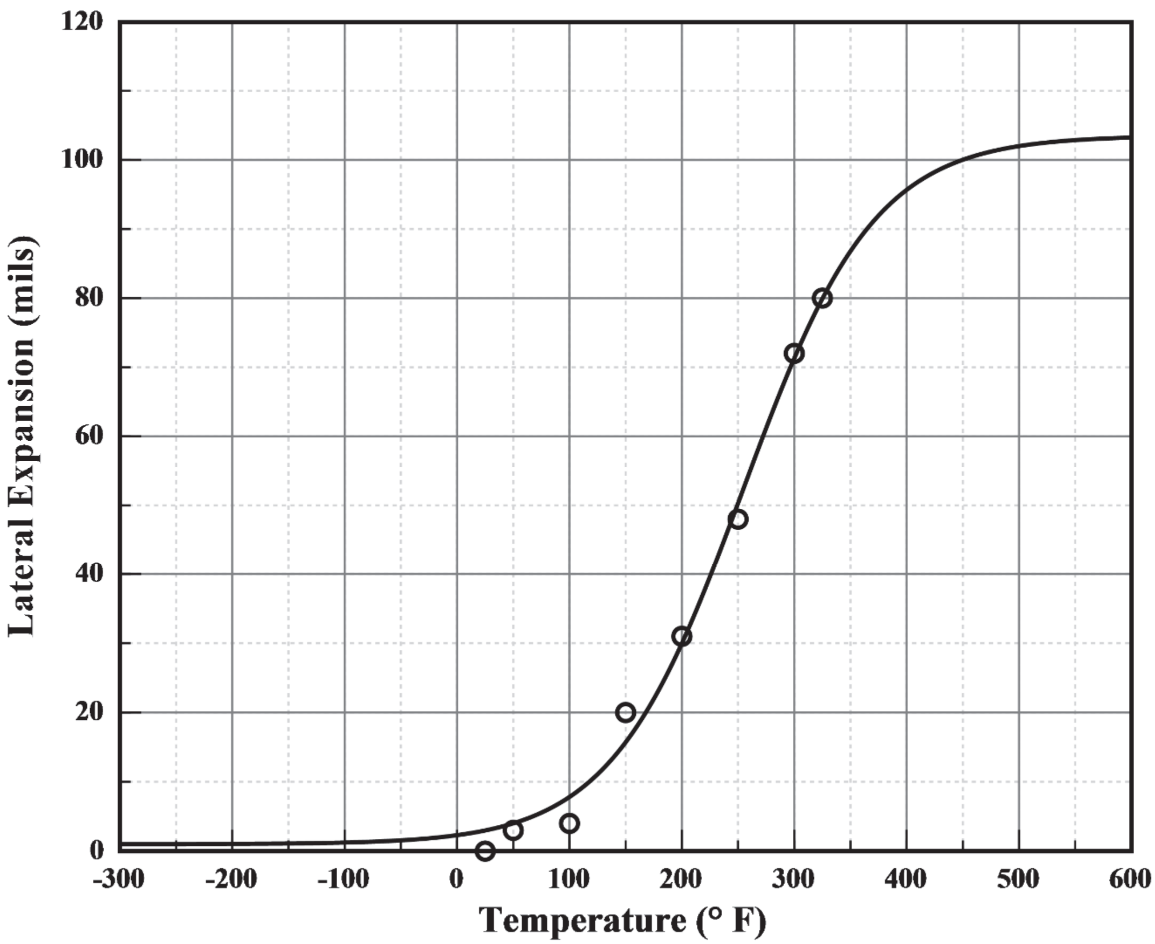

CVGraph 6.02 05/29/2026 Page 1/2

Note: This is a replot of data from a previously tested capsule.

Plant: **Diablo Canyon 1** Material: **SA533B1** Heat: **HSST02**
Orientation: **NA** Capsule: **V** Fluence: **1.35E+019 n/cm²**

Capsule V Correlation Monitor Material
Charpy V-Notch Data

Temperature (° F)	Input L. E.	Computed L. E.	Differential
25	0.0	3.0	-2.99
50	3.0	4.0	-1.02
100	4.0	7.8	-3.82
150	20.0	15.7	4.28
200	31.0	30.0	1.01
250	48.0	50.3	-2.32
300	72.0	71.3	0.72
325	80.0	79.9	0.08

CVGraph 6.02 05/29/2026 Page 2/2

Capsule B Correlation Monitor Material

CVGraph 6.02: Hyperbolic Tangent Curve Printed on 5/18/2026 4:08 PM

A = 35.22 B = 34.22 C = 70.21 T0 = 236.65 D = 0.00

Equation is A + B * [Tanh((T-T0)/(C+DT))]

Upper Shelf L.E. = 69.43 Lower Shelf L.E. = 1.00 (Fixed)

Temp@35 mils=236.20° F

Plant: **Diablo Canyon 1** Material: **SA533B1** Heat: **HSST02**

Orientation: **NA** Capsule: **B** Fluence: **3.62E+019 n/cm²**

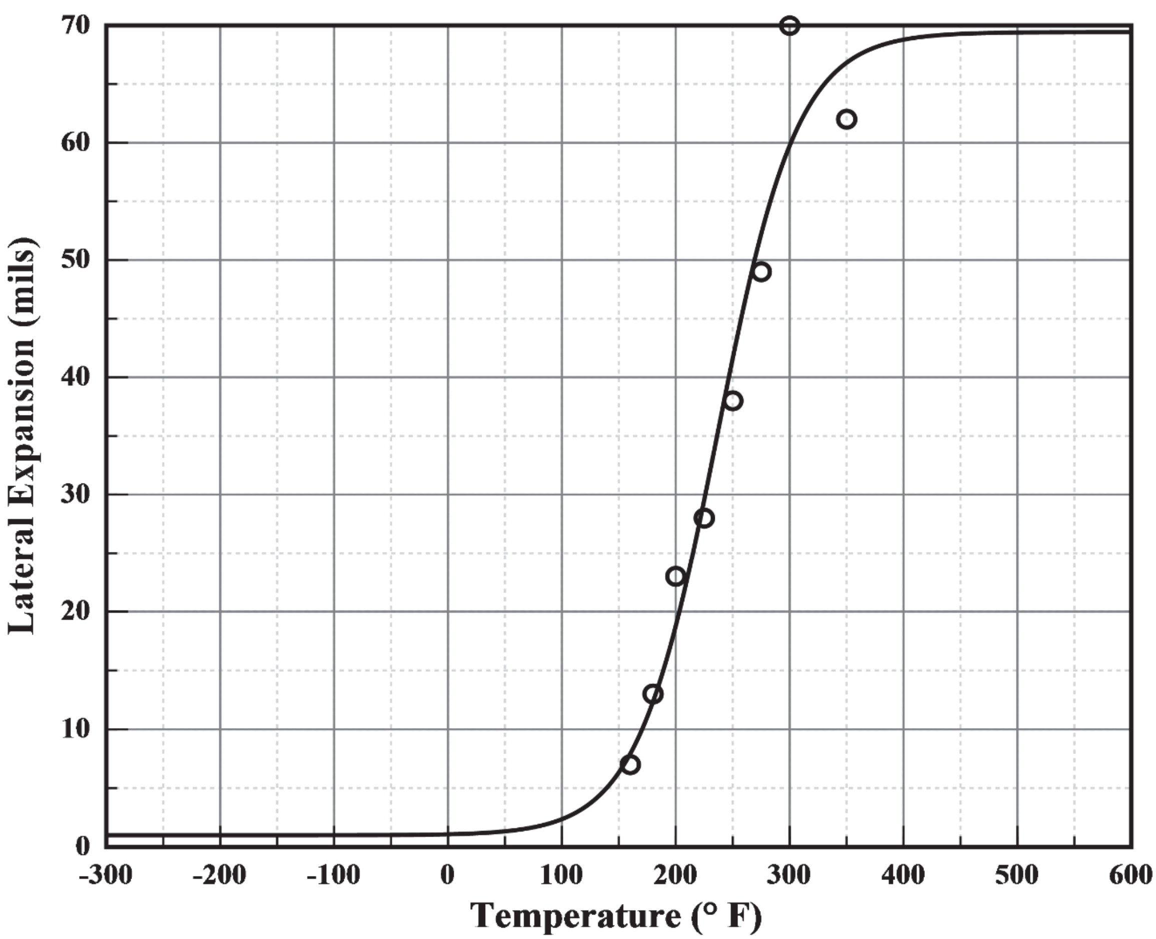

CVGraph 6.02 05/18/2026 Page 1/2

Plant: **Diablo Canyon 1** Material: **SA533B1** Heat: **HSST02**
Orientation: **NA** Capsule: **B** Fluence: **3.62E+019 n/cm²**

Capsule B Correlation Monitor Material
Charpy V-Notch Data

Temperature (° F)	Input L. E.	Computed L. E.	Differential
160	7.0	7.9	-0.93
180	13.0	12.4	0.64
200	23.0	18.8	4.18
225	28.0	29.6	-1.59
250	38.0	41.6	-3.64
275	49.0	52.2	-3.24
300	70.0	59.8	10.24
350	62.0	66.8	-4.82

CVGraph 6.02 05/18/2026 Page 2/2

Unirradiated Correlation Monitor Material

CVGraph 6.02: Hyperbolic Tangent Curve Printed on 5/18/2026 3:10 PM

A = 50.00 B = 50.00 C = 100.78 T0 = 85.68 D = 0.00

Equation is A + B * [Tanh((T-T0)/(C+DT))]

Upper Shelf %Shear = 100.00 (Fixed) Lower Shelf %Shear = 0.00 (Fixed)

Temperature at 50% Shear = 85.70

Plant: **Diablo Canyon 1** Material: **SA533B1** Heat: **HSST02**

Orientation: **LT** Capsule: **Unirrad** Fluence: **0.00E+000 n/cm²**

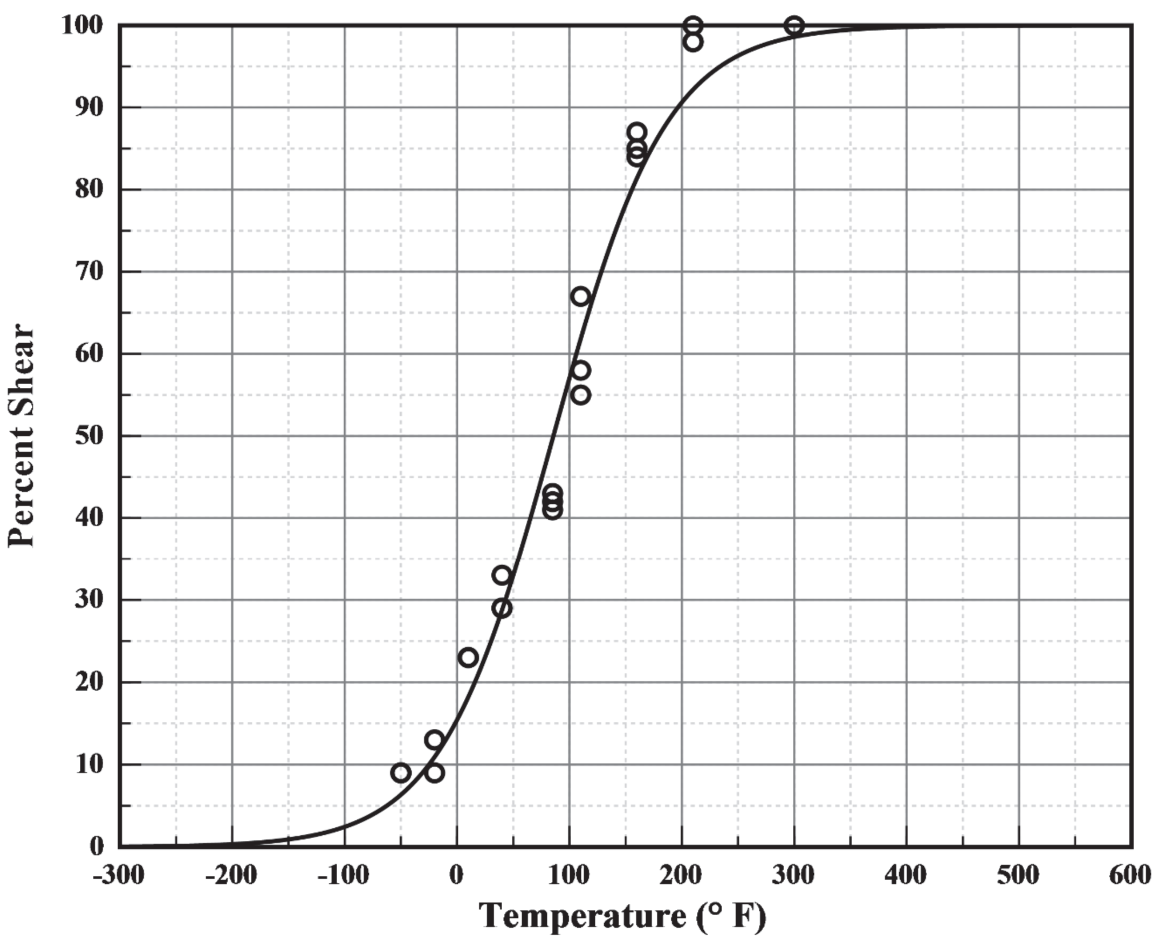

CVGraph 6.02 05/18/2026 Page 1/2

Plant: **Diablo Canyon 1** Material: **SA533B1** Heat: **HSST02**
Orientation: **LT** Capsule: **Unirrad** Fluence: **0.00E+000 n/cm²**

Unirradiated Correlation Monitor Material
Charpy V-Notch Data

Temperature (° F)	Input %Shear	Computed %Shear	Differential
-50	9.0	6.3	2.66
-50	9.0	6.3	2.66
-50	9.0	6.3	2.66
-20	9.0	10.9	-1.94
-20	13.0	10.9	2.06
-20	13.0	10.9	2.06
10	23.0	18.2	4.79
10	23.0	18.2	4.79
10	23.0	18.2	4.79
40	33.0	28.8	4.23
40	29.0	28.8	0.23
40	29.0	28.8	0.23
85	43.0	49.7	-6.66
85	41.0	49.7	-8.66
85	42.0	49.7	-7.66
110	58.0	61.8	-3.84
110	67.0	61.8	5.16
110	55.0	61.8	-6.84
160	84.0	81.4	2.62
160	85.0	81.4	3.62
160	87.0	81.4	5.62
210	98.0	92.2	5.82
210	98.0	92.2	5.82
210	100.0	92.2	7.82
300	100.0	98.6	1.40
300	100.0	98.6	1.40
300	100.0	98.6	1.40

CVGraph 6.02 05/18/2026 Page 2/2

Capsule S Correlation Monitor Material

CVGraph 6.02: Hyperbolic Tangent Curve Printed on 5/28/2026 1:30 PM

A = 50.00 B = 50.00 C = 89.95 T0 = 157.59 D = 0.00

Equation is A + B * [Tanh((T-T0)/(C+DT))]

Upper Shelf %Shear = 100.00 (Fixed) Lower Shelf %Shear = 0.00 (Fixed)

Temperature at 50% Shear = 157.60

Plant: **Diablo Canyon 1** Material: **SA533B1** Heat: **HSST02**

Orientation: **NA** Capsule: **S** Fluence: **2.93E+018 n/cm²**

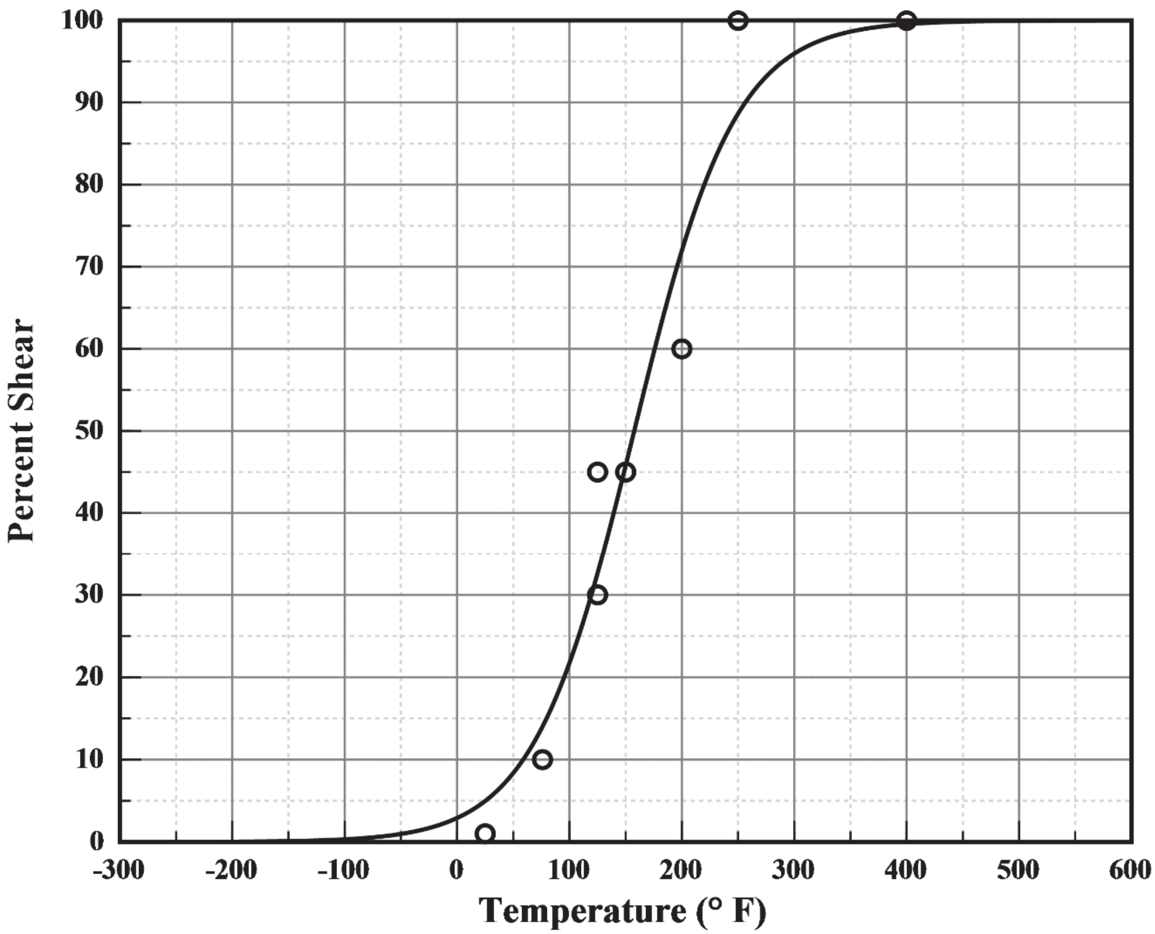

CVGraph 6.02 05/28/2026 Page 1/2

Note: This is a replot of data from a previously tested capsule.

Plant: **Diablo Canyon 1** Material: **SA533B1** Heat: **HSST02**
Orientation: **NA** Capsule: **S** Fluence: **2.93E+018 n/cm²**

Capsule S Correlation Monitor Material
Charpy V-Notch Data

Temperature (° F)	Input %Shear	Computed %Shear	Differential
25	1.0	5.0	-3.98
76	10.0	14.0	-4.01
125	45.0	32.6	12.36
125	30.0	32.6	-2.64
150	45.0	45.8	-0.79
200	60.0	72.0	-11.97
250	100.0	88.6	11.36
400	100.0	99.5	0.45

CVGraph 6.02 05/28/2026 Page 2/2

Capsule Y Correlation Monitor Material

CVGraph 6.02: Hyperbolic Tangent Curve Printed on 5/28/2026 1:36 PM

A = 50.00 B = 50.00 C = 67.42 T0 = 188.32 D = 0.00

Correlation Coefficient = 0.988

Equation is A + B * [Tanh((T-T0)/(C+DT))]

Upper Shelf %Shear = 100.00 (Fixed) Lower Shelf %Shear = 0.00 (Fixed)

Temperature at 50% Shear = 188.40

Plant: **Diablo Canyon 1** Material: **SA533B1** Heat: **HSST02**

Orientation: **NA** Capsule: **Y** Fluence: **1.07E+019 n/cm²**

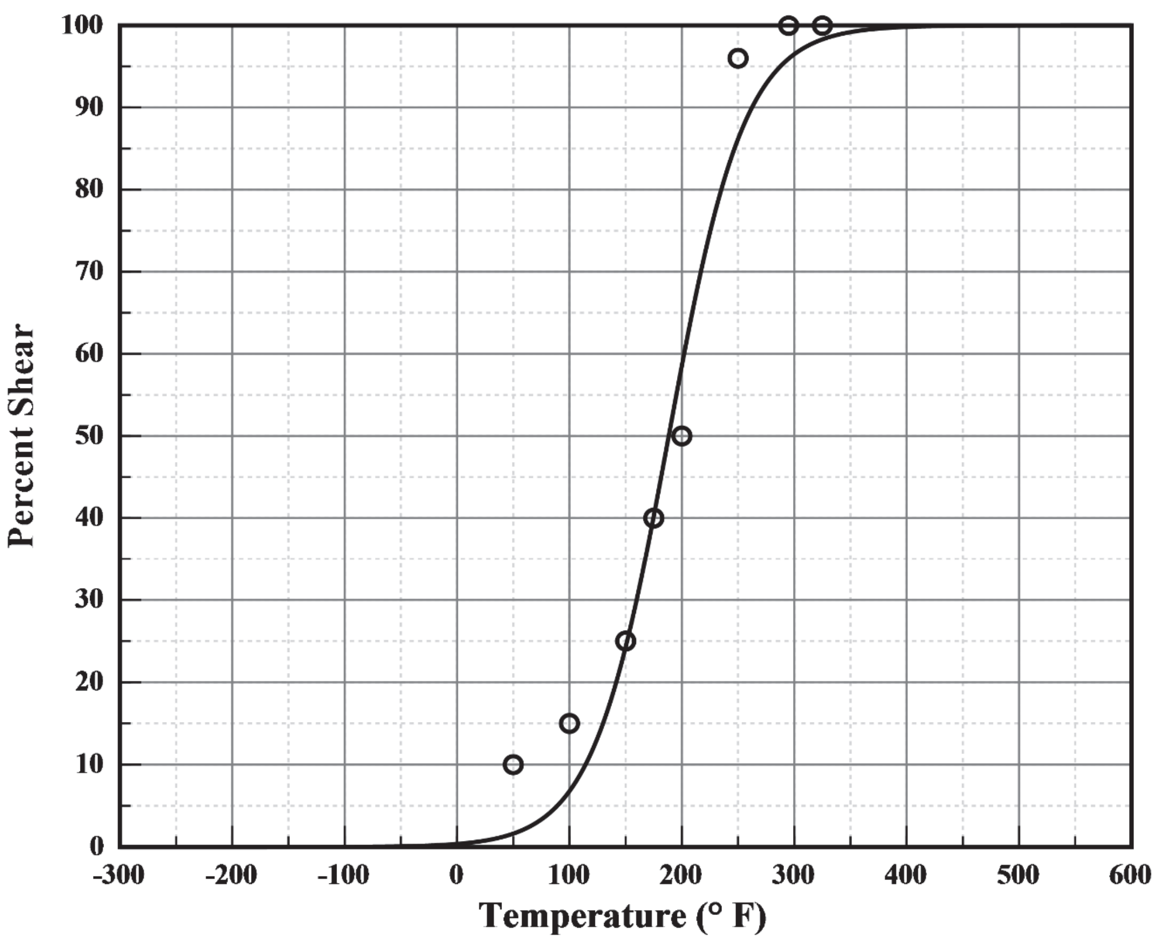

CVGraph 6.02 05/28/2026 Page 1/2

Note: This is a replot of data from a previously tested capsule.

Plant: **Diablo Canyon 1** Material: **SA533B1** Heat: **HSST02**
Orientation: **NA** Capsule: **Y** Fluence: **1.07E+019 n/cm²**

Capsule Y Correlation Monitor Material
Charpy V-Notch Data

Temperature (° F)	Input %Shear	Computed %Shear	Differential
50	10.0	1.6	8.38
100	15.0	6.8	8.21
150	25.0	24.3	0.71
175	40.0	40.2	-0.25
200	50.0	58.6	-8.58
250	96.0	86.2	9.83
295	100.0	95.9	4.05
325	100.0	98.3	1.70

CVGraph 6.02 05/28/2026 Page 2/2

Capsule V Correlation Monitor Material

CVGraph 6.02: Hyperbolic Tangent Curve Printed on 5/28/2026 1:41 PM

A = 50.00 B = 50.00 C = 98.27 T0 = 203.44 D = 0.00

Equation is A + B * [Tanh((T-T0)/(C+DT))]

Upper Shelf %Shear = 100.00 (Fixed) Lower Shelf %Shear = 0.00 (Fixed)

Temperature at 50% Shear = 203.50

Plant: **Diablo Canyon 1** Material: **SA533B1** Heat: **HSST02**

Orientation: **NA** Capsule: **V** Fluence: **1.35E+019 n/cm²**

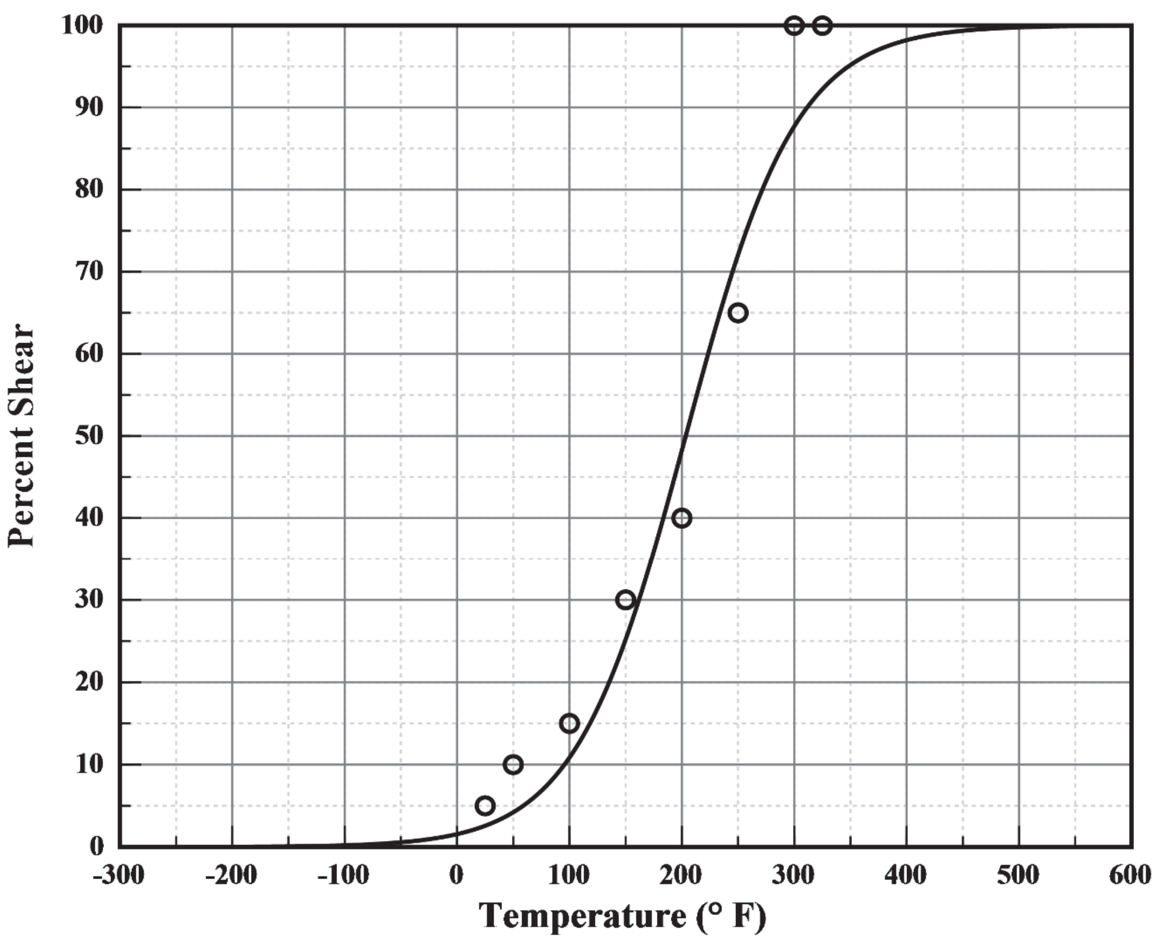

CVGraph 6.02 05/28/2026 Page 1/2

Note: This is a replot of data from a previously tested capsule.

Plant: **Diablo Canyon 1** Material: **SA533B1** Heat: **HSST02**
Orientation: **NA** Capsule: **V** Fluence: **1.35E+019 n/cm²**

Capsule V Correlation Monitor Material
Charpy V-Notch Data

Temperature (° F)	Input %Shear	Computed %Shear	Differential
25	5.0	2.6	2.42
50	10.0	4.2	5.78
100	15.0	10.9	4.14
150	30.0	25.2	4.79
200	40.0	48.2	-8.25
250	65.0	72.1	-7.06
300	100.0	87.7	12.29
325	100.0	92.2	7.77

CVGraph 6.02 05/28/2026 Page 2/2

Capsule B Correlation Monitor Material

CVGraph 6.02: Hyperbolic Tangent Curve Printed on 5/18/2026 4:09 PM

A = 50.00 B = 50.00 C = 90.49 T0 = 249.75 D = 0.00

Equation is A + B * [Tanh((T-T0)/(C+DT))]

Upper Shelf %Shear = 100.00 (Fixed) Lower Shelf %Shear = 0.00 (Fixed)

Temperature at 50% Shear = 249.80

Plant: **Diablo Canyon 1** Material: **SA533B1** Heat: **HSST02**

Orientation: **NA** Capsule: **B** Fluence: **3.62E+019 n/cm²**

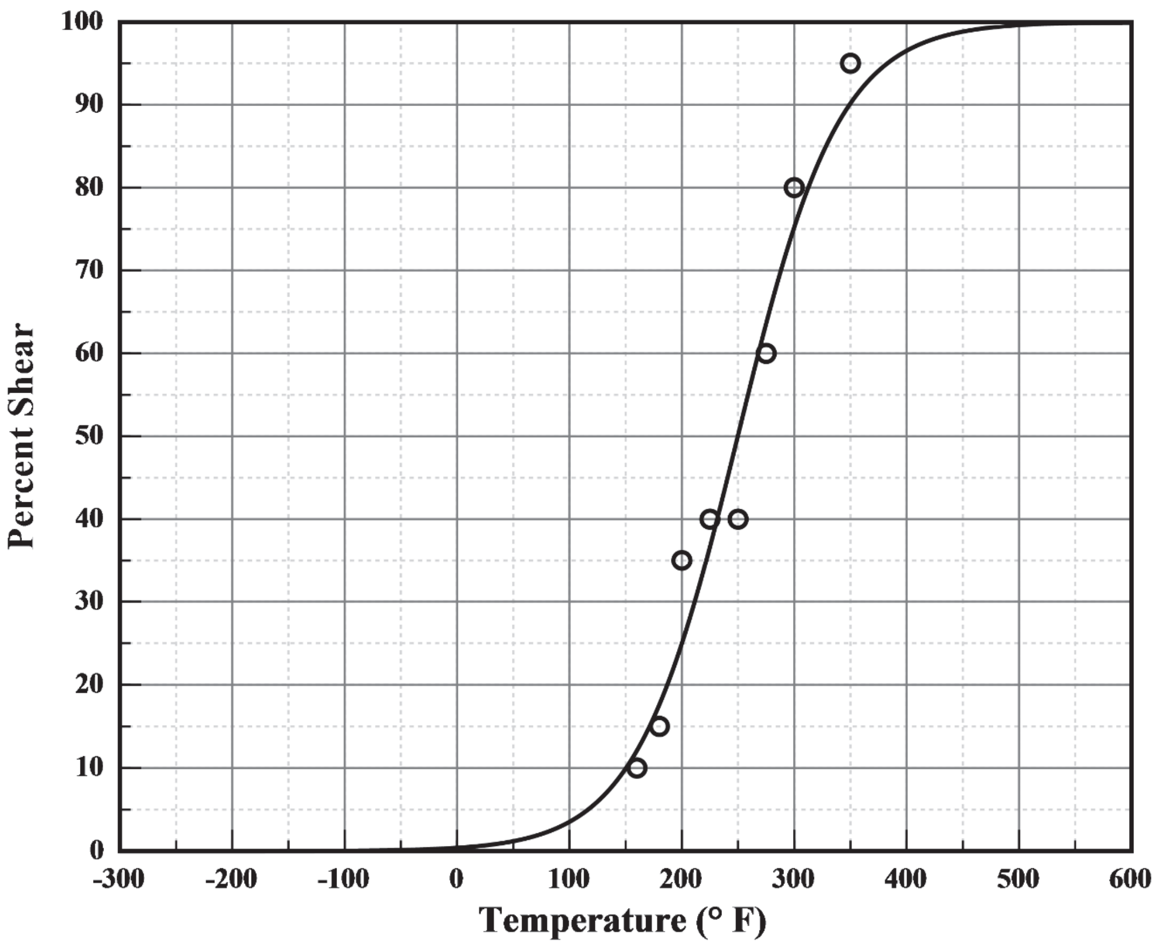

CVGraph 6.02 05/18/2026 Page 1/2

Plant: **Diablo Canyon 1** Material: **SA533B1** Heat: **HSST02**
Orientation: **NA** Capsule: **B** Fluence: **3.62E+019 n/cm²**

Capsule B Correlation Monitor Material
Charpy V-Notch Data

Temperature (° F)	Input %Shear	Computed %Shear	Differential
160	10.0	12.1	-2.09
180	15.0	17.6	-2.63
200	35.0	25.0	10.02
225	40.0	36.7	3.34
250	40.0	50.1	-10.14
275	60.0	63.6	-3.60
300	80.0	75.2	4.78
350	95.0	90.2	4.83

CVGraph 6.02 05/18/2026 Page 2/2

APPENDIX D DIABLO CANYON UNIT 1 SURVEILLANCE PROGRAM CREDIBILITY EVALUATION

D.1 INTRODUCTION

Regulatory Guide 1.99, Revision 2 [D-1] describes general procedures acceptable to the NRC staff for calculating the effects of neutron radiation embrittlement of the low-alloy steels currently used for light-water-cooled reactor vessels. Positions 2.1 and 2.2 of Regulatory Guide 1.99, Revision 2, describe the method for calculating the adjusted reference temperature and Charpy upper-shelf energy of reactor vessel beltline materials using surveillance capsule data. The methods of Positions 2.1 and 2.2 can only be applied when two or more surveillance data sets become available from the reactor in question.

To date, there have been four surveillance capsules removed from the Diablo Canyon Unit 1 reactor vessel. To use these surveillance data sets, the credibility must be determined. In accordance with Regulatory Guide 1.99, Revision 2, the credibility of the surveillance data will be judged based on five criteria.

Table D-1 provides the five criteria in Regulatory Guide 1.99, Revision 2. The following subsections evaluate each of these five criteria for Diablo Canyon Unit 1 to determine the credibility of the surveillance data for use in neutron radiation embrittlement calculations.

Table D-1 Regulatory Guide 1.99, Rev. 2, Credibility Criteria

Criterion No.	Description
1	Materials in the capsules should be those judged most likely to be controlling with regard to radiation embrittlement.
2	Scatter in the plots of Charpy energy versus temperature for the irradiated and unirradiated conditions should be small enough to permit the determination of the 30 ft-lb temperature and upper-shelf energy unambiguously.
3	When there are two or more sets of surveillance data from one reactor, the scatter of ΔRT_{NDT} values about a best-fit line drawn as described in Regulatory Position 2.1 normally should be less than 28°F for welds and 17°F for base metal. Even if the fluence range is large (two or more orders of magnitude), the scatter should not exceed twice those values. Even if the data fail this criterion for use in shift calculations, they may be credible for determining decrease in upper-shelf energy if the upper shelf can be clearly determined, following the definition given in ASTM E185-82.
4	The irradiation temperature of the Charpy specimens in the capsule should match the vessel wall temperature at the cladding/base metal interface within +/- 25°F.
5	The surveillance data for the correlation monitor material in the Capsule should fall within the scatter band of the database for that material.

D.2 EVALUATION

Criterion 1: Materials in the capsules should be those judged most likely to be controlling with regard to radiation embrittlement.

The beltline region of the reactor vessel is defined in Appendix G to 10 CFR Part 50, "Fracture Toughness Requirements" [D-2], as follows:

> *"the region of the reactor vessel (shell material including welds, heat affected zones, and plates or forgings) that directly surrounds the effective height of the active core and adjacent regions of the reactor vessel that are predicted to experience sufficient neutron radiation damage to be considered in the selection of the most limiting material with regard to radiation damage."*

The Diablo Canyon Unit 1 reactor vessel beltline region consists of the following materials:

- Intermediate Shell Plates B4106-1, B4106-2, B4106-3
- Lower Shell Plates B4107-1, B4107-2, B4107-3
- Intermediate Shell Longitudinal Weld Seams 2-442 A, B, and C (Heat # 27204, Linde 1092 Flux, Lot # 3724)
- Intermediate Shell to Lower Shell Circumferential Weld Seam 9-442 (Heat # 21935, Linde 1092 Flux, Lot # 3869)
- Lower Shell Longitudinal Weld Seams 3-442 A, B, and C (Heat # 27204, Linde 1092 Flux, Lot # 3774)

The initial surveillance program developed in WCAP-8465 [D-3], was based on the guidance in ASTM E185-70. At the time the program was developed, the Intermediate Shell Plates were identified as the most limiting base metal; therefore, specimens from each Intermediate Shell Plate were included. The capsules previously removed and tested contained only Intermediate Shell Plate B4106-3 material, which was considered limiting at the time based on its low initial upper shelf energy and high initial RT_{NDT}. This initial surveillance program was supplemented as documented in WCAP-13440 [D-4] to provide embrittlement data for a period beyond that intended by the original program. The supplemental surveillance program includes base metal specimens from Lower Shell Plate B4107-1, which was identified as the limiting beltline plate as the vessel experiences higher fluences.

The weld metal in the initial surveillance program was fabricated using weld wire Heat # 27204 with Linde 1092 Flux, Lot # 3714, which is the same wire heat as the reactor vessel Intermediate Shell and Lower Shell longitudinal weld seams. This represents six of the seven beltline welds. The seventh weld, the Intermediate to Lower Shell circumferential weld, was fabricated using Heat # 21935, which has higher initial upper shelf energy and lower copper content; therefore, Heat # 27204 was selected as the surveillance weld. The supplemental surveillance program, documented in WCAP-13440 [D-4], includes additional weld specimens. These include surrogate weld specimens of Heat # 27204 and Linde 1092 Flux, Lot # 3714, provided by ABB / Combustion Engineering, and specimens reconstituted from previous irradiated and tested specimens from Capsule S. ASTM E185-70 [D-8] only requires that the surveillance material be representative of welds in the irradiated region. Since the surveillance weld fabricated from the same heat and flux type as the Intermediate Shell and Lower Shell longitudinal reactor vessel welds, Criterion 1 is satisfied for the Diablo Canyon Unit 1 surveillance program.

Hence, Criterion 1 is met for the Diablo Canyon Unit 1 surveillance program.

Criterion 2: Scatter in the plots of Charpy energy versus temperature for the irradiated and unirradiated conditions should be small enough to permit the determination of the 30 ft-lb temperature and upper-shelf energy unambiguously.

Plots of Charpy energy versus temperature for the unirradiated and irradiated conditions are presented in Appendix C.

Based on engineering judgment, the scatter in the data presented in these plots, as documented in Section 5 and Appendix C, is small enough to permit the determination of the 30 ft-lb temperature and the upper-shelf energy of the Diablo Canyon Unit 1 surveillance materials unambiguously.

Hence, Criterion 2 is met for the Diablo Canyon Unit 1 surveillance program.

Criterion 3: When there are two or more sets of surveillance data from one reactor, the scatter of ΔRT_{NDT} values about a best-fit line drawn as described in Regulatory Position 2.1 normally should be less than 28°F for welds and 17°F for base metal. Even if the fluence range is large (two or more orders of magnitude), the scatter should not exceed twice those values. Even if the data fail this criterion for use in shift calculations, they may be credible for determining decrease in upper-shelf energy if the upper shelf can be clearly determined, following the definition given in ASTM E185-82.

The functional form of the least squares method as described in Regulatory Position 2.1 will be utilized to determine a best-fit line for this data and to determine if the scatter of these ΔRT_{NDT} values about this line is less than 28°F for welds and less than 17°F for the plates.

Following is the calculation of the best-fit line as described in Regulatory Position 2.1 of Regulatory Guide 1.99, Revision 2. The NRC methods were presented to the industry at a meeting held by the NRC on February 12 and 13, 1998 [D-6]. At this meeting the NRC presented five cases. Of the five cases, Case 4 ("Surveillance Data from Plant and Other Sources") most closely represents the situation for the Diablo Canyon Unit 1 weld.

This evaluation excludes the data from Lower Shell Plate B4107-1 and Intermediate Shell Plate B4106-3. Lower Shell Plate B4107-1 is not included because the credibility evaluation requires two or more surveillance data sets of shifts in reference temperature (ΔRT_{NDT}). Since the only available data set is from Capsule B, there is insufficient data to determine credibility, and the surveillance data will not be used to perform embrittlement projections for Lower Shell Plate B4107-1. Intermediate Shell Plate B4106-3 is not included because Capsule B did not contain any additional data for it; therefore, the credibility conclusion in WCAP-18924-NP [D-9], which identifies the Intermediate Shell Plate B4106-3 data as non-credible, remains unchanged.

Heat # 27204: Evaluation of Diablo Canyon Unit 1 Data and Palisades Data (Case 4)

This weld heat pertains to Intermediate Shell and Lower Shell Longitudinal welds in the Diablo Canyon Unit 1 reactor vessel. This weld heat is contained in the Diablo Canyon Unit 1 surveillance weld as well as the Palisades surveillance weld and the surrogate weld. NRC Case 4 most closely represents the situation for Diablo Canyon Unit 1 weld Heat # 27204.

Following the NRC Case 1 ("Surveillance Data Available from Plant but No Other Source") guidelines, the Diablo Canyon Unit 1 weld (Heat # 27204) will be evaluated using Diablo Canyon Unit 1 surveillance weld data only. First, the interim chemistry factor is calculated with an adjusted factor due to the mean operating temperature for the surveillance capsules. The mean operating temperature of the Diablo Canyon Unit 1 surveillance capsules is calculated in Table D-2. The mean operating temperature is then subtracted from the temperature during each period of operation to obtain the capsule-specific temperature adjustments as shown in Table D-2.

Table D-2 Mean Operating Temperature for Diablo Canyon Unit 1

Capsule	Inlet Temperature during Period of Irradiation (°F)	Temperature Adjustment (°F)
S	544.0	2.4
Y	541.6	0.0
V	541.1	-0.5
B	539.6	-2.0
MEAN	541.6	-

These temperature adjustments are applied to the Diablo Canyon Unit 1 surveillance material ΔRT_{NDT} values in Table D-3 to account for variations in capsule irradiation temperature. The adjustments normalize the surveillance results to a common temperature basis, thereby ensuring that differences in ΔRT_{NDT} values reflect material behavior and irradiation exposure rather than variations in irradiation temperature.

Table D-3 Calculation of Interim Chemistry Factors for the Credibility Evaluation Using Diablo Canyon Unit 1 Surveillance Weld Data Only

Material	Capsule	Capsule Fluence(1) (x 10^{19} n/cm^2, E > 1.0 MeV)	FF(2)	Adjusted (Measured) ΔRT_{NDT}(3) (°F)	FF*ΔRT_{NDT} (°F)	FF^2
Surveillance Welds (Heat # 27204)	S	0.293	0.664	112.5 (110.1)	74.72	0.441
	Y	1.07	1.019	232.0 (232.0)	236.39	1.038
	V	1.35	1.083	199.8 (200.2)	216.47	1.174
	B	3.913(4)	1.351	306.7 (308.7)	414.49	1.826
				SUM:	941.96	4.480
	$CF_{Heat\ \#\ 27204} = \Sigma(FF * \Delta RT_{NDT}) \div \Sigma(FF^2) = (941.96) \div (4.480) =$ **210.3°F**					

Notes:

1. Fluence taken from Table 6-2.
2. FF = Fluence Factor = $f^{(0.28 - 0.10*\log(f))}$.
3. Measured ΔRT_{NDT} taken from Table 5-10. These measured ΔRT_{NDT} values for the surveillance weld do not include the adjustment ratio procedure of Regulatory Guide 1.99, Revision 2, Position 2.1 [D-1] since data are for the samples of the same weld. However, as shown in Table D-2, the Diablo Canyon Unit 1 surveillance capsules were irradiated at different temperatures. Therefore, the ΔRT_{NDT} values are adjusted by the temperature adjustment values summarized in Table D-3. Pre-adjusted values are listed in parentheses.
4. The surveillance weld specimens are reconstituted tested specimens previously irradiated in Capsule S. The fluence is the sum of the fluences of Capsule S (0.293E+19 n/cm^2) and Capsule B (3.62E+19 n/cm^2).

The scatter of ΔRT_{NDT} values about the functional form of a best-fit line drawn as described in Regulatory Position 2.1 is presented in Table D-4.

Table D-4 Best-Fit Evaluation for Diablo Canyon Unit 1 Surveillance Weld Only

Material	Capsule	CF(1) (°F)	Capsule Fluence(2) (x 10^{19} /cm^2, E > 1.0 MeV)	FF(3)	Adjusted ΔRT_{NDT}(4) (°F)	Predicted ΔRT_{NDT}(5) (°F)	Scatter ΔRT_{NDT}(6) (°F)	< 28°F (Weld)
Surveillance Welds (Heat # 27204)	S	210.3	0.293	0.664	112.5	139.7	27.2	Yes
	Y	210.3	1.07	1.019	232	214.3	17.7	Yes
	V	210.3	1.35	1.083	199.8	227.8	28.1	No
	B	210.3	3.913	1.351	306.7	284.2	22.5	Yes

Notes:

1. CF calculated in Table D-3.
2. Fluence taken from Table D-3.
3. FF = fluence factor = $f^{(0.28 - 0.10*\log(f))}$.
4. Measured ΔRT_{NDT} taken from Table D-3.
5. Predicted ΔRT_{NDT} = CF x FF.
6. Scatter ΔRT_{NDT} = Absolute Value [Predicted ΔRT_{NDT} – Adjusted ΔRT_{NDT}].

The scatter of ΔRT_{NDT} values about the best-fit line, drawn as described in Regulatory Guide 1.99, Rev. 2, Position 2.1 should be less than 28°F for welds. From a statistical point of view, +/-1σ would be expected to encompass 68% of the data. Table D-4 indicates that three of the four (75%) surveillance data points falls inside the +/-1σ of 28°F scatter band for surveillance welds; therefore, the weld (Heat # 27204) data are deemed "credible" when solely considering the Diablo Canyon surveillance weld. Furthermore, the surveillance weld will be evaluated using the surrogate and Palisades surveillance weld data to determine if it is credible when considering all available data.

Weld Heat # 27204 (All data)

In accordance with the NRC Case 4 guidelines, the data from Diablo Canyon Unit 1 and Palisades will now be analyzed together. The values are adjusted to the mean chemical composition and operating temperature of the surveillance capsules to obtain the capsule-specific temperature adjustments as shown in Table D-5.

Table D-5 Mean Chemical Composition and Operating Temperature Adjustments for Weld Heat # 27204 for Diablo Canyon Unit 1 and Palisades

Material	Capsule	Cu(1) (Wt. %)	Ni(1) (Wt. %)	Inlet Temperature During Irradiation(2) (°F)	Temperature Adjustment(3) (°F)
Surrogate Weld (Heat # 27204) (Diablo Canyon Unit 1)	B	0.220	1.000	539.6	0.1
Surveillance Weld (Heat # 27204) (Diablo Canyon Unit 1 Data)	S	0.198	0.999	544.0	4.5
	Y	0.198	0.999	541.6	2.1
	V	0.198	0.999	541.1	1.6
	B	0.198	0.999	539.6	0.1
Surveillance Weld Heat # 27204 (Palisades Data)	SA-60-1	0.194	1.067	535.0	-4.5
	SA-240-1	0.194	1.067	535.7	-3.8
Mean Values	-	0.200	1.019	539.5	-
Chemistry Factor(4)		225.1			

Notes:
1. Weight percent Cu and Ni for Diablo Canyon Unit 1 taken from Table 4-1. Weight percent Cu and Ni for Palisades taken from WCAP-19077-NP [D-10].
2. Inlet temperature for Diablo Canyon Unit 1 taken from Table D-2. Inlet temperature for Palisades taken from WCAP-19077-NP [D-10].
3. Temperature Adjustment = Inlet Temperature - Mean Operating Temperature.
4. Regulatory Guide 1.99, Revision 2 [D-1] Position 1.1 Chemistry Factor calculated using the average chemistry for the surveillance weld (Heat # 27204).

The Diablo Canyon Unit 1 and Palisades surveillance capsule data will be adjusted to the mean chemical composition and operating temperature calculated in Table D-5. The ratio procedure is used to account for differences in the surveillance weld chemistry and the beltline weld chemistry as follows:

<u>Diablo Canyon Unit 1 Surrogate Weld Data</u>

$CF_{MeanChemistry}$	=	225.1°F	(calculated per Table 1 of Regulatory Guide 1.99, Revision 2 using Cu Wt. % = 0.200 and Ni Wt. % = 1.019 per Table D-5)
$CF_{Surr.. Weld (Diablo Canyon Unit 1)}$	=	232.0°F	(Cu Wt. % = 0.22 and Ni Wt. % = 1.0)
Ratio = 225.1 ÷ 232.0	=	0.97	(applied to Diablo Canyon Unit 1 surrogate weld data for weld Heat # 27204 in the credibility evaluation)

<u>Diablo Canyon Unit 1 Surveillance Weld Data</u>

$CF_{MeanChemistry}$	=	225.1°F	
$CF_{Surv. Weld (Diablo Canyon Unit 1)}$	=	222.3°F	(Cu Wt. % = 0.198 and Ni Wt. % = 0.999)
Ratio = 225.1 ÷ 222.3	=	1.01	(applied to Diablo Canyon Unit 1 surveillance weld data for weld Heat # 27204 in the credibility evaluation)

<u>Palisades Data</u>

$CF_{MeanChemistry}$	=	225.1°F	
$CF_{Surv. Weld (Palisades)}$	=	227.8°F	(Cu Wt. % = 0.194 and Ni Wt. % = 1.067)
Ratio = 225.1 ÷ 227.8	=	0.99	(applied to Palisades surveillance data for weld Heat # 27204 in the credibility evaluation)

Using the chemical composition and operating temperature adjustments described and calculated above, an interim chemistry factor is calculated for weld Heat # 27204 using the Diablo Canyon Unit 1 and Palisades data. This calculation is shown in Table D-6.

Table D-6 Calculation of Interim Chemistry Factors for the Credibility Evaluation Using Diablo Canyon Unit 1 and Palisades Surveillance Capsule Data (Heat # 27204)

Material	Capsule	Capsule Fluence(1) (x 10^{19} n/cm^2, E > 1.0 MeV)	FF(2)	Adjusted ΔRT_{NDT} with CF Ratio (Measured)(3) (°F)	FF*ΔRT_{NDT}	FF^2
Surrogate Weld (Heat # 27204) (Diablo Canyon Unit 1)	B	3.62	1.334	235.4 (242.6)	314.10	1.780
Surveillance Weld Heat # 27204 (Diablo Canyon Unit 1)	S	0.293	0.664	116.4 (110.1)	77.28	0.441
	Y	1.07	1.019	236.4 (232.0)	240.92	1.038
	V	1.35	1.083	203.8 (200.2)	220.82	1.174
	B	3.913(4)	1.351	311.9 (308.7)	421.50	1.826
Surveillance Weld Heat # 27204 (Palisades Data)	SA-60-1	1.50	1.112	246.1 (253.1)	273.74	1.237
	SA-240-1	2.40	1.236	261.4 (267.8)	323.03	1.528
				SUM:	1870.98	9.024
	$CF_{Heat\ \#\ 27204} = \Sigma(FF * \Delta RT_{NDT}) \div \Sigma(FF^2) = (1870.98) \div (9.024) =$ **207.3°F**					

Notes:

1. Diablo Canyon fluence values are taken from Table D-3. Palisades fluence values are taken from WCAP-19077-NP [D-10].
2. FF = fluence factor = $f^{(0.28 - 0.10*\log(f))}$.
3. Measured Diablo Canyon ΔRT_{NDT} data are taken from Table 5-10. Measured Palisades ΔRT_{NDT} data are taken from WCAP-19077-NP [D-10]. These measured ΔRT_{NDT} values are adjusted by the temperature adjustment values summarized in Table D-5. Then the values are adjusted by the ratios calculated using the ratio of the chemistry factor for the mean beltline weld chemistry to the chemistry factor for the applicable surveillance or surrogate weld chemistry. The pre-adjusted (measured) values are listed in parenthesis.
4. The surveillance weld specimens are reconstituted tested specimens previously irradiated in Capsule S. The fluence is the sum of the fluences of Capsule S (0.293E+19 n/cm^2) and Capsule B (3.62E+19 n/cm^2).

Using the chemical composition and operating temperature adjustments described and calculated above, an interim chemistry factor is calculated for weld Heat # 27204 using data from the Diablo Canyon Unit 1 surveillance weld, surrogate weld, and Palisades surveillance weld. This calculation is shown in Table D-7.

Table D-7 Diablo Canyon Unit 1 and Palisades Surveillance Capsule Data Scatter About the Best-Fit Line

Material	Capsule	CF(1) ($Slope_{best-fit}$) (°F)	Capsule Fluence(2) (x 10^{19} n/cm², E > 1.0 MeV)	FF(3)	Adjusted ΔRT_{NDT}(4) (°F)	Predicted ΔRT_{NDT}(5) (°F)	Scatter ΔRT_{NDT}(6) (°F)	< 28°F (Weld)
Surrogate Weld (Heat # 27204) (Diablo Canyon Unit 1)	B	207.3	3.62	1.334	235.4	276.6	41.2	No
Surveillance Weld Heat # 27204 (Diablo Canyon Unit 1)	S	207.3	0.293	0.664	115.7	137.7	21.9	Yes
	Y	207.3	1.07	1.019	236.4	211.2	25.2	Yes
	V	207.3	1.35	1.083	203.8	224.6	20.8	Yes
	B	207.3	3.913	1.351	311.9	280.2	31.7	No
Surveillance Weld Heat # 27204 (Palisades Data)	SA-60-1	207.3	1.50	1.112	246.1	230.6	15.5	Yes
	SA-240-1	207.3	2.40	1.236	261.4	256.2	5.1	Yes

Notes:
1. CF calculated in Table D-6.
2. Fluence taken from Table D-6.
3. FF = fluence factor = $f^{(0.28 - 0.10*\log(f))}$.
4. Adjusted ΔRT_{NDT} taken from Table D-6.
5. Predicted ΔRT_{NDT} = CF x FF.
6. Scatter ΔRT_{NDT} = Absolute Value [Predicted ΔRT_{NDT} – Measured ΔRT_{NDT}].

The scatter of ΔRT_{NDT} values about the best-fit line, drawn as described in Regulatory Guide 1.99, Revision 2, Position 2.1, should be less than 28°F for weld metal. Table D-7 indicates that 71% (5/7 * 100) of the surveillance data points fall inside the +/- 1σ of 28°F scatter band for surveillance welds; therefore, the weld (Heat # 27204) data are deemed "credible" per the third criterion when all available data are considered.

Criterion 4: The irradiation temperature of the Charpy specimens in the capsule should match the vessel wall temperature at the cladding/base metal interface within +/- 25°F.

The Diablo Canyon Unit 1 Capsule B specimens are located in the reactor between the thermal shield and the vessel wall and are positioned opposite the center of the core. The test capsules are in baskets attached to the thermal shield. The location of the specimens with respect to the reactor vessel beltline provides assurance that the reactor vessel wall and the specimens experience equivalent operating conditions and will not differ by more than 25°F.

Hence, Criterion 4 is met for the Diablo Canyon Unit 1 surveillance program.

Criterion 5: The surveillance data for the correlation monitor material in the Capsule should fall within the scatter band of the database for that material.

The Diablo Canyon Unit 1 surveillance program does contain CMM, which was supplied by Oak Ridge National Laboratory. The material was obtained from a 12-inch-thick A533 Grade B, Class 1 plate (HSST02), which was provided to ASTM to serve as CMM in reactor vessel surveillance programs.

NUREG/CR-6413, ORNL/TM-13133 [D-7] contains a plot of residual vs. Fast Fluence for the CMM (Figure 11 in the report). This Figure shows a 2σ uncertainty of 50°F. The data used for this plot is contained in Table 14 in the report. However, the NUREG Report does not consider the recalculated fluence values as documented herein nor does it include data pertaining to Capsule B. Thus, Table D-8 contains an updated calculation of Residual vs. Fast fluence, considering the recalculated capsule fluence values as well as data from Capsule B.

Table D-8 Calculation of Residual vs. Fast Fluence for Diablo Canyon Unit 1 CMM

Capsule	Wt. % Cu(1)	Wt. % Ni(1)	Chemistry Factor (CF)(1)	Capsule Fluence(2) (x 10^{19} n/cm^2, E > 1.0 MeV)	Fluence Factor (FF)(3)	Measured Shift(4) (°F)	Adjusted Shift(5) (°F)	RG 1.99 Shift(6) (°F)	Residual(7) (°F)
S	0.14	0.68	102	0.293	0.664	65.3	67.7	67.7	0.0
Y	0.14	0.68	102	1.07	1.019	116.2	116.2	103.9	12.3
V	0.14	0.68	102	1.35	1.083	116.4	115.9	110.5	5.4
B	0.14	0.68	102	3.62	1.334	163.8	161.8	136.1	25.7

Notes:

1. Cu and Ni values taken from Table 4-1, and used to determine the CF per Regulatory Guide 1.99, Revision 2 [D-1], Position 1.1. This is an update to the values used in previous evaluations, e.g., WCAP-15958 [D-11] and WCAP-18924-NP [D-9], which used Cu and Ni values of 0.150 and 0.650, respectively, from NUREG/CR-6413, ORNL/TM-13133 [D-7], which equates to a chemistry factor of 111.3˚F. The update was in alignment with the data within this report.
2. Fluence values taken from Table D-6.
3. FF = fluence factor = $f^{(0.28 - 0.10*\log(f))}$.
4. Measured Shift values are taken from Table 5-10.
5. Adjusted Shift = (Measured Shift + Temp. Adjustment from Table D-2).
6. Regulatory Guide 1.99, Revision 2 Shift = (CF * FF).
7. Residual = (Adjusted Shift – Regulatory Guide 1.99, Revision 2 Shift).

Table D-8 shows a 2σ uncertainty of less than 50˚F, which is the allowable scatter in NUREG/CR-6413, ORNL/TM-1313 [D-7]. Hence, Criterion 5 is met for the Diablo Canyon Unit 1 surveillance program.

Conclusion

Based on the preceding responses to the five criteria of Regulatory Guide 1.99, Rev. 2, Section B [D-1], and the application of engineering judgment, the Diablo Canyon Unit 1 surveillance weld data are deemed “credible”.

D.3 REFERENCES

D-1. U.S. Nuclear Regulatory Commission, Office of Nuclear Regulatory Research, Regulatory Guide 1.99, Rev. 2, “Radiation Embrittlement of Reactor Vessel Materials” May 1988. *[ADAMS Accession Number ML003740284].*

D-2. Code of Federal Regulations 10 CFR 50, Appendix G, “Fracture Toughness Requirements,” U.S. Nuclear Regulatory Commission, Federal Register.

D-3. Westinghouse Report, WCAP-8465, Revision 0, “Pacific Gas and Electric Co. Diablo Canyon Unit No. 1 Reactor Vessel Radiation Surveillance Program,” January 1975.

D-4. Westinghouse Report, WCAP-13440, Revision 0, “Supplemental Reactor Vessel Radiation Surveillance Program for the Pacific Gas and Electric Company Diablo Canyon Unit No. 1,” December 1992.

D-5. ASTM E185-82, “Standard Practice for Conducting Surveillance Tests for Light-Water Cooled Nuclear Power Reactor Vessels,” American Society for Testing and Materials, 1982.

D-6. K. Wichman, M. Mitchell, and A. Hiser, USNRC, “Generic Letter 92-01 and RPV Integrity Assessment, Status, Schedule, and Issues,” NRC/Industry Workshop on RPV Integrity Issues, February 12, 1998. *[ADAMS Accession Number ML110070570]*.

D-7. ORNL Report, “Analysis of the Irradiation Data for A302B and A533B Correlation Monitor Materials,” Oak Ridge National Laboratory, NUREG/CR-6413, ORNL/TM-13133, April 1996. *[ADAMS Accession Number ML20112B397]*

D-8. ASTM E185-70, “Standard Recommended Practice for Surveillance Tests for Nuclear Reactor Vessels,” American Society for Testing and Materials, 1970.

D-9. Westinghouse Report, WCAP-18924-NP, Revision 1, “Diablo Canyon Units 1 and 2 Initial License Renewal: Time-Limited Aging Analyses (TLAAs) on Reactor Vessel Integrity (RVI),” November 2024.

D-10. Westinghouse Report, WCAP-19077-NP, Revision 0, “Palisades Time-Limited Aging Analyses (TLAAs) on Reactor Vessel Integrity (RVI) for Plant Restart and Subsequent License Renewal (SLR),” April 2026.

D-11. Westinghouse Report, WCAP-15958, Rev. 0, “Analysis of Capsule V from Pacific Gas and Electric Company Diablo Canyon Unit 1 Reactor Vessel Radiation Surveillance Program,” January 2003.

This page was added to the quality record by the PRIME system upon its validation and shall not be considered in the page numbering of this document.

Approval Information
Author Approval Long Margaret L Jun-25-2026 14:56:41
Author Approval Guillen Marcos Alberto Jun-25-2026 15:11:24
Reviewer Approval Lynch Donald Jun-25-2026 15:29:23
Reviewer Approval Hawk Andrew E Jun-25-2026 16:41:09
Manager Approval Lowes Ryan R Jun-25-2026 21:11:52
Manager Approval Ruiz Gonzalez Jesus for Klingensmith Jesse J Jun-26-2026 02:21:23

Files approved on Jun-26-2026

*** This record was final approved on 06/26/2026 02:21:23. (This statement was added by the PRIME system upon its validation)